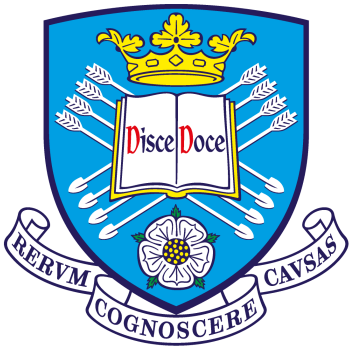

The University Of Sheffield.

Investigating the Mechanisms of Long-Lasting Within Generation Jasmonate Induced Resistance

Samuel William Wilkinson

A thesis submitted to the University of Sheffield
for the degree of Doctor of Philosophy

The University of Sheffield
Faculty of Science
Department of Animal and Plant Sciences

September 2020

Acknowledgements

First and foremost, I would like to thank my supervisors Jurriaan Ton and Melissa Magerøy for the amazing guidance, assistance and support they have provided to me throughout my PhD. Both have gone above and beyond to ensure that my PhD has been a truly fantastic experience. I have been able to conduct a range of fascinating experiments and work with an amazing diversity of different plant, microbe and insect species. Furthermore, both Jurriaan and Melissa have provided me the opportunity to get involved in numerous side projects which have developed me both as a person and a scientist.

My PhD was funded primarily by a Research Council of Norway Young Researcher Talent grant awarded to Melissa. I would like to thank the Research Council of Norway for providing this funding and Melissa for using the funding to enable me to do a PhD. I would also like to thank Paal Krokene who kindly provided additional finance to allow me to have a fully funded final year.

During my PhD I have been very fortunate to have had the assistance of several fantastic masters and summer students. In the second year of my PhD, Mike Henderson helped me considerably with several of the early insect and pathogen assays along with qPCR analysis. At the same time, Ellie Vinnicombe also provided support with conducting pathogen assays. In my third year, Rob Wilson assisted with analysing RNA-seq data and performing numerous insect assays. Finally, at the start of my fourth year, Amos Münch gave up his summer to assist me with some challenging herbivore feeding experiments and work on the analysis of RNA-seq data. I thank you all for your amazing work and willingness to put in long hours to assist me with several very large experiments. Furthermore, I wish you all luck for what I am sure will be very successful future careers.

Throughout my time in Sheffield I have been very fortunate to be part of an extremely helpful and supportive lab group. Thus, I would like to thank all the current and former members of C51/C207. I would also like to give a special mention to a couple of people. Firstly, lab manager David Pardo, who has made my PhD a much easier and enjoyable experience. Secondly, Ana López for her assistance with my early Arabidopsis experiments and for teaching me several very useful molecular biology techniques. Thirdly, Leonardo Furci who kindly assisted me with a number of

my larger experiments. Fourthly, Joost Stassen for sharing with me some of his incredible bioinformatics and plant science knowledge. Finally, Estrella Luna-Diez for introducing me to the plant-biotic interactions field and for providing me with invaluable advice and encouragement throughout my PhD. Without Estrella I almost certainly would not have had the opportunity to do this PhD.

For eight months of my PhD I lived and worked in Ås, Norway. This was my first time living outside the UK and thus was rather daunting. However, Melissa and her husband Jon provided me amazing support and assistance when I first arrived, throughout my stay and whenever I have subsequently revisited. I will be forever grateful to you both. Furthermore, I would also like to thank Paal Krokene for his academic support but also for showing me some great running routes near Ås and for lending me a bike which allowed me to explore the local area. Finally, I would like to thank all the technical and support staff at NIBIO who made my stay in H8 such a great experience.

I would also like to thank all my friends who have been there for me throughout my PhD. My PhD experience has been made a million times better as a result of the tremendous times spent with the running double Matt and Jimmy, my caterpillar co-parent Davo Rapples, my Ås friends Sia and Titta, the lunch crew, 34 Redcar Road and everyone who has attended the Friday trips to Interval pub, Click bar or Bolehill park over the last four years. I would also like to mention my long-time friend Joh, who has provided me considerable support and encouragement over the last few years. Finally, I would like to thank my amazing partner Sarah. Our Peak District walks are the highlight of my time in Sheffield and I look forward to many more adventures together in the future.

Last but certainly not least, I would like to thank my fantastic family. Without my parents', brother's and grandparents' love, attention, support and encouragement, I would not have got to this point. I am looking forward to seeing you all out in the wood following the submission of this thesis.

Declaration and Acknowledgement of Collaborative Work

The work presented in this thesis is novel and has not previously been submitted for examination at the University of Sheffield or any other University. The candidate is aware of the University's Guidance on the Use of Unfair Means (www.sheffield.ac.uk/ssid/unfair-means) and therefore all work submitted is that of the candidates. The only exception to this, is instances where additional co-authors have provided assistance with, for example, gathering data in large experiments. At the beginning of each chapter, all co-authors are acknowledged, and their contributions are listed. Additionally, acknowledgement of those who kindly provided resources such as seed stocks, pathogen isolates and insect eggs, is displayed in the methods sections of the relevant chapter. Thus far, only one publication has directly resulted from this thesis. The publication, which contributed to Chapter 1 (General Introduction) and Chapter 4 (General Discussion), is listed below.

Publications

Wilkinson SW, Magerøy MH, López Sánchez A, Smith LM, Furci L, Cotton TEA, Krokene P, Ton J (2019) Surviving in a Hostile World: Plant Strategies to Resist Pests and Diseases. *Annual Review of Phytopathology* 57: 505–529

Author contributions: SWW (the candidate) and JT conceived the original idea and structure of the review. All authors contributed to the writing of the article and/or production of the figures. SWW, MHM, PK and JT reviewed and finalised the manuscript for submission.

Abstract

Jasmonates, such as jasmonic acid (JA) or methyl jasmonate (MeJA), elicit short-term enhanced resistance in plants against chewing herbivores and necrotrophic pathogens. In Norway spruce (*Picea abies*), this jasmonate induced resistance (IR) can last for many months, whereas the long-term within-generation impact of jasmonates on biotic stress resistance in *Arabidopsis thaliana* (Arabidopsis) remains unclear. Furthermore, little is known about the mechanisms controlling long-term jasmonate-IR. This PhD study addressed these knowledge gaps by exploring the phenotypes and immunological and (epi)genetic mechanisms of long-term jasmonate-IR in Arabidopsis and Norway spruce.

Two-week-old Arabidopsis seedlings were treated with JA and then challenged three weeks later with different pests and pathogens. Long-term JA-IR against the generalist herbivore *Spodoptera littoralis* was comparable to short-term JA-IR against this pest. Whereas, plants from JA-treated seedlings displayed enhanced susceptibility to the necrotrophic fungus *Plectosphaerella cucumerina* which contrasted the short-term IR against this pathogen. Transcriptome analysis revealed that the long-term response to JA is characterised by priming and/or prolonged upregulation of MYC-dependent anti-herbivore defences, but repression of anti-pathogen defences. Bioassays with DNA (de)methylation mutants and a genome-wide methylome analysis suggested that long-term JA-IR against herbivores is based on ROS1-dependent hypomethylation of transposable elements, particularly those from the *ATREP2* family.

Spruce experiments were performed with two-year-old seedlings that were treated with MeJA and challenged four weeks later. MeJA elicited IR against the necrotrophic pathogen *Grosmannia penicillata*. A transcriptome analysis suggested that establishment and maintenance of MeJA-IR in spruce involves RNA-directed DNA methylation and defence hormone signalling. The analysis also revealed distinct temporal patterns of global gene expression in response to MeJA treatment.

This thesis has advanced our understanding of the (epi)genetic and immunological basis of long-term jasmonate-IR in Arabidopsis and Norway spruce. The results have implications for the exploitation of IR in agriculture and forestry.

Table of Contents

Table of Figures

List of Supplemental Figures

List of Tables

List of Equations

List of Supplemental Data Sets

As a consequence of their size, all of the supplemental data sets listed below have been provided separately as standalone excel workbooks.

Supplemental Data Set 2.1. RNA-seq read counts for genes displaying an altered response to JA challenge as a result of prior JA seedling treatment.

Supplemental Data Set 2.2. RNA-seq read counts for JA inducible genes which were more strongly expressed post JA challenge in plants from JA treated seedlings compared to water pre-treated controls.

Supplemental Data Set 2.3. GO terms overrepresented in the four Figure 2.6A gene expression profile clusters.

Supplemental Data Set 2.4. Overrepresented protein signatures in the four Figure 2.6A gene expression profile clusters.

Supplemental Data Set 2.5. RNA-seq read counts for genes displayed in Figure 2.7A.

Supplemental Data Set 2.6. GO terms overrepresented among the genes in Figure 2.7A.

Supplemental Data Set 2.7. Overrepresented protein signatures among the genes of Figure 2.7A.

Supplemental Data Set 2.8. Overrepresented transcription factor DNA binding motifs within the promoters of the genes of Figure 2.7A.

Supplemental Data Set 2.9. RNA-seq read counts for JA repressible genes which were more strongly repressed post JA challenge in JA seedling treated plants than in the water controls.

Supplemental Data Set 2.10. GO terms overrepresented in the three Figure 2.9A gene expression profile clusters.

Supplemental Data Set 2.11. Overrepresented protein signatures in the three Figure 2.9A gene expression profile clusters.

Supplemental Data Set 2.12. RNA-seq read counts for the genes displayed in Figure 2.10A.

Supplemental Data Set 2.13. GO terms overrepresented among the genes in Figure 2.10A.

Supplemental Data Set 2.14. Overrepresented protein signatures among the genes of Figure 2.10A.

Supplemental Data Set 2.15. Overrepresented KEGG pathways among the genes in Figure 2.10A.

Supplemental Data Set 2.16. Overrepresented transcription factor DNA-binding motifs within the promoters of the genes of Figure 2.10A.

Supplemental Data Set 2.17. DMR locations and statistics for the 1JA_Vs_3W comparisons.

Supplemental Data Set 2.18. DMR summary statistics.

Supplemental Data Set 2.19. Consensus DMRs.

Supplemental Data Set 2.20. RNA-seq raw read data and alignment statistics.

Supplemental Data Set 2.21. Whole genome bisulfite sequencing raw read data and alignment statistics.

Supplemental Data Set 3.1. RNA-seq read counts for genes displaying an altered expression profile as a result of MeJA pre-treatment.

Supplemental Data Set 3.2. Overrepresented protein signatures in the post pre-treatment transcriptome analysis gene clusters.

Supplemental Data Set 3.3. GO terms overrepresented in the post pre-treatment transcriptome analysis gene clusters.

Supplemental Data Set 3.4. Differentially expressed genes predicted to encode for defence hormone biosynthesis enzymes, downstream transcriptional regulators and defence proteins.

Supplemental Data Set 3.5. Differentially expressed genes predicted to encode for epigenetic regulators.

Supplemental Data Set 3.6. RNA-seq read counts and DESeq2 statistics for genes which were differentially expressed in one or more of the six pairwise comparisons between the post challenge treatment groups.

Supplemental Data Set 3.7. Overrepresented protein signatures in the post challenge transcriptome analysis gene clusters.

Supplemental Data Set 3.8. GO terms overrepresented in the post challenge transcriptome analysis gene clusters.

Supplemental Data Set 3.9. RNA-seq raw read data and alignment statistics.

Abbreviations

12OH-JA - hydroxylated jasmonic acid

13-HPOT - (13s)-hydroperoxyoctadecatrienoic acid

1MO-I3M - 1-methoxy-indol-3-ylmethyl-glucosinolate

4,5-ddh-JA - 4,5-didehydrojasmonate

4MO-I3M - 4-methoxy-indol-3-ylmethyl-glucosinolate

ABA - Abscisic acid

Abm - Antibiotic biosynthesis monooxygenase

ACC - 1-Aminocyclopropanecarboxylic acid

ACO - ACC oxidase

ACS - 1-AMINOCYCLOPROPANE-1-CARBOXYLIC ACID SYNTHASE

AGO - ARGONAUTE

All C - Cytosines of all possible DNA sequence contexts (All contexts).

AOC - ALLENE OXIDE CYCLASE

AOS - ALLENE OXIDE SYNTHASE

AP2/ERF - APETALA2/ETHYLENE RESPONSE FACTOR

Arabidopsis - *Arabidopsis thaliana*

ARR11 - ARABIDOPSIS RESPONSE REGULATOR11

BA - Benzoic acid

BABA - β-aminobutyric acid

bHLH - Basic helix-loop-helix

bp - Base pairs

BSMT1 - SALICYLIC ACID METHYL TRANSFERASE1

BTH - Benzothiadiazole

CBP60g - CALMODULIN BINDING PROTEIN60g

CDPK - calcium-dependent protein kinase

CEND - Carboxyl terminal end

cfu - Colony forming unit

ChIP-seq - Chromatin Immunoprecipitation Sequencing

CMOS - Complementary metal-oxide-semiconductor

CMT - CHROMOMETHYLASE-class

COI1 - CORANTINE INSENSITVE1

Col-0 - Columbia-0

COR - Coronatine

CTR1 - CONSTITUTIVE TRIPLE RESPONSE1

CUL3 - CULLIN3

CYP - CYTOCHROME P450

CYP83A1 - CYTOCHROME P450, FAMILY 83, SUBFAMILY A, POLYPEPTIDE 1

DAMP - Damage-associated molecular pattern

DCL - DICER-LIKE

DDM1 - DECREASED DNA METHYLATION1

DE – Differential expression

dH_2O - deionised H2O

DMC - Differentially methylated cytosines

DME - DEMETER

DML1 - DEMETER-LIKE1

DMP - Differentially methylated position

DMR - Differentially methylated region

dnOPDA - 2,3-dinor-12-oxo-10,15(Z)-phytodienoic acid

dpi – Days post inoculation

DRM - DNA (cytosine-5)-methyltransferase

DRM - DOMAINS REARRANGED METHYLASE

dsRNA - double stranded RNA

DSS - Dispersion shrinkage for sequencing data

EBF - ETHYLENE-INSENSITIVE3-BINDING F-BOX

EDS5 - ENHANCED DISEASE SUSCEPTIBILITY5

EIL1 - ETHYLENE-INSENSITIVE3-LIKE 1

EIN - ETHYLENE-INSENSITIVE

ENAP1 - ETHYLENE-INSENSITIVE2 NUCLEAR-ASSOCIATED PROTEIN1

epiQTLs - epigenetic quantitative trait loci

epiRILs - epigenetic recombinant inbred lines

EPS1 - ENHANCED PSEUDOMONAS SUSCEPTIBILITY 1

ERF - ETHYLENE RESPONSE FACTOR

ET - Ethylene

ETI - Effector triggered immunity

ETR1 - ETHYLENE RESPONSE1

FAIRE - Formaldehyde-Assisted Isolation of Regulatory Elements

FDR - False discovery rate

Flg22 - Flagellin 22

$FMO_{GS\text{-}OX}$ - FLAVIN-MONOOXYGENASE GLUCOSINOLATE S-OXYGENASE

FPP - Farnesyl diphosphate

GAPC2 - GLYCERALDEHYDE-3-PHOSPHATE DEHYDROGENASE C2

GGPP - Geranylgeranyl diphosphate

GLYI4 - GLYOXYLASE I4

GO - Gene ontology

GPP - Geranyl diphosphate

GS - Glucosinolate

GWA - Genome-wide association

H3K4me3 - Triple methylation of lysine residue 4 of histone H3

H3K9ac - Acetylation of lysine 9 of histone H3

H3K9me2 - Dimethylation of lysine residue 4 of histone H3

HAI1 - HIGHLY ABSCISIC ACID-INDUCED clade A protein phosphatase 2C GENE1

HAMP - Herbivore-associated molecular pattern

HCA – Hierarchical Clustering Analysis

HIPV - Herbivore-induced plant volatile

HR - Hypersensitive cell death response

hrs - Hours

HSI - Hyperspectral imaging

I3M - indol-3-ylmethyl-glucosinolate

IC-9-Glu - Isochorismate-9-glutamate

ICS - ISOCHORISMATE SYNTHAE

IDS - Isoprenyl diphosphate synthases

Ile - Isoleucine

IR - Induced resistance

IS - Induced susceptibility

ISR - Induced systemic resistance

JA - Jasmonic acid

JA-Ile - Jasmonic acid-isoleucine

JAR1 - JASMONATE RESISTANT1

JAT1 - JASMONATE TRANSPORTER1

JAZ - JAZMONATE ZIM DOMAIN

jazD - jaz1 jaz2 jaz3 jaz4 jaz5 jaz6 jaz7 jaz9 jaz10 jaz13

jazQ - jaz1 jaz3 jaz4 jaz9 jaz10

jin1 - jasmonate insensitive1

KEG - KEEP ON GOING

KEGG - Kyoto Encyclopedia of Genes and Genomes

KYP - KRYPTONITE

LOX - 13-Lipoxygenase

MAMP - Microbe-associated molecular pattern

MAPK - Mitogen-activated protein kinase

MED25 - MEDIATOR COMPLEX SUBUNIT25

MeJA - Methyl jasmonate

MET1 - METHYLTRANSFERASE1

MIR - Mycorrhiza-induced resistance

MOM1 - MORPHEAUS MOLECULE1

MON1 - MONENSIN SENSITIVITY1

MORC - Microrchidia

MPK - MITOGEN-ACTIVATED PROTEIN KINASE

MYB - MYB DOMAIN PROTEIN

myc234 - myc2 myc3 myc4

MYC234 - MYC2, MYC3 and MYC4 transcription factors

NAC - Petunia NAM and Arabidopsis ATAF1, ATAF2, and CUC2

NIBIO - Norwegian Institute of Bioeconomy Research

NINJA - NOVEL INTERACTOR OF JAZ

NLR - Nucleotide binding site-leucine-rich repeat

NPR - NONEXPRESSER OF PATHOGENESIS-RELATED GENES

NRPD1 - NUCLEAR RNA POLYMERASE D 1

NRPE1 - NUCLEAR RNA POLYMERASE E1

nt - Nucleotide

OPC - 3-oxo-2[2(Z)-pentenyl]-cyclopentane

OPDA - 12-oxo-10,15(Z)-phytodienoic acid

OPR - OPDA REDUCTASE

ORA59 - OCTADECANOID-RESPONSIVE ARABIDOPSIS AP2/ERF59

p.adj – FDR adjusted *p*-value

PAL - PHENYLALANINE AMMONIA LYASE

PAMP - Pathogen-associated molecular pattern

PBS3 - avrPphB SUSCEPTIBLE3

Pc - Plectosphaerella cucumerina

PCA - Principle component analysis

PDF1.2 - PLANT DEFENSIN1.2

PE - Paired-end

PGTS - Post-transcriptional gene silencing

Pol - RNA polymerase

PP - Polyphenolic parenchyma

PP2C - Clade A protein phosphatase 2C

PR - PATHOGENESIS-RELATED

PRR - Pattern recognition receptor

Ps - Pseudomonas syringae pv. *tomato* DC3000 *luxCDABE*

Pst-lux - Pseudomonas syringae pv. tomato DC3000 luxCDABE

PTI - Pattern triggered immunity

pv. - Pathovar

PYL6 - PYRABACTIN RESISTANCE 1-LIKE6

RBH - (R)-β-homoserine

RdDM - RNA-directed DNA methylation

RDM1 - RNA-DIRECTED DNA METHYLATION1

RDR - RNA-DEPENDENT RNA POLYMERASE

R-genes - Resistance-genes

RH – Relative humidity

RIN - RNA integrity number

RNAi - RNA interference

RNA-seq - mRNA sequencing

ROS1 - REPRESSOR OF SILENCING1

RSA - Rosette surface area

RT-qPCR - Reverse-Transcriptase Quantitative Polymerase Chain Reaction

SA - Salicylic acid

SABPs - Salicylic acid-binding proteins

SAM - S-adenosyl-L-methionine

SAR -Systemic acquired resistance

SARD1- SYSTEMIC ACQUIRED RESISTANCE-DEFICIENT1

SCF^{COI1} - S PHASE KINASE-ASSOCIATED PROTEIN1/CULLIN1/F-box CORANTINE INSENSITVE1

SHH1 - SAWADEE HOMEODOMAIN HOMOLOG1

sid2 - salicylic acid induction-deficient 2

Sl - Spodoptera littoralis

sRNA - Small RNA

ssCir DNA - single strand circle DNA

SUVH - SUPPRESSOR OF VARIEGATION 3-9 HOMOLOG

TAR - Transgenerational acquired resistance

t-CA - *trans*-cinnamic acid

TE - Transposable element

TF - Transcription factor

TGA - TGACG motif-binding

tnOPDA - tetranor-12-oxo-10,15(Z)-phytodienoic acid

TPL - TOPLESS

TRD - Traumatic resin duct

TSS - Transcription start site

UBC21 - UBIQUITIN-CONJUGATING ENZYME21

VSP - VEGETATIVE STORAGE PROTEIN

vst - variance stabilising transformation

W - Water (control/mock treatment)

WGBS - Whole genome bisulfite sequencing

wk - Week

α-LeA - α-linolenic acid (18:3)

Chapter 1

General Introduction

Adapted from:

Wilkinson SW[1,2], Magerøy MH[2], López Sánchez A[1,3], Smith LM[1], Furci L[1], Cotton TEA[1], Krokene P[2], Ton J[1] (2019) Surviving in a Hostile World: Plant Strategies to Resist Pests and Diseases. *Annual Review of Phytopathology* 57: 505–529

Affiliations:

[1] Department of Animal and Plant Sciences, The University of Sheffield, Sheffield S10 2TN, United Kingdom

[2] Department of Molecular Plant Biology, Division for Biotechnology and Plant Health, Norwegian Institute for Bioeconomy Research (NIBIO), 1431 Ås, Norway

[3] Department of Plant Molecular Genetics, Centro Nacional de Biotecnología, Consejo Superior de Investigaciones Científicas (CNB-CSIC), 28049 Madrid, Spain

Author contributions:

SWW (the candidate) and JT conceived the original idea and structure of the review. All authors contributed to the writing of the article and/or production of the figures. SWW, MHM, PK and JT reviewed and finalised the manuscript for submission.

All material in this chapter, which is not in the publication, was created by SWW.

Chapter 1. General Introduction

Our planet is inhabited by a wide range of different plant species, from short-lived desert angiosperms to long-lived coniferous species that dominate boreal forests. Although variable in phenotype, generation time, and geographical range, all plants are primary producers. Consequently, they face constant pressure from opportunistic attackers, such as viruses, bacteria, fungi, nematodes, arthropods, and large herbivores. Despite this pressure, land plants have continued to thrive for 500 million years (Morris et al., 2018), which would not have been possible without sophisticated defence strategies (Figure 1.1).

In addition to constitutive defences, all plants have an innate immune system, which provides instant protection against most attackers (Jones and Dangl, 2006; Cook et al., 2015). Plants can also acquire resistance after the perception of specific environmental stimuli (Pieterse et al., 2014; Mauch-Mani et al., 2017). This acquired or induced resistance (IR) is typically long-lasting and can even be transmitted to following generations through changes in DNA methylation and associated chromatin density (Luna et al., 2012; López Sánchez et al., 2016; Stassen et al., 2018). There is increasing evidence that these epigenetic processes can influence genetic mutations and the rate at which new defence genes evolve (Stokes et al., 2002; Yi and Richards, 2009; Ossowski et al., 2010). In addition to these internal strategies, plants are capable of orchestrating multitrophic ecological interactions for their protection (Turlings and Erb, 2018; Rolfe et al., 2019). These external strategies involve above- and below-ground recruitment of beneficial insects and microbes. Recruitment of beneficial microbes can lead to the formation of disease-suppressive microbiomes that offer long-term protection to individual plants and their progeny (Berendsen et al., 2018; Hu et al., 2018). In keeping with the internal strategies, there is also recent evidence which suggests that the formation of beneficial root associated microbiomes can be regulated by epigenetic mechanisms, or more specifically DNA methylation, in the host plant (Vílchez et al., 2020; Wilkinson and Ton, 2020).

In this general introduction the focus will be on internal strategies acting over short and medium timeframes (Figure 1.1). For more information on the internal strategies acting over longer timeframes or the external strategies, please refer to the review from which this general introduction was adapted (Wilkinson et al., 2019).

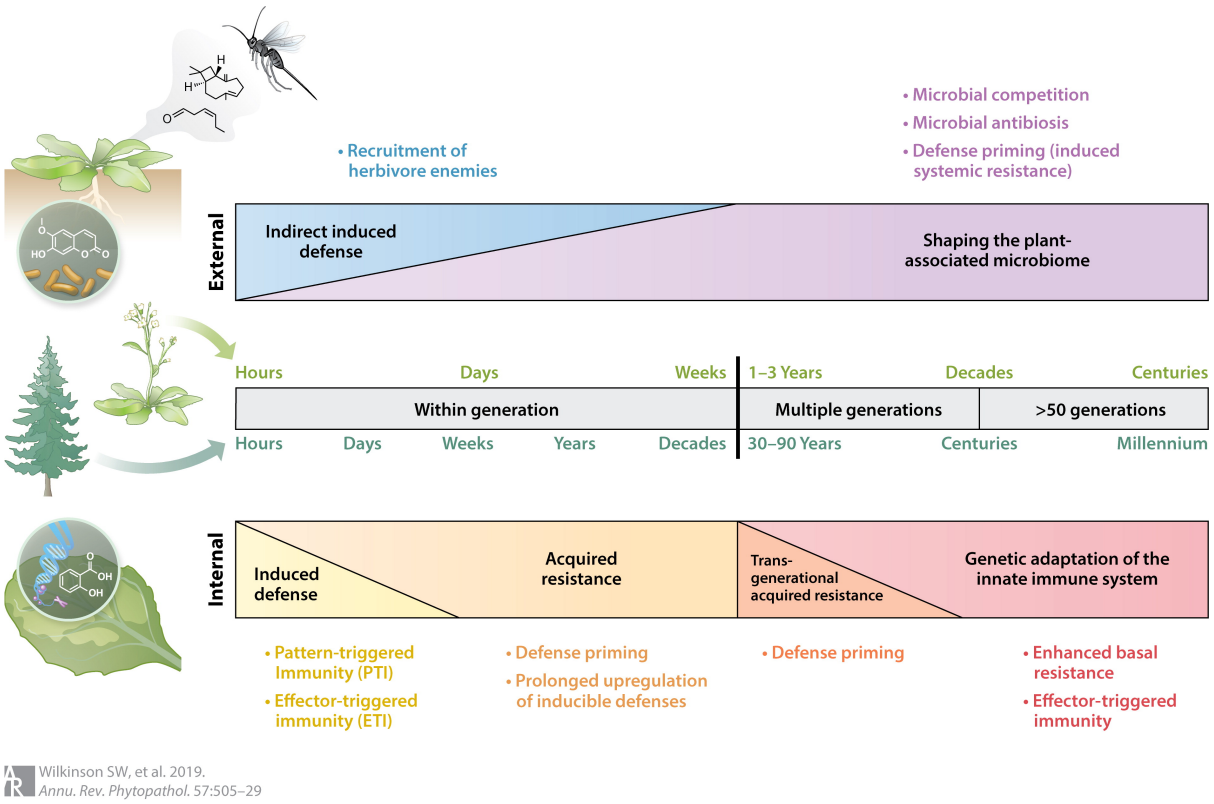

Wilkinson SW, et al. 2019.
Annu. Rev. Phytopathol. 57:505–29

Figure 1.1. Short- and Long-Term Strategies by Which Plants Adapt to Stress from Pests and Diseases.

Shown at the bottom are internal strategies, which are controlled by plant immunological pathways involving physiological, molecular, and (epi)genetic mechanisms. Shown at the top are external strategies, which involve ecological interactions with plant-beneficial organisms. Mechanisms underpinning the internal and external strategies are shown below or above, respectively, the colored triangles. All strategies are aligned against a timescale (middle), which varies depending on generation time and habitat of the plant. Reproduced with permission from the Annual Review of Phytopathology, Volume 57 © 2019 by Annual Reviews, http://www.annualreviews.org

1.1. Constitutive Defences

Constitutive defence mechanisms provide the first layer of protection and can be split into two groups, mechanical and chemical. Classic examples of mechanical constitutive defences include thorns which deter large herbivores and tissues, such as the phellem of conifers, which are rich in lignified and suberised cells (Franceschi et al., 2005). Constitutive chemical defences often exist as pools of secondary metabolites. Upon attack these metabolites are released and/or activated with the defensive action often coming through the toxic nature of the metabolite and its breakdown products. For example, glucosinolates which are generally produced by members of the Brassicales order (Halkier, 2016). In intact tissue, glucosinolates and their hydrolysing myrosinases are spatially separated (Burow and Halkier, 2017). However, upon attack, such as tissue disruption by a chewing herbivore, the

metabolites and enzymes are brought into contact resulting in the production of a range of hydrolysis products which can be toxic to the attacker (Hopkins et al., 2009; Wittstock and Burow, 2010; Wittstock et al., 2016). Terpene-rich oleoresin and polyphenolics which accumulate in the resin ducts and phloem parenchyma cells, respectively, of members of the *Pinaceae* family, are additional examples of constitutive chemical defences (Wu and Hu, 1997; Franceschi et al., 1998). Notably, oleoresin not only resists attackers via the toxicity of its terpene constituents, but due to being stored under pressure, it can also flush out and or entrap invading herbivores (Krokene, 2015). Thus, oleoresin may be defined as both a chemical and a mechanical defence.

1.2. Innate Immune System

While constitutive defences are efficient against non-adapted opportunistic aggressors, they can also be costly and are typically ineffective against more specialised attackers. Consequently, plants have evolved a regulatory system for more efficient exploitation of defence resources: the 'plant innate immune system' (Jones and Dangl, 2006; Cook et al., 2015). This genetically controlled system, which regulates the perception of attack and subsequent activation of innate defences, is subject to an evolutionary arms race with virulence strategies of pathogens and herbivores (Jones and Dangl, 2006; Anderson et al., 2010). I will briefly review the two major pillars of the plant innate immune system; pattern-triggered immunity (PTI) and effector-triggered immunity (ETI), both of which provide instant protection over relatively short timespans, ranging from hours to days (Figure 1.1).

1.2.1. Pattern Triggered Immunity (PTI)

PTI protects plants against the majority of potential attackers and involves multiple defence layers that are induced after recognition of specific molecular patterns (Jones and Dangl, 2006; Spoel and Dong, 2012; Bigeard et al., 2015). This recognition is mediated by 'pattern recognition receptors' (PRRs), which are receptor kinases and receptor-like proteins that are often localised to the surface of plant cells (Zipfel, 2014; Boutrot and Zipfel, 2017). PRRs detect attackers via molecular patterns. Some PRRs detect pathogen-/microbe-/herbivore-associated molecular patterns (PAMPs, MAMPs, and HAMPs), which indicate the presence of chemical signatures that are not from the host plant itself (non-self) (Zipfel et al., 2004; Schmelz et al., 2006). PRRs

also detect damage associated molecular patterns (DAMPs), which indicate the presence of host-derived chemical signatures from damaged cells (damaged-self) (Krol et al., 2010; Heil and Land, 2014; Boutrot and Zipfel, 2017).

Regulation of PTI is controlled by a complex signalling web that varies between plant species and the molecular patterns perceived (Bigeard et al., 2015; Couto and Zipfel, 2016; Li et al., 2016; Erb and Reymond, 2019). Despite this variation, there are common signalling components. In the immediate aftermath of molecular pattern recognition, there is often fluxes in levels of ions including Ca^{2+} (Jeworutzki et al., 2010), a burst of reactive oxygen species (Nühse et al., 2007), increased production of nitric oxide (Foissner et al., 2000) and accumulation of signalling lipids such as phosphatidic acid (van der Luit et al., 2000). These small molecules are thought to play important roles alongside protein kinases in driving the initial upregulation of inducible defences (Lippert et al., 2009; Bigeard et al., 2015; Li et al., 2016). The induction of defences is enhanced further following fluxes in the level of hormones such as jasmonic acid (JA), ethylene (ET) and salicylic acid (SA). These hormones regulate defences that are effective against different groups of attackers (Pieterse et al., 2012). While JA-dependent defences are generally more effective against necrotrophic pathogens and chewing herbivores, SA-dependent defences are mostly effective against biotrophic pathogens (Glazebrook, 2005). Defences contributing to PTI include cell wall reinforcements (Malinovsky et al., 2014), production of pathogenesis-related (PR) proteins (Van Loon et al., 2006) and accumulation of secondary metabolites, such as terpenes and tryptophan-derived metabolites including indolic glucosinolates (Piasecka et al., 2015; Celedon and Bohlmann, 2019).

A subset of specialized attackers have evolved strategies to suppress PTI. Virulent pathogens can suppress PTI via effector proteins, metabolites, and/or small RNAs (sRNAs),which can be injected into host cells (Weiberg et al., 2013; Toruño et al., 2016). This effector-triggered susceptibility can give rise to an evolutionary arms race with the host plant (Jones and Dangl, 2006).

1.2.2. Effector Triggered Immunity (ETI)

To counter immune-suppressing effectors from (hemi)biotrophic pathogens, plants have evolved resistance genes (R-genes). Most R-genes encode nucleotide binding site-leucine-rich repeat (NLR) receptor proteins, which directly or indirectly

detect pathogen effector activity (Van Der Biezen and Jones, 1998; Axtell and Staskawicz, 2003; Ade et al., 2007; Krasileva et al., 2010; Spoel and Dong, 2012; Li et al., 2014a; Cui et al., 2015; Khan et al., 2016). Activation of NLR receptors elicits ETI, which often leads to a form of programmed cell death at locally infected tissues, the hypersensitive response (HR). The HR is very effective against biotrophic pathogens that rely on living plant cells for their growth (Glazebrook, 2005; Cui et al., 2015), but can also come with costs. For instance, HR-related cell death can facilitate infection by necrotrophic pathogens (Lorang et al., 2007; Kliebenstein and Rowe, 2008; Lorang et al., 2012). Another limitation of ETI is its narrow range of effectiveness. Each R protein recognizes a limited number of effectors, thereby providing protection against one or a small number of pathogen isolates. This reliance on single R genes allows pathogens to rapidly overcome ETI, as a single mutation can give rise to a virulent pathotype (Jones and Dangl, 2006).

Attackers capable of suppressing ETI and/or PTI are still faced with a residual level of basal resistance when infecting a susceptible host (Ahmad et al., 2010; Ahmad et al., 2011). This resistance contributes to slowing disease progression. Like PTI, basal resistance is effective against a broad spectrum of attackers. Furthermore, it is regulated by many of the same signalling molecules as PTI, including the JA and SA. Due to the relevance of these hormones to this thesis, JA and SA biosynthesis, perception and downstream signalling, particularly in relation to *Arabidopsis thaliana* (Arabidopsis), will be discussed in detail. Furthermore, some of the strategies used by aggressive attackers to manipulate and/or suppress JA and SA signalling and regulated defences will also be mentioned.

1.3. Jasmonic Acid (JA) Biosynthesis, Signalling and Regulated Defences

JA is oxylipin phytohormone which regulates a number of processes related to growth, development and relevant to this review, biotic stress tolerance (Wasternack and Hause, 2013). JA accumulates in response to attack by chewing herbivores or necrotrophic pathogens (Pieterse et al., 2012; Vos et al., 2013; Goossens et al., 2016; Erb and Reymond, 2019). This accumulation, via *de novo* biosynthesis, begins very rapidly (seconds to minutes) following tissue disruption (Glauser et al., 2009; Koo et al., 2009).

The first step in the biosynthesis of JA is the release of α-linolenic acid (18:3) (α-LeA) from galactolipids of the chloroplast membrane, via the action of acyl-lipid hydrolases (Wasternack and Feussner, 2018). Excellent reviews overviewing the conversion of α-LeA to JA are available (Wasternack, 2007; Gfeller et al., 2010; Wasternack and Hause, 2013; Wasternack and Song, 2017; Wasternack and Feussner, 2018). Nevertheless, I will briefly summarise the five key steps in this biosynthesis pathway. First, 13-Lipoxygenases (LOX) catalyse the conversion of α-LeA to (13s)-hydroperoxyoctadecatrienoic acid (13-HPOT). Secondly, ALLENE OXIDE SYNTHASE (AOS) and ALLENE OXIDE CYCLASE (AOC) sequentially convert 13-HPOT to 12-oxo-10,15(*Z*)-phytodienoic acid (OPDA). This JA precursor is transported from the chloroplast, where the first three steps occur, to a peroxisome in a process which recent evidence suggests involves the chloroplast outer membrane localised transporter JASSY (Guan et al., 2019; Wasternack and Hause, 2019). Once in the peroxisome, OPDA is converted to 3-oxo-2[2(Z)-pentenyl]-cyclopentane (OPC) by OPDA REDUCTASE3 (OPR3). OPC is then converted to JA by fatty acid β-oxidation enzymes. Interestingly, a recent study demonstrated that OPDA can also be converted to JA via an OPR3-independent pathway (Chini et al., 2018). It is proposed that in three peroxisome localised steps, OPDA is converted to 2,3-dinor-OPDA (dnOPDA), tetranor-OPDA (tnOPDA) and 4,5-didehydrojasmonate (4,5-ddh-JA). In the final step, which occurs in the cytosol, OPR2 reduces 4,5-ddh-JA to JA (Chini et al., 2018).

Although known as the ‘JA pathway’, JA is not the bioactive form of the hormone. Following transport into the cytosol, which may occur before JA is produced (see OPR3 independent pathway, Chini et al 2018), JA is conjugated to the amino acid isoleucine (Ile) by the jasmonoyl isoleucine conjugate synthase enzyme JASMONATE RESISTANT1 (JAR1) (Staswick and Tiryaki, 2004; Wasternack and Feussner, 2018). While other bioactive JA amino acid conjugates exist (Yan et al., 2016) and OPDA has been shown to induce wound responsive genes and regulate defences against nematodes independently of JA (Taki et al., 2005; Gleason et al., 2016), JA-Ile, or more specifically (+)-7-iso-JA-L-Ile, is regarded as the most bioactive JA compound (Fonseca et al., 2009; Sheard et al., 2010). Following conjugation, an ABC transporter called JASMONATE TRANSPORTER1 (JAT1), transports JA-Ile from the cytosol into the nucleus (Li et al., 2017b; Nguyen et al., 2017).

Once in the nucleus, JA-Ile can activate downstream responses by binding to, and promoting the interaction of, its co-receptors, CORANTINE INSENSITVE1 (COI1), which is part of the S PHASE KINASE-ASSOCIATED PROTEIN1/CULLIN1/F-box^{COI1} (SCF^{COI1}) E3 ubiquitin-ligase complex, and JAZMONATE ZIM DOMAIN (JAZ) (Thines et al., 2007; Katsir et al., 2008; Melotto et al., 2008a; Fonseca et al., 2009; Yan et al., 2009; Sheard et al., 2010). The importance of COI1 in the JA pathway was already suggested back in 1994 by the isolation and characterisation of the *coi1-1* mutant, which is insensitive to JA and its functional analogue coronatine (Feys et al., 1994). Subsequent cloning and characterisation of the *COI1* gene revealed that it encodes an F-box protein, which function in protein ubiquitination and degradation, suggesting a role for degradation of repressive signalling proteins (Xie et al., 1998). Further work by (Devoto et al., 2002; Xu et al., 2002) suggested that JA signalling requires COI1 to combine with additional proteins to form the SCF^{COI1} E3 ubiquitin-ligase complex. In 2007, the repressive targets of COI1 were identified as JAZ proteins, which are ubiquitinated by the SCF^{COI1} E3 ubiquitin-ligase complex and subsequently degraded by the 26S proteasome (Chini et al., 2007; Farmer, 2007; Thines et al., 2007; Yan et al., 2007; Wasternack, 2015).

In Arabidopsis, 13 JAZ proteins have been identified (Chini et al., 2016; Howe et al., 2018). JAZs bind to and act as repressors of JA-pathway master regulatory transcription factors (TFs) MYC2, MYC3, MYC4 and ETHYLENE-INSENSITVE3 (EIN3) (Chini et al., 2007; Cheng et al., 2011; Fernández-Calvo et al., 2011; Niu et al., 2011; Zhu et al., 2011; Pauwels et al., 2015; Zhang et al., 2015). Various mechanisms have been proposed to explain how JAZ proteins repress the activity of MYCs at low cellular JA-Ile concentrations (Howe et al., 2018). Firstly, they can inhibit MYC activity by blocking the binding to MYC of MEDIATOR COMPLEX SUBUNIT25 (MED25), a protein which forms part of the mediator complex, which is critical for the recruitment of RNA polymerase II (Pol II) to JA-responsive genes (Zhang et al., 2015; Zhang et al., 2017a). Secondly, TOPLESS (TPL) co-repressors, which transcriptionally repress JA-responsive genes via mechanisms which include interaction with histone deacetylases, either bind directly to JAZ repressors or are recruited to them by the adaptor protein NOVEL INTERACTOR OF JAZ (NINJA) (Pauwels et al., 2010; Pauwels and Goossens, 2011; Shyu et al., 2012). Thus, JAZs can both directly and indirectly repress the activity of MYCs. This repression is relieved following the

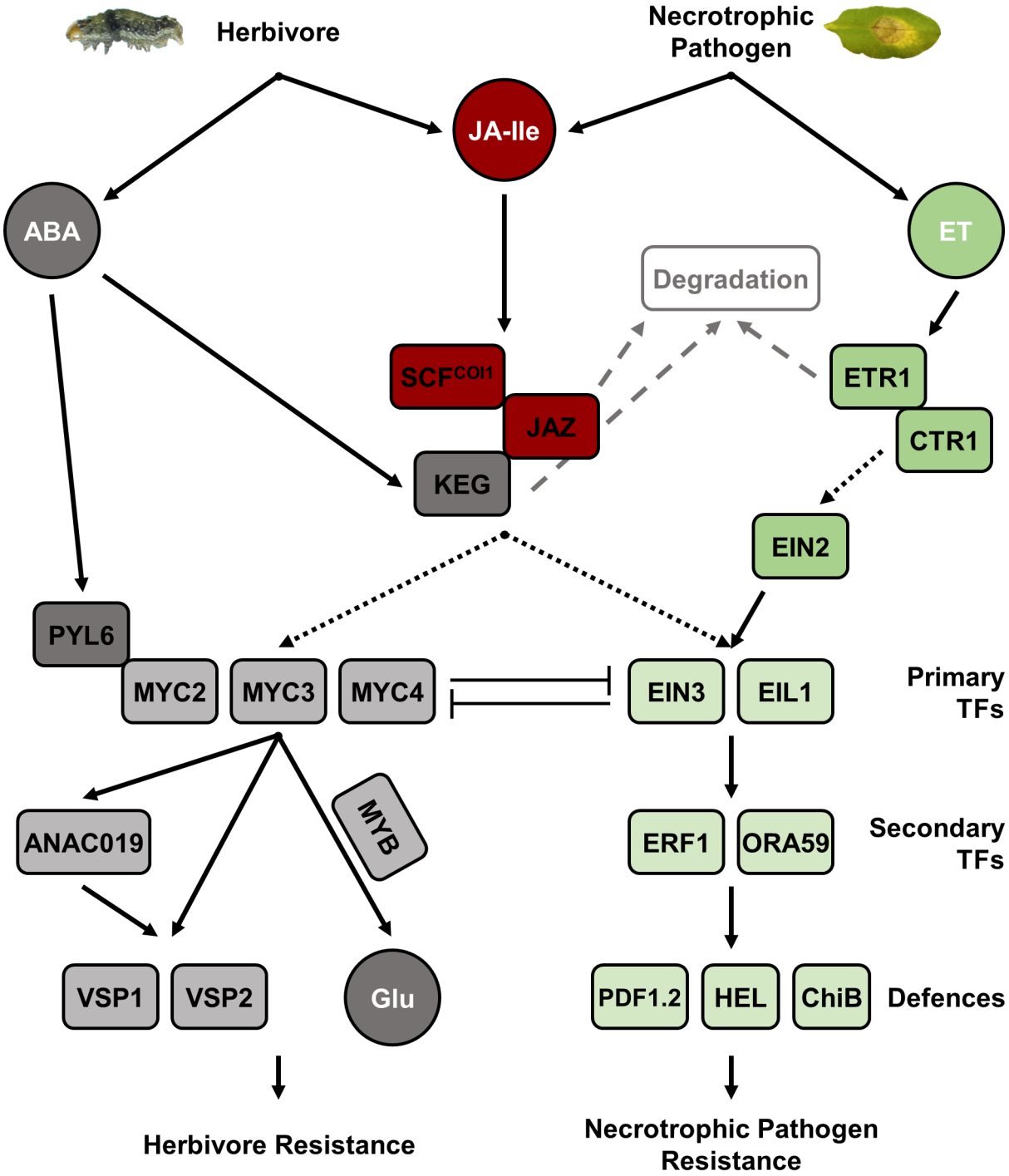

Figure 1.2. JA Dependent Defence Signalling Pathway.

In response to herbivory or infection by a necrotrophic pathogen, the bioactive jasmonate, jasmonic acid isoleucine (JA-Ile) accumulates along with abscisic acid (ABA) and ethylene (ET), respectively. JA-Ile and ABA positively regulate the 'MYC branch' (light grey) which is associated with resistance against herbivores. Whereas JA-Ile and ET positively regulate the 'EIN3/EIL1 branch' (light green) which is linked to resistance against necrotrophic pathogens. The secondary transcription factors (TFs) and defence proteins shown are examples and not a definitive list. Circles and squares are metabolites and proteins, respectively. Solid black lines with arrow heads and flat ended lines depict positive regulation and antagonism in response to stress induction, respectively. Dotted black lines depict a release from suppression in response to hormone stimulation. Dashed grey lines indicate hormone triggered degradation. To aid visualisation, the pathway has been simplified with not all interactions being shown. See the text for more details.

accumulation of higher levels of JA-Ile and the formation of the JA-Ile, COI1 and JAZ complex which also involves a inositol polyphosphate cofactor (Sheard et al., 2010; Mosblech et al., 2011; Laha et al., 2015). The SCF^{COI1} E3 ubiquitin-ligase complex ubiquitinates the JAZ proteins and thus targets them for degradation, allowing the master regulatory TFs to activate downstream JA-dependent defence responses (Lorenzo et al., 2004; Chini et al., 2007; Thines et al., 2007; Fernández-Calvo et al., 2011; Pauwels et al., 2015; Howe et al., 2018).

Although the defences providing resistance to chewing herbivores and those providing resistance to necrotrophic pathogens are both induced by JA, they are not regulated by the same downstream signalling machinery (Pieterse et al., 2012; Erb and Reymond, 2019). In fact, there is evidence that the signalling pathways controlling these defences are antagonistic to one another. Accordingly, the JA pathway is often represented as having two branches (Figure 1.2) (Anderson et al., 2004; Boter et al., 2004; Lorenzo et al., 2004; Verhage et al., 2011; Song et al., 2014; Goossens et al., 2016). The first 'MYC branch' controls resistance against chewing herbivores, is headed by the master regulatory basic helix-loop-helix (bHLH) leucine zipper MYC TFs and involves intermediate TFs such as ANAC019 and ANAC055, which are members of the NAC (petunia NAM and Arabidopsis ATAF1, ATAF2, and CUC2) TF family (Anderson et al., 2004; Boter et al., 2004; Lorenzo et al., 2004; Dombrecht et al., 2007; Bu et al., 2008; Fernández-Calvo et al., 2011; Niu et al., 2011; Schweizer et al., 2013b). The second 'EIN3/EIL1 branch' is under control by the TFs EIN3, EIN3-LIKE1 (EIL1), ETHYLENE RESPONSE FACTOR1 (ERF1) and OCTADECANOID-RESPONSIVE ARABIDOPSIS AP2/ERF59 (ORA59), which regulate defence genes that are effective against necrotrophic pathogens (Lorenzo et al., 2003; Pré et al., 2008; Zhu et al., 2011; Song et al., 2014). Both branches are activated by JA-Ile and under negative control by JAZ proteins (Chini et al., 2007; Pauwels and Goossens,

---

Figure 1.2. (continued)

Abbreviations: SCF, Skp1/Cullin/F-box; COI1, CORONATINE INSENSITIVE1; JAZ, JASMONATE ZIM DOMAIN; KEG, KEEP ON GOING; ETR1, ETHYLENE RESPONSE1; CTR1, CONSTITUTIVE TRIPLE RESPONSE1; EIN2, ETHYLENE INSENSITIVE2; EIN3, ETHYLENE INSENSITIVE3; EIL1, EIN3-LIKE1; PYL6, PYR1-LIKE6; MYC2/3/4, basic helix-loop-helix (bHLH) TFs; MYB, R2R3-MYB TFs; ANAC019, NAM/ATAF1, 2/CUC2 (NAC) TF; ERF1, ETHYLENE RESPONSE FACTOR1; ORA59, OCTADECANOID-RESPONSIVE ARABIDOPSIS AP2/ERF59; VSP, VEGETATIVE STORAGE PROTEIN; Glu, Glucosinolates; PDF1.2, PLANT DEFENSIN1.2; HEL, HEVEIN-LIKE; ChiB, BASIC CHITINASE. This figure is loosely based on Figure 3 of Pieterse et al (2012).

2011; Zhu et al., 2011; Zhang et al., 2015). This common control by a single hormone raises the question of how plants can differentially control both branches after challenge? The answer to this question is co-regulation by the plant defence hormones, abscisic acid (ABA) and ethylene (ET), which show differential accumulation in response to attack by chewing herbivores and necrotrophic pathogens (Vos et al., 2005; Vos et al., 2013; Vos et al., 2019).

The MYC branch of the JA response pathway controls resistance against chewing herbivores (Figure 1.2). This is clearly demonstrated by the vastly increased susceptibility of the Arabidopsis *myc2 myc3 myc4* triple mutant to herbivores, such as *Spodoptera littoralis* (Fernández-Calvo et al., 2011; Schweizer et al., 2013a; Schweizer et al., 2013b; Song et al., 2014). Furthermore, JA-inducible gene that are reliant on MYC TFs in Arabidopsis include *VEGETATIVE STORAGE PROTEIN1* (*VSP1*) and *2* (*VSP2*), which encode anti-insect proteins (Lorenzo et al., 2004; Liu et al., 2005; Fernández-Calvo et al., 2011; Niu et al., 2011), and genes involved in the biosynthesis of glucosinolates (Schweizer et al., 2013b; Frerigmann et al., 2014). While, as discussed above (Section 1.1), glucosinolates are a constitutive chemical defence in plants of the Brassicales order, their levels also increase in response to a JA eliciting treatments (Mewis et al., 2005; Schweizer et al., 2013b; Frerigmann and Gigolashvili, 2014). In Arabidopsis, both constitutive and JA induced biosynthesis of glucosinolates is controlled at a transcriptional level by complexes involving MYC and also MYB TFs (Schweizer et al., 2013b; Frerigmann et al., 2014).

ABA accumulates in response to herbivory (Vos et al., 2013). This hormone is required for full induction of *VSP* genes and glucosinolates and positively regulates resistance against chewing herbivores (Anderson et al., 2004; Bodenhausen and Reymond, 2007; Vos et al., 2013; Frerigmann and Gigolashvili, 2014; Vos et al., 2019). Thus, it has been suggested that ABA acts together with JA to stimulate anti-herbivore defences (Figure 1.2) (Pieterse et al., 2012). There are multiple additional lines of evidence supporting this conclusion. Firstly the regulatory TF MYC2 is both JA and ABA inducible (Lorenzo et al., 2004). Secondly, JAZ12, an interactor and negative regulator of MYC2, is degraded in response to both JA and ABA (Pauwels et al., 2015). The degradation of JAZ12 has been attributed to ABA-induced auto-ubiquitination and degradation of the RING-type E3 ligase, KEEP ON GOING (KEG), which in un-stressed cells stabilises JAZ12 (Liu and Stone, 2010; Pauwels et al., 2015). Thus,

ABA-induced degradation of KEG results in JAZ12 destabilisation, which in turn facilitates MYC2-dependent signalling. Indeed, reducing KEG expression results in reduced JAZ12 levels and increased *VSP2* gene expression (Pauwels et al., 2015). A final piece of evidence supporting the JA-ABA synergism comes from a slightly more recent study, which demonstrated that MYC2 directly interacts with the ABA receptor PYRABACTIN RESISTANCE1-LIKE6 (PYL6) (Aleman et al., 2016). This interaction, which is promoted by ABA, can influence the transcriptional regulation activity of MYC2.

In addition to positively regulating defences against chewing herbivores, ABA also negatively regulates the EIN3/EIL1-dependent resistance against necrotrophic pathogens (Audenaert et al., 2002; Anderson et al., 2004; Sánchez-vallet et al., 2012; Mine, 2019). This negative signalling cross-talk has been attributed to activity by the MYC branch of the JA pathway, which acts antagonistically on the EIN3/EIL1 branch of the JA pathway (Anderson et al., 2004; Boter et al., 2004; Lorenzo et al., 2004; Dombrecht et al., 2007; Fernández-Calvo et al., 2011; Niu et al., 2011; Verhage et al., 2011; Vos et al., 2013; Zhai et al., 2013; Song et al., 2014; Vos et al., 2015; Vos et al., 2019). Interestingly, this antagonism is not unidirectional since there is clear evidence that the EIN3/EIL1 branch repressed defences against chewing herbivores (Figure 1.2). For example, ET signalling mutants, such as *ein2* and *ein3*, show increased expression of *MYC2* and *VSP2* and are more resistant to chewing herbivores (Rojo et al., 1999; Stotz et al., 2000; Lorenzo et al., 2003; Anderson et al., 2004; Bodenhausen and Reymond, 2007; Song et al., 2014; Vos et al., 2019). A study published in 2014 provided conclusive evidence that the antagonism between the two branches of the JA pathway is at least in part mediated by interactions between the master regulatory TFs MYC2 and EIN3/EIL1 (Song et al., 2014).

The EIN3/EIL1 branch, which controls resistance against necrotrophic pathogens, is positively regulated by JA and ET (Figure 1.2) (Penninckx et al., 1996; Penninckx et al., 1998; Thomma et al., 1999; Berrocal-Lobo et al., 2002; Lorenzo et al., 2003; Anderson et al., 2004; Pré et al., 2008; Pieterse et al., 2012; Goossens et al., 2016). Both JA and ET accumulate in response to infection by necrotrophic pathogens (Vos et al., 2005; La Camera et al., 2011; Pieterse et al., 2012; Vos et al., 2019). As mentioned above, JA activates EIN3 and EIL1 by targeting JAZ repressors for degradation (Zhu et al., 2011). Furthermore, ET stabilises and facilitates the activity

of EIN3 and EIL1. Under low ET conditions, ET receptors such as ETHYLENE RESPONSE1 (ETR1) interact with and activate CONSTITUTIVE TRIPLE RESPONSE1 (CTR1), which in turn represses the endoplasmic reticulum (ER) membrane localised ETHYLENE-INSENSITIVE2 (EIN2) via phosphorylation (Alonso et al., 1999; Ju et al., 2012; Dubois et al., 2018). However, when ET levels are increased, the receptors are degraded at a faster rate than they are synthesised and thus CTR1 is inactivated, EIN2 is dephosphorylated and the carboxyl terminal end (CEND) of EIN2 is cleaved (Qiao et al., 2012; Wen et al., 2012; Shakeel et al., 2015). The CEND of EIN2 can be transported into the nucleus where, together with EIN2 NUCLEAR-ASSOCIATED PROTEIN1 (ENAP1), it's thought to influence histone acetylation and in turn the DNA binding and transcriptional regulation by EIN3 and EIL1 (Qiao et al., 2012; Wen et al., 2012; Zhang et al., 2016; Zhang et al., 2017b; Zhang et al., 2018a; Wang and Qiao, 2019). In addition, after release from the ER, the CEND of EIN2 can remain in the cytoplasm and repress the translation of *EIN3-BINDING F-BOX 1* (*EBF1*) and *EBF2* transcripts (Li et al., 2015b; Merchante et al., 2015). As EBF1 and EBF2 are F-box proteins which target EIN3 and EIL3 for degradation, this translational repression stabilises the master regulatory TFs (Guo and Ecker, 2003; Potuschak et al., 2003; Gagne et al., 2004; An et al., 2010). JA and ET activated and stabilised EIN3 and EIL1 upregulate secondary ET-responsive TFs such as the APETALA2/ETHYLENE RESPONSE FACTOR (AP2/ERF) domain containing ERF1 and ORA59 (Solano et al., 1998; Lorenzo et al., 2003; Zhu et al., 2011; Zander et al., 2012; Chang et al., 2013; Song et al., 2014). ERF1 and ORA59 directly induce the promoters of defence genes, such as *PLANT DEFENSIN1.2* (*PDF1.2*), which encode antimicrobial proteins that increase resistance against necrotrophic pathogens (Berrocal-Lobo et al., 2002; Lorenzo et al., 2003; McGrath et al., 2005; Pré et al., 2008).

This thesis Chapter only covers the basic principles of JA biosynthesis, perception and signalling in relation to plant immunity. The wider complexity of the JA response is demonstrated by recent large-scale omics studies (Hickman et al., 2017; Zander et al., 2020). Furthermore, most mechanistic knowledge about the JA response is angiosperm/Arabidopsis-centric. Nevertheless, there are similarities across all land plants. For example, recent evidence has suggested that COI1-dependent jasmonate signalling exists in the ancient nonvascular liverwort *Marchantia*

polymorpha (Monte et al., 2018). JAZ and MYC proteins are involved, with majority of their key features and functions being conserved between *M. polymorpha* and Arabidopsis (Monte et al., 2019; Peñuelas et al., 2019). For instance, MYC proteins in both species positively regulate herbivore resistance as evidenced by the enhanced susceptibility to *S. littoralis* herbivory exhibited by both At*myc* and Mp*myc* mutants (Fernández-Calvo et al., 2011; Peñuelas et al., 2019). However, despite this functional conservation, there is a key difference between jasmonate signalling in *M. polymorpha* and Arabidopsis. The MpCOI1 ligand which promotes the MpCOI1-MpJAZ interaction is dnOPDA, or more specifically two isomers of dnOPDA (dinor-*cis*-OPDA and dinor-*iso*-OPDA), not JA-Ile (Monte et al., 2018). Nevertheless, as liverworts are thought to be the earliest diverging lineage of extant land plants (Bowman et al., 2017), these results in *M. polymorpha* suggest that functional jasmonate signalling, albeit with some variation, is present across all land plants. This explains why exogenous application of jasmonates induces defences that are effective against chewing herbivores and necrotrophic pathogens in gymnosperms, such as Norway spruce (*Picea abies*) (Franceschi et al., 2002; Martin et al., 2002; Zeneli et al., 2006; Krokene et al., 2008; Zulak et al., 2009; Schiebe et al., 2012; Krokene, 2015; Mageroy et al., 2020a).

1.4. Salicylic Acid (SA) Biosynthesis, Signalling and Regulated Defences

SA is a phenolic secondary metabolite derived from the Shikimate pathway (Widhalm and Dudareva, 2015). While reported to be involved in the regulation of a variety of developmental processes, it is best known for its role in plant immunity (Vlot et al., 2009; Boatwright and Pajerowska-Mukhtar, 2013; Ding and Ding, 2020). Specifically, SA is involved in regulating defences that are effective against biotrophic pathogens and plays a role in induced resistance responses, such as Systemic acquired resistance (SAR) and β-aminobutyric acid-induced resistance (BABA-IR) (Zimmerli et al., 2000; Glazebrook, 2005; Spoel and Dong, 2012; Fu and Dong, 2013; Klessig et al., 2018).

Production of SA, as with all other benzoic acids, begins with the shikimate pathway, a seven step enzymatic pathway in the plastid which produces chorismate as an end product (Widhalm and Dudareva, 2015). There are two pathways in plants that can convert chorismate to SA (Huang et al., 2020b). The first so-called cinnamic acid pathway, includes phenylalanine as an intermediate and requires the enzyme

PHENYLALANINE AMMONIA LYASE (PAL) (Ding and Ding, 2020). Notably, the PAL-dependent conversion of phenylalanine to *trans*-cinnamic acid also represents the first step in the general phenylpropanoid pathway (Deng and Lu, 2017). The second SA biosynthesis pathway is the so-called isochorismate pathway, which begins with the conversion of chorismite to isochorismate in a reaction catalysed by ISOCHORISMATE SYNTHAE (ICS) (Huang et al., 2020b). Recent studies have clarified the later steps of the isochorismate pathway in Arabidopsis. Firstly, ENHANCED DISEASE SUSCEPTIBILITY5 (EDS5) transports isochorismate out of the plastid and into the cytosol (Rekhter et al., 2019). Secondly isochorismate is converted to isochorismate-9-glutamate (IC-9-Glu) in a reaction catalysed by avrPphB SUSCEPTIBLE3 (PBS3) (Rekhter et al., 2019; Torrens-Spence et al., 2019). Finally, IC-9-Glu is converted to SA in a reaction that can occur spontaneously, but can also be accelerated by the BAHD acyltransferase ENHANCED PSEUDOMONAS SUSCEPTIBILITY1 (EPS1) (Rekhter et al., 2019; Torrens-Spence et al., 2019). The relative importance of the two biosynthesis pathways for pathogen induced SA accumulation seems to vary between plant species (Huang et al., 2020b). In Arabidopsis, it has been suggested that the isochorismate pathway is more important as *SA induction-deficient2* (*sid2*) mutants, which are deficient in ICS1, accumulate only 5-10 % of SA of the wild-type following inoculation with (hemi)biotrophic pathogens (Nawrath and Métraux, 1999; Wildermuth et al., 2001; Klessig et al., 2018). In other plant species, such as soybean (*Glycine max*), both pathways appear to be equally important for pathogen-induced accumulation of SA (Shine et al., 2016), while in Norway spruce the PAL pathway is probably the only functional pathway for SA biosynthesis, since no *ICS* homologs have been identified in the genome of this tree species (Arnerup et al., 2013).

Considerable progress has been made in determining the transcriptional regulators of SA biosynthesis machinery in Arabidopsis (Zhang and Li, 2019; Ding and Ding, 2020). For instance, the Ca^{2+}/calmodulin binding TF CALMODULIN BINDING PROTEIN60g (CBP60g), and also SAR-DEFICIENT1 (SARD1), are very important for pathogen induced SA production via the isochorismate pathway (Zhang et al., 2010; Wang et al., 2011; Sun et al., 2015; Huang et al., 2020b). Interestingly, SA biosynthesis is also negatively regulated by TFs which promote defence against chewing herbivores and necrotrophic pathogens. For example, evidence suggests that

EIN3, and potentially EIL1, negatively regulate SA biosynthesis and in turn resistance to virulent and avirulent strains of the bacterial pathogen *Pseudomonas syringae*, by directly binding to the promoter of *ICS1* and suppressing its expression (Chen et al., 2009). Furthermore, the JA/ABA inducible NAC TFs ANAC019, ANAC055, and ANAC072, have been shown to inhibit SA accumulation via an influence on the expression of genes involved in SA biosynthesis and metabolism (Bu et al., 2008; Zheng et al., 2012).

The nature of the SA receptor and the proteins involved in triggering downstream defences has been a hotly debated topic over the past couple of decades. Tens of SA-binding proteins (SABPs) have been identified in Arabidopsis and other angiosperms (Klessig et al., 2018). However a recent study (Ding et al., 2018), which built upon considerable previous work, has resulted in the proposal of a model which suggests three SABPs, NONEXPRESSER OF PR GENES1 (NPR1), NPR3 and NPR4, are particularly important (Innes, 2018; Zhang and Li, 2019; Ding and Ding, 2020).

Multiple *npr1* mutants identified in the 1990s demonstrated the importance of NPR1 to the induction PR gene expression and resistance to biotrophic pathogens (Cao et al., 1994; Delaney et al., 1995; Shah et al., 1997). Subsequent studies provided evidence that NPR1 acts as a transcriptional co-activator as it interacts with TGACG motif-binding (TGA) TFs, which bind to the promoters of *PR* genes (Zhang et al., 1999; Després et al., 2000; Zhou et al., 2000; Fan and Dong, 2002; Rochon et al., 2006). NPR3 and NPR4 also interact with TGA TFs; however, unlike NPR1, they appear to be negative regulators of SA-dependent resistance as the *npr3 npr4* double mutant has enhanced *PR* gene expression and is more resistant than the wild-type to (hemi)biotrophic pathogens (Zhang et al., 2006). The recent study by Ding and colleagues further explored this negative regulation using a variety of genetic and molecular techniques (Ding et al., 2018). They provided evidence that under low SA conditions NPR4, and probably NPR3, act redundantly to repress SA inducible genes (e.g. *SARD1*). This repressive activity requires interaction with TGA TFs, which in turn bind to the promoters of SA inducible genes. Following binding of SA to NPR4, the transcriptional repressive activity by NPR4 is removed, even though it remains bound to TGA TFs at SA inducible genes. In parallel, SA binding to NPR1 allows it to act as a transcriptional co-activator with TGA TFs, promoting the expression of SA inducible

genes. The contrasting effects of SA on the antagonistic activities of NPR1 and NPR3/NPR4 controls SA-dependent gene expression and resistance against biotrophic pathogens.

A previous study in 2012 had concluded that NPR3/NPR4 regulate NPR1 protein levels, in an SA dependent manner, by bringing NPR1 into association with the CULLIN3 (CUL3) E3 ligase which ubiquinates and thus target NPR1 for degradation by the 26S proteasome (Fu et al., 2012). While the evidence presented by Ding et al (2018) does not support this conclusion, post-translational regulation of NPR1 is important. In non-induced cells, where SA levels are low, NPR1 mainly exists as an oligomer joined by disulphide bonds (Mou et al., 2003; Ding and Ding, 2020). Whereas upon SA induced creation of reducing conditions, and potentially SA binding, NPR1 is monomerised by the reduction of the disulphide bonds and it is translocated into the nucleus via nuclear pore proteins which includes ARABIDOPSIS THALIANA MODIFER OF SNC1/7 (Mou et al., 2003; Tada et al., 2008; Cheng et al., 2009; Spoel and Dong, 2012; Wu et al., 2012). Under reducing cellular conditions that are not caused by pathogen attack and SA, monomerised NPR1 proteins which find their way to the nucleus are quickly ubiquitinated and targeted for proteasomal degradation, preventing unnecessary defence activation (Spoel et al., 2009). Interestingly, following pathogen-induced SA production, appropriate transcriptional regulation by NPR1 also requires the addition of ubiquitin chains and subsequent modulation of ubiquitin chain length by E3 and E4 ligases and deubiquitinases (Spoel et al., 2009; Skelly et al., 2019). This highlights the complexity surrounding the link between perception of SA and the subsequent downstream changes in gene expression.

As alluded to above, NPR1 together with TGA TFs induce a number of transcriptional regulators, including SARD1 and the WKRY TFs (Ding et al., 2018). These secondary regulators can induce downstream defences, but so too can the NPR1 interacting TGAs, which directly regulate anti-microbial *PR* genes (Zhang et al., 2003; Sun et al., 2015; Zhang and Li, 2019). A classic example of an SA inducible defence gene is *PR1,* which encodes for a sterol-binding antimicrobial protein (Gamir et al., 2017). SA-induced defences provide resistance against invading biotrophic pathogen(s).

It is well documented that SA can antagonise the JA signalling pathways which regulate resistance to chewing herbivores and necrotrophic pathogens (Pieterse et al., 2012; Caarls et al., 2015). Numerous studies have shed light on the mechanisms behind this antagonistic crosstalk. For instance, the SA pathway can negatively regulate the expression of ORA59 at both the transcriptional and protein level (Van der Does et al., 2013; Zander et al., 2014). This in turn represses jasmonate-inducible genes which contain GCC-box motifs in their promoters that act as the binding site for AP2/ERF TFs (Van der Does et al., 2013). More recently, a genome-wide association (GWA) study was conducted using 100s of natural accessions of Arabidopsis and a measure of antagonism being the impact of SA treatment on jasmonate induced *PDF1.2* expression (Proietti et al., 2018). This approach, coupled with follow up analysis with T-DNA insertion mutants, identified the glyoxalase GLYOXYLASE I4 (GLYI4) and the cytokinin signalling related ARABIDOPSIS RESPONSE REGULATOR11 (ARR11) as regulators of SA-induced repression of jasmonate-dependent defence gene expression and resistance against necrotrophic pathogens (Proietti et al., 2018). Moreover, a study published this year found that NPR1 can bind to EIN3 and interfere with its regulation of apical hook formation (Huang et al., 2020a). This provides tentative evidence that SA can antagonise JA/ET signalling in a NPR1-EIN3 dependent manner. NPR1 has previously been shown to be essential for the SA suppression of jasmonate induced *PDF1.2* and *VSP* gene expression (Spoel et al., 2003; Koornneef et al., 2008). However, interestingly under high cellular ethylene levels this SA suppression of JA induced gene expression becomes NPR1-independent (Leon-reyes et al., 2009). Thus, future studies are required to explore exactly how an NPR1-EIN3 interaction could be involved in crosstalk between SA and JA/ET signalling pathways. Furthermore, all the studies presented in this paragraph were conducted with Arabidopsis. There has been some debate surrounding whether SA-JA antagonistic crosstalk is present in other species, such as Norway spruce (Arnerup et al., 2013; Mageroy et al., 2020b). Nevertheless, SA has been demonstrated to repress the upregulation of JA-inducible genes in lima bean (*Phaseolus lunatus*) following feeding by a JA inducing herbivore (Zhang et al., 2009).

1.5. Aggressive Attackers Suppress JA and SA Defence Pathways

It is often stated that crosstalk between the SA and JA signalling pathways allows plants to be more efficient in their allocation of defensive resources and to

prioritise defences effective against the attacking organism. However, certain attackers have evolved to exploit this crosstalk. For example, specific strains of the hemibiotrophic pathogen *P. syringae* (e.g. pathovar (pv.) *tomato* DC3000) which secrete coronatine (COR) (Xin and He, 2013). COR is polyketide which mimics JA-Ile and thus binds to the COI1-JAZ co-receptor complex to initiate the above-detailed JA signalling pathway (Katsir et al., 2008; Sheard et al., 2010). In Arabidopsis, COR releases MYC2, MYC3 and MYC4 from JAZ suppression and in turn transcriptionally activates the downstream NAC TFs ANAC019, ANAC055 and ANAC072 (Figure 1.2) (Bu et al., 2008; Fernández-Calvo et al., 2011; Zheng et al., 2012; Gimenez-Ibanez et al., 2017). These NAC TFs repress the SA biosynthesis gene *ICS1* and positively regulate *SA METHYL TRANSFERASE1* (*BSMT1*), which converts SA to volatile methyl salicylate (Zheng et al., 2012). Consequently, SA accumulation in response to *P. syringae* infection is inhibited. As SA promotes stomatal closure, this inhibition of SA accumulation could explain the COR induced stomatal opening which allows enhanced entry of bacteria into the leaf (Melotto et al., 2006; Melotto et al., 2008b; Zheng et al., 2012; Gimenez-Ibanez et al., 2017; Melotto et al., 2017). Furthermore, COR-induced inhibition of SA accumulation has also been reported to promote virulence of *P. syringae* in the apoplast (Zheng et al., 2012). COR-induced susceptibility can also be promoted by MYC2-dependent upregulation of *HIGHLY ABA-INDUCED PP2C GENE1* (*HAI1*), which encodes for a clade A protein phosphatase 2C (PP2C) (Mine et al., 2017). HAI1 phosphorylates and in turn inactivates MITOGEN-ACTIVATED PROTEIN KINASE3 (MPK3) and MPK6, which are a key signalling link between PRRs and downstream immune responses (Bigeard et al., 2015; Mine et al., 2017). While the HAI1 clade of PP2Cs appears to be restricted to the Brassicaceae, the COR-induced suppression of immunity in an NAC TF dependent manner also occurs in tomato (*Solanum lycopersicum*) (Du et al., 2014b; Mine et al., 2017).

A second example of an invader which suppresses host SA or JA regulated immune responses, is provided by the necrotrophic fungal pathogen *Botrytis cinerea*. El Oirdi et al (2011) demonstrated how virulent isolates of *B. cinerea* release the exopolysaccharide β-(1,3)(1,6)-D-glucan which triggers an accumulation of SA which via NPR1 antagonises JA-dependent defences, including PROTEINASE INHIBITOR I, that provide resistance against the necrotrophic fungus. Furthermore, the rice blast

fungus *Magnaporthe oryzae* also appears to reduce the JA-dependent defence response. The fungus transfers an antibiotic biosynthesis monooxygenase (Abm) to its host, which converts JA to hydroxylated JA (12OH-JA) (Patkar et al., 2015).

In addition to suppressing host defences against themselves, pathogens can also suppress hormone-dependent defences to promote success of their insect vector. For instance, the *Tomato yellow leaf curl China virus* can suppress terpene production which resists whitefly (*Bemisia tabaci*), the vector of this type of virus (Li et al., 2014b). The virus accomplishes this suppression by interfering with the activity of terpene biosynthesis regulating MYC2. Herbivores themselves can also counteract plants defences to reduce resistance. There are multiple examples of defences being detoxified or suppressed by herbivores (Erb and Reymond, 2019). For instance, the corn earworm (*Helicoverpa zea*) secretes glucose oxidase in its saliva and this reduces the accumulation of the anti-herbivore and JA-inducible compound nicotine in tobacco (*Nicotiana tabacum*) plants (Musser et al., 2002).

The above examples show that aggressive attackers have the ability to suppress innate immune responses regulated by the hormones JA and SA. As a second layer of defence, plants have evolved a form of acquired immunity that allows them to counter these aggressive attackers.

1.6. Induced Resistance (IR)

An augmented level of basal resistance to pest and/or pathogens following exposure to specific stimuli is known as induced or acquired resistance (IR/AR). IR is an example of phenotypic plasticity as it allows plants with the same genotype to have different resistance phenotypes. The classic example is systemic acquired resistance (SAR). SAR, first characterised in tobacco in the middle of the 20th century, is a systemic increase in resistance resulting from primary exposure to localised pathogen attack (Ross, 1961; Spoel and Dong, 2012; Fu and Dong, 2013; Pieterse et al., 2014). It soon became apparent that SAR is a long-lasting resistance response, which could still be detected at 42 days after induction (Bozarth and Ross, 1964). Over subsequent decades, a range of biotic and abiotic stimuli (Erbilgin et al., 2006; Kunz et al., 2008; Van Der Ent et al., 2009; Luna et al., 2014a) have been reported to elicit IR in taxonomically distant plant species and against a wide spectrum of pests and pathogens (Kuc, 1982; Ryals et al., 1994; Krokene et al., 1999; Ton et al., 2007; Eyles

Induced Resistance: A Costly Business?

Induced resistance (IR) is often associated with costs. For instance, allocation costs can arise from the redirection of resources from growth or reproduction to defense (Neilson et al., 2013). Allocation costs can result in severe reductions in growth and seed production, particularly when IR is based on a prolonged upregulation of inducible defenses (Van Hulten et al., 2006). Defense priming also comes with allocation costs, which can make it unfavorable under stress-free conditions (Van Hulten et al., 2006; Walters et al., 2009; Douma et al., 2017). Opportunity costs occur when the allocation of resources to defense occurs at a sensitive life stage, resulting in reduced ability to thrive at later developmental stages (De Vries et al., 2018). The loss of interactions with beneficial symbionts (Heil, 2001; De Román et al., 2011) and increased susceptibility to other attackers due to signaling cross-talk (Kliebenstein and Rowe, 2008; Luna et al., 2012; Pieterse et al., 2012) are examples of ecological costs. In some cases, priming can incur loss-of-specificity costs, whereby the primed defense state mediates an augmented defense response to an inappropriate stimulus (e.g. water) (Beckers et al., 2009; Jaskiewicz et al., 2011; Baum et al., 2019). However, despite these examples of costs, the benefits of protection often outweigh the costs, making IR a valuable strategy helping plants to survive in hostile environments (Douma et al., 2017).

et al., 2010; Wilkinson et al., 2018; Mageroy et al., 2020a). For instance, colonisation of roots by beneficial rhizobacteria or mycorrhizal fungi can result in induced systemic resistance (ISR) and mycorrhiza-induced resistance (MIR), respectively (Cameron et al., 2013; Pieterse et al., 2014). Furthermore, a multitude of natural and synthetic chemicals, such as MeJA, β-Aminobutyric acid (BABA) and (R)-β-homoserine (RBH), have been reported to elicit IR (Walters et al., 2013; Cohen et al., 2016; Buswell et al., 2018; Wilkinson et al., 2018; Mageroy et al., 2020a).

IR is generally based on two non-exclusive mechanisms: prolonged upregulation of inducible defences or defence priming (Figure 1.3). Following exposure to a resistance-inducing stimulus, inducible defences can remain upregulated, providing IR against subsequent attack (Figure 1.3A). Alternatively, the resistance-inducing stimulus may ‘prime’ the plant immune system, providing resistance through faster and/or stronger upregulation of inducible defences after subsequent pathogen/herbivore attack (Figure 1.3B). The optimal strategy depends on the cost-benefit balance of the resistance in a given environment (Burow and Halkier, 2017) (see the sidebar titled Induced Resistance: A Costly Business?). Here, we will outline both mechanisms in more detail, and explain how their cost/benefit balance depends on plant life history strategies.

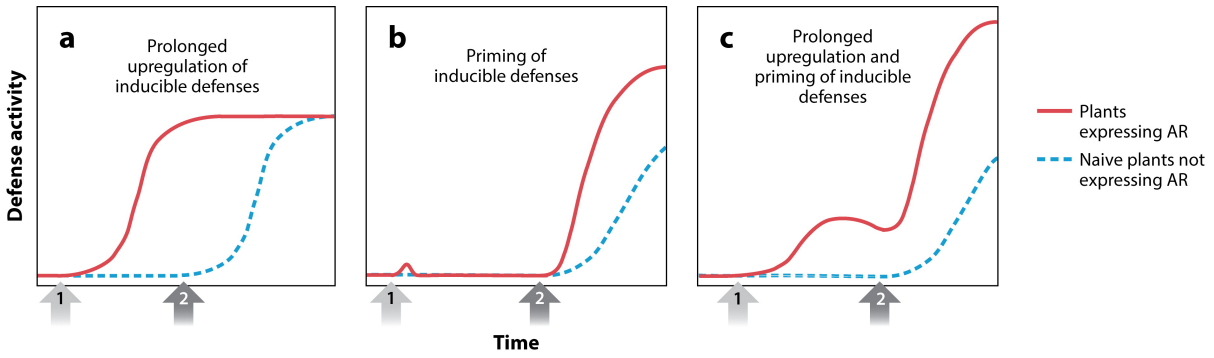

Wilkinson SW, et al. 2019.
Annu. Rev. Phytopathol. 57:505–29

Figure 1.3. Mechanisms of Induced Resistance.

Graphical models show levels of plant defence activity against time for the different mechanisms of induced resistance, otherwise known as acquired resistance (AR). **(A)** Prolonged upregulation of inducible defences. **(B)** Priming of inducible defences. **(C)** Combination of prolonged upregulation and priming of inducible defences. Light grey arrows (1) represent different AR-eliciting treatments (e.g., localized attack by a pathogen, β-aminobutyric acid). Dark grey arrows (2) represent defence elicitation by pest or pathogen. Red lines represent plants expressing AR. Blue dashed lines represent naive plants that do not express AR. Reproduced with permission from the Annual Review of Phytopathology, Volume 57 © 2019 by Annual Reviews, http://www.annualreviews.org

1.6.1. Prolonged Upregulation of Inducible Defences

Examples of stress-inducible defences that can remain upregulated for prolonged periods of time (Figure 1.3A) include benzoxazinoids and glucosinolates in Poaceae and Brassicaceae, respectively. Although these defence metabolites are produced constitutively, they can accumulate to higher levels at the site of herbivore feeding. For instance, leaf benzoxazinoid concentrations can remain elevated for seven days after feeding by moth larvae, resulting in increased resistance to secondary attack at the same location (Maag et al., 2016). Moreover, glucosinolates can remain locally upregulated in Brassicaceae roots for eight weeks after herbivore attack (Birch et al., 1992). The formation of anatomical defence features in response to pathogen infection can also be regarded as a prolonged upregulation of inducible defences. MeJA application results in increased trichome density in newly formed leaves of tomato for up to 21 days after treatment (Boughton et al., 2005). Furthermore, in spruce, treatment with MeJA, wounding and fungal infection induce the formation of traumatic resin ducts (TRDs) which enhance resistance by increasing the reservoir of defence-related oleoresin (Nagy et al., 2000; Martin et al., 2002; Franceschi et al., 2005; Celedon and Bohlmann, 2019). TRDs are maintained for several years, but are gradually buried inside the wood as the stem grows (Krokene

et al., 2003; DeRose et al., 2017). Finally, proteinaceous defences can be upregulated by IR-eliciting stimuli and potentially provide enhanced resistance to subsequent attack. For instance, in Arabidopsis, high concentrations of the SA homologue benzothiadiazole (BTH) can directly induce the defence gene *PR1* (Van Hulten et al., 2006). This gene can remain strongly upregulated for at least two days which correlates with an enhanced resistance to biotrophic pathogens inoculated at two days post BTH treatment (Van Hulten et al., 2006).

Although prolonged upregulation of inducible defences provides resistance, it can also be costly to maintain. For instance, production of constitutive glucosinolates is estimated to increase the photosynthetic requirements in Arabidopsis plants by 15% (Bekaert et al., 2012). Some of the cost of maintaining specialized metabolites may be offset if the metabolites are multifunction and synthesized by multifunctional enzymes (Neilson et al., 2013). Furthermore, in the case of terpenes stored in TRDs, although the initial investment cost is high, the maintenance cost is relative low (Gershenzon, 1994). It is also plausible that the fitness cost of a given investment may vary between short-lived annuals and long-lived perennials. For Arabidopsis, a two-week upregulation of chemical defences and trichome density could equate to 25% of the plant's life span and thus be relatively costly, whereas this type of investment would be less costly for large long-lived tree species with a lifespan of tens to hundreds of years. Nevertheless, keeping costly defences upregulated for much of a plant's lifespan will be maladaptive for any plant species. This is probably why plants have evolved an alternative IR strategy that is based on the more cost-efficient priming of inducible defences (Martinez-Medina et al., 2016; Douma et al., 2017).

1.6.2. Priming of Inducible Defences

Upon perception of specific environmental signals plants can sensitize or 'prime' their immune system. This enables a faster, stronger and/or more sustained upregulation of inducible defences upon subsequent attack (Figure 1.3B) (Conrath et al., 2006; Pastor et al., 2013; Conrath et al., 2015; Martinez-Medina et al., 2016; Mauch-Mani et al., 2017). A variety of cues can elicit priming including: natural and synthetic chemicals, localised pathogen attack, herbivore-induced plant volatiles, and beneficial microbes (Thulke and Conrath, 1998; Ton et al., 2005; Ton et al., 2007; Van Der Ent et al., 2009; Jung et al., 2009; Buswell et al., 2018). Different mechanisms of

Epigenetics: What's in a Name?

Waddington (Waddington, 1942) introduced the term epigenetics in 1942 to describe phenotype-altering interactions between genes and their products that cannot be explained by genetic inheritance. Since then, epigenetics has commonly been used to describe nongenetic changes that are transmittable through meiotic and/or mitotic divisions and that influence phenotypes at cellular and/or whole-organism levels. Advances in molecular biology have provided mechanisms to Waddington's definition but have also created ambiguity. First, small RNAs (sRNAs) that modify gene expression via (post)transcriptional mechanisms are commonly referred to as an epigenetic mechanism but can equally be considered a genetic mechanism because sRNAs are encoded by the organism's genotype. Second, histone modifications, sRNA production, and DNA methylation typically co-occur, making it difficult to separate cause and effect. Third, the heritability of nongenetic changes remains unclear. Although histone modifications can be stable over mitosis, they are not necessarily stable over meiosis. There is, however, ample evidence that changes in DNA methylation can be inherited faithfully over meiosis, making methylation the prime candidate for germline transmission of metastable epigenetic traits. Despite ongoing debate about the exact definition of epigenetics, there is a consensus that the combined effects of histone modifications, sRNAs, and DNA (de)methylation are responsible for most epigenetic phenomena, providing organisms with increased phenotypic plasticity.

priming have been proposed (Conrath et al., 2006; Bruce et al., 2007; Conrath, 2011; Conrath et al., 2015). For example, inactive Mitogen-Activated Protein Kinases (MPKs), which accumulate in plants after priming treatment with BTH, facilitate augmented induction of SA-dependent defences upon subsequent challenge (Beckers et al., 2009). Furthermore, an accumulation of PRRs 48 hours after treatment with BTH (Tateda et al., 2014) could provide an explanation of the enhanced responsiveness to the PAMP flagellin 22 (Flg22) two days after SA treatment (Xu et al., 2014). An accumulation of defence regulatory TFs which is not sufficient to induce defences directly but results in a faster and stronger induction of defence genes upon subsequent attack, is another hypothesised priming mechanism (Van Der Ent et al., 2009). Priming could also be based on increased accumulation of glucosylated phytohormones (Pastor et al., 2013). Increased concentrations of SA glucosides have been reported in primed tobacco and *Arabidopsis* following localised pathogen attack (Lee and Raskin, 1998; Song, 2006; Pastor et al., 2014). Moreover, the resistance-inducing effects of the chemical priming agent BABA are reduced in *Arabidopsis* plants impaired in SA glucoside biosynthesis (Pastor et al., 2014). However, no study has yet demonstrated long-term maintenance of accumulated glucosylated hormones in

response to a priming cue, followed by a subsequent depletion upon challenge as deglucosylated hormones are released leading to an augmented defence induction.

Over recent years, increasing evidence has suggested that defence gene priming involves regulation by epigenetic mechanisms (see the sidebar titled Epigenetics: What's in a Name?) (Conrath, 2011; Pastor et al., 2013; Conrath et al., 2015). Biochemical modifications to DNA and DNA-associated proteins that control the density of chromatin, have the potential to mediate long-term changes in defence gene responsiveness without major physiological costs (Bruce et al., 2007; Conrath, 2011). In the following sections, we discuss these epigenetic mechanisms and review the evidence for epigenetic inheritance of priming.

1.6.3. Role of Epigenetic Mechanisms in Immunological Memory

Genomic DNA in the nucleus is tightly wrapped around histone protein octamers called nucleosomes, which form the basic unit of eukaryotic chromatin. The density of chromatin regulates to what extent the DNA is available for the transcriptional machinery. For this reason, tightly packed (condensed) heterochromatin is often associated with silenced genes, whereas lightly packed euchromatin is more associated with transcriptionally active genes (Bender, 2004). Chromatin density is controlled by methylation and acetylation of histone tail residues and the presence of specific histone variants inside nucleosomes (Deal and Henikoff, 2011). Jaskiewicz and co-workers were the first to report that SAR-related priming of *WRKY* gene promoters in Arabidopsis is associated with increased methylation and acetylation at lysine residues 4 and 9 of histone H3 (H3K4me3 and H3K9ac, respectively) (Jaskiewicz et al., 2011). These marks typically indicate reduced chromatin density. Similar results were reported by López and associates in BTH-primed wild-type plants and constitutively primed mutants of Arabidopsis (López et al., 2011). Recently, Schillheim and co-workers used Formaldehyde-Assisted Isolation of Regulatory Elements (FAIRE)-qPCR (Simon et al., 2012; Baum et al., 2020) to more directly demonstrate that chemical priming of the *WRKY6* gene promoter is associated with chromatin decondensation (Schillheim et al., 2018). Subsequently the same authors conducted FAIRE-seq and identified that this pattern is widespread (Baum et al., 2019; Baum et al., 2020). Genes primed by localised pathogen infection (i.e. SAR inducing stimuli) were generally associated with unpacked or open chromatin in their

RNA-directed DNA Methylation (RdDM)

The installation of new DNA methylation, *de novo* DNA methylation, and the maintenance of CHH context methylation at some but not all loci, is achieved by RdDM pathways. Genomic features targeted by RdDM pathways include transposable elements (TEs), particularly small TEs near genes, TEs which have recently evolved and the ends of long heterochromatin localised TEs. The canonical RdDM pathway involves the production of 24 nucleotide (nt) small RNAs (sRNAs) from transcripts of the plant specific RNA polymerase IV (Pol IV). Pol IV transcripts are made double stranded by RNA-DEPENDENT RNA POLYMERASE2 (RDR2) and then cleaved into 24 nt sRNAs by DICER-LIKE3 (DCL3). These sRNAs are loaded into ARGONAUTE4 (AGO4) or AGO6 and bind to the complementary long non-coding scaffold RNAs produced from the target loci by Pol V. This collection of RNAs and AGO recruits DOMAINS REARRANGED METHYLASE2 (DRM2) which implements methylation of cytosines. Various additional proteins have been identified which are involved in the canonical RdDM pathway such as the AGO4 and DRM2 interacting RNA-DIRECTED DNA METHYLATION1 (RDM1).

Multiple non-canonical RdDM pathways exist which involve sRNAs derived from alternative sources than the Pol IV, RDR2 and DCL3 route. For instance, 21 and 22 nt sRNAs produced from Pol II TE transcripts via the action of post-transcriptional gene silencing machinery including RDR6 and DCL2 and DCL4. Furthermore, DCL3-dependent but RDR2- and 6-independent mechanisms can generate 24 nt sRNAs from Pol II transcripts. Downstream of sRNAs binding to AGO proteins the canonical and non-canonical pathways appear to be conserved (i.e. all pathways involve Pol V and DRM2).

The non-canonical RdDM pathways are thought to be key for initiating the methylation and thus silencing of transcriptionally active TEs. Once a heterochromatic landscape is established at TEs and Pol II transcripts decline, the canonical RdDM pathway likely takes over. Pol IV and Pol V recruitment requires SAWADEE HOMEODOMAIN HOMOLOGUE1 (SHH1) and SUPPRESSOR OF VARIEGATION 3-9 HOMOLOG2 (SUVH2) and SUVH9, respectively, which bind heterochromatin associated methylated histone H3 lysine 9 and methylated cytosines, respectively. All the information displayed in this sidebar came from the following three excellent reviews: (Matzke and Mosher, 2014; Cuerda-Gil and Slotkin, 2016; Zhang et al., 2018b).

5' upstream promoters (Baum et al., 2019). This pattern is aligned with a previous study which demonstrated that at 24 hours post SA treatment, SA-induced genes such as *PR1* generally had a reduced nucleosome density in their promoters (Singh et al., 2015). Together, these studies suggest that histone modifications and related changes in chromatin density, *cis*-regulate priming of defence genes.

In addition to histone modifications, there is increasing evidence that DNA methylation regulates priming. Unmethylated DNA is often associated with

A Whistle-Stop Tour of Transposable Elements

Transposable elements (TEs, or transposons) can be broadly classified into DNA transposons and RNA transposons. DNA transposons (class 2 TEs) move within a genome via single- or double-stranded DNA intermediates and are characterized by terminal inverted repeats. The six superfamilies of DNA elements transpose via either a classic cut-and-paste mechanism of excision followed by reinsertion (Ac/Ds/hAT, MuDR/Mutator/Mu/MULE, En/Spm/dSpm/CACTA, Tc1/Mariner/Stowaway, and PIF/Harbinger/Tourist superfamilies) or rolling circle replication (Helitron superfamily). The more prevalent RNA transposons (class 1 TEs) replicate via a copy-and-paste mechanism involving an RNA intermediate. RNA transposons are grouped by the presence of long-terminal repeats (LTRs), such as retrotransposons of the Copia and Gypsy superfamilies, or absence of LTRs, as in the long and short interspersed nuclear elements (LINEs and SINEs). Both DNA and RNA transposons can be classified as autonomous elements, which encode all required proteins to replicate and transpose, or non-autonomous elements, that require proteins encoded by the same subfamily or family of autonomous elements for transposition. For more comprehensive reviews describing the TE (super)families, we refer the reader to references (Wicker et al., 2007; Zhao et al., 2016; Quesneville, 2020).

euchromatin, whereas methylated DNA is more likely to be associated with heterochromatin (Chodavarapu et al., 2010; Pikaard and Mittelsten Scheid, 2014). Over recent years, various lines of evidence have established a causal link between chromatin density and DNA methylation. For instance, the chromatin-remodelling enzyme DECREASED DNA METHYLATION1 (DDM1) mediates DNA methylation at pericentromeric regions by unwinding heterochromatic DNA, thereby allowing access to DNA methyltransferases (Zemach et al., 2013). Furthermore, the CHROMOMETHYLASE-class (CMT) DNA methyltransferase CMT3 is part of a self-reinforcing feedback loop with the histone methyltransferase SUPPRESSOR OF VARIEGATION 3-9 HOMOLOG4 / KRYPTONITE (SUVH4 / KYP), which establishes a heterochromatic associated histone modification (Jackson et al., 2002; Johnson et al., 2007; Law and Jacobsen, 2010; Du et al., 2012; Du et al., 2014a).

DNA methylation in plants mostly occurs at the fifth carbon of cytosine in three DNA sequence contexts: CG, CHG, and CHH (where H indicates any base except guanine). The RNA-directed DNA methylation (RdDM) pathway(s) establish new DNA methylation at cytosines of all three sequence contexts (see the sidebar titled RNA-directed DNA methylation) (Zhang et al., 2018b). By contrast, maintenance of DNA methylation is achieved by multiple different DNA methyltransferases. In Arabidopsis,

METHYLTRANSFERASE1 (MET1) and CMT3 are largely responsible for the maintenance of CG and CHG methylation, respectively (Bartee et al., 2001; Lindroth et al., 2001; Kankel et al., 2003; Saze et al., 2003). Asymmetric CHH context DNA methylation is maintained by the RdDM pathway(s) (Zhang et al., 2018b) and CMT2, a DNA methyltransferase that is dependent on the activity of the chromatin remodeler DDM1 (Zemach et al., 2013). The three types of DNA methylation are not evenly distributed across the genome. CG methylation is found mostly at gene bodies and heterochromatic transposable elements (TEs; see the sidebar titled A whistle-stop tour of transposable elements), whereas CHG and CHH methylation mostly occur at intergenic regions and TEs in both heterochromatic and euchromatic regions (Cokus et al., 2008). It should be noted however, that these patterns are based on Arabidopsis and the distribution of DNA methylation varies across different plant species and families (Niederhuth et al., 2016; Wambui Mbichi et al., 2020). For instance, the gene bodies of conifers including loblolly pine (*Pinus taeda*) and Norway spruce contain a high amount of not only CG but also CHG context methylation (Ausin et al., 2016; Takuno et al., 2016). DNA methylation can be removed from cytosines of all three genomic contexts by both passive and active mechanisms (Zhang et al., 2018b). The failure to maintain methylation at a locus after DNA has been replicated results in a passive loss. Whereas the base excision repair pathway, which requires DNA glycosylases such as DEMETER (DME) and DEMETER-LIKE1 or REPRESSOR OF SILENCING1 (DML1/ROS1), provides a route for active removal of DNA methylation (Penterman et al., 2007; Zhu, 2009).

The first evidence for involvement of DNA methylation in defence gene priming came from Lopez and associates, who demonstrated that SA-dependent *WRKY* and *PR*-genes are constitutively primed in RdDM-deficient Arabidopsis mutants (López et al., 2011). Since then, various studies have confirmed that DNA methylation is inversely correlated with basal resistance to biotrophic pathogens and responsiveness/expression of SA-dependent genes (Luna et al., 2012; Yu et al., 2013; López Sánchez et al., 2016). Furthermore, independent groups have reported that infection of Arabidopsis with *P. syringae* alters genome-wide DNA methylation (Pavet et al., 2006; Dowen et al., 2012; Stassen et al., 2018). However, the exact mechanisms by which DNA methylation controls defence gene expression seems complex. For instance, transcriptome analysis of downy mildew-infected Arabidopsis identified

numerous defence-related genes that are transcriptionally primed in the CHH-hypomethylated RdDM mutant *nrpe1-11* and/or repressed in the hypermethylated *ros1-4* mutant, which is impaired in the active DNA demethylase ROS1 (López Sánchez et al., 2016). Interestingly, the majority of these defence genes were not targeted by NUCLEAR RNA POLYMERASE E1 (NRPE1)- and/or ROS1- dependent DNA (de)methylation, suggesting that their responsiveness is *trans*-regulated by DNA methylation (López Sánchez et al., 2016). More recently, Cambiagno and coworkers reported that *P. syringae* infection of Arabidopsis results in both the transient expression of pericentromeric TEs and the accumulation of RdDM-related sRNAs that map to both TEs and defence genes (Cambiagno et al., 2018). Interestingly, while the TEs were re-silenced over time, the complementary defence genes remained active (Cambiagno et al., 2018). Cambiagno and coworkers proposed that this antagonistic response is caused by sRNA competition, whereby sRNAs are allocated away from the defence-related genes toward the TEs (Cambiagno et al., 2018). Apart from this competition model, TE-derived sRNAs could also positively regulate the priming of distant defence genes. Recent evidence has shown that sRNAs can *trans*-activate defence-related genes through interaction with ARGONAUTE 1 (AGO1) and the SWI/SNF chromatin remodelling complex (Liu et al., 2018). Further support for *trans*-regulation of defence gene priming came from a recent study of *Arabidopsis* epigenetic recombinant inbred lines (epiRILs), which identified four hypomethylated epigenetic quantitative trait loci (epiQTLs) that control quantitative resistance against downy mildew (Furci et al., 2019). Transcriptome analysis revealed that the most resistant epiRILs were constitutively primed to activate defence-related genes. However, comprehensive comparison of gene transcription and DNA methylation failed to identify defence-regulatory genes within the pericentromeric epiQTLs that were simultaneously primed and hypomethylated, or that were located near hypomethylated TEs, suggesting that the hypomethylated epiQTLs *trans*-regulate genome-wide priming of defence genes. Apart from a possible role of sRNAs, Furci and colleagues proposed that the TE-rich heterochromatic regions *trans*-regulate priming of distant defence genes via non-coding RNAs or long-range chromatin interactions (Furci et al., 2019). Support for the latter hypothesis comes from previous high-throughput chromatin confirmation capture studies, which have shown that reductions in DNA methylation, due to mutations in *DDM1* and *MET1,* profoundly alter long-range chromatin interactions particularly in pericentromeric regions (Feng et al., 2014b).

It can be hypothesised that stress-induced DNA hypomethylation at pericentromeric TEs provides a blueprint for genome-wide defence gene priming. In addition to *cis*-regulation of defence genes by nearby TEs (Figure 1.4A), DNA methylation at pericentromeric TEs can regulate the responsiveness of distant defence genes via *trans*-acting mechanisms. Methylated TEs could control the induction of nearby regulatory genes (e.g. TFs), which in turn mediate augmented induction of downstream defence genes during secondary stress exposure (Figure 1.4B). Alternatively, disease-induced hypomethylation of pericentromeric TEs could affect long-range heterochromatic interactions, releasing repression of distant defence genes (Figure 1.4C). Finally, TE-derived sRNAs complementary to distant defence genes could *trans*-regulate defence gene priming. This can be achieved by disease-induced suppression of Pol IV-dependent RdDM gene silencing (Figure 1.4D) (Yu et al., 2013). Alternatively, Pol II-derived 21/22 nt sRNAs from disease-induced TEs could augment distant defence induction via their association with AGO1 and the SWI/SNF complex (Figure 1.4E) (Liu et al., 2018), or they could augment full-length transcription of distant defence genes with intronic TEs by alternative polyadenylation (Figure 1.4F) (Tsuchiya and Eulgem, 2013).

1.7. Transgenerational Acquired Resistance (TAR)

The first indication that plants are capable of rapid transgenerational adaptation to biotic stress, came from the finding that caterpillar-infested wild radish produces more resistant progeny to the same herbivore (Agrawal et al., 1999). In following years, other studies reported that isogenic progeny from herbivore-, wounding- or jasmonate-treated plants develop different morphological traits, such as altered leaf trichome density, specific leaf area, petal area and seed production (Holeski, 2007; Verhoeven and Van Gurp, 2012; Kellenberger et al., 2018). Furthermore, independent groups have shown that progeny from plants exposed to pathogens, herbivores and/or chemical priming agents express transgenerational acquired resistance (TAR), which is associated with priming of defence-related genes (Kathiria et al., 2010; Luna et al., 2012; Rasmann et al., 2012; Slaughter et al., 2012). Because patterns of DNA methylation can remain stable over meiosis (Niederhuth and Schmitz, 2014), subsequent research has focused on the role of DNA methylation in TAR. In Arabidopsis, mutations in DNA methylation machinery mimic TAR in terms of resistance and priming of defence genes (Luna et al., 2012; Luna and Ton, 2012;

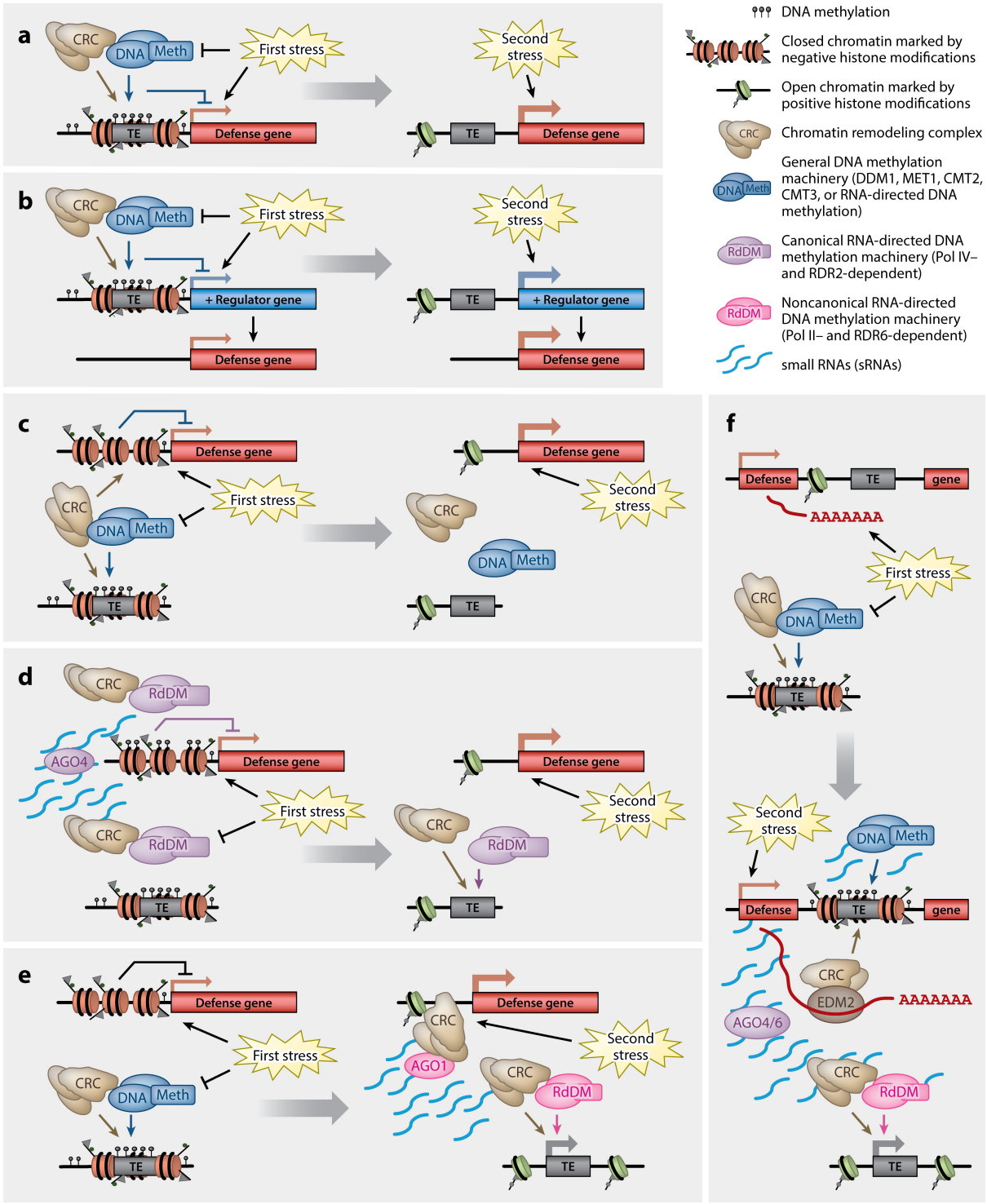

Wilkinson SW, et al. 2019.
Annu. Rev. Phytopathol. 57:505–29

Figure 1.4. Mechanistic Models of the Regulation of Defence Gene Priming by DNA Methylation at Transposable Elements (TEs).

(A) Cis-regulation by nearby TEs. Primary exposure to biotic stress induces defence gene expression and simultaneous DNA demethylation and chromatin decondensation at a nearby TE in the defence gene promoter. The open chromatin structure enables augmented defence gene induction after secondary stress exposure.

López Sánchez et al., 2016), pointing to a mechanism by which disease-induced DNA hypomethylation is transmitted to following generations to control TAR. This hypothesis is supported by Furci et al (2019), who identified hypomethylated DNA regions controlling quantitative disease resistance, which are stable over multiple generations. Furthermore, mutation of the DNA demethylase gene *ROS1* not only affects basal resistance to biotrophic pathogens (Yu et al., 2013), but also prevents TAR in progeny from diseased plants (López Sánchez et al., 2016). Hence, DNA demethylation is essential for the elicitation, transmission and/or expression of TAR. Another recent study revealed that TAR in *Arabidopsis* is associated with global shifts in DNA methylation at CG context in gene bodies, which were more pronounced after

---

Figure 1.4. (continued)

(B) Trans-regulation of defence genes through intermediate regulatory genes. Primary stress induces a transient increase in the expression of a defence regulatory gene (e.g., transcription factor encoding gene), which controls the induction of defence genes located elsewhere in the genome. Simultaneous DNA demethylation and chromatin decondensation at a TE in the promoter of the regulatory gene enable augmented induction of this gene after secondary stress exposure. This in turn enables augmented defence gene induction.
(C) Trans-regulation by long-range chromatin interactions. Primary stress induces DNA demethylation at a heterochromatic TE that forms a long-range heterochromatic connection with a distant defence gene promoter. The resultant chromatin decondensation at the TE disrupts the long-range heterochromatic interaction, enabling augmented induction of the distant defence gene after secondary stress exposure.
(D) Trans-regulation by small RNAs (sRNAs) from canonical RNA-directed DNA methylation (RdDM). Primary stress represses RNA polymerase IV (Pol IV)–, RNA-DEPENDENT RNA POLYMERASE 2 (RDR2)–, and ARGONAUTE 4 (AGO4)–dependent RdDM, reducing the production of 24-nt-long sRNAs from a TE containing complementary DNA sequences with distant defence gene promoters. This allows for augmented induction of the distant defence gene after secondary stress exposure, as the gene is no longer repressed by RdDM.
(E) Trans-regulation by sRNAs from noncanonical RdDM. Primary stress results in transcriptional reactivation of functional TEs that contain complementary DNA sequences to distant defence gene promoters. Subsequent resilencing of the TEs by Pol II– and RDR6-dependent RdDM results in the production of 21/22-nt-long sRNAs that are loaded onto AGO1 and interact with the SWI/SNF chromatin remodeling complex at distant defence gene promoters. The increased recruitment of Pol II and associated chromatin remodeling to the distant defence gene promoters enables augmented induction after secondary stress exposure.
(F) Combination of cis- and trans-regulation by local and distal TEs, respectively. The defence gene contains an intronic TE with an alternative polyadenylation site. Initially, when the intronic TE is in a demethylated and euchromatic state, the alternative polyadenylation site is in use, resulting in the majority of the defence gene transcripts being truncated and nonfunctional. Primary stress leads to demethylation and transcription of a distant TE that is partially complementary to the intronic TE. The sRNAs derived from the stress-inducible TE induce noncanonical RdDM at both TEs. The resulting heterochromatization at the intronic TE prevents the use of the alternative polyadenylation site in an EDM2/EDM3/IBM2-dependent manner, allowing for full-length transcription of the functional defence gene upon secondary stress exposure.

three generations than one generation of disease stress (Stassen et al., 2018). However, the genes carrying these differentially methylated cytosines (DMCs) were not enriched for defence-related functions and there was little overlap in DMCs between independent experiments. Since the role of gene body methylation in gene expression remains unclear (Bewick et al., 2016), it was concluded that the observed changes in DNA methylation mark TAR, but do not necessarily cause TAR (Stassen et al., 2018).

Although the exact mechanisms underpinning TAR require further study, there is little doubt about the epigenetic nature of the phenomenon (see sidebar, Epigenetics: what´s in a name?). First, TAR can still be apparent in isogenic progeny after multiple stress-free generations, indicating that TAR is transmittable through the germline and not a consequence of a physiological maternal effect (Luna et al., 2012; Rasmann et al., 2012; Stassen et al., 2018). Second, TAR requires active DNA demethylation at and around TEs by ROS1 (López Sánchez et al., 2016). Third, TAR is reversible, and its transgenerational durability seems to depend on the level of parental stress. For instance, TAR triggered by localised infection with avirulent *P. syringae* disappears after one stress-free generation (Slaughter et al., 2012). By contrast, TAR is still apparent after two stress-free generations when elicited by repeated inoculations with a virulent strain of the same pathogen (Stassen et al., 2018). The reversibility of TAR also suggests that it is associated with ecological costs (see sidebar, Induced resistance: a costly business?). Indeed, it has been reported that TAR-expressing progeny from *P. syringae*-inoculated Arabidopsis are more susceptible to necrotrophic fungal pathogens and exhibit an enhanced sensitivity to salt stress (Luna et al., 2012; López Sánchez et al., 2020). Further research is needed to clarify the ecological drivers of TAR and determine to what extent TAR provides a selective advantage to plants in a changing environment.

1.8. Knowledge Gaps and PhD Aims

Considerable progress has been made in deciphering the mechanisms underpinning the plant immune system. For instance, many components of the jasmonate biosynthesis and signalling pathway, which are key to the regulation of defences against necrotrophic pathogens and chewing herbivores, have been deciphered. Initially, our understanding came primarily from the model species

Arabidopsis. However, there is an increasing body of evidence showing conservation of many aspects of the jasmonate pathway across the plant kingdom (Monte et al., 2018; Monte et al., 2019; Peñuelas et al., 2019). Excellent progress has also been made regarding our understanding of the mechanisms of IR. For example, there is an increasing number of studies suggesting the involvement of epigenetic mechanisms in the maintenance of immune priming (e.g. Baum et al., 2019; Furci et al., 2019). However, despite this progress, there are numerous questions that remain to be answered.

Most studies of IR have focused on short-term phenotypes, whereby plants are challenged only hours or days post the initial resistance inducing treatment. Only recently has there also been a focus on TAR and the mechanisms behind it (Luna et al., 2012; López Sánchez et al., 2016; Stassen et al., 2018). Another common theme among studies on IR is the involvement of SA-dependent defences, which makes sense considering their involvement in the extremely well-studied phenomenon SAR (Spoel and Dong, 2012; Fu and Dong, 2013; Klessig et al., 2018). What is lacking, particularly in Arabidopsis, is the study of long-term consequences of jasmonates on the plant immune system. For instance, does jasmonate elicit long-term IR to chewing herbivores and necrotrophic pathogens. JA and ET signalling pathways are involved in ISR, a phenomenon that has been well studied in Arabidopsis (Pieterse et al., 2014). However, the triggering of ISR does not involve an accumulation of JA (Pieterse et al., 2000) and thus it is different to jasmonate-IR. Long-term within generation jasmonate-IR has been demonstrated in species such as tomato (Worrall et al., 2012) and Norway spruce (Mageroy et al., 2020a). However, the (epi)genetic mechanisms underpinning these phenotypes remain largely under-explored.

This thesis describes the (epi)genetic mechanisms underpinning long-term within-generation jasmonate-IR. Focus was placed on the transcriptional responses and the involvement of DNA methylation. Studies about within-generation long-term IR have often focused on the role of post-translational modifications of histones and rarely address the role of DNA methylation. Experiments were conducted with both Arabidopsis (Chapter 2) and Norway spruce (Chapter 3). Arabidopsis was selected because, in addition to the minimal knowledge about long-term within generation jasmonate-IR in this species, it is easy to work with and there is a wealth of resources available for this model species that allow establishment of causal evidence. By

contrast, Norway spruce was chosen because it is an economically and ecologically important tree species which has had its genome and methylome sequenced (Nystedt et al., 2013; Ausin et al., 2016; Caudullo et al., 2016). Moreover, the jasmonate-IR phenotype has been extensively described in Norway spruce (Kozlowski et al., 1999; Erbilgin et al., 2006; Zeneli et al., 2006; Krokene et al., 2008; Mageroy et al., 2020a). Multiple studies published over the last two decades have explored the anatomical and chemical defences underpinning jasmonate-IR (Martin et al., 2002; Krokene et al., 2008; Zulak et al., 2009; Zhao et al., 2011). However, there has been a paucity of studies investigating the signalling pathways and (epi)genetic mechanisms behind this phenomenon. Recently, together with several co-authors, I was involved in a study which began to rectify this knowledge gap (Mageroy et al., 2020b). The study explored the transcriptional response to challenge of jasmonate pre-treated trees. Chapter 3 follows on from this previous work, with the primary focus on analysing the establishment of jasmonate-IR.

Chapter 2

Long-Lasting Jasmonic Acid Induced Resistance Against a Chewing Herbivore Comes at the Cost of Enhanced Susceptibility to Pathogens in *Arabidopsis thaliana*

Authors:

Wilkinson SW[1], Wilson RS[1], Münch A[1], Henderson MA[1], Moffat EK[1], Stassen JHM[1], López Sánchez A[1], Krokene P[2], Magerøy MH[2], Ton J[1]

Affiliations:

[1] Department of Animal and Plant Sciences, The University of Sheffield, Sheffield S10 2TN, United Kingdom

[2] Department of Molecular Plant Biology, Division for Biotechnology and Plant Health, Norwegian Institute for Bioeconomy Research (NIBIO), 1431 Ås, Norway

Author contributions:

SWW, PK, MHM and JT proposed the original idea for the research. SWW conducted experiments and gathered data with assistance from RSW, AM, MAH, ALS and EKM. SWW analysed the data with assistance from RSW, AM, MAH, EKM, JHMS and ALS. SWW created all figures and wrote all the text in the chapter. JT and MHM reviewed and provided comments on the chapter. MHM, PK and JT provided funding for the research.

Chapter 2. Long-Lasting Jasmonic Acid Induced Resistance Against a Chewing Herbivore Comes at the Cost of Enhanced Susceptibility to Pathogens in *Arabidopsis thaliana*

2.1. Abstract

Jasmonic acid (JA) can elicit a short-term induced resistance (IR) response against necrotrophic pathogens and chewing herbivores but activate a short-term induced susceptibility (IS) response to (hemi-)biotrophic pathogens. While these short-term responses are relatively well-studied, the longer-lasting impacts of JA on biotic stress resistance remain unclear. Here, we have investigated the long-term effects of JA on resistance of *Arabidopsis thaliana* against pests and diseases. We show that the long-term response to this plant stress hormone is phenotypically different than the short-term response. While JA-IR against the generalist herbivore *Spodoptera littoralis* (*Sl*) and JA-IS to the biotrophic pathogen *Pseudomonas syringae* pv. *tomato* DC3000 were maintained for 3 weeks, 5-week-old plants from JA-treated seedlings showed IS to the necrotrophic fungus *Plectosphaerella cucumerina*, contrasting the short-term JA-IR response to this pathogen. A transcriptome analysis revealed that long-term JA-IR against *Sl* was associated with priming and/or prolonged upregulation of genes associated with anti-herbivore defences, while the long-term JA-IS responses to necrotrophic and biotrophic pathogens correlated with a long-lasting repression of ET- and SA-dependent defence genes. Promoters of genes associated with the long-term JA-IR against *Sl* were enriched with G-box motifs bound by the defence-regulatory MYC transcription factors. The biological relevance of this global transcriptome signal was evidenced by the inability of an *myc2 myc3 myc4* triple mutant to express long-term JA-IR against *Sl*. In addition, mutants deficient in RNA-directed DNA methylation or the DNA demethylase REPRESSOR OF SILENCING 1, which antagonistically control DNA methylation at transposable elements (TEs), were both impaired in long-term JA-IR against *Sl*. Whole genome bisulfite sequencing revealed that JA seedling treatment induces long-term variation in non-CG methylation, which can largely be attributed to randomly occurring hypomethylation at TEs. Despite this variability, the differential methylation was strongly and specifically targeted at the *ATREP2* family of TEs. Our study suggests that random hypomethylation of homologous *ATREP2* TEs primes and/or upregulates MYC-

dependent defence genes via *trans*-regulatory mechanisms, resulting in long-term immunological memory against chewing herbivores.

2.2. Introduction

Plants have evolved a wide range of defence strategies to help them survive in their variable and potentially hostile environment (Wilkinson et al., 2019). Perception of stress-indicating signals by molecular pattern-recognition receptors (PRRs) elicits pattern-triggered immunity (PTI), a highly efficient form of plant innate immunity that is effective against a broad spectrum of attackers (Jones and Dangl, 2006). Specialised pests and diseases can weaken the effectiveness of PTI using effector molecules that interfere with the signalling pathways and defence mechanisms which are required for PTI (Pel and Pieterse, 2013; Xin and He, 2013; Erb and Reymond, 2019; Irieda et al., 2019). The residual level of resistance is often referred to as basal resistance, which although too weak to prevent parasitisation, does contribute to slowing down the colonisation by a PTI suppressing attacker (Ahmad et al., 2010; Ahmad et al., 2011). Accordingly, the pathways controlling PTI and basal resistance share signalling components, which orchestrate the induction of anti-pathogen and/or -herbivore defences (Ahmad et al., 2010; Bigeard et al., 2015; Li et al., 2016; Erb and Reymond, 2019). The phytohormones salicylic acid (SA) and jasmonic acid (JA) are two examples of important signalling components in these pathways (Bari and Jones, 2009; Pieterse et al., 2012; Bigeard et al., 2015; Klessig et al., 2018). SA regulates defences which resist (hemi-)biotrophic pathogens (Glazebrook, 2005; Qi et al., 2018), whereas JA is important for the induction of defences effective against necrotrophic pathogens and chewing herbivores (McConn et al., 1997; Thomma et al., 1998; Vijayan et al., 1998; Wasternack and Hause, 2013).

Within seconds to minutes of *Arabidopsis thaliana* (Arabidopsis) leaf tissue being damaged, both JA and its bioactive form JA-isoleucine (JA-Ile) begin to accumulate in local and distal tissues (Glauser et al., 2009; Koo et al., 2009). Biosynthesis of JA-Ile begins with α-linolenic acid (18:3) being released from chloroplast membranes, and subsequently involves a series of enzyme catalysed steps in the plastid, peroxisome and cytosol (Wasternack and Hause, 2013; Wasternack and Feussner, 2018). JA-Ile is transported from the cytosol to the nucleus where it promotes the interaction of its co-receptors, a JASMONATE ZIM DOMAIN (JAZ) protein and CORONATINE-INSENSITIVE1 (COI1) (Thines et al., 2007; Katsir et al., 2008; Melotto et al., 2008a; Fonseca et al., 2009; Sheard et al., 2010). Subsequently, the F-box protein COI1, as part of the SKP1–CUL1–F-box^{COI1} protein

E3 ubiquitin ligase complex, targets the associated JAZ protein for degradation by the 26S proteasome (Chini et al., 2007; Thines et al., 2007). JAZ proteins, of which there are thirteen in Arabidopsis, repress transcriptional activators of JA-inducible genes such as the basic helix-loop-helix (bHLH) MYC transcription factors (TFs) and ETHYLENE INSENSITIVE3 (EIN3) and EIN3-LIKE1 (EIL1) (Zhu et al., 2011; Zhang et al., 2015; Chini et al., 2016; Howe et al., 2018). Thus, the COI1-dependent degradation of JAZ proteins results in the activation of TFs which upregulate JA-inducible genes. It takes less than 15 minutes following tissue wounding for the first JA-inducible genes to be upregulated (Hoo et al., 2008; Glauser et al., 2009; Koo et al., 2009).

JA-dependent responses regulated by MYC TFs include defences effective against chewing herbivores (Fernández-Calvo et al., 2011; Niu et al., 2011; Schweizer et al., 2013a; Song et al., 2017; Erb and Reymond, 2019). For instance, MYCs together with MYB TFs positively regulate the biosynthesis of glucosinolates, secondary metabolites which play a major role in defending *Brassicaceae* plants against chewing herbivores (Schweizer et al., 2013b). Additionally, MYC TFs are also required for the JA-dependent induction of genes encoding for anti-insect proteins such as *VEGETATIVE STORAGE PROTEIN2* (*VSP2*) (Lorenzo et al., 2004; Fernández-Calvo et al., 2011). There is increasing evidence suggesting that JA/MYC dependent anti-herbivore defences are co-regulated by the abiotic stress hormone abscisic acid (ABA) (Anderson et al., 2004; Bodenhausen and Reymond, 2007; Pieterse et al., 2012; Vos et al., 2013; Frerigmann and Gigolashvili, 2014). This co-regulation is thought to be in part mediated via MYC2 as it is ABA responsive at the transcriptional level and has been shown to interact with the ABA receptor PYRABACTIN RESISTANCE1-LIKE6 (PYL6) (Abe et al., 1997; Abe et al., 2003; Lorenzo et al., 2004; Aleman et al., 2016). Interestingly, in addition to positively regulating JA/ABA induced anti-herbivore defences, MYC TFs are involved in antagonising the JA and ethylene (ET) dependent defence response which controls resistance against necrotrophic pathogens (Boter et al., 2004; Lorenzo et al., 2004; Fernández-Calvo et al., 2011; Niu et al., 2011; Zhai et al., 2013; Song et al., 2014). This antagonism provides evidence that the JA signalling pathway has two branches. The current paragraph has described the first of those, the MYC-branch, which is co-regulated by ABA, requires MYC TFs and is associated with resistance to chewing

herbivores (Pieterse et al., 2012). The second branch of the JA signalling pathway is co-regulated by ET and is associated with resistance against necrotrophic pathogens (Broekgaarden et al., 2015). The master regulators of this second branch are EIN3 and EIL1 (Alonso et al., 2003; Zhu et al., 2011; Chang et al., 2013; Song et al., 2014) and thus it can be referred to as the EIN3/EIL1-branch.

As mentioned above, EIN3/EIL1 are released from repression following JA-Ile triggered COI1-dependent degradation of JAZ proteins (Zhu et al., 2011). Furthermore, an accumulation of ET promotes EIN3/EIL1 stabilisation and transcriptional regulation activity in an EIN2-dependent manner (Li et al., 2015b; Merchante et al., 2015; Zhang et al., 2017b; Dubois et al., 2018; Wang and Qiao, 2019). Thus, a simultaneous accumulation of JA and ET, as triggered by necrotrophic pathogen infection, promotes EIN3/EIL1 activity and results in the induction of downstream secondary TFs (Pieterse et al., 2012; Chang et al., 2013). Two examples of secondary TFs are the APETALA2/ETHYLENE RESPONSE FACTOR (AP2/ERF) domain containing ETHYLENE RESPONSE FACTOR1 (ERF1) and OCTADECANOID-RESPONSIVE ARABIDOPSIS AP2/ERF59 (ORA59) (Solano et al., 1998; Lorenzo et al., 2003; Pré et al., 2008; Zhu et al., 2011; Zander et al., 2012; Chang et al., 2013; Song et al., 2014). Secondary TFs are responsible for the induction of defence genes, such as *PLANT DEFENSIN1.2* (*PDF1.2*), which encode for antimicrobial peptides (Penninckx et al., 1996; Penninckx et al., 1998; Berrocal-Lobo et al., 2002; Lorenzo et al., 2003; McGrath et al., 2005; Pré et al., 2008). Consequently, the EIN3/EIL1-branch is essential for resistance to necrotrophic pathogens. However, in parallel, it antagonises the MYC-branch as indicated by the enhanced defence expression and resistance to chewing herbivores in *ein2* and *ein3* mutants (Rojo et al., 1999; Stotz et al., 2000; Lorenzo et al., 2003; Anderson et al., 2004; Bodenhausen and Reymond, 2007). The negative crosstalk is thought to be at least in part facilitated by interactions between EIN3/EIL1 and MYC TFs (Song et al., 2014)

In addition to the two branches of the JA signalling pathway, crosstalk also occurs between JA- and SA-dependent defence pathways. In Arabidopsis, this SA/JA crosstalk is often antagonistic and therefore prioritisation of defence against one type of threat (e.g. biotrophic pathogens) can come at the cost of enhanced susceptibility to another class of attackers (e.g. herbivore or necrotrophic pathogen) (Spoel et al., 2007; Koornneef et al., 2008; Pieterse et al., 2012). Certain pathogens have evolved

to exploit this antagonistic crosstalk. For example, the hemi-biotrophic pathogen *Pseudomonas syringae*. Virulent *P. syringae* strains (e.g. *P. syringae* pathovar (pv.) *tomato* strain DC3000) produce the functional JA-Ile analogue coronatine to suppress SA-dependent defences (Kloek et al., 2001; Brooks et al., 2005; Laurie-berry et al., 2006; Fernández-Calvo et al., 2011; Zheng et al., 2012; Xin and He, 2013; Gimenez-Ibanez et al., 2017). In summary, the JA response does not operate in isolation, but is co-regulated by ABA and ET to specify defence responses against herbivores and necrotrophic pathogens, respectively, and can suppress defence allocation against biotrophic pathogens through repression of the SA pathway.

The short-term (hours/days) effects of JA on biotic stress resistance are well-documented and consistent with the well-characterised effects of the JA pathway within the wider plant immune signalling network. Application of JA or its methyl ester methyl jasmonate (MeJA), induces resistance to chewing herbivores (Stotz et al., 2002; Cipollini et al., 2004; Cui et al., 2005; Johnson et al., 2011; Vos et al., 2019) and necrotrophic pathogens (Thomma et al., 2000; Ton and Mauch-Mani, 2004; Spoel et al., 2007; Pétriacq et al., 2016), but can also induce susceptibility to (hemi-)biotrophic pathogens due to the signalling cross-talk with the SA pathway (Cui et al., 2005; Murmu et al., 2014). The phenomenon whereby plants enhance their basal resistance to pest and/or pathogen attack following exposure to specific environmental stimuli (e.g. JA or MeJA), is known as acquired or induced resistance (IR). It is thought that IR can be underpinned by two overlapping mechanisms (Wilkinson et al., 2019). The first is a prolonged upregulation of inducible defences, whereby the resistance inducing or induction stimuli upregulates defences and those defences remain upregulated until subsequent challenge. With the second mechanism, defence priming, following induction treatment defences remain at basal level until the subsequent attack upon which they are upregulated faster and/or stronger (Martinez-Medina et al., 2016; Mauch-Mani et al., 2017). Many studies have focused on short-term IR. However, it has been shown in Arabidopsis that elevated resistance can last many weeks within a generation (Luna et al., 2014b) and even be transmitted across generations (Luna et al., 2012; Rasmann et al., 2012; Slaughter et al., 2012). Nevertheless, the longer term within generation impact of JA on biotic stress resistance in Arabidopsis has been poorly characterised.

The maintenance of longer lasting IR and defence gene priming, within and across generations, has been linked with epigenetic mechanisms such as DNA methylation (Luna et al., 2012; Luna et al., 2014b; López Sánchez et al., 2016; Furci et al., 2019). In Arabidopsis, DNA methylation, the addition of a methyl group to the fifth carbon of cytosine, occurs at all three sequence contexts: CG, CHG and CHH (H being any base other than G) and predominantly targets heterochromatic transposable elements (TEs). The establishment of DNA methylation is largely controlled by *de novo* RNA-directed DNA methylation (RdDM) (Zhang et al., 2018b), which depends on the activity of small RNAs (sRNAs) targeting the DNA methyltransferase DOMAINS REARRANGED METHYLASE2 (DRM2) to specific genomic locations (Matzke and Mosher, 2014; Cuerda-Gil and Slotkin, 2016). Maintenance of DNA methylation across rounds of DNA replication is generally facilitated by different enzymes for each of the different sequence contexts. DNA methylation at CG and CHG contexts is maintained by METHYLTRANSFERASE1 (MET1) and CHROMOMETHYLASE-class methyltransferase3 (CMT3), respectively (Lindroth et al., 2001; Kankel et al., 2003; Saze et al., 2003). Whereas, DNA methylation at CHH context is mostly maintained by RdDM and CMT2 (Zemach et al., 2013; Matzke and Mosher, 2014). DNA demethylation occurs through both passive and active mechanisms (Zhang et al., 2018b). Active DNA demethylation involves specific DNA glycosylases, such as REPRESSOR OF SILENCING 1 (ROS1) (Gong et al., 2002). Expressed in all vegetative tissues, ROS1 often targets genomic loci that are within TEs and are methylated by the RdDM pathway (Penterman et al., 2007; Tang et al., 2016). The antagonism between RdDM and ROS1 provides a mechanism by which dynamic changes in methylation can occur in response to environmental stress, such as a localised pathogen attack or a hormone treatment. Furthermore, as DNA methylation has been associated with the direct induction and/or priming of defence gene expression (Yu et al., 2013; López Sánchez et al., 2016; Furci et al., 2019), environmental stress induced methylome alterations provide a mechanism for long-lasting immunological memory in plants.

In this study, we have examined the long-term effects of JA on the defence-related phenotype, transcriptome and DNA methylome of Arabidopsis. We show that the long-term effects of JA (weeks) are phenotypically different than the short-term effects of JA (days). Seedlings treated with JA developed long-term IR against the

generalist chewing herbivore *Spodoptera littoralis* (*Sl*) but long-term induced susceptibility (IS) to the necrotrophic fungus *Plectosphaerella cucumerina* (*Pc*) and the hemi-biotrophic bacterium *P. syringae* pv. *tomato* DC3000 *luxCDABE* (*Ps*). Transcriptome analysis identified clusters of JA/ET- and SA-dependent defence genes which displayed long-lasting reduced expression. In contrast, genes associated with defence against herbivores exhibited enhanced constitutive expression and/or transcriptional priming. The promoters of these augmented genes were enriched for G-box containing MYC TF binding motifs and the long-lasting IR against herbivory was dependent on MYC2, MYC3 and MYC4. The long-term IR also required intact RdDM- and ROS1-dependent regulation of DNA methylation at TEs. A comprehensive methylome analysis revealed that the long-term MYC/ROS1/RdDM-dependent JA-IR is associated with DNA hypomethylation which occurs at inconsistent locations between replicates but is often targeted at TEs, particularly those of the *ATREP2* TE family.

2.3. Results

2.3.1. JA Induces Long-Term Resistance to a Generalist Herbivore and Long-Term Susceptibility to both Necrotrophic and Hemi-biotrophic Pathogens

Treatment of Arabidopsis with JA or MeJA has been demonstrated to elicit short-term IR against both chewing herbivores and necrotrophic pathogens (Thomma et al., 2000; Stotz et al., 2002; Cipollini et al., 2004; Ton and Mauch-Mani, 2004; Johnson et al., 2011; Pétriacq et al., 2016), but short-term IS to biotrophic pathogens that are resisted through SA-dependent defences (Cui et al., 2005; Murmu et al., 2014). We validated these previously observed short-term jasmonate IR and IS phenotypes by treating 5-week-old Arabidopsis plants with water (control) or 1 mM JA and then 1 day later challenging those plants with the generalist chewing herbivore *Spodoptera littoralis* (*Sl*), a necrotrophic fungal pathogen *Plectosphaerella cucumerina* (*Pc*) or the virulent biotrophic bacterial pathogen *Pseudomonas syringae* pv. *tomato* DC3000 *luxCDABE* (*Ps*; Figure 2.1A). Plants pre-treated with JA were more resistant than the water controls to both the generalist chewing herbivore and the necrotrophic pathogen, as evidenced by the lower larval weights and smaller lesions diameters, respectively (Figure 2.1B). Furthermore, the JA pre-treated plants allowed more bacterial growth to occur and were thus more susceptible than the water controls to *Ps* (Figure 2.1B).

Having validated the short-term resistance phenotypes, we next assessed the less well characterised long-lasting impacts of JA treatment on resistance to pests and pathogens. Five-week-old plants, from 2-week-old seedlings treated with water or 1 mM JA, were challenged with *Sl*, *Pc* or *Ps* (Figure 2.1A). *Sl* larvae reared on water seedling treated controls grew much faster and were substantially bigger after 5 days of feeding than those reared on plants from JA treated seedlings (Figure 2.1C). Thus, JA seedling treatment elicited long-term IR to the generalist chewing herbivore. In contrast, JA seedling treatment resulted in long-lasting IS to both pathogens as evidenced by the larger lesions (*Pc*) and enhanced bacterial growth (*Ps*) in plants from JA treated seedlings, when compared to the water controls (Figure 2.1C). The long-lasting IS to *Pc* was weaker or non-existent when lower concentrations of JA were used for the seedling treatment (Supplemental Figure 2.1). This suggests that only a

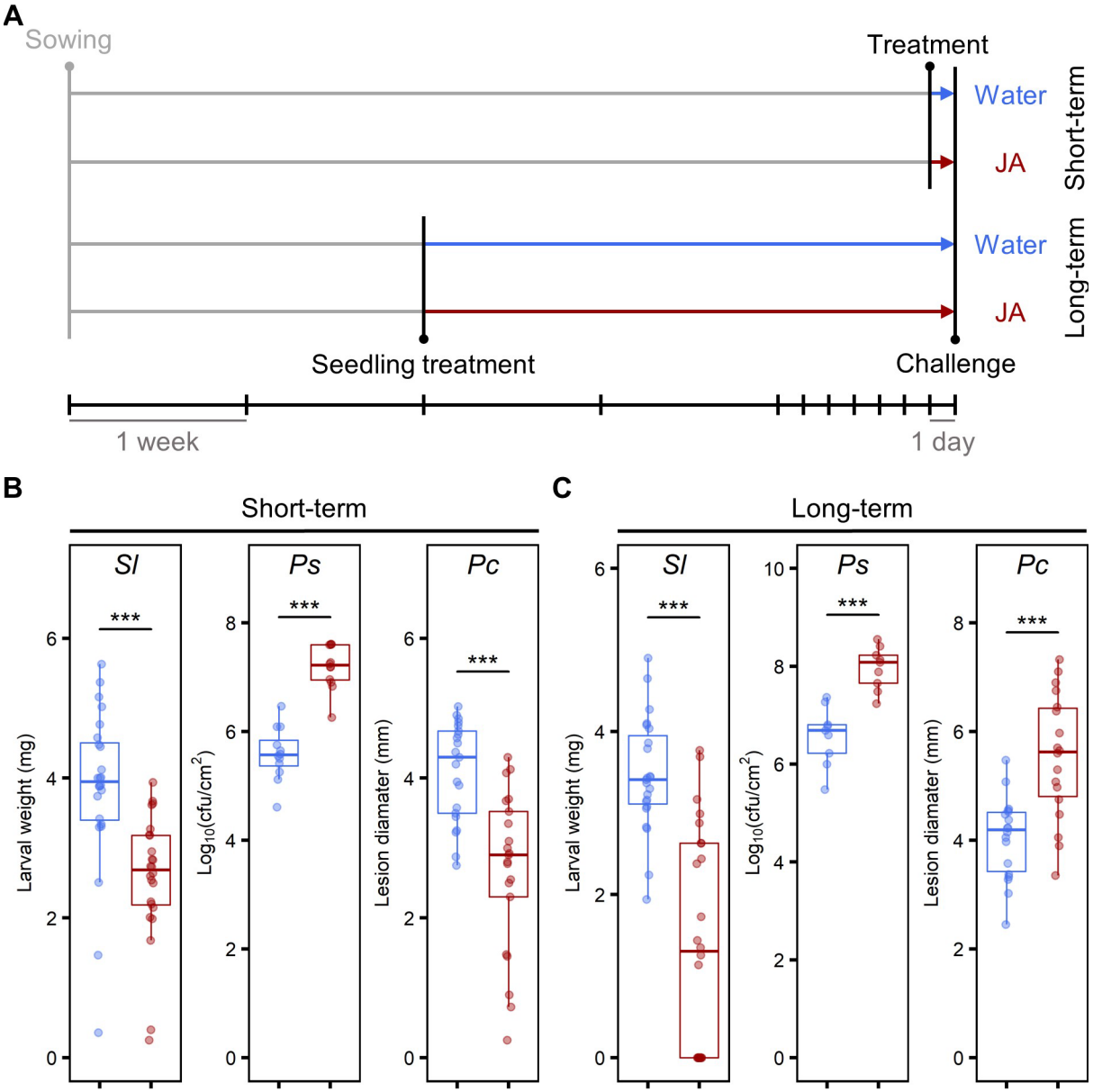

Figure 2.1. Short and Long-Term Impact of JA Treatment on Resistance to *Spodoptera littoralis*, *Pseudomonas syringae* pv. *tomato* DC3000 *luxCDABE* and *Plectosphaerella cucumerina.*

(A) Experimental setup for the analysis of the short- and long-term impacts of JA on biotic stress resistance. Plants were either treated with water (control, blue) or 1 mM JA (red) 1 day (treatment; short-term) or 3 weeks (seedling treatment; long-term) prior to challenge with a chewing herbivore, pathogen or hormone application. Horizontal lines represent plants, with one plant being shown per treatment group. Grey line colouring indicates plants are naïve and untreated. Whereas blue and red colouring indicates that plants have received a water or JA pre-treatment, respectively. Major events are indicated by vertical lines labelled above or below the rounded ends. A time scale bar is provided at the bottom of the diagram. The treatment groups are labelled to the right of the diagram (e.g. short-term JA).
(B) and **(C)** The short- **(B)** and long-term **(C)** impact of JA pre-treatment on the resistance of 5-week-old wild-type Col-0 plants to *S. littoralis* (*Sl*), *P. syringae* pv. *tomato* DC3000 *luxCDABE* (*Ps*) and *P. cucumerina* (*Pc*). One neonate *Sl* was fed on each plant (n = 23-24) for 5- (long-term) or 6-days (short-term) prior to measurement of larval weight. A *Pc* spore suspension (5 x 10^6 spores per ml) was droplet inoculated onto four leaves of each plant (n = 18-21). Points represent the mean per plant lesion diameters at 6- (short-term) or 8-days (long-term) post inoculation. A *Ps* bacterial suspension (OD_{600} = 0.0002) was syringe infiltrated into four leaves per plant (n = 9-12). Bacterial counts at 3 days post

strong activation of the JA pathway results in a long-lasting impact on resistance and confirms the suitability of the 1 mM JA seedling treatment for studying the long-lasting impact of JA on resistance to biotic stress.

To verify the biological relevance of the long-term effects of JA seedling treatment, we subjected seedlings to transient feeding by *Sl* larvae, which induces endogenous JA accumulation (Scholz et al., 2014), and quantified resistance against *Sl* and *Pc* in 5-week-old plants. As with the JA seedling treatment, *Sl* infestation of seedlings resulted in long-term IR against *Sl* larvae but long-term IS to the necrotrophic pathogen *Pc* (Figure 2.2).

In summary, the short- and long-term effects of JA on biotic stress resistance are not identical (Figure 2.1). Against chewing herbivores, JA elicits both short- and long-term IR. Furthermore, JA treatment results in both short- and long-term IS against biotrophic pathogens. However, against necrotrophic pathogens, although JA triggers short-term IR, it elicits long-term IS.

2.3.2. JA Seedling Treatment Primes Herbivore Defences and Represses Pathogen Defences

The long-lasting JA-IR to *Sl* could be explained by a prolonged activity and/or priming of the herbivore resistance associated MYC-branch of the JA signalling pathway. Furthermore, the JA-IS to *Pc* and *Ps* may be explained by a long-lasting repression of EIN3/EIL1- and SA-dependent resistance, respectively. To test this hypothesis, we performed a series of RT-qPCR experiments. Five-week-old plants from water and 1 mM JA treated 2-week-old seedlings were challenged with either water (mock) or defence-eliciting hormones. At 4, 8 and 24 hours (hrs) post challenge, we quantified expression of three Arabidopsis defence marker genes: the MYC-dependent anti-insect gene *VSP2* (*AT5G24770*) (Liu et al., 2005), the JA/ET- and EIN3/EIL1-controlled antifungal gene *PDF1.2* (*AT5G44420*) (Penninckx et al., 1996),

---

Figure 2.1. (continued)

inoculation are displayed as $\log_{10}$(colony forming units (cfu) per cm^2 of leaf tissue). The lower, middle and upper horizontal lines in the boxplots equate to the first, second and third quartiles. Whiskers extend to the lowest and highest data points within 1.5*interquartile range below and above the first and third quartiles. Asterisks indicate that pre-treatment (water or JA) had a significant effect on resistance (Two-sample t-test (**(B)** *Pc* and *Ps* **(C)** *Pc* and *Ps*), welch two-sample t-test (**(B)** *Sl*) or Mann-Whitney test (**(C)** *Sl*) , *** $p < 0.001$).

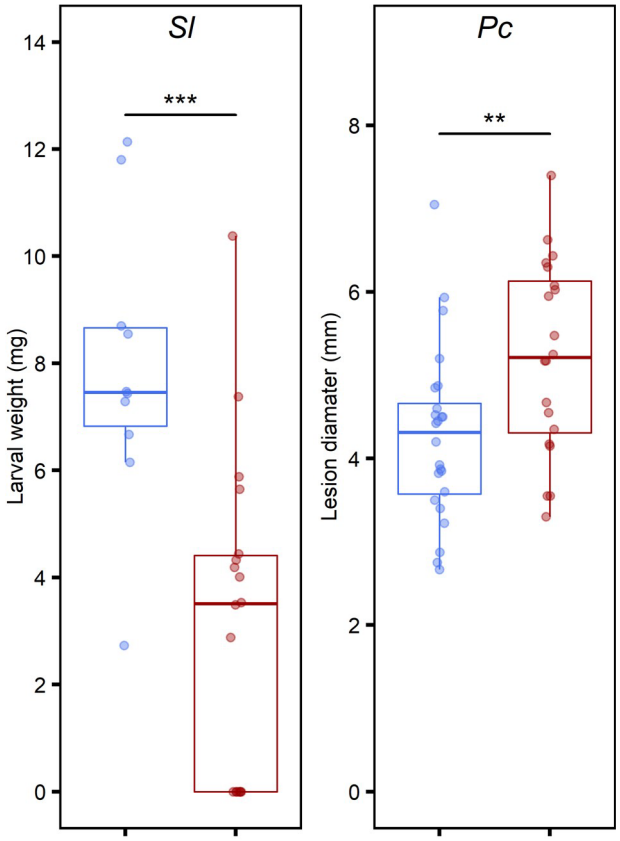

Figure 2.2. Herbivory Damage at the Seedling Stage Mimics the Long-Lasting Impact of JA Treatment on Resistance to the Chewing Herbivore *Spodoptera littoralis* and the Necrotrophic Pathogen *Plectosphaerella cucumerina*.

Two-week-old seedlings were either left undamaged (blue) or had 50-75% of their leaf area removed by *S. littoralis* larvae (red). Plants were challenged 3 weeks post seedling treatment with *S. littoralis* (*Sl*) larvae or *P. cucumerina* (*Pc*). Resistance to *Sl* was assessed with no-choice assays where one neonate was fed on each 5-week-old plant (n = 10-18) for 7-days prior to measurement of larval weight. Resistance to *Pc* was assessed by droplet inoculating a *Pc* spore suspension (5 x 10^6 spores per ml) on to four leaves of each 5-week-old plant (n = 20-24) and then measuring lesion size 6 days later. Points represent the mean per plant lesion diameters. Asterisks indicate that seedling treatment had a significant effect on resistance (Mann-Whitney test (*Sl*) or two sample t-test (*Pc*); ** $p < 0.01$, *** $p < 0.001$).

and the SA-dependent antimicrobial gene *PATHOGENSIS-RELATED1* (*PR1*, *AT2G14610*) (Gamir et al., 2017). To ensure we were able to observe the induction of the defence marker genes, the concentrations of defence eliciting hormones used for the challenge, together with the post-challenge harvesting timepoints, were selected based on previous studies (Luna et al., 2014b; Zhang et al., 2014; López Sánchez et al., 2016). Furthermore, the concentration of JA used for the challenge was less than that used for the seedling treatment as we predicted that if the MYC-dependent marker gene *VSP2* was primed, a strong activation of the JA pathway following a 1 mM JA treatment would induce the gene too quickly to be easily studied.

JA seedling treatment increased the constitutive expression of *VSP2* (Figure 2.3A). However, the most noticeable long-term effect of JA on *VSP2* expression appeared after subsequent challenge treatment with 0.1 mM JA, as *VSP2* exhibited a much faster and stronger induction in JA pre-treated plants compared to plants from water-treated seedlings (Figure 2.3A). The magnitude of this long-term priming effect was most evident at the relatively early timepoint of 4 hrs after challenge (Figure 2.3A). In contrast, the JA/ET-controlled *PDF1.2* showed a prolonged repression in plants from JA treated seedlings (Figure 2.3B), which was statistically significant at 4 and/or

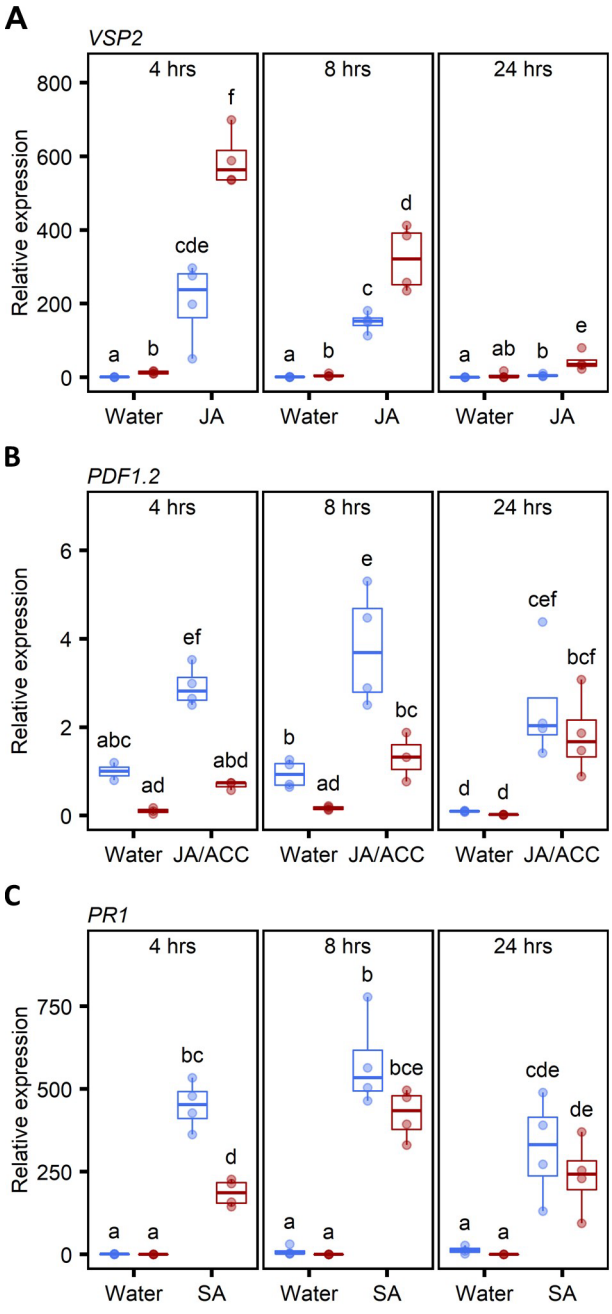

Figure 2.3. JA Seedling Treatment Induces Long-Lasting Priming of Herbivore Defences and Repression of Pathogen Defences.

RT-qPCR analysis of defence pathway marker gene expression in plants treated at 2-weeks-old with water (blue) or 1 mM JA (red) and then challenged 3 weeks later with either water (mock) or, 0.1 mM JA **(A)**, 0.1 mM JA + 0.1 mM ACC **(B)** or 0.5 mM SA **(C)**. *VSP2*, *PDF1.2* and *PR1* expression was assessed at 4, 8 and 24 hours (hrs) post challenge. Points represent the expression of individual replicates (n = 2-4) relative to the mean expression (set to 1) at 4 hrs post water challenge of plants from water treated seedlings. Those seedling treatment, challenge and timepoint groups which do not share the same letter are significantly different (*VSP2* - pairwise Wilcoxon rank sum test, adjusted *p*-value < 0.05; *PDF1.2* and *PR1* - Tukey post-hoc test, $p < 0.05$).

8 hrs after mock challenge or application of a *PDF1.2* inducing solution of 0.1 mM JA and 0.1 mM of the precursor of ET 1-Aminocyclopropanecarboxylic acid (ACC; Figure 2.3B). Following challenge with a 0.5 mM SA solution, *PR1* exhibited a repressed induction in plants treated at the seedling stage with JA compared to those treated at the seedling stage with water (Figure 2.3C). Taken together, these marker gene expression profiles support our hypothesis. JA seedling treatment enhances the long-term activity and responsiveness of the MYC-branch of the JA response, whereas it represses the activity and/or responsiveness of both the EIN3/EIL1-branch and the SA-defence pathway.

2.3.3. The Transcriptome Associated with Long-Lasting JA-IR Against *Spodoptera littoralis* is Characterised by Prolonged Upregulation and Priming of Genes Related to Herbivore Defence

To explore the long-term impacts of JA seedling treatment on global gene expression, we performed mRNA sequencing (RNA-seq) of all RNA samples from 5-

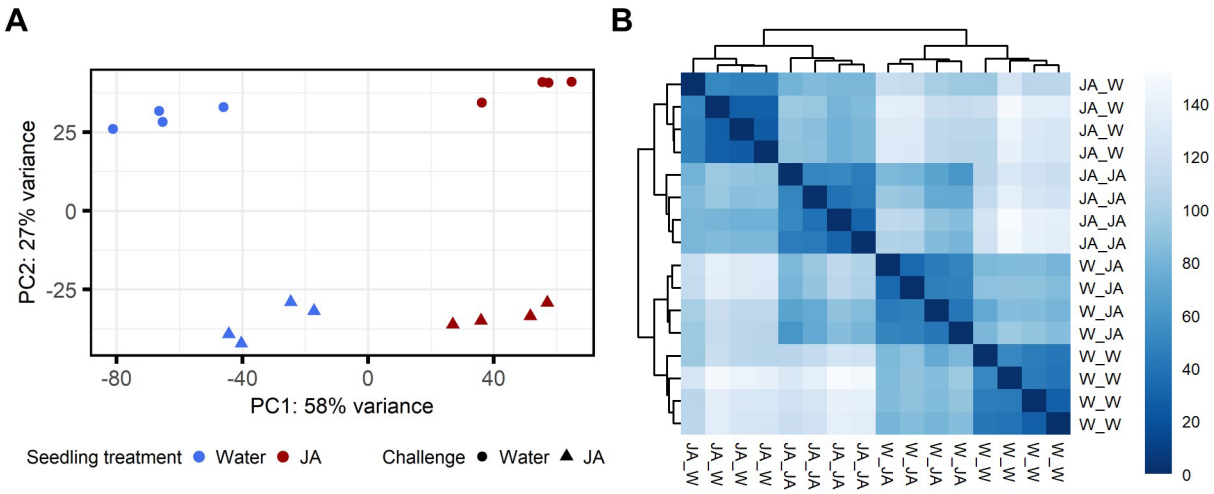

Figure 2.4. Both JA Seedling Treatment and Challenge have a Profound and Consistent Impact on the Leaf Transcriptome.

A principle component analysis (PCA) **(A)** and hierarchical clustering analysis (HCA) **(B)** displaying how treating plants with water or 1 mM JA at 2-weeks-old and then challenging them 3 weeks later with either water or 0.1 mM JA, impacts on global gene expression in leaf tissue. RNA-seq was performed on samples from 4 hours post challenge. All genes with a total read count of ≥ 100 across the 16 samples (four replicates per seedling treatment and challenge combination) were included in the analyses. Both the PCA and HCA utilised read counts normalised for library size and transformed, to homogenise variances of genes from different expression levels, using the DESeq2 function vst (Love et al., 2014). The dendrogram and heatmap display the outcome of clustering samples using Euclidean distances (darker colours equate to a higher similarity) and the complete-linkage method. W_W, water seedling treatment and water challenge; JA_W, JA seedling treatment and JA challenge; W_JA, water seedling treatment and JA challenge; JA_JA, JA seedling treatment and JA challenge.

week-old plants of water- and JA-treated seedlings at 4 hrs after challenge with either water or 0.1 mM JA (Figures 2.1A and 2.3A). The 4 hrs post challenge timepoint was selected as out of the three used in the RT-qPCR experiments, it was the timepoint which showed the most pronounced impact of JA seedling treatment on marker gene expression (Figure 2.3). Furthermore, a previous study reported that maximal transcriptional change for most genes occurred during the first few hrs post MeJA treatment of 5-week-old Columbia-0 (Col-0) plants (Hickman et al., 2017). Thus, using the 4 hrs timepoint increased the likelihood of identifying changes in JA-responsive gene expression patterns due to seedling treatment with JA.

Four replicates were sequenced for each of the 4 hrs post challenge treatment groups: water seedling treatment and water challenge (W_W), JA seedling treatment and water challenge (JA_W), water seedling treatment and JA challenge (W_JA) and JA seedling treatment and JA challenge (JA_JA). A principle component analysis (PCA; Figure 2.4A) and hierarchical cluster analysis (HCA; Figure 2.4B) of normalised and transformed read counts, revealed a clear separation between the four treatment

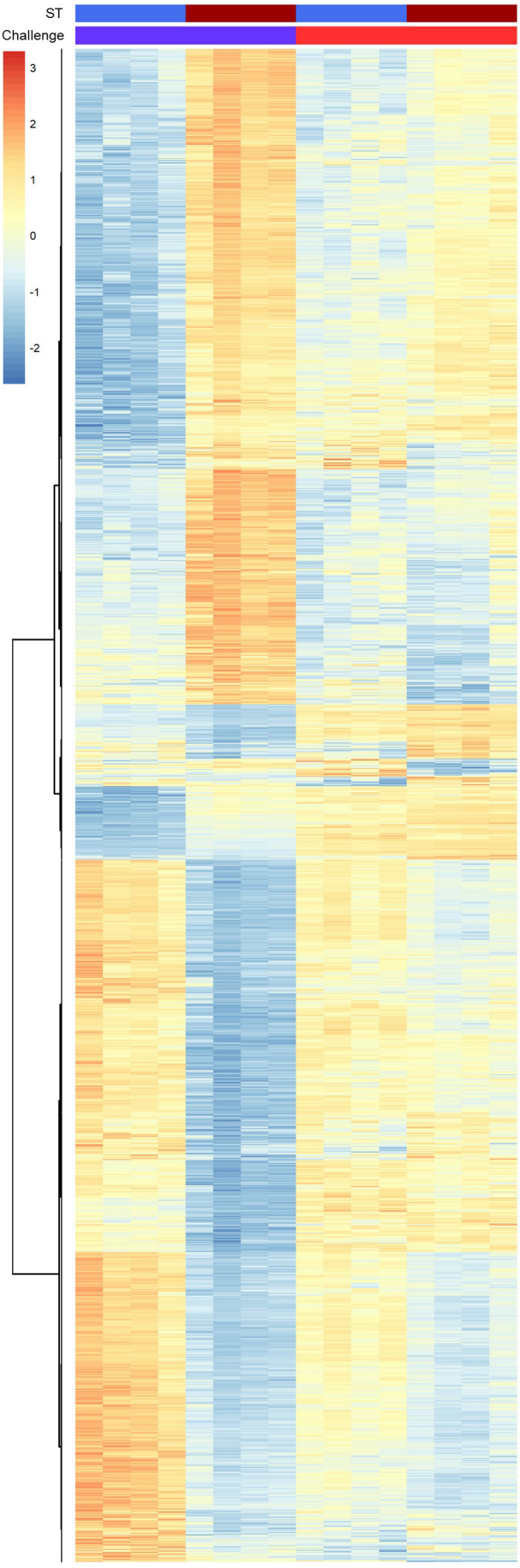

Figure 2.5. Genes Which Responded Differently to JA Challenge as a Result of JA Seedling Treatment.

Five-week-old plants, from water or 1 mM JA treated seedlings, were challenged with water or 0.1 mM JA. RNA-seq was performed on samples (n = 4) from 4 hours post challenge. 2409 genes were selected which exhibited a significantly (false discovery rate (FDR) adjusted *p*-value < 0.01) altered response to JA challenge as a result of JA seedling treatment (ST). Pearson distances and Ward's method were used to cluster the selected genes. Read counts normalised for library size and transformed using the DESeq2 function vst (Love et al., 2014), are displayed as per gene z-scores. Blue and red coloured column annotations equate to water and JA treatments, respectively. Each column is an individual replicate.

combinations. This not only indicated that there were no mis-labelled or outlier samples but also that both JA seedling treatment and JA challenge had a profound impact on global gene expression (Figure 2.4).

To identify gene expression profiles associated with the long-term JA-induced changes in resistance against JA-eliciting attackers (Figures 2.1 and 2.2), we used a DESeq2 (Love et al., 2014) based approach. Expression profiles were selected which displayed a statistically significant interaction between seedling treatment and challenge and thus which represented genes which responded differently to JA challenge as a consequence of prior JA seedling treatment. Using a stringent false discovery rate (FDR) adjusted

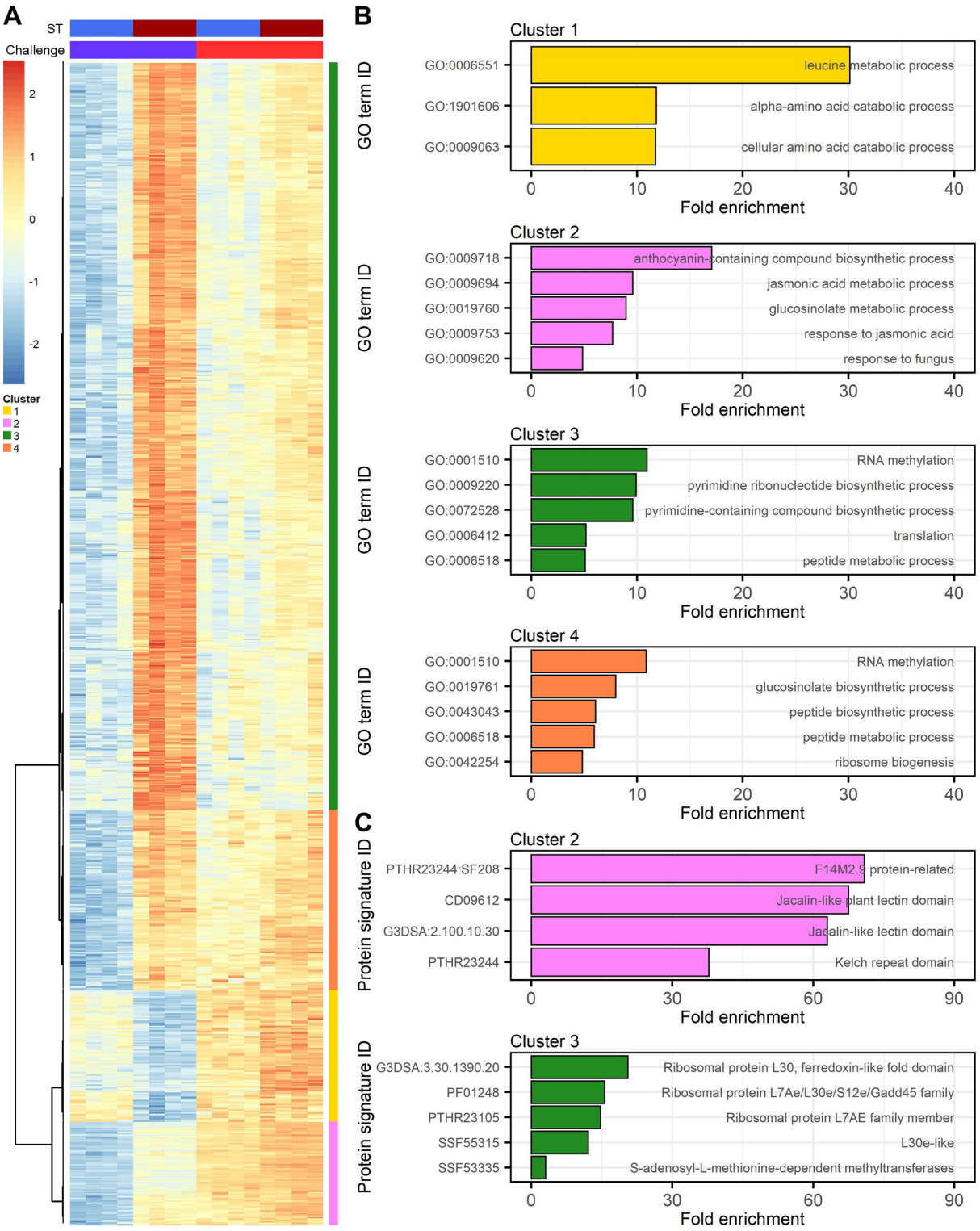

Figure 2.6. Enrichment for Anti-herbivore Defence Function Among Primed and Prolonged Upregulated Genes.

(A) Expression profiles of genes which responded differently to JA challenge as a result of JA seedling treatment (adjusted *p*-value ≤ 0.01, Figure 2.5) and which met the following criteria (i) W_JA > W_W (ii) JA_JA > W_JA (the 1st and 2nd letters equate to seedling treatment (ST) and challenge, respectively; W = water). Genes were clustered using Spearman's distances and Ward's method. The dendrogram was split into four distinct clusters as indicated by the coloured boxes. Read counts normalised for library size and transformed using the DESeq2 function vst (Love et al., 2014), are displayed as per gene

p-value cut-off of 0.01 (*p.adj* < 0.01), 2409 genes were selected (Supplemental Data Set 2.1). Hierarchical clustering of this gene set revealed a range of expression patterns, including genes showing prolonged up- or down-regulation by JA seedling treatment, as well as genes showing an altered response to JA challenge as a consequence of JA seedling treatment (Figure 2.5 and Supplemental Data Set 2.1).

In order to focus on JA-dependent genes with expression profiles that correlated positively with long-term IR against *Sl*, we performed additional filtering steps. Out of the 2409 originally selected genes we identified a sub-set of 832 which were (i) inducible by JA in 5-week-old plants (W_JA > W_W) and (ii) were more highly expressed post JA challenge in plants from JA treated seedlings (JA_JA > W_JA; Supplemental Data Set 2.2). Hierarchical clustering was used to group the 832 selected genes by expression pattern (Figure 2.6A). Four clear distinct gene expression profile clusters were identified. The genes of cluster 1 switched from having lower constitutive expression (JA_W < W_W) to having higher post JA challenge expression in plants from JA treated seedlings compared to plants from water treated seedlings (Figure 2.6A). In contrast, cluster 2 genes, which included *VSP2*, displayed prolonged upregulation by JA seedling treatment (JA_W > W_W) and/or augmented expression after subsequent JA challenge (JA_JA > W_JA). Genes in clusters 3 and 4 were also prolonged up-regulated in mock challenged plants from JA-treated seedlings (JA_W > W_W). However, for the cluster 3 genes, this elevated expression was strongly repressed after subsequent JA challenge (JA_JA < JA_W; Figure 2.6A).

To understand what types of genes were in the sub-set of 832, functional analysis, gene ontology (GO) and protein signature enrichment, was performed on each of the gene expression profile clusters (Figures 2.6B and 2.6C and Supplemental Data Sets 2.3 and 2.4). Overrepresented functional categories were identified for all

---

Figure 2.6. (continued)

z-scores. Blue and red coloured column annotations equate to water and JA treatments, respectively. Each column is an individual replicate (n = 4).
(B) and **(C)** Enriched (adjusted *p*-value ≤ 0.05) Gene Ontology (GO) terms **(B)** and protein signatures in each of the four gene clusters annotated in **(A)**. Post enrichment analysis, the enriched GO terms and protein signatures were simplified to remove analogous annotations. From the simplified lists, the top five most significantly enriched annotations or the total number of enriched annotations, whichever is smaller, are displayed. Clusters 1 and 4 did not have any enriched protein signatures. Simplified and non-simplified lists of enriched functional annotations can be found in Supplemental Data Sets 2.3 and 2.4.

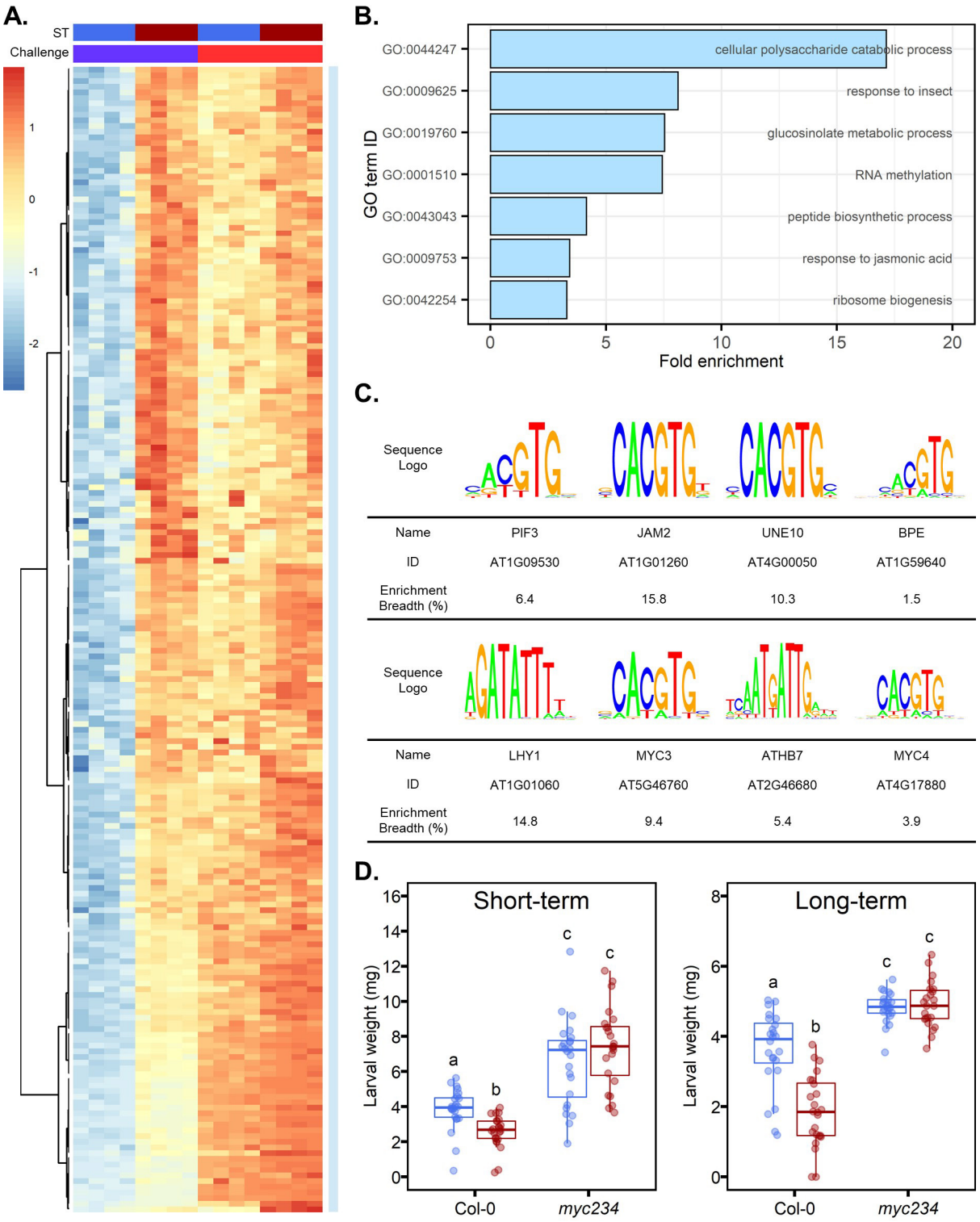

Figure 2.7. Primed and Prolonged Upregulated Genes have Anti-Herbivore Defence Related Functions and are Regulated by G-box (CACGTG) Binding MYC2, MYC3 and MYC4.

(A) The expression profiles of 203 genes from two JA-IR related clusters identified in Figure 2.6. Genes were clustered using Pearson distances and Ward's method. Read counts normalised for library size and transformed using the DESeq2 function vst (Love et al., 2014), are displayed as per gene z-scores. Blue and red coloured column annotations equate to water and JA treatments, respectively. Each column is an individual replicate from one of the four seedling treatment (ST) and challenge combinations (n = 4).

four clusters however only clusters 2 and 4 were enriched for categories associated with resistance to herbivores. Overrepresented GO terms associated with clusters 2 and/or 4 included: “response to wounding” (GO:0009611), “jasmonic acid metabolic process” (GO:0009694) and “glucosinolate biosynthetic process” (GO:0019761; Figure 2.6B and Supplemental Data Set 2.3). Glucosinolates are a class of secondary metabolites, produced by members of the Brassicales order, that are well documented to play an important role in defence against herbivory (Mithöfer and Boland, 2012; Halkier, 2016). Thus, the genes in clusters 2 and 4 showed long-term up-regulation and/or augmented expression after subsequent JA challenge in plants from JA treated seedlings and were predicted to function in defence against herbivores (Figure 2.6A). Based on these results, we selected the 203 genes of clusters 2 and 4 for further investigation (Figures 2.6 and 2.7A and Supplemental Data Set 2.5).

The prolonged upregulated and/or primed genes in clusters 2 and 4 included anti-insect protein encoding *VSP1* (*AT5G24780*) and *VSP2* and glucosinolate homeostasis genes *MYB DOMAIN PROTEIN34* (*MYB34, AT5G60890*), *CYTOCHROME P450 79F1* (*CYP79F1*, *AT1G16410*), *CYP83A1* (*AT4G13770*) and *FLAVIN-MONOOXYGENASE GLUCOSINOLATE S-OXYGENASE1-3* (*FMO$_{GS\text{-}OX1\text{-}3}$, AT1G65860*, *AT1G62540, AT1G62560*; Figure 2.7A, Supplemental Figure 2.2 and Supplemental Data Set 2.5). Furthermore, when all 203 genes were analysed together, prominent enriched functional annotations included the GO terms ‘response to insect’ (GO:0009625) and ‘glucosinolate metabolic process’ (GO:0019760; Figure 2.7B and Supplemental Data Sets 2.6 and 2.7). Thus, in summary, the results of the

---

Figure 2.7. (continued)

(B) Enriched (adjusted *p*-value < 0.05) Gene Ontology (GO) terms among the 203 genes displayed in **(A)**. Only non-overlapping terms are displayed. All enriched GO terms are listed in Supplemental Data Set 2.6.
(C) Overrepresented transcription factor (TF) DNA-binding motifs ($p < 0.01$) in the 1000 bp upstream promoter sequences of the genes displayed in **(A)**. The enriched motifs were reduced to one per TF and the top eight most significantly enriched motifs are displayed. Enrichment breadth indicates the proportion of promoters of genes displayed in **(A)** where the motif was within the top 5% of enriched motifs. The name and ID are for the TF binding the motif. A full list of overrepresented motifs can be found in Supplemental Data Set 2.8.
(D) The weights of larvae reared on 5-week-old wild-type (Col-0) and *myc2 myc3 myc4* (*myc234*) plants, which had been treated with either water (blue) or 1 mM JA (red) 1 day (short-term) or 3 weeks (long-term) previously. Larvae were fed for 5 and 6 days in the long- and short-term experiments, respectively. Each point represents the post feeding weight of a single larvae reared from neonate stage on a single plant (n = 23-24). Those genotype and pre-treatment combinations which do not share the same letter are significantly different (pairwise Wilcoxon rank sum test, adjusted *p*-value < 0.05).

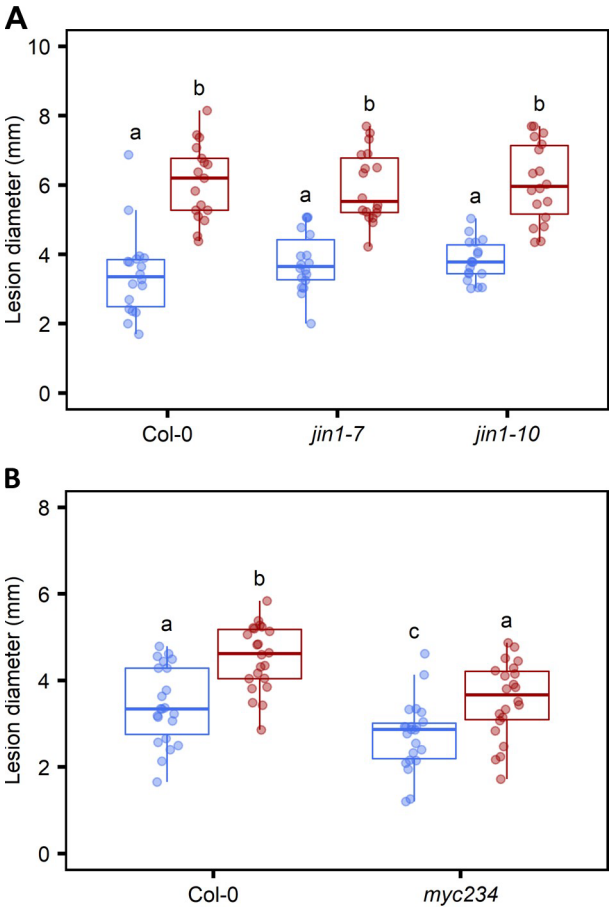

Figure 2.8. Long-Term JA-IS to the Necrotrophic Fungal Pathogen *Plectosphaerella cucumerina* is not Dependent on MYC2 (JIN1), MYC3 and MYC4.

The size of *P. cucumerina* lesions 6 days after inoculation of 5-week-old wild-type (Col-0) or myc mutant plants, **(A)** *myc2* (*jin1-7* and *jin1-10*) **(B)** *myc2 myc3 myc4* (*myc234*). Plants were from water (blue) or 1 mM JA (red) treated 2-week-old seedlings and were inoculated with a 5 x 10^6 spores per ml *P. cucumerina* spore suspension. Each point represents the mean lesion diameter of four leaves from a single plant (n = 17-22). Those genotype and seedling treatment groups which do not share the same letter are significantly different (Tukey post-hoc test, $p < 0.05$).

global transcriptome analysis suggest that the long-lasting JA-IR against *Sl* is underpinned by a JA seedling treatment elicited prolonged upregulation and/or priming of genes associated with resistance to chewing herbivores.

2.3.4. Long-Lasting JA-IR against *Spodoptera littoralis* is Dependent on the MYC-Dependent Branch of the JA Signalling Pathway

To search for transcriptional regulators of the 203 IR-related genes (Figure 2.7A), we conducted statistical enrichment analysis of TF DNA-binding motifs in the genes 1000 bp upstream promoter regions (Figure 2.7C and Supplemental Data Set 2.8). Many of the overrepresented motifs within the promoters of the 203 IR-related genes contained the canonical G-box (CACGTG), which is the annotated preferred core binding site for many bHLH TFs including the defence regulatory TFs MYC2, MYC3 and MYC4 (MYC234; Figure 2.7C and Supplemental Data Set 2.8) (Dombrecht et al., 2007; Carretero-Paulet et al., 2010; Fernández-Calvo et al., 2011; Lian et al., 2017). Previous studies have shown that these MYCs are essential for the activity of basal defences against herbivory, including the expression of the JA-dependent *VSP2* and genes controlling glucosinolate biosynthesis (Fernández-Calvo et al., 2011; Schweizer et al., 2013b). *VSP2* and multiple glucosinolate biosynthesis related genes were primed or prolonged upregulated in response to JA seedling treatment (Figure 2.3A and 2.7A and

Supplemental Figure 2.2). Taken together, the evidence would suggest that MYC234 are critical for the long-lasting JA-IR against *Sl*. To test this hypothesis, 5-week-old *myc2 myc3 myc4* (*myc234*) triple mutant (Fernández-Calvo et al., 2011) and wild-type Col-0 plants from water and 1 mM JA treated seedlings, were challenged with *Sl.* As in previous studies (Fernández-Calvo et al., 2011; Schweizer et al., 2013b; Schweizer et al., 2013a), we found that the *myc234* triple mutant allowed higher larval growth and was thus basally more susceptible than wild-type Col-0 to *Sl* (Figure 2.7D). Furthermore, as in Figure 2.1, we found that in the wild-type, a 1 mM JA pre-treatment elicited both short- and long-term IR to the generalist chewing herbivore, as evidenced by statistically significant reductions in larval growth on JA pre-treated plants (Figure 2.7D). In contrast, the *myc234* triple mutant failed to express IR against *Sl* (Figure 2.7D). Regardless of whether the pre-treatment was 1 day or 3 weeks before challenge (Figure 2.1A), the weights of larvae reared on water and 1 mM JA pre-treated *myc234* plants were strongly overlapping and thus there was not a significant difference in larval weight between pre-treatment groups (Figure 2.7D). The absence of long-term JA-IR in the *myc234* triple mutant was not a consequence of the MYCs being pleiotropic and also regulating the inhibition of growth by JA, as the triple mutant displayed an analogous level of JA induced growth reduction as the wild-type (Supplemental Figure 2.3). Taken together, these results suggest that the MYC-branch of the JA-signalling pathway not only contributes to basal resistance against *Sl* but that it is also essential for short- and long-term JA-IR against chewing herbivores.

2.3.5. The MYC-Dependent JA Response does not Control Long-Term JA-IS to the Necrotrophic Fungus *Plectosphaerella cucumerina*

Previous studies have reported that MYC2 negatively regulates defences effective against necrotrophic pathogens (Lorenzo et al., 2004; Dombrecht et al., 2007; Song et al., 2014). Combined with our clear demonstration of the importance of MYC TFs in the expression of long-lasting JA-IR against *Sl* (Figure 2.7D), these previous results suggest that the long-term JA-IS to *Pc* could be controlled by MYC2. To test this hypothesis, we assessed *Pc* disease progression in Col-0 and two previously characterised *myc2* mutants, *jasmonate insensitive1-7* (*jin1-7*) and *jin1-10* (Anderson et al., 2004; Boter et al., 2004; Dombrecht et al., 2007). Both *myc2* mutant lines

expressed similar levels of long-term JA-IS to *Pc* as wild-type plants (Figure 2.8A). Thus, MYC2 alone is not the master regulator of long-term JA-IS against *Pc*.

The possibility of functional redundancy between MYC2, MYC3 and MYC4, prompted us to test the *myc234* triple mutant. Interestingly, while the *myc234* mutant had higher basal resistance than the wild-type to *Pc*, it still expressed the long-lasting JA-IS (Figure 2.8B). Thus, in contrast to the long-lasting JA-IR against *Sl*, the long-term JA-IS to *Pc* is not dependent on the MYC234 TFs and is not controlled by the MYC-regulated branch of the JA response.

2.3.6. The Transcriptome Associated with Long-Lasting JA-IS to *Plectosphaerella cucumerina* Reveals Prolonged Repression of Genes Related to Pathogen Resistance

To focus on genes with expression profiles that correlated positively with the long-lasting and MYC234-independent JA-IS response to *Pc* (Figures 2.1 and 2.8), we applied different filtering criteria to the 2409 genes which showed a significantly (*p.adj* < 0.01) altered response to JA challenge as a result of JA seedling treatment (Figure 2.5 and Supplemental Data Set 2.1). A total of 904 genes were selected which were (i) repressed by JA challenge in 5-week-old plants (W_JA < W_W) and (ii) were more weakly expressed following JA challenge in plants from JA-treated seedlings compared to naïve (water) pre-treated plants (JA_JA < W_JA; Supplemental Data Set 2.9). Based on their expression profiles, the selected genes were grouped into three distinct clusters (Figure 2.9A). In contrast to cluster 3 genes, which exhibited increased expression after JA seedling treatment only and repressed expression after subsequent JA challenge, the genes in clusters 1 and 2 showed transcriptional repression after both JA seedling treatment and subsequent JA challenge (Figure 2.9A). GO term and protein signature enrichment analysis identified multiple significantly overrepresented functional categories for all three clusters however only clusters 1 and 2 were enriched with terms related to pathogen resistance. For example, “systemic acquired resistance, salicylic acid mediated signalling pathway” (GO:0009862), “defense response to fungus” (GO:0050832), “ethylene biosynthetic process” (GO:0009693), “regulation of immune system process” (GO:0002682) and “WRKY domain” (G3DSA:2.20.25.80) were enriched among genes in cluster 1 (Figure 2.9B and 2.9C and Supplemental Data Sets 2.10 and 2.11). Enriched GO terms

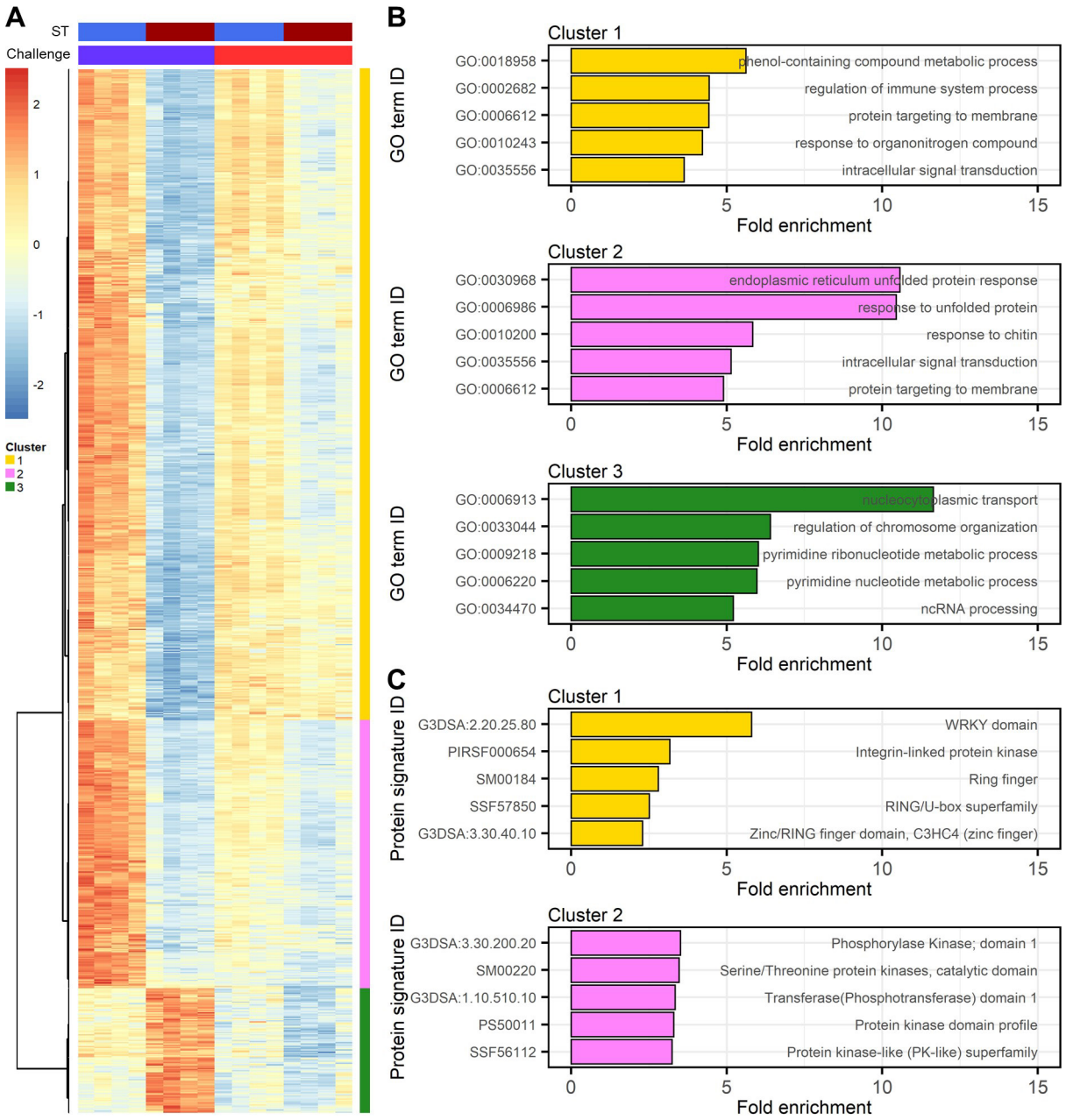

Figure 2.9. Expression Profiles and Functional Annotations of Genes Repressed by JA Seedling Treatment and JA Challenge.

(A) Expression profiles of 904 genes which responded differently to JA challenge as a result of JA seedling treatment (adjusted *p*-value ≤ 0.01, Figure 2.5) and which met the following criteria: (i) W_JA < W_W and (ii) JA_JA < W_JA (the 1st and 2nd letters equate to seedling treatment (ST) and challenge, respectively; W = water). Genes were clustered using Spearman's distances and Ward's method. The dendrogram was split into three clusters as indicated by the coloured boxes. Read counts normalised and transformed using the DESeq2 function vst (Love et al., 2014), are displayed as per gene z-scores. Blue and red coloured column annotations equate to W and JA treatments, respectively. Each column is an individual replicate from one of the four seedling treatment and challenge combinations (n = 4). **(B)** and **(C)** Enriched (adjusted *p*-value ≤ 0.05) Gene Ontology (GO) terms **(B)** and protein signatures **(C)** in each of the three gene clusters annotated in **(A)**. Cluster 3 did not have any enriched protein signatures. Post enrichment analysis, the enriched GO terms and protein signatures were simplified to remove analogous annotation categories. From the simplified lists, the top five most significantly enriched categories or the total number of enriched categories, whichever is smaller, are displayed. See Supplemental Data Sets 2.10 and 2.11 for full lists of enriched terms and signatures, respectively.

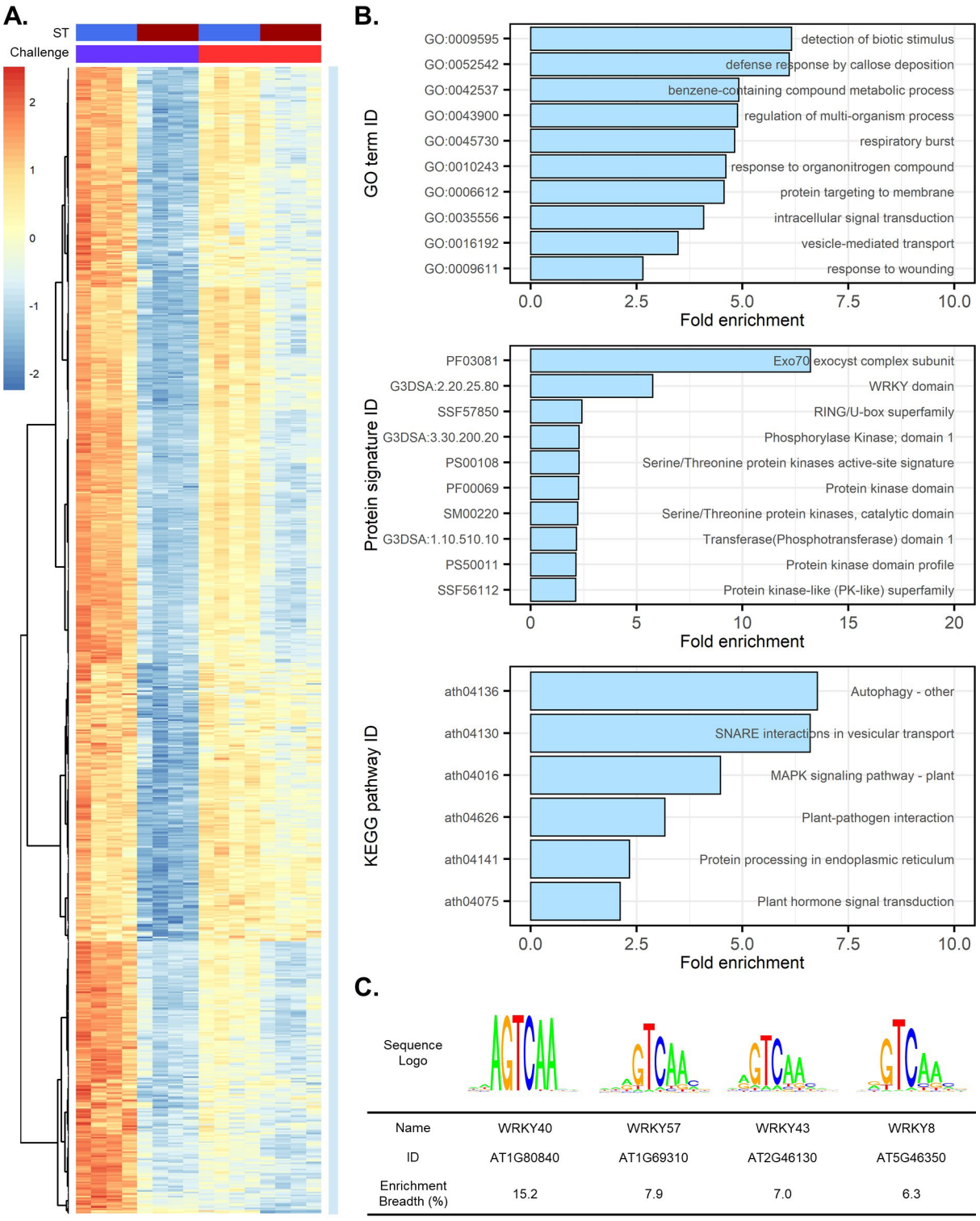

Figure 2.10. Genes Repressed by JA Seedling Treatment and Challenge are Associated with Pathogen Resistance and may be Regulated by WRKY TFs.

(A) The expression profiles of 796 genes from two defence related clusters identified in Figure 2.9. Genes were clustered using Pearson distances and Ward's method. Read counts normalised for library size and transformed to homogenise variances using the DESeq2 function vst (Love et al, 2014), are displayed as per gene z-scores. Blue and red coloured column annotations equate to water and JA treatments, respectively. ST = seedling treatment. Each column is an individual replicate from one of the four seedling treatment and challenge combinations (n = 4).

among the cluster 2 genes included “ethylene-activated signaling pathway” (GO:0009873), “salicylic acid mediated signaling pathway” (GO:0009863), “response to chitin” (GO:0010200), “defense response by callose deposition” (GO:0052542) and “defense response to bacterium” (GO:0042742; Figure 2.9B and Supplemental Data Set 2.10). The overrepresented functional categories together with the gene expression profiles suggested that the 796 genes of clusters 1 and 2 could be associated with the long-term JA-IS and therefore they were selected for further analysis.

A clustered heatmap of the 796 selected genes, displayed in Figure 2.10A, demonstrates that the genes were both repressed long-term following JA seedling treatment (JA_W < W_W) and at 4 hrs post JA challenge more weakly expressed in plants from JA treated seedlings when compared to the water controls (JA_JA < W_JA; Supplemental Data Set 2.12). Furthermore, GO terms, protein signatures and KEGG pathways enriched among this combined set of 796 genes included: “defense response to fungus” (GO:0050832), “systemic acquired resistance” (GO:0009627), “response to salicylic acid” (GO:0009751), “response to ethylene” (GO:0009723), “defense response to bacterium” (GO:0042742), “defense response by callose deposition” (GO:0052542), “Protein kinase domain” (PF00069) and “Plant-pathogen interaction” (ath04626; Figure 2.10B and Supplemental Data Sets 2.13, 2.14 and 2.15). Examples of genes which contributed to the enrichment of these or other closely associated functional categories are, ET biosynthesis and signalling related: *ACC SYNTHASE6* (*ACS6*, *AT4G11280*), *ETHYLENE RESPONSE FACTOR1* (*ERF1*, *AT3G23240*), *ERF5* (*AT5G47230*) and *ERF72* (*AT3G16770*) and regulator of SA biosynthesis and signalling *SAR-DEFICIENT1* (*SARD1*, *AT1G73805*; Supplemental Data Sets 2.12, 2.13, 2.14 and 2.15). Thus, in summary, the transcriptome analysis

---

Figure 2.10. (continued)

(B) Enriched (adjusted *p*-value < 0.05) Gene Ontology (GO) terms, protein signatures and KEGG pathways among the 796 genes displayed in **(A)**. Only the top ten most significantly enriched non-overlapping terms/signatures/pathways are displayed. A full list of enriched terms, signatures and pathways can be found in Supplemental Data Sets 2.13, 2.14 and 2.15.
(C) Overrepresented TF DNA-binding motifs ($p < 0.01$) in the 1000 bp upstream promoter sequences of the genes displayed in **(A)**. The enriched motifs were reduced to one per TF and the top four most significantly enriched motifs are displayed. Enrichment breadth indicates the proportion of promoters of genes displayed in **(A)** where the motif was within the top 5% of enriched motifs. The name and ID are for the TF binding the motif. A full list of overrepresented motifs can be found in Supplemental Data Set 2.16.

suggests that the long-lasting JA-IS against *Pc* and *Ps* is a consequence of long-lasting JA seedling treatment induced repression of JA/ET and SA regulated defences effective against necrotrophic and biotrophic pathogens, respectively.

2.3.7. Promoters of Repressed Genes Associated with Long-Term JA-IS are Enriched with WRKY and TGA DNA-Binding Motifs

To identify putative regulators of the 796 JA-IS associated genes, we performed statistical enrichment analysis of TF DNA-binding motifs in the genes 1000 bp upstream promoter regions (Figure 2.10C and Supplemental Data Set 2.16). Overrepresented motifs included 14 that were bound to by TGACG motif-binding (TGA) TFs, such as TGA2, TGA5 and TGA6 (Supplemental Data Set 2.16). These TGA TFs have been reported to control the expression of SA-induced and NPR-regulated defence genes (Ding et al., 2018; Innes, 2018; Zhang and Li, 2019). However, more pronounced was the fact that just over half (51%) of the overrepresented motifs, including the most significantly enriched motifs, were the binding sites of WRKY TFs (Figure 2.10C and Supplemental Data Set 2.16). Members of the WRKY family of TFs are known to play important roles in regulating JA/ET- and SA- dependent defences effective against necrotrophic and biotrophic pathogens, respectively (Chen et al., 2017). Moreover, the “WRKY domain” (G3DSA:2.20.25.80) was identified as overrepresented among the repressed genes (Figure 2.10B and Supplemental Data Set 2.14). Thus, together these results suggest that long-term JA-IS to *Pc* and *Ps* involves repressed activity of defence regulatory TGA and WRKY TFs.

2.3.8. Regulation of DNA Methylation at TEs is Required for Long-Lasting JA-IR against *Sl* but not Long-Term JA-IS against *Pc*

The transcriptome analysis and subsequent mutant bioassays indicated that long-lasting JA-IR to *Sl* is associated with a prolonged upregulation and priming of a suite of MYC-dependent anti-herbivore defence genes (Figure 2.7 and Supplemental Data Sets 2.6, 2.7 and 2.8). Whereas the long-term JA-IS to *Pc* and *Ps* is associated with long-lasting repression of JA/ET and SA regulated defences, respectively (Figure 2.10 and Supplemental Data Sets 2.13, 2.14, 2.15 and 2.16). Previous studies have revealed a functional link between long-term changes in the constitutive expression and/or responsiveness of defence genes, on the one hand, and active DNA (de)methylation of TEs, on the other hand (López et al., 2011; Luna et al., 2012; López

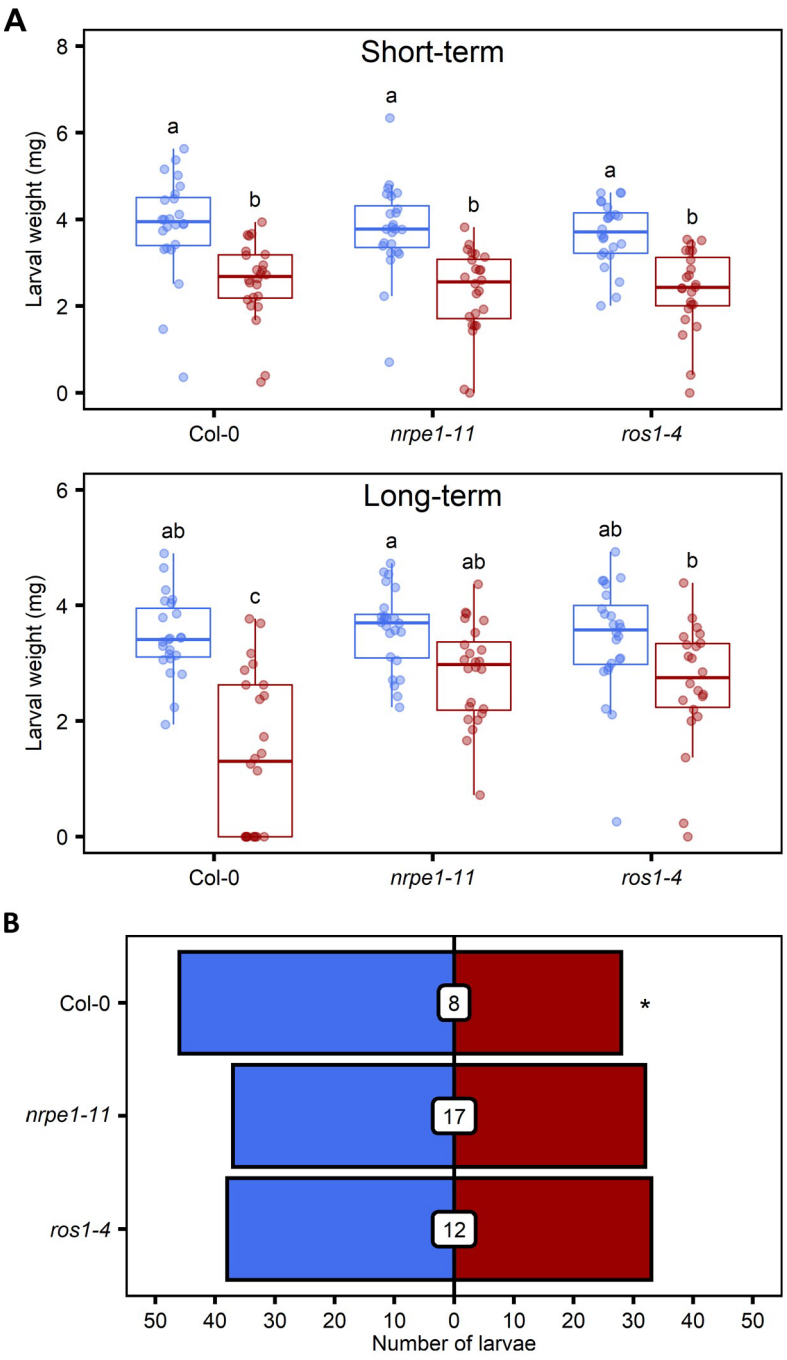

Figure 2.11. Long-Term but not Short-Term JA-IR to the Chewing Herbivore *Spodoptera littoralis* Requires RdDM- and ROS1-Dependent Regulation of DNA Methylation at TEs.

(A) The weights of *S. littoralis* larvae fed on 5-week-old wild-type (Col-0) and RdDM (*nrpe1-11*) and ROS1 (*ros1-4*) mutant plants, treated with either water (blue) or 1 mM JA (red) 1 day (short-term) or 3 weeks (long-term) previously. Larvae were fed for 5 (long-term) or 6 (short-term) days. Each point represents the post-feeding weight of a single larvae fed on a single plant (n = 23-24). Those genotype and pre-treatment combinations which do not share the same letter are significantly different (Tukey post-hoc test, $p < 0.05$).
(B) Within genotype dual-choice tests between 5-week-old plants treated 3 weeks previously, as 2-week-old seedlings, with water (blue) or 1 mM JA (red). Five *S. littoralis* larvae were placed in each choice arena (n = 18 for every genotype) and given 20 hrs to make a choice. The number of larvae which did not make a choice are shown in the white boxes. Asterisks indicate that for a given genotype the distribution of larvae across plants from water and JA treated seedlings, is significantly uneven (Goodness-of-fit test, * $p < 0.05$).

Sánchez et al., 2016; Furci et al., 2019). In Arabidopsis, DNA methylation at TEs is regulated in part by the antagonistic activities of RdDM and the DNA demethylase ROS1 (Zhang et al., 2018b). Thus, to investigate whether this epigenetic regulatory system is required for JA-IR or JA-IS, we acquired two previously characterised mutants which are deficient in RdDM (*nrpe1-11*) and ROS1 (*ros1-4*) (Pontier et al., 2005; López et al., 2011; López Sánchez et al., 2016). *nrpe1-11* has a T-DNA insertion in the gene *NUCLEAR RNA POLYMERASE E1* which encodes the largest subunit of RNA polymerase V (Pol V), an essential component of both canonical and non-

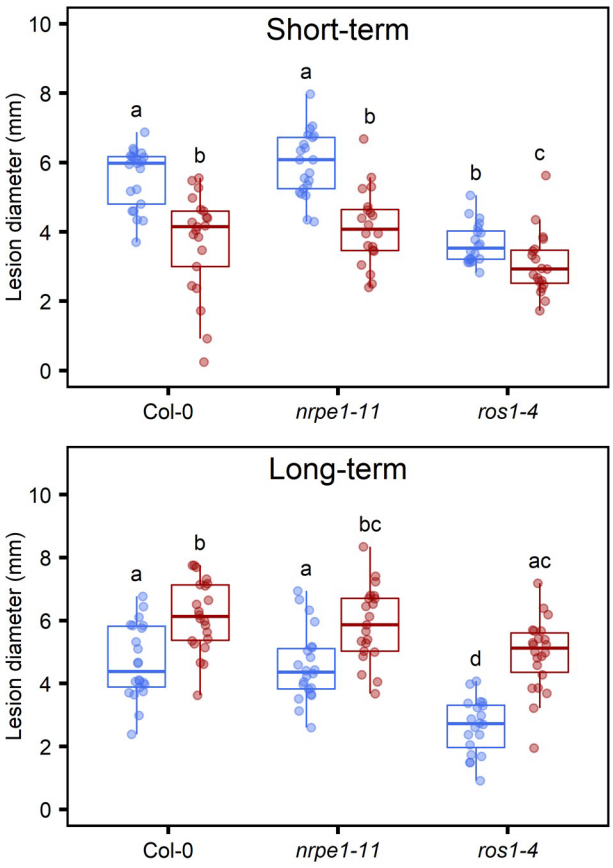

Figure 2.12. Short-Term JA-IR and Long-Term JA-IS to the Necrotrophic Fungal Pathogen *Plectosphaerella cucumerina* does not Require RdDM- and ROS1-Dependent Regulation of DNA Methylation at TEs.

Lesion diameters 7 days after leaves of 5-week-old plants (Col-0, *nrpe1-11* and *ros1-4*) were inoculated with a *P. cucumerina* spore suspension (5 x 10^6 spores per ml). Inoculated plants were pre-treated with water (blue) or 1 mM JA (red) either 1 day (short-term) or 3 weeks (long-term) previously. Each point represents the mean diameter of lesions on the four inoculated leaves of one plant (n = 19-22). Those genotype and pre-treatment groups which do not share the same letter are significantly different (Short-term - Pairwise Wilcoxon rank sum test, adjusted *p*-value < 0.05; Long-term - Tukey post-hoc test, $p < 0.05$).

canonical RdDM pathways (Matzke and Mosher, 2014; Cuerda-Gil and Slotkin, 2016). To test for the presence of JA-IR, wild-type Col-0 and *nrpe1-11* and *ros1-4* mutant plants were treated with water or 1 mM JA 1 day or 3 weeks prior to challenge with *Sl* (Figure 2.1A). Both mutants expressed similar levels of short-term JA-IR as the wild-type, as evidenced by the reduction in growth of larvae fed on JA-pre-treated plants of all genotypes (Figure 2.11A). In contrast, expression of long-term JA-IR was strongly reduced in both *nrpe1-11* and *ros1-4* compared to the wild-type (Figure 2.11A). This impaired expression of JA-IR was not due to a pleiotropic effect of RdDM or ROS1 on JA's regulation of growth as both of the mutants exhibited wild-type levels of JA induced growth reduction (Supplemental Figure 2.3). Thus, the results in Figure 2.11A provide support for the conclusion that short- and long-term JA-IR are controlled by different mechanisms. Furthermore, they also indicate that RdDM- and ROS1-dependent regulation of DNA methylation at TEs is critical for long-term JA-IR against herbivory. To provide additional evidence for the latter conclusion, we quantified long-lasting JA-IR against *Sl* using dual-choice tests. In each test, five *Sl* larvae were given 20 hrs to choose between two plants of the same genotype, one was from a water treated seedling and one was from a JA treated seedling. As is shown in Figure 2.11B, for the wild-type, a higher number of larvae choose naïve plants over plants from JA treated seedlings,

indicating that long-term JA-IR affects the attractiveness of leaves to larvae. In contrast, for both *nrpe1-11* and *ros1-4*, plants from water and JA treated seedlings attracted a similar number of larvae (Figure 2.11B). Hence, RdDM/ROS1-dependent regulation of DNA methylation at TEs plays a critical role in long-term JA-IR against herbivory.

In contrast to long-lasting JA-IR against *Sl*, long-lasting JA-IS to *Pc* was not dependent on RdDM or ROS1. The increased susceptibility in plants from JA-treated seedlings was just as strong in *nrpe1-11* and *ros1-4* mutants as in the wild-type Col-0 (Figure 2.12). Furthermore, JA treatment 1 day prior challenge induced short-term enhanced resistance to *Pc* in all three genotypes (Figure 2.12). This short-term JA-IR response appeared to be weaker in the *ros1-4* mutant than in Col-0 however this can probably be explained by the enhanced basal resistance phenotype which was obvious in our experiments and which has previously been reported (Figure 2.12) (López Sánchez et al., 2016). In summary, RdDM/ROS1-dependent regulation of DNA methylation is not involved in the short-term JA-IR or long-term JA-IS to *Pc.*

2.3.9. JA Seedling Treatment Induces Long-Lasting Increased Variation in DNA Methylation at Transposable Elements

Having demonstrated that active regulation of DNA methylation at TEs is required for long-lasting JA-IR against *Sl* (Figure 2.11), we next explored the impact of JA seedling treatment on the Arabidopsis DNA methylome. Whole genome bisulfite sequencing (WGBS) was employed to profile the methylomes of 5-week-old plants from 2-week-old seedlings treated with water or 1 mM JA. Three replicate leaf samples were sequenced per seedling treatment (water and JA). Genome-wide weighted methylation levels were consistent across replicates and were not significantly impacted by JA seedling treatment (Supplemental Figure 2.4A). This was true when all cytosines were considered together (All C or All contexts) and when cytosines were split up into the three sequence contexts: CG, CHG and CHH (Supplemental Figure 2.4A). Furthermore, the context specific genome-wide weighted methylation level estimates were analogous to those previously reported for Arabidopsis (Niederhuth et al., 2016).

As JA seedling treatment did not significantly impact genome-wide DNA methylation levels, we next investigated whether it altered the global patterning of DNA

methylation by performing a PCA and HCA of methylation levels at an individual cytosine resolution. Both analysis techniques revealed that when cytosines of all contexts were analysed together (All C), the samples from plants of JA-treated seedlings were comparably much more variable than those from naïve (water pre-treated) controls (Figures 2.13A and 2.13B). Interestingly, this difference in variation between water and JA pre-treated plants was largely driven by CHG and CHH sequence contexts, rather than CG context (Figure 2.13B and Supplemental Figure 2.4B). Considering that non-CG methylation mostly occurs at intergenic TE sequences (Cokus et al., 2008) and that RdDM/ROS1-dependent regulation of DNA methylation at TEs is required for the long-term JA-IR to *SI* (Figure 2.11), these results suggest that the JA seedling treatment induces long-lasting variation in TE methylation.

To identify whether TEs are indeed the location of JA seedling treatment induced increased variation in cytosine methylation, we analysed the genome for differentially methylated regions (DMRs) between each individual JA replicate and all three water replicates (1JA_vs_3W). In contrast to statistical comparison between all three replicates from both treatments (3JA_vs_3W), which selects for regions where cytosine methylation is consistently altered by JA treatment, the 1JA_vs_3W approach selects for regions displaying enhanced variation in cytosine methylation induced by JA pre-treatment. The analysis was performed at different sequence contexts (All C, CG, CHG and CHH), using the dispersion shrinkage for sequencing data methodology of the DSS R package (Feng et al., 2014a). In the three All C 1JA_vs_3W comparisons, 325, 291 and 260 DMRs were identified, respectively (Figure 2.13C and Supplemental Data Sets 2.17 and 2.18). Although the DMRs were generally quite small (41 bp average length), they were rich in cytosines (13 cytosines on average per DMR) and generally involved a substantial shift in methylation level (average difference in methylation level of 43 percentage points; Supplemental Data Set 2.18). The CHH sequence context specific analysis revealed 588 DMRs on average per 1JA_vs_3W comparison (Figure 2.13C and Supplemental Data Sets 2.17 and 2.18). Whereas only 52 and 28 DMRs were identified on average per CHG and CG 1JA_vs_3W comparison, respectively (Figure 2.13C and Supplemental Data Sets 2.17 and 2.18). As with All C, the context specific DMRs were generally quite small (53 bp, 50 bp and 42 bp average DMR length for CG, CHG and CHH, respectively) but involved a substantial shift in methylation (average methylation level difference of

45, 37 and 41 percentage points for CG, CHG and CHH, respectively; Supplemental Data Set 2.18). Majority of the DMRs identified across all contexts and all comparisons, occurred at TEs which were located in intergenic regions and to a lesser extent gene promoters (transcription start site (TSS) to 1000 bp upstream; Figure 2.13C). Furthermore, almost all DMRs (> 90 %) were hypomethylated in the individual samples from JA-treated seedlings compared to the three samples from water-treated naïve plants (Figure 2.13C and Supplemental Data Set 2.18). Hence, the long-term increased variation in DNA methylation following JA seedling treatment is largely driven by non-CG context hypomethylation at TEs.

2.3.10. Long-term JA-IR to *Spodoptera littoralis* is Unlikely to be Associated with *cis*-Regulation of Defence Genes by DNA Methylation

Previous studies have linked DNA (de)methylation within the promoters of genes to changes in those genes basal expression and/or responsiveness to stress (Yu et al., 2013; Williams et al., 2015; López Sánchez et al., 2016; Gallego-Bartolomé et al., 2018; Vílchez et al., 2020). Thus, long-term IR may be underpinned by long-lasting changes in DNA methylation in the promoters of specific genes which encode for key defence proteins or regulators. On the face of it, the results of our WGBS analysis suggest that such *cis*-regulation by DNA methylation (Figure 1.4) is unlikely to be involved in the long-term RdDM/ROS1-dependent JA-IR to *Sl*, as the changes in methylation induced by JA seedling treatment appear to occur at variable locations (Figure 2.13). However, it is possible that although DMRs of each JA replicate do not occur at exactly the same location, they could occur in broadly the same region. Thus, rather than DMRs being targeted at specific loci in defence genes promoters they could instead be targeted at the defence genes promoter regions more broadly. Considering that DNA methylation is thought to influence gene expression by effecting the binding of TFs and the expression of genes is often controlled by multiple TFs which have different preferred binding sites (O'Malley et al., 2016; Zhang et al., 2018b), plausibly the broad targeting of JA-induced DMRs could result in a similar effect on defence gene expression and in turn resistance.

To begin to test our broad targeting hypothesis, we searched for consensus DMRs, regions overlapped by one DMR from each of the three 1JA_vs_3W comparisons. The pipeline used to identify consensus DMRs was as follows: (i)

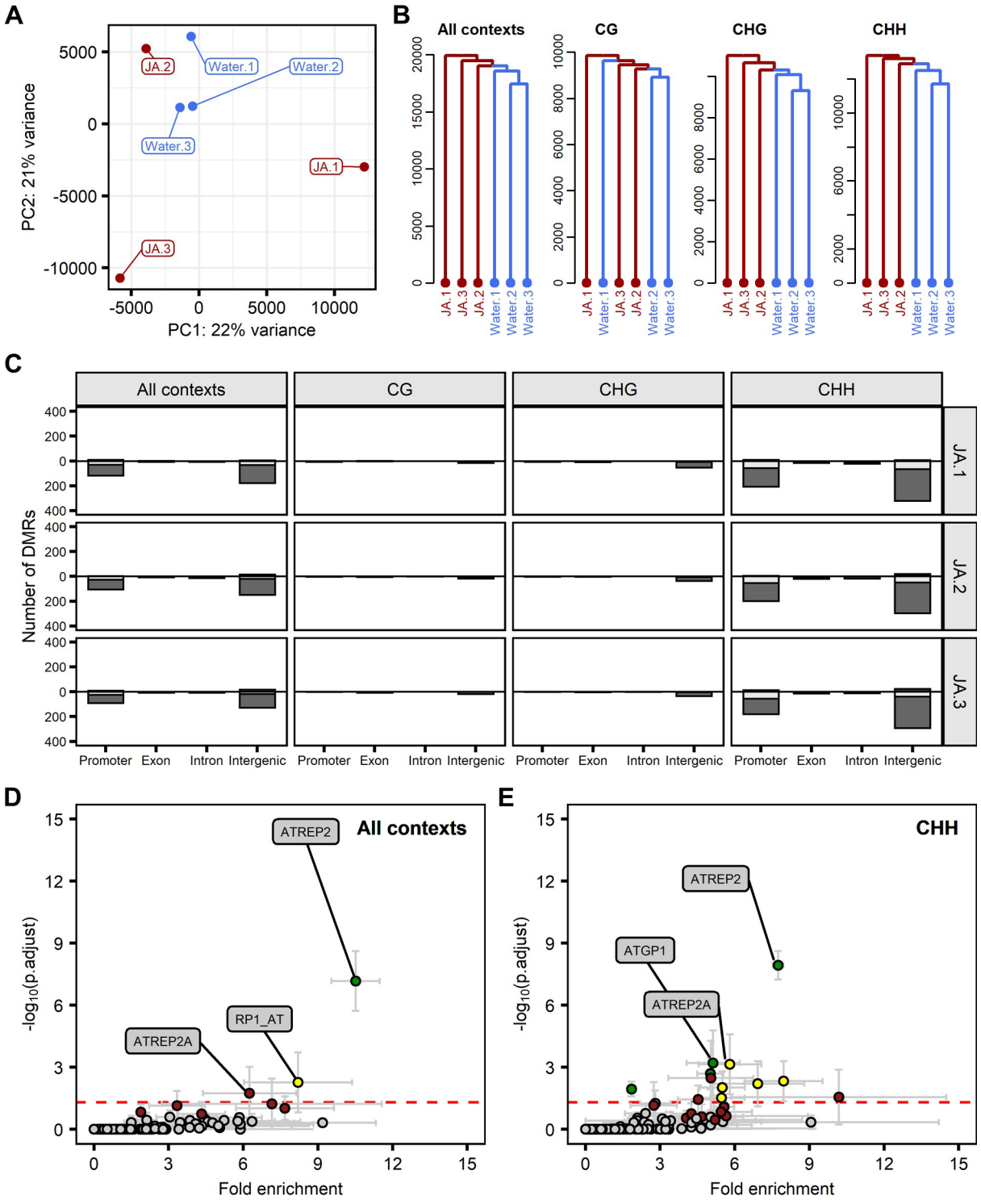

Figure 2.13. JA Seedling Treatment Induces CHH Context DNA Hypomethylation Targeted at *ATREP2* TEs.

(A) A PCA of the percentage methylation at cytosine positions of all sequence contexts. Positions with low coverage (< 5 reads in one or more samples) and minimal between sample variation (standard deviation less than or equal to the 0.5 quantile of all positions standard deviations), were excluded from the analysis. Data was mean centred but not scaled. Each point represents a sample of 5-week-old plants from 2-week-old seedlings treated with water (blue) or 1 mM JA (red).
(B) A hierarchical clustering analysis (HCA) was performed using the same data as the PCA (All contexts). HCAs were also performed separately for cytosines of the three different sequence contexts: CG, CHG and CHH (H = any base other than G). Euclidean distances and Ward's method were used

identified DMRs from pairs of comparisons which were within 100 bp of one another (ii) for each 'overlapping' pair of DMRs created a merged DMR, using the lowest and highest coordinates from across the two (iii) identified DMRs from the comparison not in the original pair which occurred within 100 bp of merged DMRs (iv) created consensus DMRs using the lowest and highest coordinates from across the three 'overlapping' DMRs. For All C, only two consensus DMRs were identified and both mapped to the same region on chromosome 1 (Supplemental Data Set 2.19). Increasing the gap allowed between DMRs from 100 to 500 bp had no impact on the result (Supplemental Data Set 2.19). No consensus DMRs were identified for either CG or CHG. Furthermore, for the CHH sequence context, only 10 and 25 consensus DMRs were identified with 100 and 500 bp maximum gaps, respectively (Supplemental Data Set 2.19). The low number of consensus DMRs further supports the conclusion that JA seedling treatment does not induce changes in methylation at consistent locations but instead induces increased variation in cytosine methylation. Nevertheless, it is still possible that the few identified consensus DMRs could *cis*-regulate genes associated with the long-term JA-IR to *Sl*. Thus, we next looked whether any of the consensus DMRs overlapped gene promoter regions (1000 bp upstream of TSS). Neither of the All C consensus DMRs overlapped any gene promoters whereas 7 and 19 of the CHH consensus DMRs, created using 100 and 500 bp maximum gap respectively, did overlap the promoter regions of genes including *WRKY14* (*AT1G30650*), *GAT1* (*AT1G08230*) and *CALMODULIN 7* (*CAM7*, *AT3G43810*; Supplemental Data Set 2.19). While some of the consensus DMR associated genes have been linked to plant immune responses, none were picked up

---

Figure 2.13. (continued)

for all four HCAs.
(C) Numbers of DMRs identified in comparisons between the three water replicates and each of the individual JA replicates, JA.1, JA.2 and JA.3. Separate 1JA_vs_3W comparisons were performed for each of the cytosine sequence contexts. Hyper- and hypo-methylated DMRs are shown above and below the x-axis, respectively. DMRs are split up based on what genomic context (e.g. promoter) they occurred at and whether (dark grey) or not (light grey) they overlapped a TE.
(D) and **(E)** Overrepresented TE families among the TEs overlapped by DMRs identified in the three 1JA_vs_3W comparisons using cytosines of all sequence contexts (All contexts, **(D)**) or CHH only **(E)**. Points represent the mean $-\log_{10}$(hypergeometric test adjusted *p*-value) vs mean fold enrichment (± SEM), of individual TE families. Enrichment is relative to the background of all TEs annotated in genome. The labelled families have a mean $-\log_{10}$(adjusted *p*-value) of greater than the red dashed line which equals $-\log_{10}(0.05)$ **(D)** or $-\log_{10}(0.001)$ **(E)**. The multi-coloured families were significantly (adjusted *p*-value ≤ 0.05) overrepresented in one (red), two (yellow) or three (green) 1JA_vs_3W comparisons, respectively.

in our RNA-seq analysis as showing an altered response to JA challenge as a result of JA seedling treatment (Figure 2.5 and Supplemental Data Set 2.1). Thus, we conclude that the long-term RdDM/ROS1-dependent JA-IR against *Sl* is unlikely to be associated with *cis*-acting DMRs in the promoters of anti-herbivore defence genes and/or their regulators.

2.3.11. The *ATREP2* TE Family is Specifically Targeted for Long-Term Hypomethylation Following JA seedling treatment

There is increasing evidence that TE methylation can *trans*-regulate distant defence genes across the genome (Cambiagno et al., 2018; Furci et al., 2019; Wilkinson et al., 2019; Wilkinson and Ton, 2020), which would offer an alternative mechanism by which TE methylation homeostasis controls long-term IR against *Sl* Figure 2.11). It has been proposed that this mode of *trans*-regulation is mediated by small RNAs (sRNAs) that are transcribed and processed from TEs with complementary sequences to defence genes and/or their promoters (Section 1.6.3 and Figure 1.4). However, the relatively low number of consensus DMRs, and the even lower number of consensus DMRs which overlap TEs (Supplementary dataset 2.19), suggests that if a *trans*-regulatory mechanism is involved in long-term JA-IR to *Sl*, it is unlikely be under control by specific individual TEs. Nevertheless, as TEs within the same family and/or related families are highly homologous (Wicker et al., 2007), it is plausible that there is a high degree of redundancy between TEs in the production of similar *trans*-acting sRNAs. In turn, this would enable different TEs of the same family or closely related families, to have similar activities. To address this hypothesis, we investigated whether there were TE families and/or superfamilies' that were specifically enriched among the DMR overlapped TEs. Strikingly, the *HELITRON* TE family *ATREP2* was on average 11-fold (All C) and 8-fold (CHH) more prevalent among TEs overlapped by JA-induced DMRs relative to the background of all TEs in the genome (Figures 2.13D and 2.13E). This enrichment was highly significant across all three 1JA_vs_3W comparisons, for both All C and CHH (Figures 2.13D and 2.13E). The *MuDR* TE superfamily and the *ATGP1*, *META1* and *ATREP3* TE families were also consistently overrepresented among the TEs overlapped by DMRs of the CHH context 1JA_vs_3W comparisons (Figures 2.13E and Supplemental Figure 2.5A). However, these additional TE (super)families were much less strongly enriched than *ATREP2* (Figures 2.13E and Supplemental Figure 2.5A). Furthermore, they were not

consistently enriched across the three All C comparisons (Figures 2.13D and Supplemental Figure 2.5B). The pattern for CG and CHG contexts was somewhat different with the only consistently overrepresented TE (super)family being the *Gypsy* superfamily of LTR retrotransposons (Supplemental Figures 2.5C and 2.5D). However not only was this enrichment borderline statistically significant but also it did not translate into consistent enrichment of specific TE families (Supplemental Figures 2.5C and 2.5D). Thus, JA seedling treatment induced variation in DNA methylation is specifically targeted at TEs from the *ATREP2* family.

Further analysis revealed that per comparison, between 12 and 16 All C DMRs and 17 and 20 CHH DMRs overlapped *ATREP2* TEs (Supplemental Figure 2.6A). The majority of these DMRs were hypomethylated and located in promoters or intergenic regions across all chromosome arms (Supplemental Figure 2.6). In total three consensus DMRs overlapped *ATREP2* TEs (2 All C and 1 CHH; Supplemental Data Set 2.19). One of these consensus DMRs overlapped the promoters of three genes (Supplemental Data Set 2.19), however, as mentioned above (section 2.3.10), these genes were not differentially expressed in our RNA-seq analysis. Thus, it seems unlikely that specific JA-IR associated defence genes are consistently regulated in *cis* by *ATREP2* DMRs. Combined with our finding that long-term JA-IR against *Sl* requires active DNA (de)methylation at TEs by ROS1 and RdDM (Figures 2.11), the results of our WGBS analysis strongly suggest that long-term JA-IR against chewing herbivores is underpinned by defence genes regulated in *trans* by hypomethylated *ATREP2* TEs.

2.4. Discussion

2.4.1. Long-Term and Short-Term Responses to Jasmonates are Controlled by Different Pathways

Decades of intense research has provided a detailed understanding of the short-term signalling responses to the plant defence hormone JA (Wasternack, 2015). For instance, in Arabidopsis JA positively regulates the short-term defence responses to chewing herbivores and necrotrophic pathogens (Wasternack and Hause, 2013; Erb and Reymond, 2019) and therefore JA application elicits short-term induced resistance (IR) against these two classes of biotic threats (Figure 2.1B) (Thomma et al., 2000; Stotz et al., 2002; Cipollini et al., 2004; Ton and Mauch-Mani, 2004; Johnson et al., 2011; Pétriacq et al., 2016). Furthermore, due to antagonistic signalling cross-talk with the SA pathway, JA also elicits short-term induced susceptibility (IS) against biotrophic pathogens (Cui et al., 2005; Murmu et al., 2014). In contrast, much less is known about the long-term consequences of JA signalling. The present study provides the first evidence that long-lasting responses to JA are controlled by partially different mechanisms than the short-term response to JA. We have demonstrated that JA elicits long-term IR to the generalist chewing herbivore *Spodoptera littoralis* (*Sl*) but long-lasting IS to the necrotrophic pathogen *Plectosphaerella cucumerina* (*Pc*) and hemi-biotrophic pathogen *Pseudomonas syringae* pv. *tomato* DC3000 (*Ps*, Figures 2.1 and 2.2). Although scarce, long-term IR responses to jasmonates have been reported in other species. For instance, treatment of Norway spruce (*Picea abies*) with MeJA has been reported to induce resistance against infestation by the European spruce bark beetle *Ips typographus* beginning 35 days later (Mageroy et al., 2020a). This long-lasting IR in Norway spruce is not associated with the costs of IS to necrotrophic fungi observed in Arabidopsis (Figures 2.1 and 2.2), since the MeJA treatment also elicits long-lasting IR in Norway spruce against the necrotrophic pathogen *Endoconidiophora polonica* (Zeneli et al., 2006). Considering the evolutionary distance and life history differences between the gymnosperm tree species Norway spruce and short-lived annual angiosperm Arabidopsis, a difference in response to jasmonate treatment is hardly surprising. Nevertheless, long-lasting JA-IS has previously been reported in other species. For instance, Bruce and colleagues found that *B. cinerea* spreads more rapidly across leaves of 7-week-old tomato plants from 1-week-old seedlings treated with JA (Bruce et al., 2017). Interestingly, when less time was left between JA seedling

treatment and *B. cinerea* inoculation (e.g. 3 weeks), a JA-IR phenotype was observed (Luna et al., 2016; Bruce et al., 2017). A JA-IR phenotype was also observed when a seed treatment was used, with 4-week-old tomato plants from JA treated seeds being more resistant to *B. cinerea* than water controls (Worrall et al., 2012). The JA seed treatment was also shown to elicit long-lasting (> 8 weeks) IR against spider mites (*Tetranychus urticae*) and a lepidopteran chewing herbivore (*Manduca sexta*) (Worrall et al., 2012). Thus, together this data could suggest that as we observed in Arabidopsis, in tomato JA elicits short-term (days to weeks) IR to herbivores and necrotrophic pathogens but long-term (months) IR to only the former group of biotic stressors. Future studies should aim to investigate whether this long-lasting resistance trade-off is common across plant species. It would be particularly interesting to study this trade-off in different *Arabidopsis* species and *A. thaliana* ecotypes, which are taxonomically related, but have adapted to a wide range of different habitats. Nevertheless, it is clear from the resistance phenotypes presented in this study (Figures 2.1 and 2.2) that the short-term and long-term responses to JA in the Col-0 ecotype of Arabidopsis are under control by partially different pathways. This notion is further confirmed by our finding that the *ros1-4* and *nrpe1-11* mutants show unaffected levels of short-term JA-IR, while being impaired in long-term JA-IR against *Sl* (Figure 2.11).

2.4.2. Long-Term JA-IR against *Spodoptera littoralis* Requires the MYC-Dependent Branch of the JA Signalling Pathway

IR can be based on a combination of priming and prolonged upregulation of inducible defences (Wilkinson et al., 2019). Our transcriptome analysis confirmed that long-term JA-IR against *Sl* fits this pattern, as evidenced by a suite of 203 defence-related genes showing long-term priming and/or prolonged upregulation in response to JA seedling treatment (Figures 2.7A and 2.7B). The promoters of these 203 genes showed a statistically significant enrichment for transcription factor (TF) DNA-binding motifs which contained the canonical G-box at their core (Figure 2.7C). The G-box element is the binding site of many bHLH TFs (Carretero-Paulet et al., 2010) including the MYC2-4 TFs (Dombrecht et al., 2007; Fernández-Calvo et al., 2011; Lian et al., 2017), which play a critical role in regulating JA- and ABA-controlled defences against herbivores (Fernández-Calvo et al., 2011; Schweizer et al., 2013b). Indeed, our characterisation of the *myc234* triple mutant revealed a critical role for these TFs in

long-term JA-IR against *Sl* (Figure 2.7D). This mutant has previously been shown to be severely compromised in basal resistance to *Sl* and impaired in a range of anti-herbivore defences, such as the induction of the anti-herbivore gene *VSP2* and the production of defence-related glucosinolates (GSs) (Fernández-Calvo et al., 2011; Schweizer et al., 2013b; Schweizer et al., 2013a). Our selection of 203 IR-related genes not only included the *VSP2* gene itself, which showed long-term priming by JA seedling treatment (Figure 2.3A), but was also enriched with a variety of the GO terms related to insect resistance, such as GS metabolism (Figure 2.7B). GSs are sulphur rich secondary metabolites which are produced by members of the Brassicales order, can be classified into three groups, aliphatic, benzenic and indolic, and play a major role in defence against generalist chewing herbivores (Beekweelder et al., 2008; Müller et al., 2010; Sønderby et al., 2010b; Halkier, 2016). The main anti-herbivory activity of the GSs comes from tissue disruption triggered myrosinase-dependent cleavage of the glucoside and subsequent release of the sulphur-nitrogen containing breakdown products (Barth and Jander, 2006; Hopkins et al., 2009). While the exact structure and activity of the breakdown products depends on the GS precursor and other specifier enzymes (Wittstock and Burow, 2010; Wittstock et al., 2016), GS products are generally toxic and typically kill, reduce the growth of, and/or repel generalist chewing herbivores (Li et al., 2000; Hopkins et al., 2009; Jeschke et al., 2016). Interestingly, these activities by GSs are consistent with the phenotype of long-term JA-IR, which not only reduced the growth of *Sl* larvae in single choice assays (Figures 2.1 and 2.2), but also increased the repellence of larvae in a dual choice assay (Figure 2.11B). Collectively, the enrichment of herbivore defence-related GO terms and MYC-binding G-box motifs in our selection of 203 IR-related genes, combined with the inability of the *myc234* triple mutant to express long-term JA-IR against *Sl* (Figure 2.7D), adds biological relevance to the expression profiles of these genes and demonstrates that the immunological memory of long-term JA-IR is retained at the MYC-dependent branch of the JA response.

2.4.3. Glucosinolates: Essential for JA-IR to Chewing Herbivores and JA-IS to Pathogens?

GSs can be defined as both phytoanticipins and phytoalexins as they are produced both constitutively and in increased amounts after challenge (VanEtten et al., 1994; Müller et al., 2010; Schweizer et al., 2013b; Frerigmann and Gigolashvili,

2014). Our gene expression data suggests that JA seedling treatment may adjust the basal GS level, rather than alter the accumulation of GSs in response to subsequent challenge (Supplemental Figure 2.2). Previous studies on species other than Arabidopsis have found that following herbivory or a JA treatment, GS levels can remain enhanced for one, two or more weeks (Bodnaryk, 1994; Van Dam et al., 2004; Hopkins et al., 2009; Fritz et al., 2010). It is thus not implausible that long-lasting JA-IR to *Sl* is underpinned by a long-term accumulation of glucosinolates. However, expression patterns of glucosinolate homeostasis genes do not always correlate well with glucosinolate levels (Sønderby et al., 2010a). Thus, future studies using liquid chromatography coupled to mass spectrometry (LC-MS) are required to confirm that GS levels are enhanced in 5-week-old plants from 2-week-old JA treated seedlings.

Despite the importance of GSs in herbivore resistance, not all the GS homeostasis genes were upregulated in our transcriptome experiment (Supplemental Figure 2.2). For instance, in contrast to *MYB34* which showed a prolonged upregulation, *MYB51* exhibited a prolonged downregulation by JA seedling treatment (Supplemental Figure 2.2). MYB34 and MYB51, together with MYB122, play an important role in the transcriptional regulation of indolic GSs (Gigolashvili et al., 2007; Frerigmann, 2016). Interestingly, while their functions are overlapping, the two MYBs differ in the role they play in regulating the accumulation of indolic GSs in response to different stresses (Frerigmann and Gigolashvili, 2014). For example, the indolic GSs 1-methoxy-indol-3-ylmethyl-glucosinolate (1MO-I3M) and indol-3-ylmethyl-glucosinolate (I3M) accumulate in response to a JA or ABA in a MYB34-dependent manner. Whereas, in response to elevated levels of SA or ET, 4-methoxy-indol-3-ylmethyl-glucosinolate (4MO-I3M) and to a lesser extent I3M are induced with MYB51 being the key regulator (Frerigmann and Gigolashvili, 2014). Furthermore, MYB51 seems to be the most important MYB for the regulation of indolic GS accumulation in response to pathogens such as *Pc* (Frerigmann et al., 2016). These results support the previously reported role of 4MO-I3M in resistance against SA and JA/ET eliciting pathogens (Bednarek et al., 2009; Sanchez-Vallet et al., 2010). For example, a *cyp81f2* mutant which is deficient in the enzyme required to produce 4MO-I3M, was shown to have enhanced susceptibility to the same *Pc* strain (BMM) as used in our experiments (Sanchez-Vallet et al., 2010). Furthermore, *Pc* (BMM) infection of wild-type Col-0 induced the accumulation of 4MO-I3M, but not 1MO-I3M (Sanchez-Vallet

et al., 2010). In contrast, 2 days of *Sl* feeding caused only a marginal increase in 4MO-I3M (130 %) but a substantial increase in 1MO-I3M (760 %) (Schweizer et al., 2013b). Moreover, *cyp81f2* mutant plants which have severely reduced 4MO-I3M levels are not more susceptible to ABA- and JA-inducing generalist chewing herbivores than wild-type plants (Pfalz et al., 2009). Taken together, it would seem plausible that the observed long-term induction of *MYB34* and long-term repression of *MYB51* after JA seedling treatment causes a shift in the indole GS composition towards MYB34-dependent 1MO-I3M and I3M and away from the MYB51-dependent 4MO-13M. In turn, this would result in enhanced resistance to generalist chewing herbivores and susceptibility to pathogens, providing 1MO-I3M is the important indole GS for generalist chewing herbivore resistance yet does not play a role in defence against pathogens. Future work is required quantify the levels of individual indole GSs following JA seedling treatment and to determine the susceptibility of plants deficient in 1MO-I3M to generalist chewing herbivores and pathogens. It would also be interesting to test the ability of *myb34*, *myb51* and *myb34 myb51* mutants to express JA-IR to *Sl* and JA-IS to *Pc* and *Ps*.

2.4.4. Long-Lasting JA-IS to Necrotrophic and Biotrophic Pathogens is Associated with Repression of JA/ET- and SA-Dependent Defence Genes but does not Require MYC TFs

The MYC2 TF suppresses the EIN3/EIL3-dependent branch of the JA defence response, which is co-regulated by ET and controls resistance against necrotrophic pathogens (Stotz et al., 2000; Bodenhausen and Reymond, 2007; Song et al., 2014; Broekgaarden et al., 2015). However, this MYC-dependent signalling crosstalk does not explain long-term JA-IS against necrotrophic pathogens, since *myc2* and *myc234* mutants displayed wild-type levels of JA-IS to *Pc* (Figure 2.8). Our transcriptome analysis identified a set of 796 IS-related genes showing long-term repression by JA seedling treatment (Figure 2.10). Functional analysis highlighted that many of these genes are involved in the Arabidopsis anti-pathogen defence response (Figures 2.9 and 2.10 and Supplemental Data Sets 2.10-2.15). For example, multiple genes involved in ET biosynthesis and signalling were among the JA-IS gene set. In response to a variety of stimuli, including necrotrophic pathogen infection, ET is synthesised from S-adenosyl-L-methionine (SAM) (Wang et al., 2002; Li et al., 2012a). ACC-synthase (ACS) converts SAM into 1-aminocyclopropane-1-carboxylic acid

(ACC). In turn, ACC is converted to ET via an exothermic reaction catalysed by ACC oxidase (ACO) (Wang et al., 2002; Lin et al., 2009). ET biosynthesis is often considered to be controlled via the regulation of ACS activity as this is generally the rate-limiting enzyme in ET production (Xu and Zhang, 2014; Dubois et al., 2018). Interestingly, *ACS6* (*AT4G11280*) showed long-term transcriptional repression (Supplemental Data Set 2.12). The ACS isoform ACS6 is known to play a major role in necrotrophic pathogen induced ET production (Li et al., 2012a). Other genes showing long-term repression were multiple members of the mitogen-activated protein kinase (MAPK) and calcium-dependent protein kinase (CDPK) families (Supplemental Data Set 2.12). This is evidenced by the GO term “MAPK cascade” (GO:0000165), the KEGG pathway “MAPK signaling pathway – plant” (ath04016) and the protein signature “Protein kinase domain” (PF00069) functional categories which were associated with the repressed genes (Figure 2.10 and Supplemental Data Sets 2.13-15). MAPKs and CDPKs can be activated by biotic stress and may provide a connection between PRR-dependent extracellular pathogen perception and downstream intracellular defence signalling (Bigeard et al., 2015). For example, the collective evidence from multiple studies suggests that both MAPKs and CDPKs can regulate ACS activity and therefore ET biosynthesis in response to stress (Liu and Zhang, 2004; Joo et al., 2008; Han et al., 2010; Li et al., 2012a; Luo et al., 2014; Gravino et al., 2015; Li et al., 2018). ACS enzymes, including ACS6, are stabilised by MAPK phosphorylation, resulting in increased ACS activity and in turn enhanced ethylene production (Liu and Zhang, 2004; Joo et al., 2008; Han et al., 2010). ACS enzymes are also thought to be regulated by MAPKs at a transcriptional level, as the induction of *ACS2* and *ACS6* in response to *B. cinerea* infection is partially dependent on WRKY33, a TF which is activated upon pathogen stress by MAPK phosphorylation (Mao et al., 2011; Li et al., 2012a). Interestingly, the *WRKY33* gene itself also showed long-term repression by JA seedling treatment (Supplemental Data Set 2.12).

ET is best known for its positive regulation of defences and resistance against necrotrophic pathogens (Thomma et al., 1999; Tsuchisaka et al., 2009). The anti-microbial plant defensin encoding *PDF1.2* is a classic example of an ET-inducible defence mechanism (Penninckx et al., 1996; Penninckx et al., 1998) and we found it to be repressed long-term by JA seedling treatment (Figure 2.3B). ET also plays a role in resistance against biotrophic pathogens. Evidence for this comes from *acs* mutants

that are impaired in stress-induced ET emission and exhibit enhanced susceptibility to *Ps* (Guan et al., 2015). Thus, a repression of genes encoding for an ET biosynthesis enzyme (*ACS6*) and its regulators (e.g. *WRKY33*), may well have contributed to the long-lasting JA-IS to both *Pc* and *Ps*. Future studies are needed to determine whether ET accumulation in response to pathogen infection is reduced in plants from JA treated seedlings. Furthermore, it would be interesting to test whether JA-IS is absent in plants which have enhanced ET levels due to ACS6 having been artificially stabilised via the overexpression of a form of ACS6 which behaves as if it was phosphorylated (e.g. Liu and Zhang, 2004; Luo et al., 2014).

Aside from ET biosynthesis, MAPKs and CDPKs also activate numerous other downstream responses (Bigeard et al., 2015). For instance, the biosynthesis of camalexin, an important anti-pathogen phytoalexin (Ren et al., 2008; Piasecka et al., 2015). As with ET biosynthesis, WKRY33 functions downstream of MAPK cascades in the regulation of camalexin biosynthesis in response to necrotrophic pathogen infection (Mao et al., 2011). Interestingly, as evidenced by the overrepresented "WRKY domain" (G3DSA:2.20.25.80) protein signature among the 796 JA-IS associated genes (Figure 2.10 and Supplemental Data Set 2.14), *WRKY33* was among a group of 14 WRKY encoding genes that were repressed by JA seedling treatment. The majority of these repressed WRKYs regulate defences effective against necrotrophic and/or biotrophic pathogens (Li et al., 2004; Xu et al., 2006; Zheng et al., 2006; Kim et al., 2008; Lai et al., 2008; Li et al., 2010; Pandey et al., 2010; Gao et al., 2011; Li et al., 2017a; Yan et al., 2018). For instance, genome-wide DNA-binding data suggests that WRKY18 and WRKY40 may regulate numerous ET and SA biosynthesis and signalling genes (Birkenbihl et al., 2017). Thus, unsurprisingly, plants with either reduced or increased expression of these two WRKY TFs show altered resistance to *Ps* and *B. cinerea* (Xu et al., 2006). Considering that WRKY-binding W-box containing motifs were enriched in the promoters of the 796 IS-related genes (Figure 2.10 and Supplemental Data Set 2.16), it is plausible that the long-lasting repression of the 14 WRKY TFs plays a role in the JA-IS to *Pc* and *Ps*. Future studies should assess whether long-term JA-IS is alleviated in plants overexpressing a combination of the repressed WRKYs.

In addition to W-box elements, the promoters of the 796 IS-related genes were also enriched with TGA TF-binding motifs (Supplemental Data Set 2.16). The current

model of SA perception indicates that promoter-localised protein complexes of NONEXPRESSER OF PR GENES (NPR) and TGA proteins are the primary regulators of SA-dependent gene induction (Ding et al., 2018; Innes, 2018). One example of a gene that is activated in a NPR- and TGA-dependent manner in response to SA inducing pathogens is *SAR DEFICIENT1* (*SARD1*, *AT1G73805*), a regulator of both pathogen induced SA biosynthesis and numerous other genes related to plant immunity (e.g. *PR1*) (Zhang et al., 2010; Sun et al., 2015; Ding et al., 2018). This regulatory gene of SA-dependent defences was amongst our selection of 796 IS-related genes showing long-lasting repression after JA seedling treatment (Supplemental Data Set 2.12), which offers an attractive explanation for long-lasting IS to *Ps* (Figure 2.1C) and the long-lasting repression of SA-induced *PR1* expression (Figure 2.3C). To confirm the role of SARD1 in JA-IS to *Ps*, future studies should test whether JA-IS to *Ps* is repressed in *SARD1* overexpressor lines (Zhang et al., 2010).

2.4.5. JAZ Repressors: Master Regulators of Long-Term JA-IR and JA-IS?

Since MYC234 TFs are essential for the long-lasting JA-IR against *Sl* (Figure 2.7) but not for JA-IS to *Pc* (Figure 2.8), it remains unclear whether there are master regulators of both the long-term JA-IR and JA-IS. It is, however, tempting to speculate that the upstream JAZ repressors could fulfil this role. The authors of recent reviews have hypothesised that specificity in the response to JA can be at least partially explained by the JAZ repressors having subtly different targets (Chini et al., 2016; Howe et al., 2018). It is therefore plausible that JAZ repressors which preferentially target and are important negative regulators of the EIN3/EIL1 TFs, are upregulated and/or stabilised long-term by the JA seedling treatment. However, if JAZs are upregulated and/or stabilised how can the JA seedling treatment still enhance the activity of the MYC branch? It is thought that MYCs are regulated by most JAZs (Chini et al., 2016). Thus, a larger subset of JAZs which do not have a major regulatory impact on EIN3/EIL1 would also need to be repressed for JA seedling treatment to enhance the activity of the MYC branch in parallel to repressing the EIN3/EIL1 branch. This hypothesis can not only explain the JA-IR to *Sl* and JA-IS to *Pc* but also the JA-IS to *Ps*, as it has previously been shown that this hemi-biotrophic pathogen hijacks the MYC branch of the JA signalling pathway to repress SA-dependent defences and stomatal immunity (Zheng et al., 2012; Gimenez-Ibanez et al., 2017). Recent studies using higher-order *jaz* mutants have provided some support for our hypothesis

(Campos et al., 2016; Major et al., 2017; Guo et al., 2018). The *jaz* quintuple (*jazQ*) mutant, which is deficient in *JAZ1*, *-3*, *-4*, *-9* and *-10*, has a strikingly similar phenotype to plants from JA-treated seedlings. Compared to the wild-type Col-0, *jazQ* is more resistant to the generalist chewing herbivore *Trichoplusia ni* (Campos et al., 2016; Major et al., 2017; Guo et al., 2018) yet more susceptible to the necrotrophic and biotrophic pathogens *B. cinerea* (Guo et al., 2018) and *Ps* (Major et al., 2017), respectively. Furthermore, much like the JA seedling treated plants, the *jazQ* mutant has a reduced leaf area (Supplemental Figure 2.3) (Campos et al., 2016). The enhanced herbivore resistance of the *jazQ* mutant is also associated with an upregulation of GS homeostasis genes, along with enhanced expression of anti-insect proteins, such as VSP2 (Campos et al., 2016; Major et al., 2017). Whereas the enhanced susceptibility to *B. cinerea* correlates with reduced expression of ET signalling and downstream defence genes (Guo et al., 2018). Interestingly, this repression is reversed in the *JAZ1-7*, *-9*, *-10* and *-13* deficient *jaz* decuple (*jazD*) mutant. ET-dependent signalling and defences are constitutively upregulated and thus the *jazD* mutant is much more resistant than Col-0 to *B. cinerea* (Guo et al., 2018). Furthermore, the *jazD* mutant is also substantially more resistant than Col-0 to *T. ni* which correlates with enhanced VSP expression and GS levels. However in contrast to the *jazQ* mutant, which predominantly accumulates aliphatic glucosinolates, it is mainly indolic glucosinolates that accumulate in the *jazD* plants (Campos et al., 2016; Guo et al., 2018). Nevertheless, the phenotypes and molecular/metabolite analyses of the *jazQ* and *jazD* mutants suggest that one or more of JAZ2, -5, -6, -7 or -13 may act as major regulators of the *EIN3/EIL1*-dependent branch of the JA pathway. The transcriptome analysis by Campos et al (2016) shows that all but *JAZ6* have somewhat enhanced expression in the *jazQ* mutant, suggesting a compensatory effect. Thus, much like we proposed in our hypothesis at the start of this paragraph, in the *jaz*Q mutant, a subset of JAZ's are upregulated whereas another portion are absent (repressed). However, often the increase in JAZ expression in the *jazQ* mutant is marginal. Furthermore, our transcriptome analysis does not provide evidence for JA seedling treatment enhancing and repressing the same JAZ's as in the *jazQ* mutant (Supplemental Figure 2.7). In general, JA seedling treatment only had a very minor long-lasting impact on *JAZ* gene expression. Nevertheless, it is very plausible that the impact of JA seedling treatment on JAZs is post-transcriptional. For instance, maybe JA seedling treatment influences alternative splicing and changes the ratio of *JAZ*

isoforms. There is increasing evidence that alternative splicing can influence JAZ stability in the presence of JA-Ile (Chini et al., 2016; Howe et al., 2018). Thus, it would be interesting to use mass spectrometry to explore the protein levels of different JAZs in plants seedling treated with water or JA and subsequently challenged with water or JA. Furthermore, future experiments are needed to test whether JA-IR and JA-IS are affected in the *jazQ* mutant. Finally, by using a combination of overexpression and mutation of *JAZ* genes, it may be possible to determine which combinations of JAZs are key to the expression of the long-lasting JA-IR and JA-IS.

2.4.6. Long-Lasting JA-IR Against *Spodoptera littoralis* is Dependent on the Regulation of DNA Methylation at TEs and is Associated with Sporadic Hypomethylation at *ATREP2* TEs

In contrast to short-term JA-IR against the generalist chewing herbivore *Sl,* long-term JA-IR against *Sl* was impaired in the *nrpe1-11* and *ros1-4* mutants (Figure 2.11). Considering that DNA methylation at many TEs is antagonistically controlled by NRPE1-dependent RdDM and ROS1 (Tang et al., 2016; Zhang et al., 2018b), these results indicate that long-term JA-IR requires regulation of DNA methylation at TEs. Rasmann and colleagues reported that two RdDM mutants deficient in the biogenesis of sRNAs failed to express MeJA-elicited transgenerational acquired resistance (TAR) against the specialist chewing herbivore *Pieris rapae*, suggesting a similar dependency on functional RdDM (Rasmann et al., 2012). However, the RdDM mutants used by Rasmann et al (2012) exhibited increased levels of basal resistance to *P. rapae*, which suggests that RdDM is a negative regulator of resistance against this herbivore, and that the hypomethylated status of RdDM mutants mimicked the defence phenotype of transgenerational MeJA-IR. By contrast, while *nrpe1-11* and *ros1-4* were both impaired in long-term JA-IR against *Sl*, they were unaffected in basal resistance against this herbivore (Figure 2.11). Hence, RdDM and ROS1 both act as positive regulators of long-term JA-IR. A similar pattern was reported by Le et al (2014), who found that RdDM and ROS1/DEMETER-LIKE2(DML2)/DML3-dependent DNA demethylation both act as positive regulators of basal resistance against *Fusarium oxysporum*. A possible explanation for the similarity in phenotype between mutants in RdDM and ROS1 comes from the fact that RdDM mutants are strongly affected in *ROS1* gene expression, due to an RdDM-activated DNA methylation monitoring sequence in the promoter of this gene (Lei et al., 2015; Williams et al., 2015). This so-

called ‘methylstat’ allows for negative feedback on excessive DNA methylation at TEs. The implication of this regulatory system suggests that ROS1-dependent DNA hypomethylation at TEs is a key mechanism underpinning long-term JA-IR against *Sl*, which is supported by our finding that the majority of DMRs after JA seedling treatment were hypomethylated and located at TEs (Figure 2.13C).

Biotic stress induces genome-wide DNA hypomethylation in plants (Wilkinson et al., 2019). For instance, both *Ps* infection and SA treatment can induce wide-spread hypomethylation in Arabidopsis (Pavet et al., 2006; Dowen et al., 2012). Furthermore, infection of Arabidopsis roots by the beet cyst nematode *Heterodera schachtii* (Hewezi et al., 2017), as well as early gall formation by the root-knot nematode *Meloidogyne graminicola* in rice (*Oryza sativa*) (Atighi et al., 2020), have been reported to induce genome-wide hypomethylation. There is also some evidence from *Brassica rapa* that suggests MeJA treatment generally induces a loss of methylation (Kellenberger et al., 2016). Many of these studies have shown that the hypomethylation is particularly prevalent at TEs (Dowen et al., 2012; Hewezi et al., 2017; Atighi et al., 2020). Interestingly, this aligns with what we observed, long-lasting hypomethylation at TEs induced by JA seedling treatment (Figure 2.13C). However, previously reported methylomes of stressed plants show consistent DNA hypomethylation at the same loci, whereas our plants from JA-treated seedlings showed little consensus in the locality of the hypo-methylated DMRs across replicate comparisons (Supplemental Data Set 2.19).

The low number of consensus DMRs, coupled with the fact that those which did exist did not occur in the promoters of primed and/or prolonged upregulated IR-related defence genes, suggests involvement of *trans*-acting mechanisms in JA-IR against *Sl*. Recent studies have suggested that DNA methylation at TEs can *trans*-regulate distal defence genes (Cambiagno et al., 2018; Furci et al., 2019). It has been hypothesised that sRNAs could be important for this mode of defence gene regulation (Figure 1.4) (Wilkinson et al., 2019). With this in mind we propose a model (Figure 2.14) to explain both how the observed JA seedling treatment induced DMRs came about, and how differential methylation at TEs links to the long-term ROS1-dependent JA-IR against *Sl*. (i) Treatment of 2-week-old seedlings with JA results in genome-wide ROS1-dependent hypomethylation of TEs leading to a loss of silencing and increased TE expression (Panda and Slotkin, 2020). (ii) The reduced methylation levels feedback

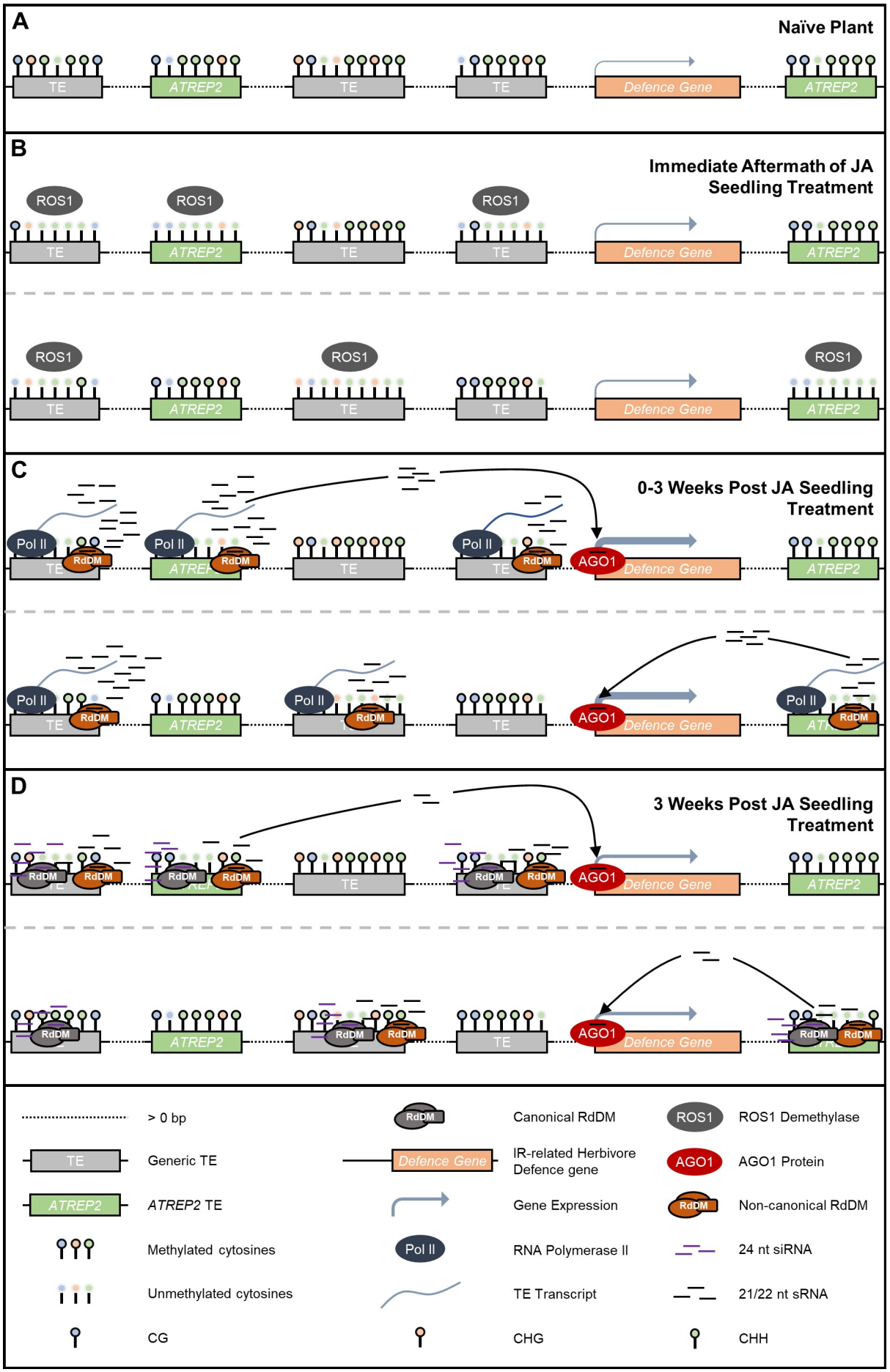
A
Naïve Plant
TE
ATREP2
Defence Gene
B
Immediate Aftermath of JA Seedling Treatment
ROS1
C
0-3 Weeks Post JA Seedling Treatment
Pol II
RdDM
AGO1
D
3 Weeks Post JA Seedling Treatment
> 0 bp
Generic TE
ATREP2 TE
Methylated cytosines
Unmethylated cytosines
CG
Canonical RdDM
IR-related Herbivore Defence gene
Gene Expression
RNA Polymerase II
TE Transcript
CHG
ROS1 Demethylase
AGO1 Protein
Non-canonical RdDM
24 nt siRNA
21/22 nt sRNA
CHH

on ROS1 activity via a 'methylstat' dependent downregulation of *ROS1* gene expression (Lei et al., 2015; Williams et al., 2015). (iii) Pol II derived TE transcripts are degraded to 21/22 nt sRNAs by the post-transcriptional gene silencing (PGTS) pathway (Ito et al., 2011; McCue et al., 2012; Cuerda-Gil and Slotkin, 2016). The 21/22 nt sRNAs function as part of a non-canonical Pol IV-independent RdDM pathway to begin to restore methylation at the activated TEs (Nuthikattu et al., 2013; Matzke and Mosher, 2014; McCue et al., 2015; Cuerda-Gil and Slotkin, 2016; Panda et al., 2016). (iv) Due to sequence homology, the 21 nt sRNAs produced from upregulated TEs recruit AGO1 to distal IR-associated JA inducible defence genes. In turn AGO1 promotes the transcription of these genes. (Note - A recent study has demonstrated that AGO1 plays a 21 nt sRNA dependent role in promoting transcription, particularly of JA inducible genes (Liu et al., 2018)). (v) Symmetric CG and CHG sites which were only partially hypomethylated, or which have been partially remethylated by non-canonical RdDM, are quickly fully re-methylated by MET1 and CMT3 which are recruited to the hemi-methylated sites by VIM and SUVH4 proteins (Du et al., 2014a; Kim et al., 2014). The CHH sites are slower to be remethylated as the redirection of sRNAs to AGO1 results in a smaller pool available for RdDM at TEs. (vi) The histone methyltransferase KRYPTONITE/SUPPRESSOR OF VARIEGATION 3-9

Figure 2.14. JA Seedling Treatment Induced DNA Hypomethylation at *ATREP2* TEs Controls Long-term Expression of Herbivore Defence Genes (*Figure appears on previous page*).

(A) The TE DNA methylation status and basal expression of a representative herbivore defence gene in a naïve plant. The TEs and herbivore defence gene may be nearby or far apart on the same or different chromosomes.
(B) JA treatment of 2-week-old seedlings induces genome-wide ROS1-dependent hypomethylation at TEs. The exact location of the hypomethylation varies between plants (two plants are depicted, above and below the grey dashed line respectively).
(C) Pol II transcripts from hypomethylated and unsilenced TEs, are degraded to 21/22 nt sRNAs. Based on sequence homology, sRNAs from particularly *ATREP2* TEs, target AGO1 to IR-related herbivore defence genes. In turn AGO1 promotes transcription. The 21/22 nt sRNAs also play a role in a non-canonical RdDM pathway which begins to re-establish methylation at TEs.
(D) The establishment of some methylation by non-canonical RdDM enables recruitment of MET1 and CMT3 (not shown) which ensure symmetric CG and CHG sites, respectively, are fully remethylated. Pol IV is also recruited resulting in the production of 24 nt sRNAs and in turn canonical RdDM. TE expression declines and although some 21/22 nt sRNAs are generated in a Pol IV dependent manner, levels of 21/22 nt sRNAs also decline. AGO1's promotion of defence gene transcription is reduced, however as AGO1 remains associated with the herbivore defence genes upon subsequent stress the genes can be upregulated more rapidly. The gradual and imprecise nature of the sRNA reliant RdDM pathways mean that small CHH context rich hypomethylated regions remain long-term post JA seedling treatment. It is important to note that the exact timing of many aspects of this model remain unclear (e.g. the transition from non-canonical to canonical RdDM). A more detailed description of the model is provided in the text.

HOMOLOG4 (KYP/SUVH4) binds to CHH and CHG context DNA methylation and implements di-methylation of histone H3 lysine 9 (H3K9me2) (Johnson et al., 2007; Du et al., 2014a). In turn, SAWADEE HOMEODOMAIN HOMOLOG1 (SHH1) binds to this histone mark and recruit Pol IV (Law et al., 2013; Zhang et al., 2013). (vii) The canonical 24 nt sRNA and Pol IV dependent RdDM pathway gradually take over the reestablishment of DNA methylation and transcriptional TE silencing. (viii) TE expression declines and thus so too does the production of 21/22 nt sRNAs from the degradation of TE transcripts. However a low level of 21 nt sRNAs are produced in a Pol IV dependent manner and are incorporated into AGO1 (Panda et al., 2020). Thus AGO1 continues to associate with the JA inducible IR-associated defence genes (Liu et al., 2018). However, due to the overall lower level of 21 nt sRNAs this association will be weaker. In turn the expression of IR-related genes will decline although the genes will remain primed for a faster upregulation in response to future attack. (ix) By 3 weeks post JA seedling treatment, due to the gradual and imprecise restoration of CHH context DNA methylation by the RdDM pathways, only small hypomethylated regions remain. Occasionally, due to overcompensation by the RdDM pathways at specific loci, hypermethylated DMRs appear. The DMRs do not occur in the same locations between replicates due to inter-tissue and -individual variation in both the TEs which are originally de-repressed and the silencing re-establishment procedure. To begin to test this nine stage model, future studies should perform WGBS, sRNA sequencing, long read RNA sequencing (e.g. Panda and Slotkin, 2020) and ROS1/NRPE1 Chromatin Immunoprecipitation Sequencing (ChIP-seq) on leaf tissue harvested at various timepoints following the treatment of 2-week-old seedlings with JA. Not only should these omics approaches be conducted on wild-type Col-0 but also Pol IV mutants as this would allow for determination of when post JA seedling treatment the canonical RdDM pathway begins to become important. While our model suggests that canonical RdDM has taken over by 3 weeks post JA seedling treatment, it is plausible that this is incorrect and non-canonical RdDM pathways are still playing a major role in DNA methylation re-establishment. Finally, it would also be interesting to determine whether JA-IR against *Sl* is repressed in *ago1* mutants.

Our model explains how the small mainly hypomethylated CHH context DMRs can be generated and how DNA methylation at TEs can *trans*-regulate JA-IR related defence genes. However, what it currently does not explain is how major variation

between samples in which TEs remain differentially methylated long term, can lead to consistent priming and/or upregulation of JA-dependent defence genes. A plausible explanation to this question comes from the high degree of homology between TEs (Wicker et al., 2007), which generates redundancy in the ability of TEs of the same family and/or related families to generate similar defence inducing sRNAs. In this context, perhaps the most remarkable outcome of our methylome analysis is the very significant enrichment of the *ATREP2* TE family among the TEs overlapped by CHH context rich and predominantly hypomethylated DMRs (Figures 2.13D and 2.13E). Based on our model of RdDM-dependent recovery of CHH methylation, this targeting suggests a very specific role of *ATREP2* TEs in the genome-wide orchestration of plant immune memory after exposure to JA-related biotic stress (Figure 2.14).

2.5. Methods

2.5.1. Plant Materials and Growth Conditions

Arabidopsis thaliana var. Columbia (Col-0) seeds were originally obtained from Maarten Koornneef (University of Wageningen, The Netherlands). Seeds of the *jin1-7* (SALK_040500), *jin1-10* (SALK_083483) and *ros1-4* (SALK_135293) mutants were obtained from the Nottingham Arabidopsis Stock Centre (NASC). Seeds of the *nrpe1-11* (SALK_029919) single mutant and the *myc2 myc3 myc4* (*myc234*) (Fernández-Calvo et al., 2011) triple mutant were kindly provided by Pablo Vera (Instituto de Biología Molecular y Celular de Plantas, Spanish National Research Council, Spain) and Roberto Solano (Centro Nacional de Biotecnología, Consejo Superior de Investigaciones Científicas (CNB-CSIC), Spain), respectively. The seeds were stored at 4 ºC, in the dark and suspended in deionised H_2O (dH_2O) for 4 days to break the dormancy. Seeds were sown in soil consisting of Scott's Levington M3 compost (Everris) and sand in a 3:1 ratio and cultivated under Arabidopsis short-day growth conditions (8.5 hour day at 21 ºC and 15.5 hour night at 21 ºC; 45-70% relative humidity; 100 – 150 µE m^{-2} s^{-1}).

2.5.2. Pathogen Strains and Cultivation

Plectosphaerella cucumerina strain *BMM* (*Pc*) was originally obtained from Professor Brigitte Mauch-Mani (University of Neuchâtel, Switzerland). *Pc* was continuously cultured on potato dextrose agar (Oxoid, CM0139), in the dark and at room temperature (15-25 ºC). Four weeks prior to spore collection for each assay, a plug of *Pc* potato dextrose agar was transferred to a new plate.

Pseudomonas syringae pv. *tomato* DC3000 *luxCDABE* (*Ps*) was originally obtained from Fan et al (2008). Glycerol stocks of *Ps* were stored at -80 ºC. Two days prior to inoculation, a glycerol stock was thawed on ice and then cultured at 28 ºC on King's B agar plates supplemented with rifampicin (50 µg ml^{-1}) and kanamycin (50 µg ml^{-1}).

2.5.3. Insect Rearing

Spodoptera littoralis (*Sl*) eggs were kindly provided by Professor Ted Turlings (University of Neuchatel, Switzerland). Larvae were reared in house on a semi-artificial Haricot-bean based diet, which was formulated based on the diets in Gupta et al

(2005), Roeder et al (2010) and Bricchi et al (2013). A full diet ingredient list is provided in Table 2.1. Diet was prepared by first autoclaving the agar with half of water (300 ml) and then second mixing that autoclaved agar with all the other ingredients. Eggs were hatched in 55 mm petri dishes containing a layer of diet across the bottom. To prevent cannibalism, larvae were gradually thinned out until there was only one third instar larvae in each petri dish. Following pupation in the diet containing petri dishes, pupae were transferred to a BugDorm-4 Insect Rearing Cage (Natural History Book Service, #211478). A 5% sugar solution was provided as a food source for the adult moths. Eggs were collected from the side wall of the BugDorm-4 Insect Rearing Cage.

Table 2.1. – *Spodoptera littoralis* Diet Ingredients List

Ingredient	Amount	Supplier	Product code
Haricot Beans	125 g	Real foods	NA
Agar	20 g	NEOGEN	MC006
Ascorbic Acid	4 g	Sigma Aldrich	A1417
Multivitamin A-Z Daily Tablets	2 Tablets	Lindens Health and Nutrition	5060332533763
Ethyl 4-hydroxybenzoate	2.25 g	Sigma Aldrich	111988
Formaldehyde Solution (approx. 35-40% Formaldehyde)	325 µl	Sigma Aldrich	F8775
Propionic Acid	836 µl	BDH	296884k
Phosphoric Acid solution	84 µl	Sigma Aldrich	W290017
Sorbic Acid	0.016 g	Sigma Aldrich	S1626
Benzoic Acid	0.008 g	Sigma Aldrich	242381
Chloramphenicol	0.002 g	BioVision	2486
Distilled Water	600 ml	NA	NA

2.5.4. Hormone Treatments

All treatments were performed in the same manner, with a control or hormone solution being sprayed over a plant until its upper leaf surfaces were entirely covered. Hormone stock solutions were made by diluting or resuspending Jasmonic acid (JA; Sigma Aldrich, J2500), 1-Aminocyclopropanecarboxylic acid (ACC; Sigma Aldrich, A3903) and Salicylic acid (SA; Sodium salicylate, Sigma Aldrich, S3007) in absolute

ethanol (JA and SA; Fisher Scientific, E/0650DF/17) or dH_2O (ACC). All hormone solutions for both induction (pre-) and challenge treatments were prepared by diluting stocks with dH_2O. Pre-treatments were performed with 1 mM JA solutions apart from in a single dose-response experiment where 0.05, 0.1 and 0.5 mM JA solutions were also used. Challenge treatments were performed with 0.5 mM SA, 0.1 mM JA or 0.1 mM JA + 0.1 mM ACC solutions. The controls of both the pre-treatments (named 'control') and challenge treatments (named 'mock') consisted of dH_2O supplemented with the same percentage of ethanol as in the hormone solution or the strongest hormone solution in the case of the dose-response experiment. To ensure even distribution over the surface of leaves, all solutions were supplemented with 0.02% of the surfactant silwet L-77 (LEHLE SEEDS, VIS-30). Pre-treatments were performed when plants were either 2 weeks old (long-term experiments; seedling treatment; three weeks prior to challenge) or nearly 5 weeks old (short-term experiments; 1 day prior to challenge; Figure 2.1A). Challenge treatments were performed when plants were 5 weeks old.

2.5.5. Seedling Induction Treatment by Herbivory

To test the long-term effects of seedling herbivory, second instar *Sl* larvae were placed on 2-week-old wild-type plants and allowed to feed until 50 - 75% of above ground tissue had been removed. To encourage larvae to feed, particularly on the leaves and not the stem, soil was piled up around the stem and a 15 ml falcon tube was placed over each plant. To account for the impact of any damage caused by soil piling or covering the plants with falcon tubes, control plants received the same treatment.

2.5.6. Necrotrophic Pathogen (*Plectosphaerella cucumerina*) Bioassays

At three weeks (long-term experiments) or 1 day (short-term experiments) post pre-treatments (Figure 2.1A), four leaves of similar age and developmental stage from 5-week old plants (Col-0, *myc234*, *nrpe1-11*, *ros1-4*, *jin1-7* or *jin1-10)* were droplet inoculated with 6 µl droplets containing 5 x 10^6 spores per ml of *Pc*, as described previously (Ton and Mauch-Mani, 2004; Pétriacq et al., 2016). The inoculum was prepared by inundating a 4-week old *Pc* culture on PDA agar with dH_2O, gently scraping the spores into suspension, quantifying the spore density using a hemocytometer (Improved Neubauer, Hawksley, UK) and diluting the inoculum to the

required density with dH_2O. Inoculated plants were maintained at 100% relative humidity (RH) to promote disease progression. Lesion diameters were measured between 6 and 8 days post inoculation (dpi), using Vernier callipers. The exact time-point of measuring lesion diameters depended on the speed of disease progression. We aimed to select a day when the lesions were both visible on the most resistant plants but also not so large in the most susceptible plants that they had covered whole leaves and become unmeasurable. A single replicate lesion diameter equates to the average diameter of lesions from four inoculated leaves of a single plant. All assays had between 16 and 22 replicates per pre-treatment/genotype combination.

2.5.7. Hemi-Biotrophic Pathogen (*Pseudomonas syringae*) Bioassays

At three weeks (long-term experiments) or 1 day (short-term experiments) after pre-treatments (Figure 2.1A), four leaves of 5 week old Col-0 plants were syringe infiltrated with a 10 mM $MgSO_4$ inoculum containing *Ps* bacteria at OD_{600nm} = 0.0002 (Morel and Dangl, 1999; Yang et al., 2015). Plants were maintained at 80-100% RH. At three dpi, four leaf disks of 0.2 cm^2 were harvested per plant, with one plant equating to one biological replicate. Leaves were ground in 10 mM $MgSO_4$ and then a 5-fold dilution series was plated on King's B agar plates supplemented with rifampicin (50 µg ml^{-1}) and kanamycin (50 µg ml^{-1}). Plates were incubated at 28 ºC for 20 hours and 4 ºC for 17 hours prior to the counting of colonies. Colonisation was expressed as the number of colony forming units (cfu's) per cm^2. All assays had between 9 and 12 biological replicates per pre-treatment group.

2.5.8. Chewing Herbivore (*Spodoptera littoralis*) No-Choice Bioassays

Plants (Col-0, *myc234*, *nrpe1-11* and *ros1-4*) were grown in separate 425 ml transparent plastic cups (event supplies, 5055202181045) which had three ~ 0.8 cm^2 holes drilled in the bottom to allow water drainage. At three weeks (long-term experiments) or 1 day (short-term experiments) post pre-treatments (Figure 2.1A), a single *S. littoralis* neonate was placed on each plant with a fine paintbrush. A transparent lid (event supplies, 5055202181113) was placed on each cup to prevent larval escape. After 5 to 7 days of feeding, larvae were removed and weighed. The feeding period length was adjusted between experiments to prevent complete consumption of the most susceptible plants. Each biological replicate consisted of the

weight of one single larva fed on an individual plant. All assays had between 23 and 24 replicates per pre-treatment/genotype group.

2.5.9. Chewing Herbivore (*Spodoptera littoralis*) Dual Choice Bioassay

To test the effect of long-term JA-IR on *Sl* behaviour and confirm the involvement of RdDM and ROS1 in long-term JA-IR against this herbivore, dual-choice assays were performed with 5-week-old plants (Col-0, *npre1-11* and *ros1-4*) at three weeks after seedling treatments. Every choice assay arena contained two 5-week old plants of the same genotype. One plant in the arena was from a 2-week-old seedling treated with a 1 mM JA, while the other (naïve) plant was from a 2-week-old seedling treated with water (control). The plants were positioned in a 1000 ml transparent plastic container backfilled with soil. The two plant pots were separated by a 30 mm upturned petri dish lid. Five second and third instar *Sl* larvae were placed in the petri dish lid. A lid with pin prick holes was placed over the choice arena to prevent larval escape. After 20 hours, the position of each larvae was recorded. If a larva was not on a plant, or on the soil immediately under a plant, it was recorded as having not made a choice. Eighteen choice arena's were used for each of the genotypes: Col-0, *nrpe1-11* and *ros1-4*. The total numbers of larvae choosing the water or JA pre-treated plants, across all arenas of each genotype, were used for Goodness-of-fit tests ($p < 0.05$). The null hypothesis was that the proportion of larvae on plants from water- and JA-treated seedlings of a single genotype was equally distributed (50% vs. 50%).

2.5.10. Hyperspectral Quantification of Plant Size

Five-week-old plants (Col-0, *myc234*, *nrpe1-11* and *ros1-4*), from water or 1 mM JA treated two-week-old seedlings, were imaged using a Photon Systems Instruments PlantScreen HC 900 hyperspectral imaging (HSI) system. The system consisted of a push-broom scanner which had a halogen lamp light source and complementary metal-oxide-semiconductor (CMOS) detector (spatial resolution = 1000 pixels and spectral resolution = 0.8 nm) mounted on a motorised carriage, which travelled directly over trays of plants at 15 mms^{-1}. The lens of the camera was positioned ~ 20 cm above the rosettes and an 0.09 s exposure time was used. Raw intensity values were acquired for 480 wavebands across a 350 to 900 nm spectral range.

Plant size was approximated based on rosette surface area (RSA). A plants RSA was measured by counting the number of pixels in an image which were associated with that plant only and not the background or neighbouring plants. The separation or segmentation of a plant of interest from its background was achieved by using the following four step pipeline (i) A calibrated reflectance image (R) was produced, with reflectance values for all wavebands and pixels being generated using Equation 2.1 and the intensity values from a raw hyperspectral image (I_{raw}) and two reference images of the same white Teflon standard, one of which was taken in the light (I_{light}) and one in complete darkness (I_{dark}). See Mishra et al (2017) for more information about calibration procedures.

Equation 2.1. - Raw Hyperspectral Image Calibration

$$R = \frac{I_{Raw} - I_{dark}}{I_{light} - I_{dark}}$$

(ii) The broad area of the calibrated image containing the plant of interest was defined. (iii) All pixels within the defined area with a plant index (Equation 2.2) > 0.53 were selected. The plant index (Equation 2.2) utilises wavebands which show differential reflection between plant leaves and the background (e.g. soil).

Equation 2.2. - Plant Index

$$Plant\ index = 1.2\big(2.5(R_{740} - R_{672}) - 1.3(R_{740} - R_{556})\big)$$

(iv) The selected group of plant-associated pixels ('plant mask') was eroded to remove noise associated with the edge of leaves. Approximately one layer of pixels was removed from the edge of the plant mask. Photo analysis was performed using PlantScreen Data Analyser software (Photon Systems Instruments) and an in house developed R version 3.6.1 (R Core Team, 2019) package.

2.5.11. RNA Extractions

Two-week-old wild-type (Col-0) plants were treated either water (control) or JA and challenged three weeks later with water (mock), JA, SA, or JA + ACC. At 4, 8 and 24 hours post challenge, leaf material was harvested and snap frozen. Each treatment/timepoint combination had up to four biological replicates. Each replicate consisted of eight leaves, four from each of two plants. All leaves were of a similar age

and developmental stage. Frozen leaf tissue was ground to a powder using 3 mm diameter steel ball bearings (Atlas Ball & Bearing Co Ltd) and a TissueLyser (Qiagen). RNA extractions were performed exactly as described by López Sánchez et al (2016) and Furci et al (2019). Total RNA concentration and quality was determined used a Nanodrop 8000 Spectrophotometer (Thermo Scientific) and gel electrophoresis, respectively.

2.5.12. Reverse Transcriptase-Quantitative Polymerase Chain Reactions (RT-qPCRs)

Genomic DNA removal and cDNA synthesis were performed as described by López Sánchez et al (2016) and Furci et al (2019) or the instructions of the "Maxima First Strand cDNA Synthesis Kit for RT-qPCR, with dsDNase" (Thermo Scientific, K1672). Approximately 1 µg of total RNA was used for cDNA synthesis. The qPCRs were conducted using the Rotor-Gene SYBR Green PCR Kit (Qiagen) and Rotor-Gene Q (Qiagen) real-time PCR cycler. Reactions were run with the following cycling conditions: 1 cycle of 10 mins @ 95 ºC and 35-40 cycles of 10 seconds @ 95 ºC and 40 seconds @ 60 ºC. C_t values were based on the 'take-off' values calculated by the Rotor-Gene Q 2.3.5 software. C_t values from reactions with primers targeting

Table 2.2. – RT-qPCR Primers

Target Gene	Forward primer (5'-3')	Reverse primer (5'-3')	Reference
VSP2 *AT5G24770*	GGACTTGCCCTAAAGAACGACACC	GTCGGTCTTCTCTGTTCCGTATCC	This Study
PDF1.2 *AT5G44420*	CTTGTTCTCTTTGCTGCTTTCGAC	TTGGCTCCTTCAAGGTTAATGCAC	This Study
PR1 *AT2G14610*	ACACGTGCAATGGAGTTTGTGG	TTGGCACATCCGAGTCTCACTG	This Study
GAPC2 *AT1G13440*	GCCATCCCTCAATGGAAAATT	GAGACATCAACGGTTGGAACA	This Study
UBC21 *AT5G25760*	CTGCGACTCAGGGAATCTTCTAA	TTGTGCCATTGAATTGAACCC	(Czechowski et al., 2005)
MON1 *AT2G28390*	AACTCTATGCAGCATTTGATCCACT	TGATTGCATATCTTTATCGCCATC	(Czechowski et al., 2005)

VEGETATIVE STORAGE PROTEIN2 (*VSP2*, *AT5G24770*), *PLANT DEFENSIN1.2* (*PDF1.2*, *AT5G44420*) and *PATHOGENESIS-RELATED1* (*PR1*, *AT2G14610*) were expressed relative to a single calibrator sample (a water seedling treatment and water challenge replicate from the 4 hour timepoint). Next the relative values were adjusted for amplification efficiency (E+1), normalised using the mean expression of three reference genes, *GLYCERALDEHYDE-3-PHOSPHATE DEHYDROGENASE C2* (*GAPC2*, *AT1G13440*), *UBIQUITIN-CONJUGATING ENZYME21* (*UBC21*, *AT5G25760*) and *MONENSIN SENSITIVITY1* (*MON1*, *AT2G28390*), and finally put relative to the average expression of four replicates harvested at 4 hours post water challenge of water seedling treated plants. Primer sequences for both the reference genes and the genes of interest are presented in Table 2.2.

2.5.13. Statistical Analysis of Data from Pathogen Bioassays, No-Choice Herbivore Bioassays, Hyperspectral Plant Size Assay and RT-qPCR Experiments

When all treatment groups data was normally distributed and had equal variances, two-sample t-tests (binary comparisons) or one-, two- or three-way ANOVAs followed by Tukey post-hoc tests (multiple groups), were used to determine if there was any significant differences. For comparisons between two normally distributed treatment groups with unequal variances, welch two-sample t-tests were used. If data was not normally distributed, either (i) the data was logged, squared or square-rooted and then the parametric tests above were used, or (ii) if the transformations did not normalise the data, the non-parametric Mann-Whitney test (binary comparisons) or Kruskal-wallis test followed by Pairwise Wilcoxon Rank Sum Tests (multiple groups) were used. The *p*-values from Pairwise Wilcoxon Rank Sum Tests were adjusted using the Benjamini-Hochberg correction (Benjamini and Hochberg, 1995). In all cases, a difference was deemed to be statistically significant if the (adjusted) p-value < 0.05. All statistical analyses were performed in R version 3.6.1 (R Core Team, 2019).

2.5.14. mRNA Sequencing (RNA-seq)

2.5.14.1. Library Preparation and Sequencing

RNA-seq was performed on the samples used for the JA challenge RT-qPCR experiment (Figure 2.3A). In total, 16 RNA samples were sequenced, four replicates

of each of the four combinations of the following treatments: seedling treatment (water or 1 mM JA), challenge (water or 0.1 mM JA) and time post challenge (4 hours). Quality and quantity of RNA was assessed using a nanodrop and 2100 Bioanalyzer (Agilent Technologies). All samples had RNA integrity number (RIN) of at least 6.4.

Library preparation and sequencing of all RNA samples was performed by BGI Tech Solutions (Hongkong) Company Limited (16 Dai Fu Street, Tai Po Industrial Estate, Tai Po, Hong Kong). As the BGI-seq (quantification) service was used, a standard protocol was followed for library preparation and sequencing. Briefly, total RNA was treated with DNase I to remove any contaminating genomic DNA. mRNAs were isolated via the selection for poly(A) tails using oligo dT sequences attached to magnetic beads. Following fragmentation of the purified mRNAs, first strand cDNA was synthesised with the help of random hexamer primers. Subsequent second strand cDNA synthesis was followed by end-repair and adenylation of the 3' end. Adaptors were ligated at the 3' adenylated ends before the cDNA was amplified by PCR. Purification of the amplified cDNA was performed using SPRI beads. Via denaturation and circularization with the help of a DNA splint, double stranded PCR products were converted to single strand circle DNA (ssCir DNA). The phi29 DNA polymerase created DNA nanoballs by amplifying the ssCir DNA. The DNA nanoballs were loaded onto a sequencing chip and then sequenced using the BGISEQ-500 functioning in its single end mode. More information on the technical details of BGI's in house sequencing platform, and evidence that its output is comparable to that of Illumina's HiSeq4000 platform when it comes to sequencing Arabidopsis transcriptomes, can be found in the following references: Huang et al (2017) and Zhu et al (2018).

Across all 16 samples a total of 598 million 50 bp single-end clean reads were generated, with an average of 37.4 million clean reads per sample (Supplemental Data Set 2.20). The reads were defined by BGI as 'clean' because adapter sequences, contamination and low-quality reads had been removed. As a result of this cleaning by BGI, on average 98.7% of nucleotides had a Phred quality score of > 20 (Supplemental Data Set 2.20).

2.5.14.2. Read Alignment and Counting

To check that the sequencing quality was sufficient, the read containing fastq files were analysed using the next generation sequencing data quality control tool

FASTQC version 0.11.5 (Andrews, 2010). The FASTQC reports, which were summarised using the convenient tool MultiQC version 1.7 (Ewels et al., 2016), suggested that common to all samples was the first 15 positions of reads having non-uniform contents of the four DNA bases. This is a common trait of RNA-seq libraries where the cDNA was generated using random hexamer primed reverse transcriptase. To avoid any issues this non-uniformity may cause with read alignment, the first 15 bases of reads were removed using the read trimming tool Trimmomatic version 0.38 (Bolger et al., 2014) run with the following parameter settings: 'SE', 'HEADCROP:15'. FASTQC analysis post trimming confirmed reads were ready for alignment, despite a high level of read duplication being flagged up. The high level of duplication, which is common in RNA-seq datasets, results from the deep sequencing of a small subset of the genome.

Reads were aligned to the Arabidopsis genome (Ensembl Plants version TAIR10.40) using the RNA-seq splice-aware read aligner STAR version 2.6.1b (Dobin et al., 2013), run with the default parameter settings. All samples had a read alignment efficiency between 89.3% and 90.8%, with the average being 90.3% (Supplemental Data Set 2.20). The number of reads mapping to each gene annotated in the Arabidopsis genome were counted using HTSeq-count version 0.9.1 (Anders et al., 2015) run with the following settings: '-i gene_id', '--stranded=no'.

2.5.14.3. Assessment of Global Gene Expression Patterns

Prior to differential expression analysis, global gene expression patterns across the 16 samples from the 4 hours post challenge timepoint were assessed. Read count tables were loaded into R using the DESeqDataSetFromHTSeqCount function from the DESeq2 package version 1.24.0 (Love et al., 2014). Genes with a total read count across all samples of < 100 were removed. To account for between-sample variation in sequencing depth and homogenise variances across genes of different expression levels, read counts were normalized for library size and transformed with a variance stabilising transformation (vst) (Anders and Huber, 2010). The transformation was conducted using the DESeq2 vst function run with the following option settings: 'blind=TRUE', 'nsub=1000', 'fitType = "parametric"'. Transformed count data was used for a principle component analysis (PCA) and a clustered heatmap of sample to sample distances. PCAs were performed using DEseq2's plotPCA function run with

the following parameter settings: ‘intgroup=c("Seedling.Treatment","Challenge")’, ‘ntop = (number of genes with ≥ 100 total read count)’, ‘returnData = TRUE’. The outcome of the PCA was displayed using the R package ggplot2 version 3.2.1 (Wickham, 2016). Another R package, pheatmap version 1.0.12 (Kolde, 2019), was used to generate a clustered heatmap which was based on Euclidean distances and the complete linkage clustering method.

2.5.14.4. Differential Expression Analysis and Selection of Genes Related to JA-IR and JA-IS

The aim of the differential expression (DE) analysis was to identify genes with expression profiles which correlated with either long-lasting JA induced resistance (IR) to *Sl* or long-lasting JA induced susceptibility (IS) to *Pc* and *Ps*. Genes exhibiting a prolonged upregulation and/or an augmented induction after challenge in plants from JA-treated seedlings were defined as IR-related genes (Wilkinson et al., 2019), whereas genes showing prolonged repression and/or stronger repression after challenge in plants from JA-treated seedlings were defined as IS-related genes. To identify these JA-IR and JA-IS associated genes, we first selected for genes showing a statistically significant interaction between seedling treatment and challenge treatment, which represent genes that respond differently to JA challenge as a result of JA seedling treatment. To this end, we used the DEseq function, from the DESeq2 R package, run with the following parameter settings: ‘test="LRT"’, ‘full = ~ Seedling.Treatment + Challenge + Seedling.Treatment:Challenge’, ‘reduced = ~ Seedling.Treatment + Challenge’. The DESeq2 results table, created using the results function run with the parameter options: ‘alpha = 0.01’, ‘cooksCutoff = F’, ‘lfcThreshold = 0’, was filtered to retain only genes with an adjusted *p*-value of < 0.01 (Benjamini and Hochberg correction) (Benjamini and Hochberg, 1995). A total of 2409 differentially expressed genes were selected.

For visualisation of the results of the first step of the DE analysis, count data for all 2409 significant genes was transformed by DESeq2’s vst function, run with the option settings: ‘blind=FALSE’, ‘nsub=1000’, ‘fitType = "parametric"’. The aheatmap function, from the NMF R package version 0.21.0 (Gaujoux and Seoighe, 2010), was used to calculate Pearson distances between genes, cluster genes using Ward’s method and display the relative expression values of genes in a heatmap.

The second step in the DE analysis was to reduce the number of selected genes and focus on those potentially associated with either the JA-IR or JA-IS. This was achieved by applying two sets of selection criteria. Both required that, for each gene, mean transformed counts were calculated for each of the four treatment groups: water seedling treatment and water challenge (W_W), JA seedling treatment and water challenge (JA_W), water seedling treatment and JA challenge (W_JA) and JA seedling treatment and JA challenge (JA_JA). The first set of selection criteria, which aimed to identify genes associated with JA-IR to *SI*, were as follows (i) gene must be JA inducible (W_JA > W_W) and (ii) gene must be more strongly expressed post JA challenge in replicates from plants of JA treated seedlings (JA_JA > W_JA). A heatmap displaying the resulting selection of 832 genes was created using the aheatmap function (NMF R package) run with the Spearman distance and Ward's clustering method options being specified. The dendrogram was cut into four gene clusters using the cutree function from the stats R package version 3.6.1 (R Core Team, 2019). Based on expression profile and enrichment of Gene Ontology (GO) terms related to antiherbivore defences, two clusters with a total of 203 genes were selected for further analysis. This final set of IR-related genes was displayed in a new heatmap created with the aheatmap function (NMF R package), using Pearson distances and the Ward's clustering method. Biological function analysis was also conducted on this final set of 203 IR-related genes. Genes associated with JA-IS were selected using the second set of selection criteria which were as follows (i) gene must be JA repressible (W_JA < W_W) (ii) gene must be more weakly expressed post JA challenge in replicates from plants of JA treated seedlings (W_JA > JA_JA). The resulting 904 genes were visualised in a clustered heatmap created using the aheatmap function (NMF R package), Pearson distances and Ward's clustering method. Based on enrichment with GO terms related to plant defence against biotrophic and necrotrophic pathogens, two clusters containing a total number of 796 genes were selected for further analysis and displayed in a new heatmap created as before. Further biological function analysis was performed on the combined set of 796 IS-related genes.

2.5.14.5. Gene Ontology (GO) Term Enrichment Analysis

GO term enrichment analysis was conducted in R using the clusterProfiler version 3.12.0 (Yu et al., 2012) and org.At.tair.db version 3.8.2 (Carlson, 2019),

packages. For analysis of single and multiple gene clusters, the clusterProfiler compareCluster and enrichGO functions, respectively, were used with the following parameter settings: ‘universe = all_genes_with_≥100_counts_across_all_samples’, ‘fun = "enrichGO"’ (compareCluster only), ‘OrgDb = 'org.At.tair.db'’, ‘keyType = "TAIR"’, ‘ont='BP"’, ‘minGSSize = 10’, ‘maxGSSize = 500’. Biological process GO terms were classed as enriched if they had an adjusted *p*-value of < 0.05 (Benjamini and Hochberg correction).

To reduce the redundancy of enriched GO terms, the clusterProfiler simplify function (Yu et al., 2010) was applied with the following settings: ‘cutoff = 0.7’, ‘measure = "Jiang"’, ‘semData = AtGO’ (a GOSemSimDATA object created using the function godata with the parameter settings: ‘OrgDb = "org.At.tair.db"’, ‘ont = "BP"’), ‘by = "p.adjust"’, ‘select_fun = min’. Further reduction of redundant GO terms was achieved by retaining only one term from each of the groups of terms which had the same: fold enrichment, background ratio (background genes annotated with the term / all genes in background) and list of associated genes from the input list (e.g. gene cluster, IR-related gene list). Fold enrichment plots of the most enriched non-redundant GO terms were created using the R package ggplot2. Supplemental Data Sets 2.3, 2.6, 2.10 and 2.13 display all overrepresented GO terms both pre- and post-simplification.

2.5.14.6. Protein Signature Enrichment Analysis

Protein signature annotations (e.g. protein domains) for Araport11 proteins were downloaded from TAIR. Signatures annotated in less than five proteins were removed. The enrichment function from the bc3net R package version 1.0.4 (de Matos Simoes and Emmert-Streib, 2016) was used to determine which of the remaining signatures were enriched in various candidate protein lists (e.g. gene cluster, IR-related gene list) when compared to a background. The background consisted of genes that (i) were analysed by DESeq2 (i.e. all genes with ≥ 100 reads across all samples) and (ii) encoded a protein with an annotated signature. For a signature to be classed as enriched it had to have an adjusted *p*-value ≤ 0.05 (Benjamini and Hochberg correction). Redundant enriched protein signatures were removed by only retaining one signature from each of the groups of signatures which had the same: fold enrichment, background ratio and list of proteins from the candidate list which

were annotated with the signature. Fold enrichment plots of the most enriched non-redundant protein signatures were created using the R package ggplot2. All overrepresented enriched protein signatures pre-redundancy selection are listed in Supplemental Data Sets 2.4, 2.7, 2.11 and 2.14.

2.5.14.7. Pathway Enrichment Analysis

The enrichKEGG and compareCluster functions from the R package clusterProfiler were used for enrichment analysis of Kyoto Encyclopaedia of Genes and Genomes (KEGG) pathways for single and multiple gene clusters, respectively. The parameter settings used for the two enrichment functions were as follows: ‘universe= all_genes_with_≥100_counts_across_all_samples’, ‘fun = "enrichKEGG"’ (compareCluster only), ‘organism = 'ath'', ‘keyType = 'kegg'’, ‘minGSSize = 10’, ‘maxGSSize = 500’. KEGG pathways were classed as enriched if they had an adjusted *p*-value < 0.05 (Benjamini and Hochberg correction). Fold enrichment plots of the most enriched KEGG pathways were created using the R package ggplot2.

2.5.14.8. Transcription Factor DNA-Binding Motif Enrichment Analysis

Promoter sequences (transcription start site to 1000 bp upstream) for all genes analysed by DESeq2 (≥100 reads across all samples), were downloaded from TAIR (version 10). These promoter sequences, together with the 803 Arabidopsis TF DNA-binding motifs found in the MotifDb collection version 1.26.0 (Shannon and Richards, 2019) and the functions makePriors, PFMtoPWM and makeBackground from the PWMEnrich R package version 4.20.0 (Stojnic and Diez, 2019), were used to create background distributions of TF DNA-binding motifs. To determine which of the 803 MotifDb Arabidopsis motifs were significantly overrepresented ($p < 0.01$) in a list of gene of interest promoters relative to the background, the PWMEnrich motifEnrichment (all option settings default apart from ‘group.only = F’) and groupReport (all option settings default) functions were used. Sequence logos were produced using the PWMEnrich plot function.

2.5.14.9. Visualising Expression Profiles of Glucosinolate Homeostasis and JAZ Genes

The 2409 genes displaying a significantly altered response to JA challenge as a result of JA seedling treatment (see section 2.5.14.4) were filtered to retain only

those known to be involved in glucosinolate (GS) homeostasis. This was achieved using a list of GS homeostasis genes complied from the following sources: Sønderby et al (2010b), Wittstock and Burow (2010), Yatusevich et al (2010), Schweizer et al (2013b), Frerigmann and Gigolashvili (2014), Kong et al (2016), Pfalz et al (2016), Wittstock et al (2016) and Nakano et al (2017). The selected differentially expressed GS homeostasis genes were clustered using Pearson distances and the average method. Heatmaps displaying z-scores of transformed read counts (vst-normalised; DEseq2) for the clustered GS homeostasis genes and the 13 Arabidopsis JAZ genes, were created using the aheatmap function from the NMF R package.

2.5.15. Whole Genome Bisulfite Sequencing (WGBS)

2.5.15.1. Library Preparation and Sequencing

Leaf tissue was collected from 5-week-old plants treated when they were 2 weeks old seedlings with either water (control) or 1 mM JA. Three biological replicates were collected per seedling treatment (water and JA). Each replicate consisted of twelve leaves, two leaves from each of six plants. All leaves were of a similar age and developmental stage. Leaf material was snap frozen and then ground to a powder using 3 mm diameter steel ball bearings (Atlas Ball & Bearing Co Ltd) and a TissueLyser (Qiagen). DNA was extracted using the GenElute Plant Genomic DNA Miniprep Kit (Sigma-Aldrich) and eluted in the provided elution buffer (10 mM Tris, 1 mM EDTA, pH~8.0). Quality and concentration of the DNA was determined using agarose gel electrophoresis and a Qubit fluorometer (Invitrogen), respectively.

Library preparation and sequencing was performed by BGI using their standard whole genome bisulfite sequencing (WGBS) protocol. Briefly, genomic DNA (1 µg) was randomly fragmented into 100-300 bp pieces using an ultrasonicator (Covaris) and fragment sizes were checked using gel electrophoresis. The ends of the DNA fragments were repaired, 3’ ends were adenylated and methylated adaptors were added. After each of the four aforementioned steps, DNA was purified using the MinElute PCR Purification Kit (Qiagen). The EZ DNA Methylation-Gold Kit (Zymo Research) was used to perform the bisulfite treatment and subsequent purification. DNA fragments were enriched using multiple rounds of PCR amplification. Size selections were performed before and after the PCR amplification, with DNA fragments of size 320-420 bp being selected using agarose gel electrophoresis and

then cleaned up using the QIAquick Gel Extraction kit (Qiagen). The quality of the prepared libraries was confirmed using a 2100 bioanalyzer (Agilent Technologies) and a StepOnePlus Real-Time PCR System (Applied Biosystems). 150 bp paired-end sequencing was performed using an HiSeq X Ten System (Illumina).

Across all six samples, 97 million 150 bp paired-end reads were generated, with a minimum and maximum number of read pairs per sample of 15.6 and 17 million, respectively (Supplemental Data Set 2.21). As with the RNA-seq reads, BGI defined the reads as clean because adapter sequences, contamination and low-quality reads had been removed. On average 98.2% of nucleotides had a Phred quality score of > 20.

2.5.15.2. Read Alignment

Read quality was checked using FASTQC version 0.11.7 and summarised by MultiQC version 1.5. This analysis suggested that the start of reads were generally of lower quality, with the first 5-10 positions of reads having increased numbers of uncalled bases, reduced phred quality scores and an unstable base composition. Accordingly, the first 10 bases were removed from the start of each read using Trimmomatic run with the parameter settings: ‘PE’, ‘HEADCROP:10’.

Alignment of reads to the Arabidopsis genome (Ensembl Plants version TAIR10.40) was performed using bismark version 0.21.0 (Krueger and Andrews, 2011) run with the default parameter settings which includes the use of Bowtie2 version 2.3.4.1 for read mapping (Langmead and Salzberg, 2012). Prior to alignment, the genome was prepared using the bismark_genome_preparation script. Alignment efficiency for each of the six samples was between 58% and 66% (Supplemental Data Set 2.21).

The pre-alignment quality control (i.e. FASTQC) and the visualisation of alignments in a genome viewer (Intergrative genomics viewer, version 2.5.0) (Robinson et al., 2011; Thorvaldsdottir et al., 2013), suggested that duplicate reads were present. Duplicates could, for example, be the result of excessive PCR amplification or artefacts of the HiSeq X Ten System (Suzuki et al., 2018). To remove the duplicates, the paired-end BAM alignment files were rearranged using samtools (‘sort’, ‘-n’; version 1.7; (Li et al., 2009)) and then passed to the Bismark tool deduplicate_bismark which was run with the parameter setting: ‘--paired’. Between

23% and 29% of aligned paired-end reads were removed from each sample in the deduplication procedure. Thus, after alignment and deduplication, between 43% and 51% of all sequenced paired-end reads per sample were retained (Supplemental Data Set 2.21).

2.5.15.3. Methylation Calling and Weighted Methylation Levels

Per cytosine position total read counts and methylated read counts were generated using the Bismark tool bismark_methylation_extractor run with the following parameter settings: '--paired-end', '--no_overlap', '--ignore_3prime_r2 90', '--comprehensive', '--bedGraph', '--CX', '--cytosine_report'. The latter 90 bases of the second read of all pairs were excluded from the methylation counting as M-bias plots highlighted that there was a gradual and unexplained increase in the average per cytosine position % methylation across the latter 80-90 positions of the second read. The outputted CX reports were split into three, with one file for cytosine positions located in the plastid, mitochondrial and nuclear genomes, respectively. Using the latter file of each of the six samples, the per sample average coverage of nuclear genome cytosine positions was calculated as ranging from 4.8 and 6.1 (Supplemental Data 2.21).

Since cytosines in the plastid genome are unmethylated, any "methylated" reads mapping to the plastid genome indicate non-conversion by the bisulfite treatment. Thus, we used counts for all cytosine positions in the plastid genome to estimate the per sample bisulfite non-conversion rate. Generally it is considered that a non-conversion rate of less than 2% is acceptable (Stuart et al., 2018) and the non-conversion rates across our six samples were between 0.37% and 0.48% (Supplemental Data Set 2.21).

The counts for all cytosine positions in the nuclear genome were used for downstream analysis. This included the estimation of the genome-wide methylation level for all cytosine positions together (All C or All contexts) and separately for each of the three cytosine sequence contexts: CG, CHG and CHH (H equals any base other than G). The more deeply sequenced a cytosine position, the more reliable an estimate of methylation level it provides. To account for this in the genome-wide methylation level estimates, per replicate and cytosine context weighted methylation levels were calculated using Equation 2.3 adapted from (Schultz et al., 2012):

Equation 2.3. - Genome-Wide Weighted Methylation Level

$$Genome - Wide\ Weighted\ Methylation\ level = \frac{\sum_{i=1}^{n} C_i}{\sum_{i=1}^{n} C_i + T_i}$$

In this equation, *n* is the total number of cytosines positions in the genome of the relevant context (e.g. CG), *i* is cytosine position, C_i is a read methylated at *i* and T_i is a read not methylated at *i*. Thus, the sum of C_i and T_i is the total number of reads covering *i*.

2.5.15.4. Global Analysis of Positional Cytosine Methylation

A hierarchical clustering analysis (HCA) and PCA was conducted for each of the four nuclear genome sequence context groups: All C, CG, CHG and CHH. Both HCA and PCA are suitable methods to detect global shifts in DNA methylation and were performed on datasets consisting of per position methylation levels, calculated using Equation 2.4 adapted from (Schultz et al., 2012):

Equation 2.4. - Position Methylation Level

$$Position\ Methylation\ Level = \frac{C_i}{C_i + T_i}$$

To ensure that the analyses were performed only on positions with accurate estimations of methylation, all positions with a coverage of less than five in one or more samples were removed. Furthermore, to focus the analysis on cytosine positions that varied in methylation between the six samples, positions with a standard deviation of methylation levels across samples of less than or equal to the 0.5 quantile of standard deviations from all cytosine positions were also removed. PCAs were conducted using the prcomp function from the R stats package run with the parameter settings: ‘center = TRUE’, ‘scale. = FALSE’. HCA was performed using the dist and hclust functions, also from the R stats package, run with the options ‘method = "euclidean"’ and ‘method = “average”’, respectively. PCA and HCA plots were created using the ggplot2, graphics version 3.6.1 (R Core Team, 2019) and dendextend version 1.13.4 (Galili, 2015) R packages.

2.5.15.5. Differential Methylation Analysis

Based on the outcome of the global analysis of positional cytosine methylation, which revealed increased variation in cytosine methylation between replicate samples from plants of JA-treated seedlings, the analysis of differentially methylated regions (DMRs) was designed to select positions that in individual samples from JA-treated plants are statistically different relative to the three replicate samples from water-treated plants. This 1JA_vs_3W approach is not confounded by the elevated variation between JA samples. To identify DMRs in all three 1JA_vs_3W comparisons, the R package dispersion shrinkage for sequencing data (DSS; version 2.26.0) (Feng et al., 2014a; Wu et al., 2015) was used. Since DSS accounts for coverage depth information, all cytosine positions in the nuclear genome were used without prior filtering based on minimum coverage. Statistical tests were performed at all positions, using the DMLtest function run with the arguments: 'equal.disp = TRUE', 'smoothing = FALSE'. DMRs were called using the callDMR function run with the following option settings: 'delta = 0.1', 'p.threshold = 0.05', 'minlen = 25', 'minCG = 5', 'dis.merge = 50', 'pct.sig = 0.5'. Context specific DMRs were identified by running the same DSS analysis pipeline with only CG, CHG or CHH context cytosine positions.

Arabidopsis genome and transposable element (TE) annotation files were downloaded from Ensembl (version TAIR10.40) and TAIR (version 10), respectively. Analysis of genomic features overlapped by DMRs was conducted using the R packages GenomicRanges version 1.36.1 (Lawrence et al., 2013) and genomation version 1.16.0 (Akalin et al., 2015). The order of precedence used for counts of genomic features overlapped by DMRs was promotor > exon > intron > intergenic. Overrepresented TE families and superfamilies among the DMR overlapped TEs were identified using hypergeometric tests with all TEs annotated in TAIR10 as the background and an adjusted *p*-value threshold of 0.05 (Benjamini and Hochberg correction). Plots of DMR numbers and TE (super)family enrichment were created using the R packages ggplot2 and ggrepel version 0.8.1 (Slowikowski, 2019). A chromosome map displaying the distribution of *ATREP2* TEs, was generated using the TAIR10 gaps track downloaded from the UCSC genome browser, the centromere coordinates obtained from the TAIR9 genome assembly and the R package chromPlot version 1.12.0 (Verdugo and Orostica, 2019).

Consensus DMRs, regions overlapped by DMRs from all three of the 1JA_vs_3W comparisons, were identified using the following pipeline: (i) identified 'overlapping' DMRs from a pair of 1JA_vs_3W comparisons using the findOverlaps function from the GenomicRanges R package (note – DMRs were not necessarily overlapping but instead may just have been close to one another, see below for more information) (ii) created new merged DMRs with the highest and lowest coordinates of each pair of 'overlapping' DMRs (iii) identified DMRs from the third 1JA_vs_3W comparison which 'overlapped' with the merged DMRs using the findOverlaps function (iv) created consensus DMRs using the highest and lowest coordinates from across 'overlapping' merged and 3rd comparison DMRs (v) repeated steps i to iv three times, once for each possible combination of initial pairs of 1JA_vs_3W comparisons (vi) removed consensus DMR duplicates (sometimes the same consensus DMR was identified on multiple occasions in step v). The consensus DMR identification pipeline was run twice for each of the four cytosine sequence contexts (All C, CG, CHG and CHH). The first time the pipeline was run, DMRs were classed as 'overlapping' if they were within 100 bp of one another and the second time if they were within 500 bp of one another.

2.6. Supplemental Figures

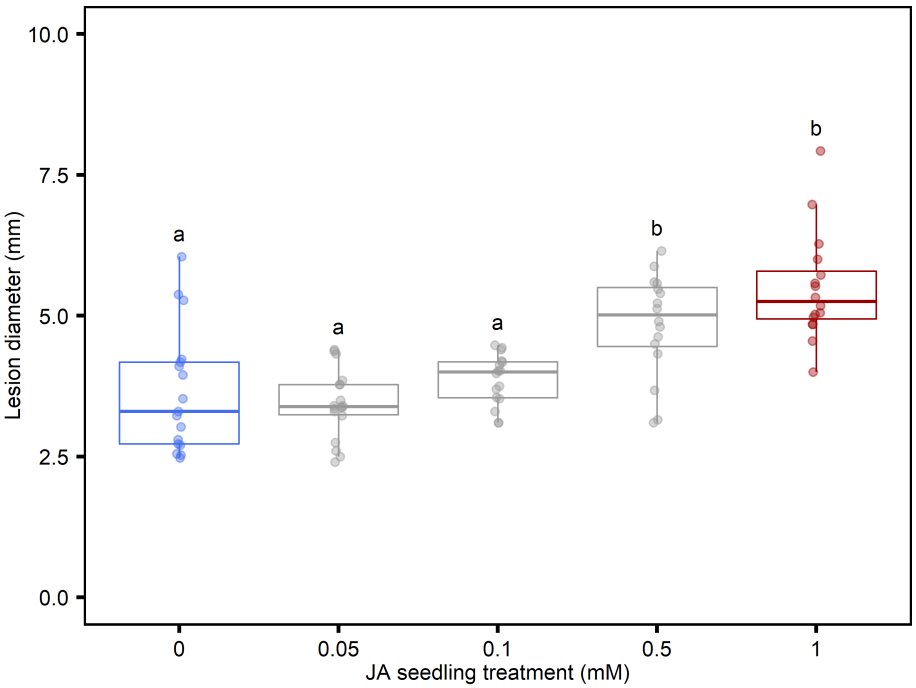

Supplemental Figure 2.1. JA Seedling Treatment Induces Long-term Susceptibility to the Necrotrophic Fungal Pathogen *Plectosphaerella cucumerina* in a Concentration Dependent Manner.

The size of *P. cucumerina* lesions 6 days after inoculation of 5-week-old wild-type plants treated 3 weeks previously as 2-week-old seedlings with one of five JA solutions. The "water" and "JA" seedling treatments used for the remainder of Chapter 2 are shown in blue (0 mM) and red (1 mM), respectively. Plants were inoculated with a 5 x 10^6 spores per ml *P. cucumerina* spore suspension. Each point represents the mean lesion diameter of four leaves from a single plant (n = 16-18). Those seedling treatment groups which do not share the same letter are significantly different (Tukey post-hoc test, $p < 0.05$).

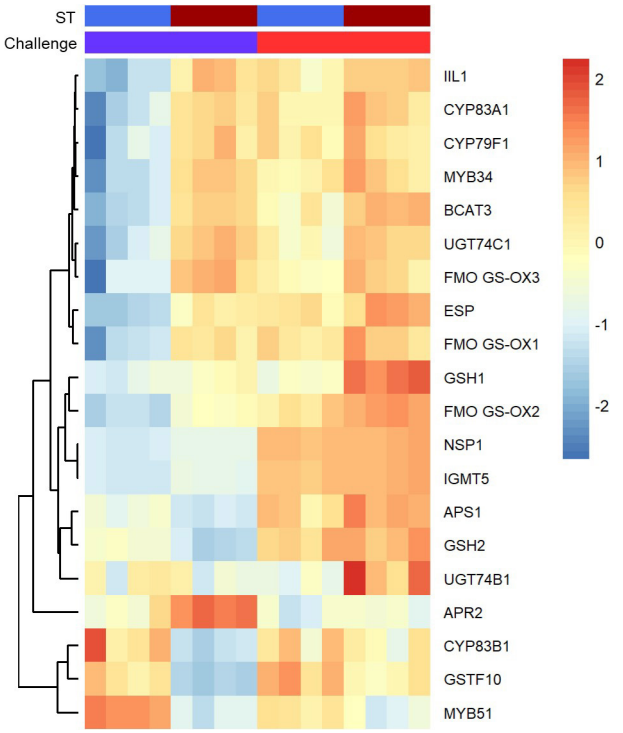

Supplemental Figure 2.2. JA Seedling Treatment Alters Numerous Glucosinolate Homeostasis Genes Constitutive Expression and/or Responsiveness to Subsequent JA Challenge.

The expression profiles of glucosinolate homeostasis genes which responded differently to JA challenge as a result of JA seedling treatment (ST; adjusted *p*-value ≤ 0.01). Genes were clustered using Pearson distances and the Average method. Read counts normalised for library size and transformed using the DESeq2 function vst (Love et al, 2014) are displayed as per gene z-scores. Blue and red coloured column annotations equate to water and JA treatments respectively. Each column is a separate replicate.

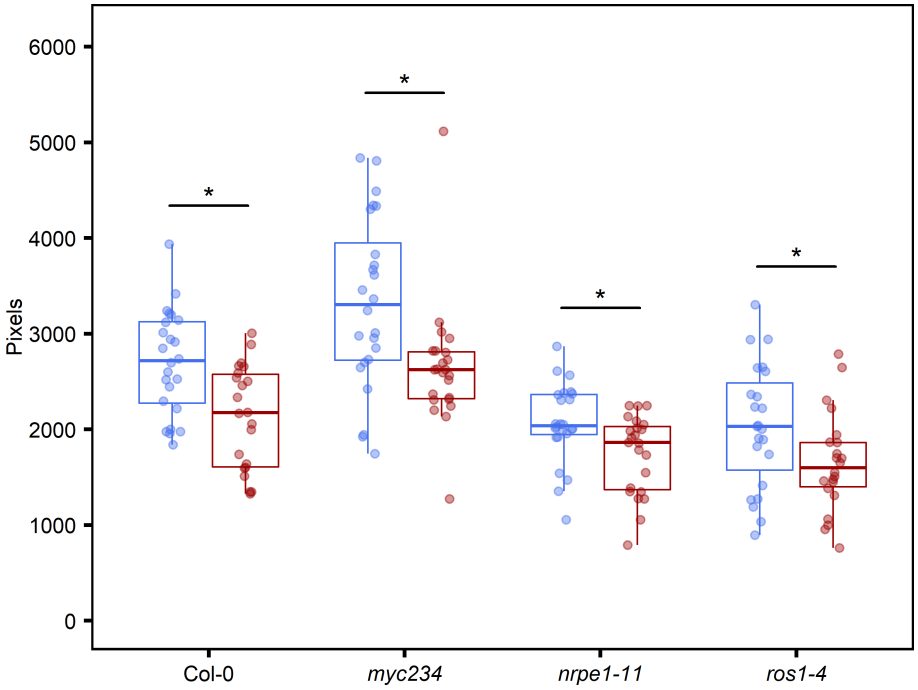

Supplemental Figure 2.3. JA Seedling Treatment Represses Growth Independently of both MYC TFs and RdDM- and ROS1-Dependent Regulation of DNA Methylation at TEs.

The rosette surface area of 5-week-old plants (Col-0, *myc2 myc3 myc4* (*myc234*), RdDM mutant (*nrpe1-11*) and *ros1-4*) from 2-week-old seedlings treated with water (blue) or 1 mM JA (red). Each point represents the area in pixels of a single plant (n = 22-24). Asterisks indicate significant within genotype differences in plant size (Wilcoxon rank sum test, * $p < 0.05$).

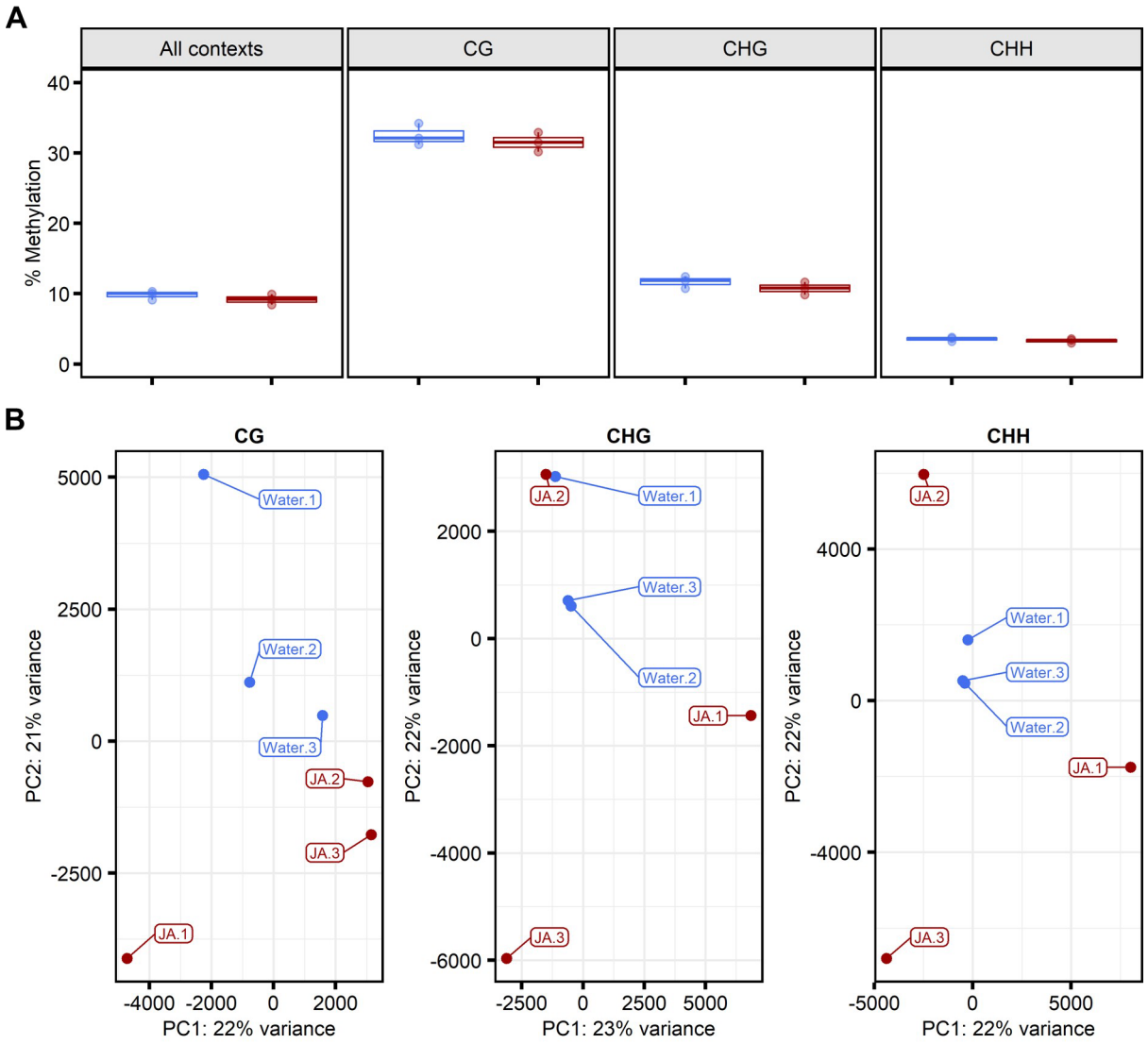

Supplemental Figure 2.4. Impact of JA Seedling Treatment on Global DNA methylation Levels and Patterning.

(A) Genome-wide weighted methylation levels for all cytosines together and split up by sequence context (H = any base other than guanine). Whole genome bisulfite sequencing was performed on leaf material from 5-week-old plants treated when they were 2 weeks old with water (blue) or 1 mM JA (red). Each point represents the genome-wide methylation level of a single replicate (n = 3). JA seedling treatment did not have a significant impact on methylation level for any of the four sequence contexts (two-sample t-test, $p > 0.05$).
(B) Principle component analyses of the percentage methylation at CG, CHG or CHH context cytosine positions. Positions with low coverage (< 5 reads in one or more samples) and minimal between sample variation (standard deviation less than or equal to the 0.5 quantile of all positions standard deviations), were excluded from the analysis. Data was mean centred but not scaled.

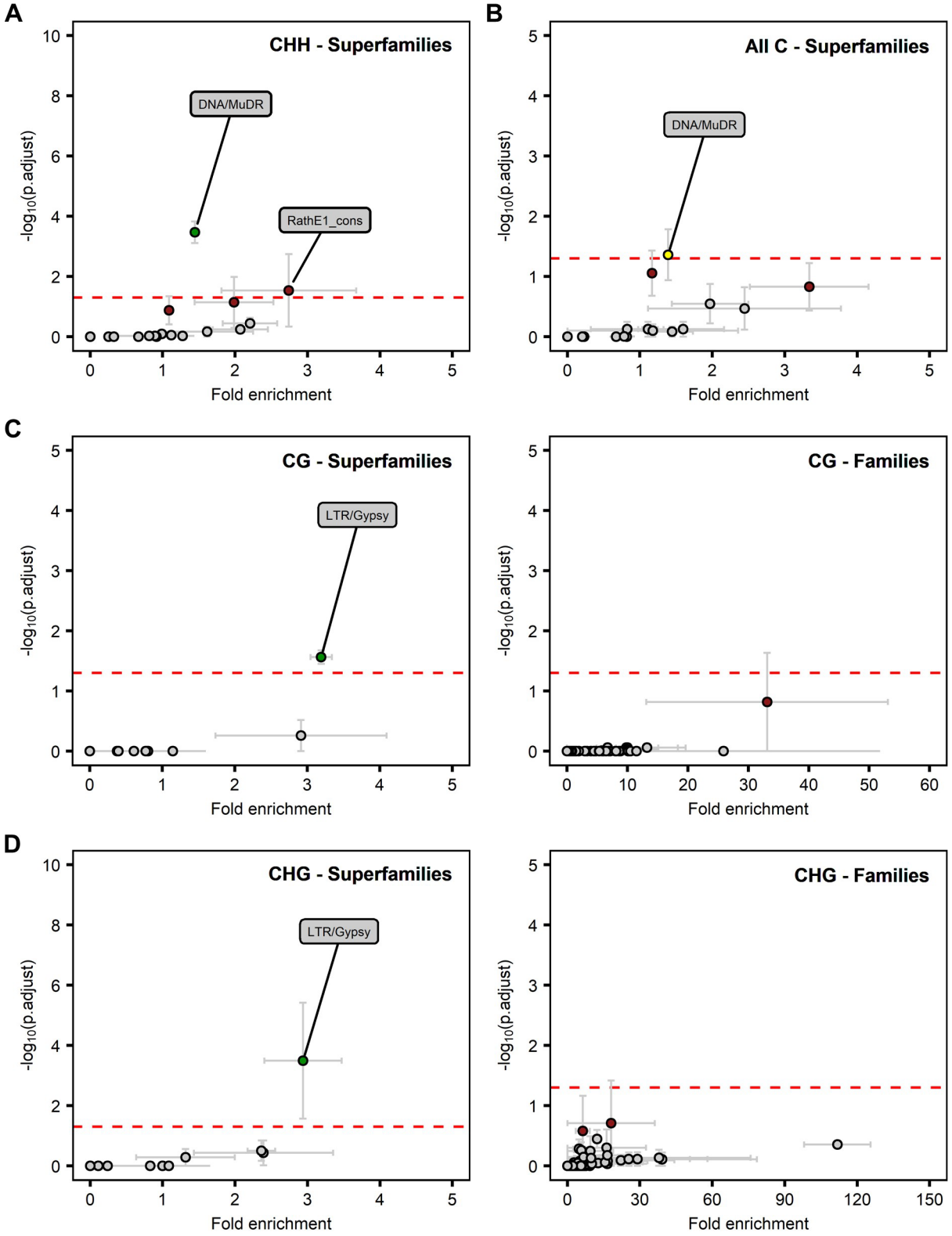

Supplemental Figure 2.5. Overrepresented TE (Super)Families Among DMR Overlapped TEs.

TE (super)families overrepresented among the TEs overlapped by DMRs identified in comparisons between the three water WGBS replicates and individual JA WGBS replicates. Overrepresented (super)familes are displayed for CHH **(A),** All C **(B)**, CG **(C)** and CHG **(D)** sequence context groups. Overrepresented TE families for CHH and All C are displayed in Figure 2.13. Points represent the mean

Supplemental Figure 2.5. (continued)

$-\log_{10}$(hypergeometric test adjusted *p*-value) vs mean fold enrichment (± SEM), of individual (super)families. Enrichment is relative to the background of all TEs annotated in genome. The labelled (super)families have a mean $-\log_{10}$(adjusted *p*-value) of greater than $-\log_{10}(0.05)$ (red dashed line). The multi-coloured (super)families were significantly (adjusted *p*-value ≤ 0.05) overrepresented in one (red), two (yellow) or three (green) comparisons, respectively.

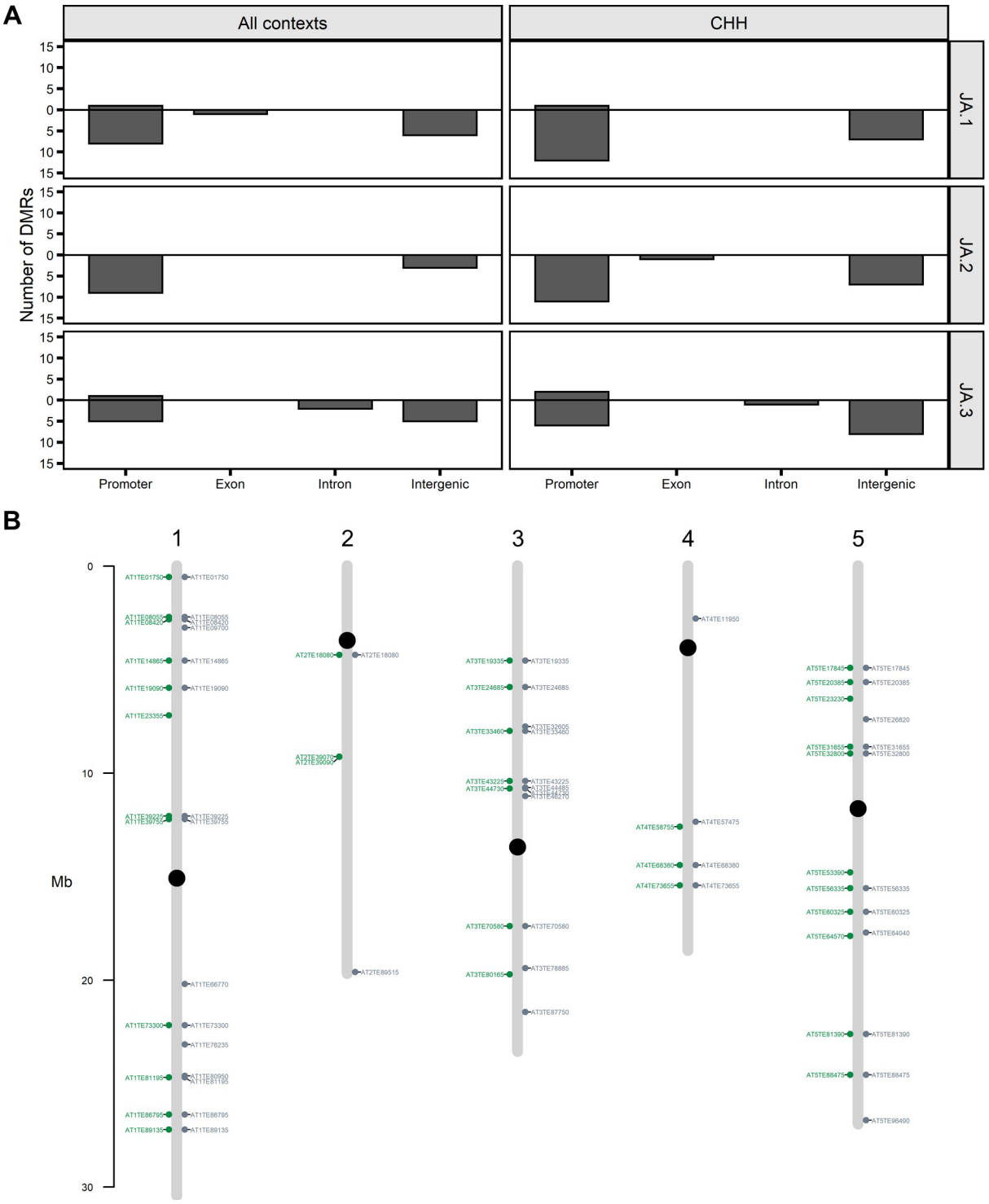

Supplemental Figure 2.6. DMRs Which Overlap *ATREP2* TEs are Predominantly Hypomethylated and Located in Gene Promoters or Intergenic Regions Spread Across the Genome.

(A) The genomic locality of *ATREP2* overlapping DMRs, identified in comparisons between individual JA seedling treatment replicates (JA.1, JA.2 and JA.3) and all three replicates from plants of water treated seedlings. Hyper- and hypo-methylated DMRs are shown above and below the x-axis, respectively.
(B) Distribution of DMR overlapped *ATREP2* TEs across the five Arabidopsis chromosomes. Black dots signify centromeres and grey bars indicate chromosomes. The TEs labelled in green and grey were overlapped by DMRs from the All contexts or CHH sequence context comparisons, respectively. An individual TE had to be overlapped by a DMR from at least one comparison (e.g. JA.1 All contexts) to be displayed.

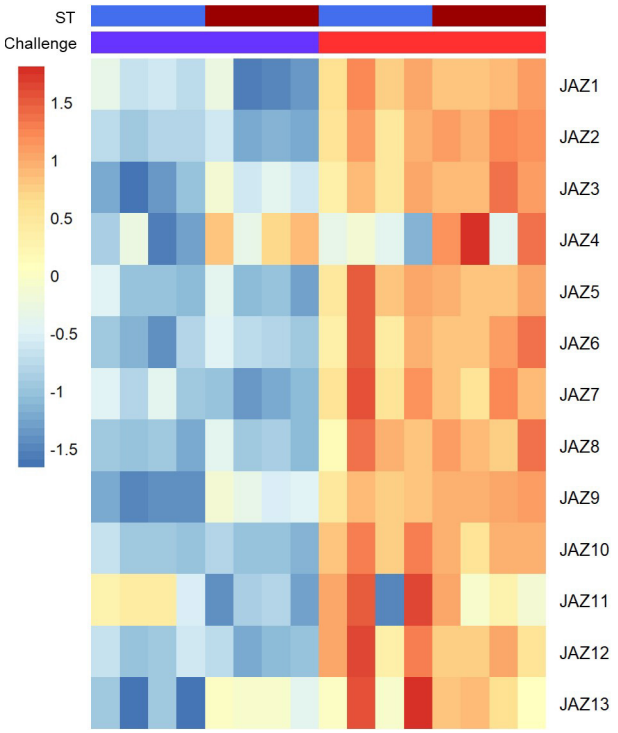

Supplemental Figure 2.7. Expression Profiles of the 13 Arabidopsis JAZ Repressor Genes.

Read counts normalised for library size and transformed using the DESeq2 function vst (Love et al, 2014) are displayed as per gene z-scores. Blue and red coloured column annotations equate to water and JA treatments respectively. Each column is a separate replicate. ST = Seedling Treatment.

Chapter 3

The Norway Spruce Transcriptome of Methyl Jasmonate Induced Resistance

Authors:

Wilkinson SW[1,2], Ton J[1], Krokene P[2], Magerøy MH[2]

Affiliations:

[1] Department of Animal and Plant Sciences, The University of Sheffield, Sheffield S10 2TN, United Kingdom

[2] Department of Molecular Plant Biology, Division for Biotechnology and Plant Health, Norwegian Institute for Bioeconomy Research (NIBIO), 1431 Ås, Norway

Author contributions:

SWW, JT, PK and MHM proposed the original idea for the research. SWW conducted experiments and gathered data with assistance from MHM. SWW analysed the data with assistance from MHM. SWW created all figures and wrote all the text in the chapter. MHM and JT reviewed and provided comments on the chapter. MHM, PK and JT provided funding for the research.

Chapter 3. The Norway Spruce Transcriptome of Methyl Jasmonate Induced Resistance

3.1. Abstract

Norway spruce (*Picea abies*) is an economically and ecologically important tree species which is grown widely across northern and central Europe. Jasmonate treatments have been shown to have long-lasting beneficial effects on the resistance of this tree species against damaging pests, such as the European spruce bark beetle *Ips typographus* and its fungal associates. The potential involvement of (epi)genetic mechanisms underpinning this long-lasting jasmonate-induced resistance (IR) have gained much recent interest but remain largely unknown. In this study, we pre-treated 2-year-old spruce seedlings with methyl jasmonate (MeJA) and challenged them four weeks later. The MeJA pre-treatment elicited IR to the *I. typographus* vectored fungus *Grosmannia penicillata,* which is a necrotrophic pathogen affecting bark tissues. A transcriptome analysis was performed to explore the transcriptional response of bark to MeJA pre-treatment and subsequent challenge. Key findings from this analysis included evidence that MeJA treatment induced a transient upregulation of jasmonic acid, salicylic acid and ethylene biosynthesis and downstream signalling genes. Additionally, genes encoding components of the RNA-directed DNA methylation pathway showed long-term repression, suggesting a possible role of DNA hypomethylation in the maintenance of MeJA-IR. Whole genome bisulfite sequencing is currently being used to test this hypothesis. Interestingly, analysis of the transcriptomic response at 6 hours after secondary challenge with MeJA did not provide evidence for majorly augmented defence gene induction, suggesting that transcriptional priming of JA-dependent genes may not play a major role in long-term MeJA-IR in spruce seedlings. In summary, this study has generated a detailed characterisation of the temporal transcriptional changes in bark tissues of Norway spruce after MeJA treatment. In addition, the results provide new clues about the potential mechanisms underpinning long-term MeJA-IR in Norway spruce.

3.2. Introduction

Norway spruce (*Picea abies*) is an economically and ecologically important coniferous tree species which occurs widely throughout northern and central Europe (Caudullo et al., 2016). However, across the majority of its range, Norway spruce is threatened by the aggressive European spruce bark beetle, *Ips typographus* (Wermelinger, 2004; Jeger et al., 2017; Biedermann et al., 2019). Large swathes of Norway spruce plantations across central and eastern Europe have been decimated in recent years by this bark beetle (Jeger et al., 2017; Hlásny et al., 2019). The exhaustion of tree defences and ultimately the success of bark beetle attacks, is thought to be aided by infection of the tree with necrotrophic Ophiostomatoid fungal pathogens which the beetles vector and are intimately associated with (Lieutier et al., 2009; Krokene, 2015; Kandasamy et al., 2019; Zhao et al., 2019). Common fungal phytopathogens associates of *I. typographus* include *Grosmannia penicillata*, *Endoconidiophora polonica* and *Ophiostoma bicolor* (Furniss et al., 1990; Krokene and Solheim, 1996; Linnakoski et al., 2016). Additional biotic threats faced by Norway spruce include the large pine weevil (*Hylobius abietis*), which is a major problem for seedling establishment, and the necrotrophic fungus *Heterobasidion annosum* which causes root and butt rot (Caudullo et al., 2016).

Norway spruce, as with other members of the *Pinaceae* family, has a comprehensive suite of defences that it can use to try and defend itself against potentially deadly attackers. In addition to constitutive defences such as lignified sclerenchyma cells and intracellular deposits of calcium oxalate crystals, it also has a range of inducible defences (Franceschi et al., 2005; Krokene, 2015). A classic example of a spruce inducible defence is the production of sapwood located traumatic resin ducts (TRDs), which are filled with a terpene rich oleoresin that acts as both a chemical and physical barrier to attackers (Nagy et al., 2000; Krokene et al., 2003; Krekling et al., 2004; Celedon and Bohlmann, 2019). However, it has been suggested that often the formation of TRDs may not be fast enough to be of benefit for resisting the attacker which induced them (Krokene, 2015). Nevertheless, in response to challenge, there is also a rapid upregulation of terpene biosynthesis in bark localised cortical resin ducts (Zulak et al., 2009; Abbott et al., 2010; Zulak et al., 2010; Celedon and Bohlmann, 2019). Phenolic compounds such as stilbenes and flavonoids are also important defence compounds in spruce (Faccoli and Schlyter, 2007; Hammerbacher

et al., 2011; Hammerbacher et al., 2014; Hammerbacher et al., 2019). In response to challenge of bark tissue, phenolic biosynthesis is induced which is in turn linked to the swelling of phenolic compound rich polyphenolic parenchyma (PP) cells (Franceschi et al., 1998; Franceschi et al., 2000; Hammerbacher et al., 2011; Li et al., 2012b; Hammerbacher et al., 2014; Hammerbacher et al., 2019). An entirely new layer of PP cells can also form in response to severe challenge (Krokene et al., 2003; Krekling et al., 2004; Krokene, 2015). Aside from enhanced production of terpenes and phenolics, a hypersensitive cell death response and pathogenesis-related (PR) proteins are also inducible defences which are thought to play a role in providing resistance against biotic stress in conifers (Franceschi et al., 2005). However, despite this extensive repertoire of inducible defences, Norway spruce is far from fully protected. This is evidenced by the widespread damage caused by *I. typographus* and its Ophiostomatoid fungal associates (Hlásny et al., 2019). Thus, there is a desire to develop novel pest and disease strategies to protect Norway spruce. One possibility is to enhance trees' innate defence capacity.

Exposure of plants to specific environmental stimuli such as localised pathogen infection, beneficial microbes and specific chemicals, can make them more resistant to subsequent attack (Fu and Dong, 2013; Pieterse et al., 2014). This phenomenon is known as induced resistance (IR) and provides a feasible route by which particularly young trees in a nursery setting could be protected against pests and/or diseases. Two models have been proposed to explain the IR phenomenon (Wilkinson et al., 2019). The first is referred to as a "direct induction defences" or a "prolonged upregulation of inducible defences". Following exposure to a resistance inducing stimulus, inducible defences are upregulated and maintained upregulated until subsequent attack (Wilkinson et al., 2019). The second model is the "priming of inducible defences" (Conrath et al., 2015; Mauch-Mani et al., 2017). The resistance inducing stimulus or priming cue, may or may not result in a transient induction of defences. However, crucially, defences return to basal levels where they are maintained until subsequent challenge upon which they are upregulated faster and/or stronger than in control unprimed plants. While long-term IR may be underpinned by just a prolonged upregulation or priming of inducible defences, as demonstrated in Chapter 2 often a combination of the two can explain the enhanced resistance.

Considerable research has been conducted in model angiosperms investigating the mechanisms involved in IR. For example, there is an increasing wealth of evidence which suggests that maintenance of particularly longer lasting IR, which is often underpinned by a priming of inducible defences, involves epigenetic mechanisms (Wilkinson et al., 2019). Studies have provided evidence that in response to priming cues, specific histone modifications are implemented and chromatin is unpacked in the promoters of genes which show a primed response to subsequent challenge (Jaskiewicz et al., 2011; Schillheim et al., 2018; Baum et al., 2019). Furthermore, Chapter 2 of this thesis provided evidence that DNA methylation can play a role in long-lasting within generation IR in *Arabidopsis thaliana* (Arabidopsis). Nevertheless, despite this ever-increasing knowledge in model angiosperms, our understanding of the mechanisms of IR in tree species including Norway spruce remains limited in comparison.

Research in angiosperms has demonstrated the importance of jasmonic acid (JA) in positively regulating defences effective against insect herbivores and necrotrophic pathogens (Wasternack and Hause, 2013). Thus, it is unsurprising that studies in Norway spruce have found that application of JA, or its methyl ester methyl jasmonate (MeJA), to seedlings and mature trees can induce resistance against both threats (Kozlowski et al., 1999; Erbilgin et al., 2006; Zeneli et al., 2006; Krokene et al., 2008; Mageroy et al., 2020a). This MeJA-IR is linked to a direct induction of defences. For instance, MeJA triggers an increased production of terpenes in bark localised cortical resin ducts, an enhanced production of phenolics leading to swelling of existing PP cells, the formation of TRDs and the creation of new PP cells (Franceschi et al., 2002; Martin et al., 2002; Krokene et al., 2008; Zulak et al., 2009; Schiebe et al., 2012; Celedon and Bohlmann, 2019). Interestingly, a study with another *Pinaceae* species, *Pseudotsuga menziesii* (Douglas fir), provided evidence that the induction of a number of the aforementioned defences by MeJA is somewhat dependent on ethylene (ET) (Hudgins and Franceschi, 2004). Thus, as in Arabidopsis, JA and ET probably act together to regulate certain inducible defences in conifers.

In addition to a prolonged upregulation or direct induction of defences, MeJA-IR has also been associated with a priming of inducible defences in Norway spruce. In 2011, Zhao et al (2011) provided evidence that although MeJA treatment alone does induce an increase in terpene levels in the bark, it is very minor in comparison to

accumulation of terpenes following the wounding of bark treated with MeJA 4 weeks previously. However, this accumulation does not appear to be the result of *de novo* biosynthesis as terpene biosynthesis enzymes are generally not primed at a transcriptional level (Mageroy et al., 2020b). Thus, the high levels of terpenes could be the result of a rapid mobilisation and concentration of terpenoids at the localised wound site. These terpenes may be derived from the sapwood located TRDs and transported to the bark through radial resin ducts. If this hypothesis is true, then the strong accumulation of terpenes in MeJA pre-treated and wound challenge trees could arguably be the result of a prolonged upregulation or direct induction of defences. Nevertheless, in a recent study where we began to explore the molecular mechanisms behind MeJA-IR, we demonstrated that MeJA pre-treatment likely primed a swathe of *PR* genes to respond faster and stronger to wounding (Mageroy et al., 2020b). Despite these recent findings, much is still unknown about the workings of MeJA-IR. For instance, what are the molecular mechanisms underpinning the establishment and maintenance of MeJA-IR? In a previous study, we provided evidence that wounding induces differential expression of epigenetic regulators (Mageroy et al., 2020b). While wounding can prime plant defences and induce resistance, it is not the same as MeJA treatment. Thus, a detailed analysis with multiple timepoints post MeJA pre-treatment is required to obtain a fuller understanding of how expression of epigenetic regulators is modulated in response to the resistance-inducing stimulus. Furthermore, in the previous study, we used the 24 hours post challenge timepoint. Considering the number of genes significantly differentially expressed (Wounded Vs Control) at this timepoint (1000s), coupled with the speed with which genes can be induced in response to MeJA treatment or Herbivory (e.g. Ralph et al., 2006b; Hickman et al., 2017), this was almost certainly too late to study the more rapid responses to jasmonate inducing challenge which will include the differential expression of defence regulators. Thus, there is also a need to study an earlier timepoint post challenge.

The current study builds on our previous work (Mageroy et al., 2020b), although this time we used more tractable seedlings rather than mature trees. The overall aim of the study was to further explore the molecular mechanisms of MeJA-IR. More specifically, we aimed to (1) examine the transcriptional response to MeJA pre-treatment, (2) investigate the establishment and maintenance of MeJA-IR, (3) explore the transcriptional response to challenge with a particular focus on the early responses

and (4) compare transcriptional responses of bark tissues from seedlings to those from mature trees following pre-treatment and challenge with MeJA.

3.3. Results

3.3.1. Design of a Study to Explore the Molecular Mechanisms of Methyl Jasmonate (MeJA) Induced Resistance (IR)

In follow up to our previous work in mature Norway spruce trees (Mageroy et al., 2020b), this study aimed to further explore the molecular mechanisms behind MeJA-induced resistance (MeJA-IR). To achieve this goal, an experiment was setup with 2-year-old seedlings which were pre-treated with water (control) or 10 mM MeJA (Figure 3.1). The pre-treatment was performed by spraying plants until they were saturated using a pressurised spray bottle (see methods for details). In Chapter 2 JA rather than MeJA was used as it is less volatile which is more suitable when plants are grown in enclosed climate chambers that also contain the control plants and plants from other experiments. However, in this chapter, we choose to use MeJA because (a) plants were grown outside and (b) MeJA has been used in the majority of previous studies exploring jasmonate-IR in spruce. The concentration of MeJA was chosen based on previous studies showing that 10 mM elicits a strong defence response without severely impacting growth and development (Martin et al., 2002; Skrautvol, 2018) and therefore would very likely elicit a strong IR response which could be dissected in the present study. Seedlings rather than mature trees were used as they are much easier to work with and manipulate. Furthermore, the use of seedlings allowed for a higher number of treatments and replicates to be included in the experiment. Following pre-treatment, bark tissue was harvested at various timepoints allowing for the assessment of the transcriptional response to MeJA treatment and also enabling the exploration of how MeJA-IR is established and maintained (Figure 3.1). Additionally, some seedlings were kept intact until 4 weeks post pre-treatment when they were used to study the response to subsequent challenge.

To confirm both the effectiveness of the MeJA pre-treatment and that, as shown in previous studies (Erbilgin et al., 2006; Zeneli et al., 2006; Mageroy et al., 2020a), MeJA induces resistance to biotic stress, plants from both of the pre-treatment groups were challenged with the necrotrophic Ophiostomatoid fungal pathogen, *Grosmannia penicillata* or a mock agar control (Figure 3.1). *G. penicillata* was chosen for the experiment as it causes substantial necrosis in the phloem tissue making it easy to study the spread of infection (Zhao et al., 2019). In order to study the transcriptional

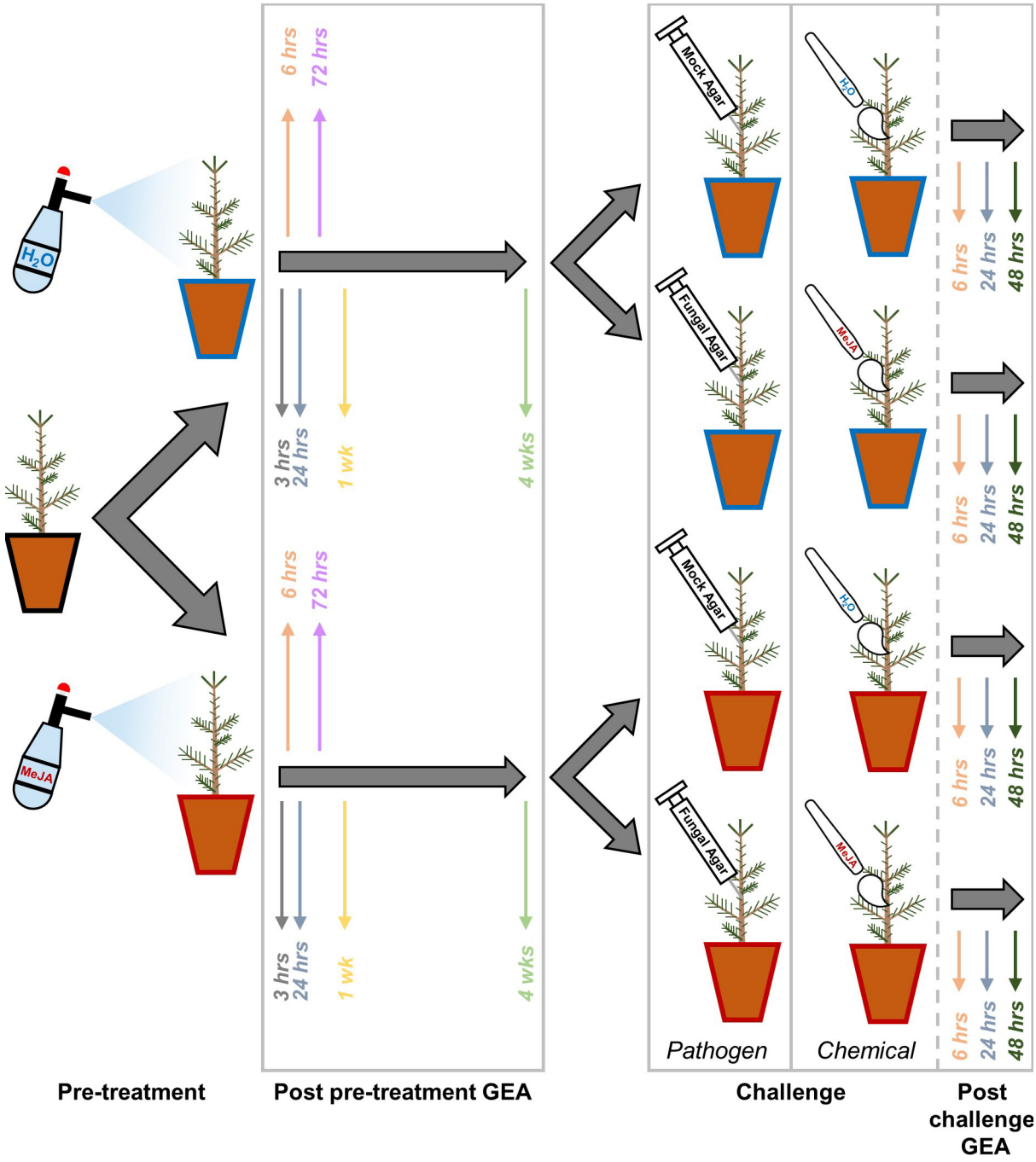

Figure 3.1. Experimental Setup for the Study of the Molecular Mechanisms Underpinning Methyl Jasmonate (MeJA) Induced Resistance (IR) in Norway Spruce Seedlings.

Two-year-old seedlings were pre-treated with either water (blue pots) or 10 mM MeJA (red pots). At 3 hours (hrs), 6 hrs, 24 hrs, 72 hrs, 1 week (wk) and 4 wks post pre-treatment, the bark of the first internode of four seedlings from both pre-treatment groups, was harvested for gene expression analysis (GEA). At 4 wks post pre-treatment, the remaining seedlings were either challenged with a pathogen or chemical treatment. The pathogen challenged plants were either inoculated in a wound in the bark of their first internode with the necrotrophic fungus *Grosmannia penicillata* or mock agar. For the chemical challenge, a water or 5 mM MeJA solution was painted onto the first internode. At 6 hrs, 24 hrs and 48 hrs post chemical challenge, bark from the first internode was harvested for GEA.

response and thus the release of MeJA-IR, plants not used for the fungal bioassay were painted with 5 mM MeJA or water (mock) solution on the same region of bark as challenged with the fungal pathogen. Bark material was harvested at multiple timepoints post chemical challenge (Figure 3.1). An MeJA rather than fungal challenge was used for the molecular studies as a chemical challenge induces a homogenous response across a wider bark tissue area making it easier to study the transcriptional response to challenge. Furthermore, MeJA is at least a partial mimic of fungal infection as it is known that JA and JA-Ile accumulate in spruce phloem tissue in response to infection with *G. penicillata* (including the isolate used in this study) and other Ophiostomatoid fungi (Zhao et al., 2019).

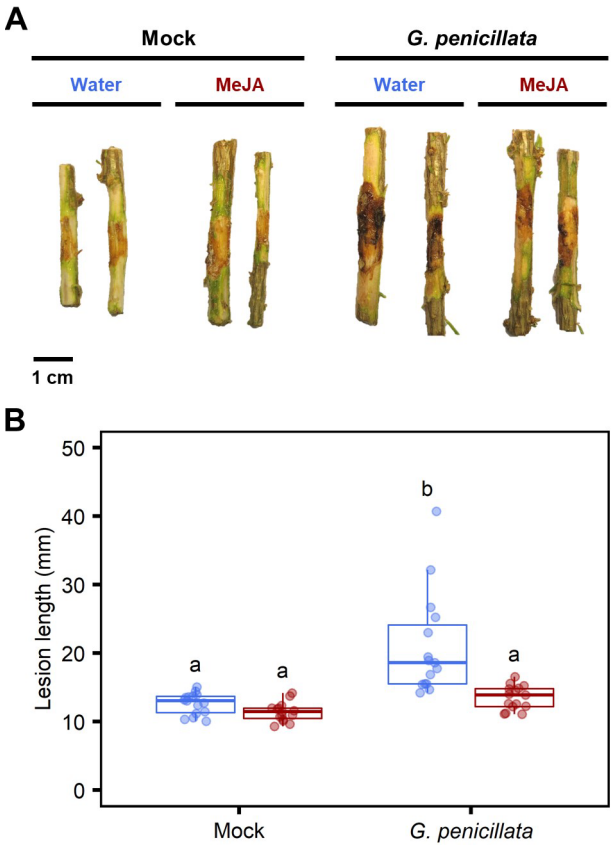

Figure 3.2. MeJA Elicits IR Against the Necrotrophic Fungal Pathogen *Grosmannia penicillata*.

Two-year-old Norway spruce seedlings were pre-treated with either water (blue) or 10 mM MeJA (red) 4 weeks prior to challenge by wounding and the addition of either a *G. penicillata* or sterile malt agar (mock) inoculum. Symptoms were assessed 8 weeks post inoculation. **(A)** The 1st internode stem sections, with wound and/or fungal induced cell death, from all plants of one representative experimental block. **(B)** Lesion lengths were measured in a direction parallel to the stem and from the uppermost to lowermost areas of darkened tissue of the continuous lesions situated at the wounded locations. Points represent individual replicates (n = 15). The lower, middle and upper horizontal lines in the boxplots equate to the first, second and third quartiles. Whiskers extend to the lowest and highest data points within 1.5*(interquartile range) below and above the first and third quartiles. Those treatment groups which don't share the same letter are significantly different (Tukey post-hoc test, $p < 0.01$).

3.3.2. MeJA Elicits IR to a Necrotrophic Pathogen in Spruce Seedlings

To assess the resistance of water and MeJA pre-treated seedlings to *G. penicillata*, the lengths of phloem necrotic lesions were measured at 8 weeks post inoculation. Lesion length provides an indication of the speed of fungal spread through the phloem and therefore the resistance of trees. Plants pre-treated with MeJA generally exhibited shorter fungal induced phloem necrotic lesions than the water controls (Figure 3.2). In fact, the lengths of the lesions in the MeJA pre-

treated and fungal challenged plants phloem were analogous to those of the mock inoculated control plants (Figure 3.2). A difference in plant height or yearly growth could not explain the lesion length results as MeJA pre-treatment did not impact on plant height (Supplemental Figure 3.1A) and there was no increase in apical leader height during the 4 weeks between pre-treatment and challenge (Supplemental Figure 3.1B). Taken together, these results provide evidence of MeJA-IR and therefore confirm the suitability of the experimental setup for investigating the mechanisms behind this phenomenon.

3.3.3. Targeted Transcriptomics Identifies Similarities and Differences Between Seedlings and Mature Trees Response to MeJA Pre-treatment and Subsequent Challenge

The first step in exploring the molecular mechanisms behind MeJA-IR in seedlings was to perform a targeted transcriptomics analysis using RT-qPCR. This preliminary analysis aimed to explore the establishment, maintenance and release of MeJA-IR while also investigating whether findings from our previous study in mature trees carried over to seedlings. One key finding from our previous study was that MeJA pre-treatment of mature tree bark primes numerous *PR* genes to respond faster and/or stronger to wounding challenge (Mageroy et al., 2020b). *PR* genes encode proteins with a variety of modes of action (e.g. chitinase, β-1-3-glucanase) that are important for resisting biotic stress (Van Loon et al., 2006; Ali et al., 2018). In our previous study, we also found that epigenetic regulators were differentially expressed in response to a resistance and defence priming inducing stimulus (wounding). Thus, we studied the expression of five of the primed *PR* genes and two genes which encode regulators of DNA methylation, an epigenetic modification linked to the maintenance of defence priming (Wilkinson et al., 2019). Additionally, we profiled the expression of genes encoding MYC, ETHYLENE INSENSITIVE3 (EIN3) / ETHYLENE-INSENSITIVE3-LIKE1 (EIL1) and WRKY transcription factors (TFs) as these are known to regulate defences against biotic stress in Arabidopsis and other angiosperms (Alonso et al., 2003; Pieterse et al., 2009; Fernández-Calvo et al., 2011; Song et al., 2014; Chen et al., 2017; Du et al., 2017).

The five *PR* genes studied were relatively unresponsive to MeJA (Figure 3.3A and Supplemental Figure 3.2A). While at 72 hrs and 1 week (wk) post pre-treatment

PR4 was more highly expressed in the MeJA compared to water pre-treatment group, none of the *PR* genes showed a rapid transient upregulation in response to MeJA treatment as might be expected. Furthermore, the five *PR* genes did not respond to MeJA challenge and therefore did not exhibit a faster and/or stronger upregulation in the MeJA pre-treated plants (Figure 3.3B and Supplemental Figure 3.2B). Thus, a subset of *PR* genes showing a primed response in mature trees did not exhibit the same pattern in seedlings.

DNA methylation is thought to be established in plants by RNA directed DNA methylation (RdDM) pathways, which require the DNA dependent RNA polymerase, polymerase (Pol) V (Matzke et al., 2015; Cuerda-Gil and Slotkin, 2016). The largest subunit of Pol V is NUCLEAR RNA POLYMERASE E1 (NRPE1). Notably, a spruce gene predicted to encode for NRPE1, was repressed by MeJA pre-treatment (Figure 3.3A). The MeJA induced reduction in *NRPE1* expression was not immediate but came into effect by 24 hrs post challenge. Furthermore, the reduced expression was also not permanent as by 4 wks post MeJA pre-treatment *NRPE1* expression was back to basal levels (i.e. the expression of the water controls). Similarly, a spruce homolog of the Arabidopsis DNA demethylase *DEMETER-LIKE 1* (*DML1* or *ROS1*), was also transiently repressed in response to MeJA pre-treatment (Figure 3.3A). However, it was not until 72 hrs to 1 wk post pre-treatment that the expression of the DNA glycosylase in the MeJA samples dropped significantly below that in the water controls (Figure 3.3A). Neither of the genes involved in DNA methylation regulation responded to MeJA challenge (Figure 3.3B). Nevertheless, the targeted transcriptome analysis suggests that as in mature trees DNA methylation could play a role in the maintenance of MeJA-IR in seedlings.

The *MYC* and *EIN3/EIL1* but not *WRKY* genes were transiently upregulated in response to MeJA pre-treatment (Figure 3.3A and Supplemental Figure 3.2A). In response to subsequent challenge, the *WRKY* again showed no difference in expression between treatment groups (Supplemental Figure 3.2B). The *EIN3/EIL1* gene was also not significantly differentially expressed post challenge, although there was some suggestion of it being upregulated by MeJA challenge in plants of both pre-treatment groups at 6 hrs and the water pre-treatment group only at 24 and 48 hrs (Figure 3.3B). This pattern was more obvious for the *MYC* gene. At 6 hrs, *MYC* was significantly upregulated by MeJA challenge in plants of both pre-treatment groups,

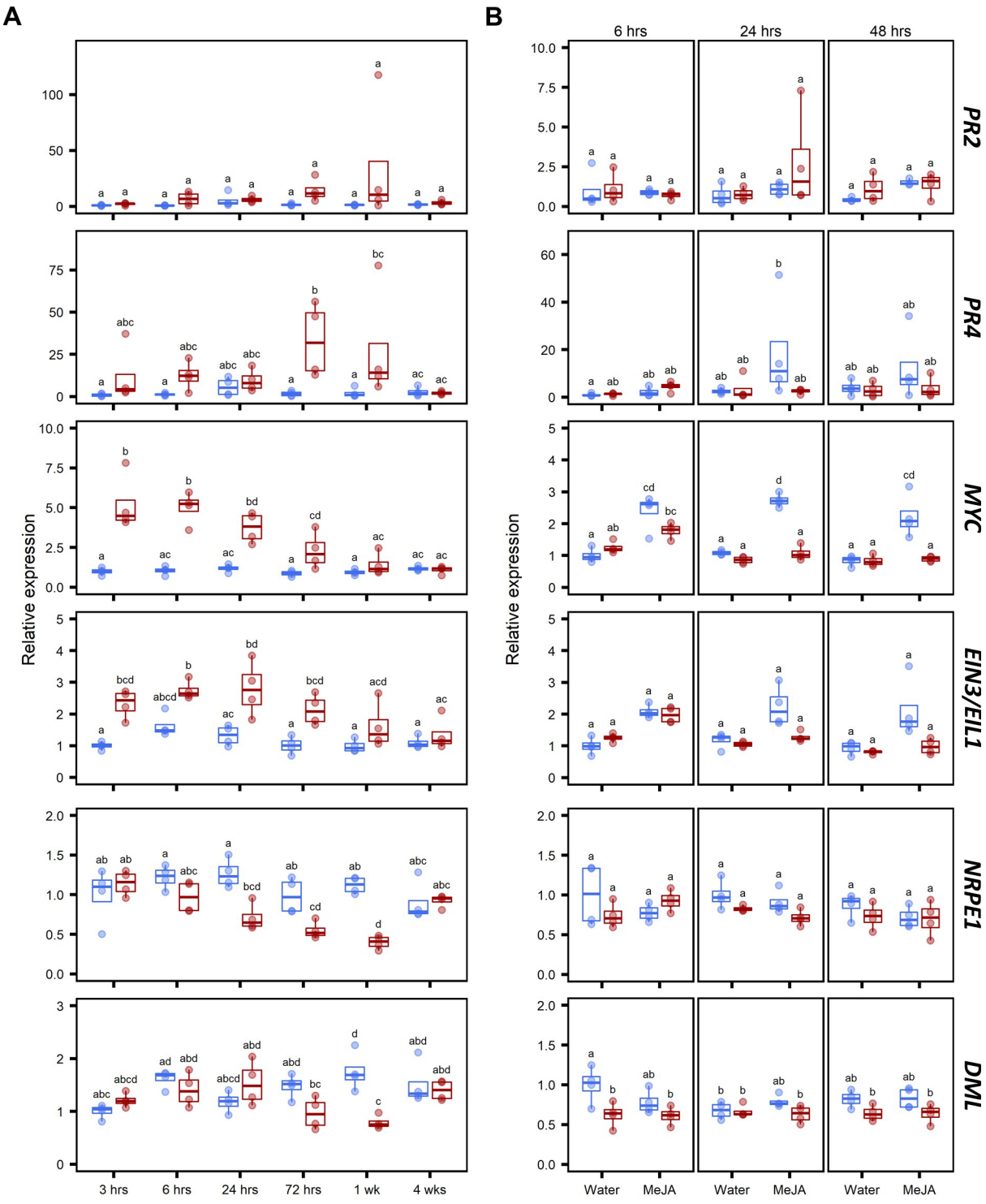

Figure 3.3. Expression Patterns of Pathogenesis-related (PR), Transcription Factor (TF) and DNA Methylation Related Genes in Response to MeJA Pre-treatment and Challenge.

The expression pattern of two *PR* genes (*PR2 - MA_10432716g0010* and *PR4 - MA_394599g0010*), two defence regulatory TFs (*MYC - MA_10435905g0020* and *EIN3/EIL1 - MA_52817g0010*) and two genes involved in DNA methylation homeostasis (*NRPE1 - MA_8720349g0010* and *DML - MA_68384g0010*), in response to water (blue) or 10 mM MeJA (red) pre-treatment and subsequent challenge four-weeks-later with water or 5 mM MeJA. Expression of the six genes was assessed at six timepoints post pre-treatment **(A)** and three timepoints post challenge **(B)**. Points represent individual replicates (n = 4) with expression relative to the mean, which equals 1, of the 3 hrs water pre-treated

when compared to the water pre-treated and water challenge control (Figure 3.3B). Whereas at 24 and 48 hrs, *MYC* only remained upregulated in the water pre-treatment group. Taken together, these results suggest that MeJA pre-treatment either primes specific defence regulatory TFs to respond very rapidly to subsequent MeJA challenge or reduces their responsiveness to future challenge.

The RT-qPCR results provide additional support for the quality of the experimental setup as replicates were generally consistent and we could identify differential expression (Figure 3.3 and Supplemental Figure 3.2). However, this analysis also highlighted potential differences between seedlings and mature trees in their response to challenge following MeJA pre-treatment. Furthermore, this targeted analysis together with our previous work, only just begins to scratch the surface regarding the mechanisms of MeJA-IR. This is particularly true for the response to the initial resistance inducing MeJA pre-treatment. Thus, we conducted mRNA sequencing (RNA-seq) on the 3 hrs, 24 hrs and 1 wk post pre-treatment and 6 hrs post challenge RNA samples (Figure 3.1). There were 40 RNA samples sequenced in total, with four replicate samples per pre-treatment/timepoint/(challenge) combination (e.g. 3 hrs post MeJA pre-treatment). In order to use this global transcriptome data to assess the establishment, maintenance and release of MeJA-IR, two separate transcriptomics analyses were conducted. The first characterised the response to MeJA pre-treatment (Chapter Sections 3.3.4, 3.3.5, 3.3.6 and 3.3.7) and the second characterised the response to subsequent MeJA challenge (Chapter Section 3.3.8).

3.3.4. Profiling the Transcriptional Response to a MeJA Pre-treatment

To analyse the transcriptional response to the resistance inducing MeJA pre-treatment, we used the RNA-seq samples from the three post pre-treatment timepoints (3 hrs, 24 hrs and 1 wk) in addition to the samples from mock challenged plants, from both pre-treatments (water and MeJA), which acted as the 4 wk timepoint (Figure 3.1). Both a principle component analysis (PCA) and a hierarchical clustering analysis

---

Figure 3.3. (continued)

samples **(A)** or the 6 hrs water pre-treated and water challenged replicates **(B)**. Those treatment groups which do not share the same letter are significantly different (ANOVA followed by Tukey post hoc test, $p < 0.05$ (**(A)** *PR.2, MYC, EIN3, NRPE1* and *DML* **(B)** *PR.2, MYC* and *DML*); Welch ANOVA followed by Pairwise t-test, $p.adj < 0.05$ (**(B)** *PR.1*); Kruskal-wallis test followed by Pairwise wilcox test, $p.adj < 0.05$ (**(A)** *PR.1* **(B)** *EIN3*); No pairwise comparison as no significant effect of treatment group (**(B)** *NRPE1*).

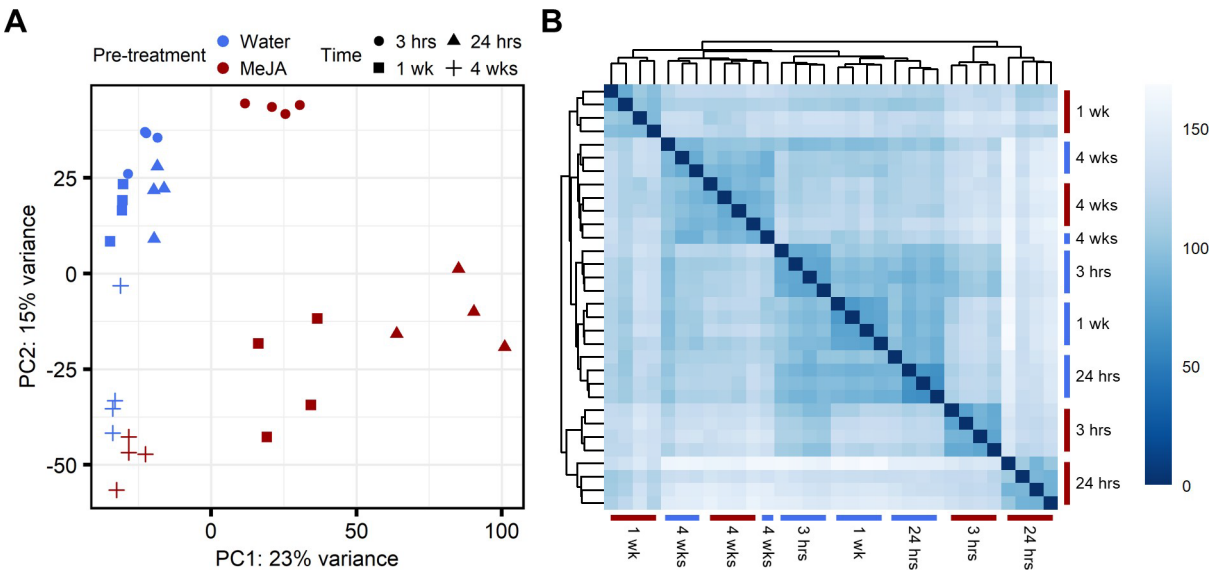

Figure 3.4. MeJA Pre-treatment Induces a Transient Shift in the Bark Transcriptome.

A principle component analysis (PCA) **(A)** and hierarchical clustering analysis (HCA) **(B)** demonstrating how treatment of 2-year-old seedlings with water (blue) or 10 mM MeJA (red) impacted on the bark transcriptome over the subsequent 4 weeks. All genes with a total read count of ≥ 100 across the 32 samples (four replicates per pre-treatment and timepoint combination) were included in the analyses. Both the PCA and HCA utilised read counts normalised for library size and transformed, to homogenise variances of genes from different expression levels, using the DESeq2 function vst (Love et al, 2014). The dendrogram and heatmap display the outcome of clustering samples using Euclidean distances (darker colours equate to a higher similarity) and the complete-linkage method.

(HCA) were performed to confirm the consistency of replicates and check the global patterns in the data. Both analysis methods suggested that MeJA pre-treatment induced a transient shift in the bark transcriptome (Figure 3.4). Although the 3 hrs samples were somewhat similar, by 24 hrs post pre-treatment the MeJA samples were distinct from the water controls. The separation between the two treatments was reduced at 1 wk and by 4 wks post pre-treatment, the MeJA samples were very similar to the water controls (Figure 3.4). This was evidenced by the 4 wks samples not perfectly clustering by pre-treatment (Figure 3.4B). Nevertheless, apart from the 4 wks timepoint, the replicates of all other treatment groups clustered together, further confirming the quality of the dataset.

Having found that MeJA induces a transient shift in the global transcriptome (Figure 3.4), next we profiled the expression patterns of genes which responded to the MeJA pre-treatment. The R package DESeq2 (Love et al., 2014) was used to identify the genes which showed a significantly (FDR adjusted *p*-value (*p.adj*) < 0.001) altered expression profile across time as a result of MeJA pre-treatment. In total 6330 significant genes were identified (Supplemental Data Set 3.1). Based on expression

pattern, these differentially expressed genes were grouped into thirteen clusters (Figure 3.5A). While each cluster had a subtly different expression profile, there were broadly four main patterns (Figure 3.5B). The genes in clusters 1 (yellow), 2 (dark pink), 4 (orange), 5 (purple) and 13 (sandy brown) were transiently upregulated in response to MeJA pre-treatment before returning to basal (i.e. the expression level in the water controls; clusters 2 and 5), or near basal (clusters 1, 4 and 13), expression levels by 4 wks post challenge (group 1; Figures 3.5A and 3.5B and Supplemental Data Set 3.1). Peak upregulation was probably reached earliest for the genes of cluster 2. Furthermore, peak upregulation of the group 1 genes generally occurred before 1 wk post pre-treatment. An exception to this was that some of the genes of cluster 13 likely reached peak upregulation later, between 1 and 4 wks post pre-treatment. Notably, the basal expression level of the genes of cluster 13 increased substantially between 1 and 4 wks post pre-treatment and therefore the expression levels of these genes did not substantially change from 1 wk to 4 wks in the MeJA pre-treatment samples (Figure 3.5A and 3.5B). For the second group, consisting of clusters 3 (dark green) and 9 (turquoise), majority of genes were initially upregulated in response to MeJA however they then returned to basal levels before exhibiting slightly repressed expression long-term (Figures 3.5A and 3.5B and Supplemental Data Set 3.1). Clusters 6 (dark grey), 7 (fluorescent green), 8 (pale pink), 11 (light blue) and 12 (brown) made up the third group, with the genes of these clusters being repressed in response to MeJA, reaching a maximal downregulation between 3 hrs and 1 wk, before returning to basal (8 and 12) or near basal expression (6, 7 and 11) levels by 4 wks post pre-treatment. The final group, group 4, consisted of one cluster, cluster 10 (red), and its genes were at first repressed before climbing back to and above basal expression levels (Figures 3.5A and 3.5B and Supplemental Data Set 3.1).

To assess whether there were particular functional annotations associated with each of the clusters, we performed protein signature and Gene Ontology (GO) term enrichment analysis (Figure 3.5C and Supplemental Data Sets 3.2 and 3.3). The enriched Pfam accessions (the Pfam database was the source of protein signatures) and GO terms associated with the clusters displaying MeJA-induced repression (group 3) were generally related to processes involved in primary cell functioning and metabolism, such as cell division, the Krebs cycle, photosynthesis and transcription.

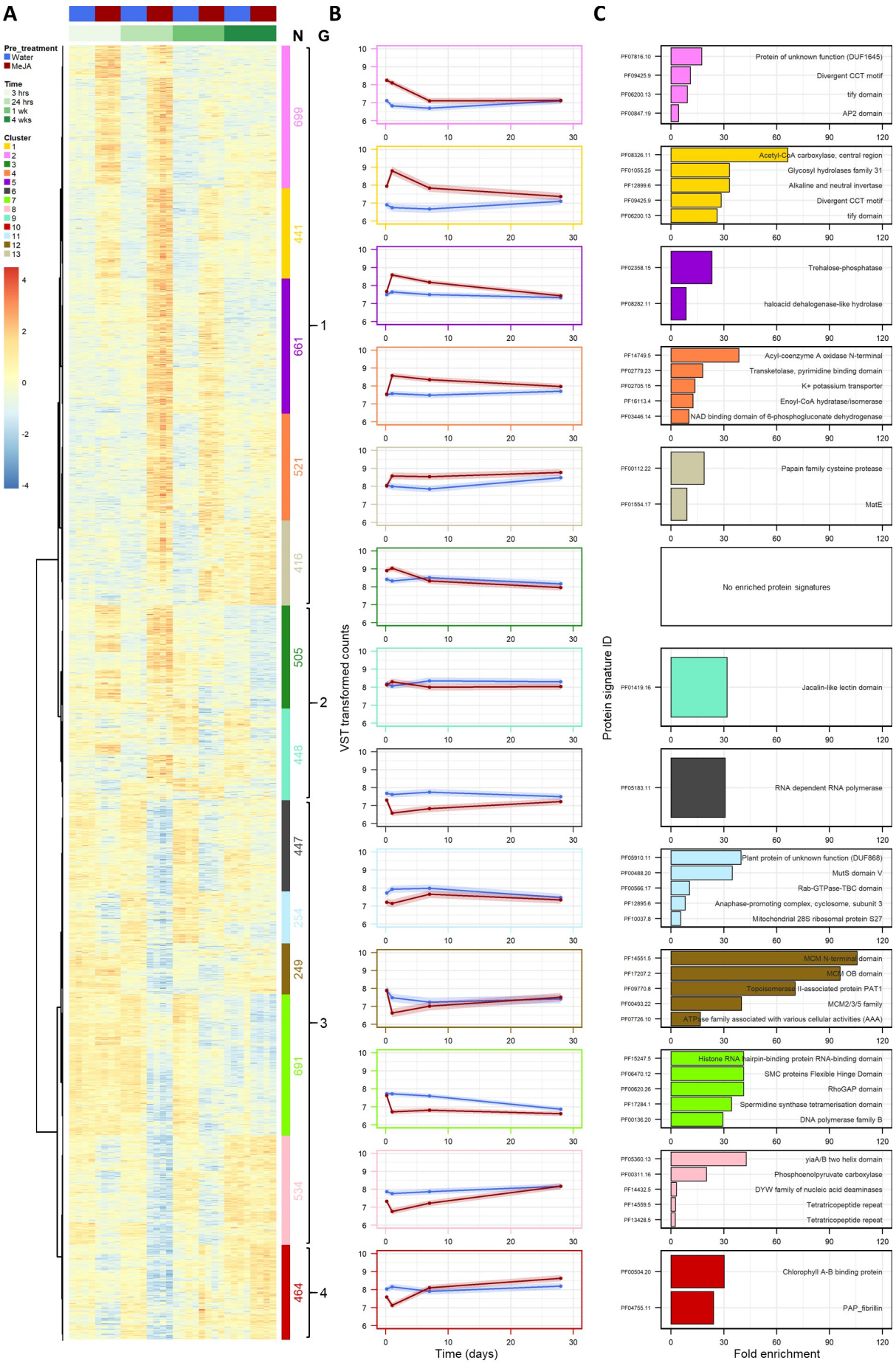
A
B
C
N
G
Pre_treatment
Water
MeJA
Time
3 hrs
24 hrs
1 wk
4 wks
Cluster
1
2
3
4
5
6
7
8
9
10
11
12
13
699
441
661
521
416
505
448
447
254
249
691
534
464
1
2
3
4
VST transformed counts
Time (days)
Protein signature ID
Fold enrichment
PF07816.10
Protein of unknown function (DUF1645)
PF09425.9
Divergent CCT motif
PF06200.13
tify domain
PF00847.19
AP2 domain
PF08326.11
Acetyl-CoA carboxylase, central region
PF01055.25
Glycosyl hydrolases family 31
PF12899.6
Alkaline and neutral invertase
PF09425.9
Divergent CCT motif
PF06200.13
tify domain
PF02358.15
Trehalose-phosphatase
PF08282.11
haloacid dehalogenase-like hydrolase
PF14749.5
Acyl-coenzyme A oxidase N-terminal
PF02779.23
Transketolase, pyrimidine binding domain
PF02705.15
K+ potassium transporter
PF16113.4
Enoyl-CoA hydratase/isomerase
PF03446.14
NAD binding domain of 6-phosphogluconate dehydrogenase
PF00112.22
Papain family cysteine protease
PF01554.17
MatE
No enriched protein signatures
PF01419.16
Jacalin-like lectin domain
PF05183.11
RNA dependent RNA polymerase
PF05910.11
Plant protein of unknown function (DUF868)
PF00488.20
MutS domain V
PF00566.17
Rab-GTPase-TBC domain
PF12895.6
Anaphase-promoting complex, cyclosome, subunit 3
PF10037.8
Mitochondrial 28S ribosomal protein S27
PF14551.5
MCM N-terminal domain
PF17207.2
MCM OB domain
PF09770.8
Topoisomerase II-associated protein PAT1
PF00493.22
MCM2/3/5 family
PF07726.10
ATPase family associated with various cellular activities (AAA)
PF15247.5
Histone RNA hairpin-binding protein RNA-binding domain
PF06470.12
SMC proteins Flexible Hinge Domain
PF00620.26
RhoGAP domain
PF17284.1
Spermidine synthase tetramerisation domain
PF00136.20
DNA polymerase family B
PF05360.13
yiaA/B two helix domain
PF00311.16
Phosphoenolpyruvate carboxylase
PF14432.5
DYW family of nucleic acid deaminases
PF14559.5
Tetratricopeptide repeat
PF13428.5
Tetratricopeptide repeat
PF00504.20
Chlorophyll A-B binding protein
PF04755.11
PAP_fibrillin

For example, cluster 7 (fluorescent green) was enriched for terms such as “DNA polymerase family B” (PF00136.20), “regulation of cell cycle phase transition” (GO:1901987), “DNA replication” (GO:0006260) and “gene silencing” (GO:0016458; Supplemental Data Sets 3.2 and 3.3). Furthermore, “Phosphoenolpyruvate carboxylase” (PF00311.16) and “photosystem II assembly” (GO:0010207) were enriched among the genes of clusters 8. Photosynthesis related terms such as “photosynthesis, light harvesting” (GO:0009765) and “chlorophyll biosynthetic process” (GO:0015995) were also enriched for cluster 10 (Figure 3.5C and Supplemental Data Sets 3.2 and 3.3), suggesting that while photosynthesis maintenance and functioning may initially be repressed by MeJA, longer term it may be upregulated to higher than basal levels in compensation. Another commonality between clusters 8 and 10 was that they both had an overrepresentation of genes involved in terpenoid biosynthesis (Supplemental Data Set 3.3). Interestingly, the group 1 clusters 1 and 4 also had enriched terms related to terpenoid production such as “Terpene synthase family, metal binding domain” (PF03936.15) and “terpenoid biosynthetic process” (GO:0016114), respectively (Supplemental Data Sets 3.2 and 3.3). Thus, the composition or quantity of terpenoids in bark tissue was likely modulated in response to MeJA as has previously been observed (Zulak et al., 2009).

In addition to terpene biosynthesis, there were numerous other ‘response to biotic stress’ related annotations overrepresented in the group 1 clusters (Figure 3.5C and Supplemental Data Set 3.2 and 3.3). This was exemplified by clusters 1 (yellow) and 2 (pink). The enriched GO terms associated with one or both of these clusters included “regulation of innate immune response” (GO:0045088), “regulation of

---

Figure 3.5. Transcriptional Response to MeJA Pre-treatment (*Figure appears on previous page*).

Expression profiles and functional characterisation of genes (6330) showing a significantly (adjusted *p*-value < 0.001) altered expression pattern, over a month-long time course, between the bark tissue of water (control, blue) and 10 mM MeJA (red) pre-treated 2-year-old seedlings.
(A) Differentially expressed genes were grouped into thirteen clusters (indicated by the coloured boxes with associated gene numbers (N)) using Spearman distances and Ward’s method. The thirteen clusters were assigned to one of four groups (G) based on their general MeJA relative to water expression pattern: 1 – Upregulated, 2 – Upregulated then downregulated, 3 – Downregulated and 4 – Downregulated then upregulated. Read counts normalised for library size and transformed using the DESeq2 function vst, are displayed as per gene z-scores.
(B) Per cluster mean expression profiles with 95% confidence intervals. Transformed counts are approximately on a $\log_2$ scale.
(C) Significantly overrepresented protein signatures (adjusted *p*-value ≤ 0.05). If a cluster had more than five significantly enriched protein signatures, only the five with the highest fold enrichment are displayed. See Supplemental Data Set 3.2 for the full list of enriched protein signatures.

defense response to fungus" (GO:1900150), "response to chitin" (GO:0010200), "regulation of plant-type hypersensitive response" (GO:0010363) and "response to wounding" (GO:0009611; Supplemental Data Set 3.3). Furthermore, given the importance of the hormones JA and salicylic acid (SA) in regulating plant defence to biotic stress in angiosperms (Pieterse et al., 2012), it is unsurprising that there was also genes in the group 1 clusters associated with these hormones. Enriched GO terms associated with the group 1 clusters including "salicylic acid mediated signaling pathway" (GO:0009863), "jasmonic acid mediated signaling pathway" (GO:0009867) and "jasmonic acid biosynthetic process" (GO:0009695; Supplemental Data Set 3.3). Furthermore, clusters 1 and 2 contain genes encoding for JAZMONATE ZIM DOMAIN (JAZ) proteins which are key regulators of the response to JA (Chini et al., 2016). This was evidenced by the "tify domain" (PF06200.13) and "Divergent CCT motif" (PF09425.9; renamed "Jas motif") which were enriched in both clusters and are characteristic of JAZ proteins (Howe et al., 2018) (Figure 3.5C and Supplemental Data Set 3.2). Notably these two group 1 clusters also contained ET and abscisic acid (ABA) responsive genes as evidence by the enriched GO terms "response to ethylene stimulus" (GO:0009723) and "response to abscisic acid stimulus" (GO:0009737; Supplemental Data Set 3.3). This result is consistent with the known co-regulation of JA signalling pathways by ET and ABA in Arabidopsis (Chapter section 1.3). In summary, MeJA-augmented gene clusters are strongly associated with the defence response to biotic stress whereas MeJA-repressed gene clusters are more linked with primary cell functioning and metabolism.

3.3.5. Biosynthesis of Defence Hormones in Response to MeJA Pre-treatment

Based on the results of the protein signature and GO term enrichment analysis, along with the known links of JA and SA to the regulation of defences effective against biotic stress (Chapter Sections 1.3 and 1.4), we performed a more detailed analysis of the response of JA and SA biosynthesis and downstream signalling genes to MeJA. This more detailed analysis involved searching the list of 6330 genes displaying an altered expression profile across time as a result of MeJA pre-treatment, for those genes annotated using blastp (Altschul et al., 1990; Altschul et al., 1997; Camacho et al., 2009) and the Swiss-Prot database (The UniProt Consortium, 2019) as encoding JA or SA: biosynthesis enzymes, receptors and related transcriptional regulators.

It is known that in other species, JA positively regulates the expression of its own biosynthesis genes (Wasternack and Song, 2017). It was therefore unsurprising that genes predicted to encode enzymes involved in all steps of the conversion of galactolipids to the bioactive form of JA, (+)-7-iso-jasmonoyl-L-isoleucine, were generally upregulated following MeJA treatment and thus were found in the group 1 clusters (Figures 3.5 and 3.6 and Supplemental Data Set 3.4). This included predicted *OPDA Reductase* (*OPR*) genes (Supplemental Data Set 3.4). The OPRs could be involved in the canonical JA biosynthesis pathway as shown in Figure 3.6 or a recently described alternative pathway which involves 4,5-didehydrojasmonate as an intermediate (Chini et al., 2018).

Interestingly, considering the antagonism between JA and SA in some angiosperms (Pieterse et al., 2012), genes predicted to encode enzymes involved in the biosynthesis of the precursors of SA, such a phenylalanine ammonia-lyase (PAL), were also predominantly found in the group 1 upregulation clusters (Figures 3.5 and 3.7 and Supplemental Data Set 3.4). The same was true for the downstream signalling pathways. Homologs of master regulators which control SA and JA dependent defence responses in Arabidopsis were generally found in the group 1 clusters and were thus transiently upregulated in response to MeJA treatment (Figures 3.5 and 3.8 and Supplemental Data Set 3.4).

Previous work in conifers has demonstrated that ET accumulates in response to MeJA treatment and in turn is an important signalling compound for the induction of defences by MeJA (Hudgins and Franceschi, 2004). Thus, we also explored in more detail the expression of ET biosynthesis genes. ET is synthesised from the amino acid methionine in a three step process involving the enzymes S-adenosyl-L-methionine (SAM) synthetase, 1-aminocyclopropane-1-carboxylic acid (ACC) synthase (ACS) and ACC oxidase (ACO) (Lin et al., 2009). All differentially expressed ET biosynthesis genes were in group 1 clusters (Figure 3.5 and Supplemental Data Set 3.4). Two genes predicted to encode for SAM synthetases were in cluster 1 and one *ACO* gene was in cluster 5 (Figure 3.5 and Supplemental Data Set 3.4). Notably, no *ACS* genes were differentially expressed in the post pre-treatment transcriptome analysis. Nevertheless, all together the results in this section suggest that the biosynthesis of the defence hormones JA, SA and ET is induced in spruce bark by MeJA.

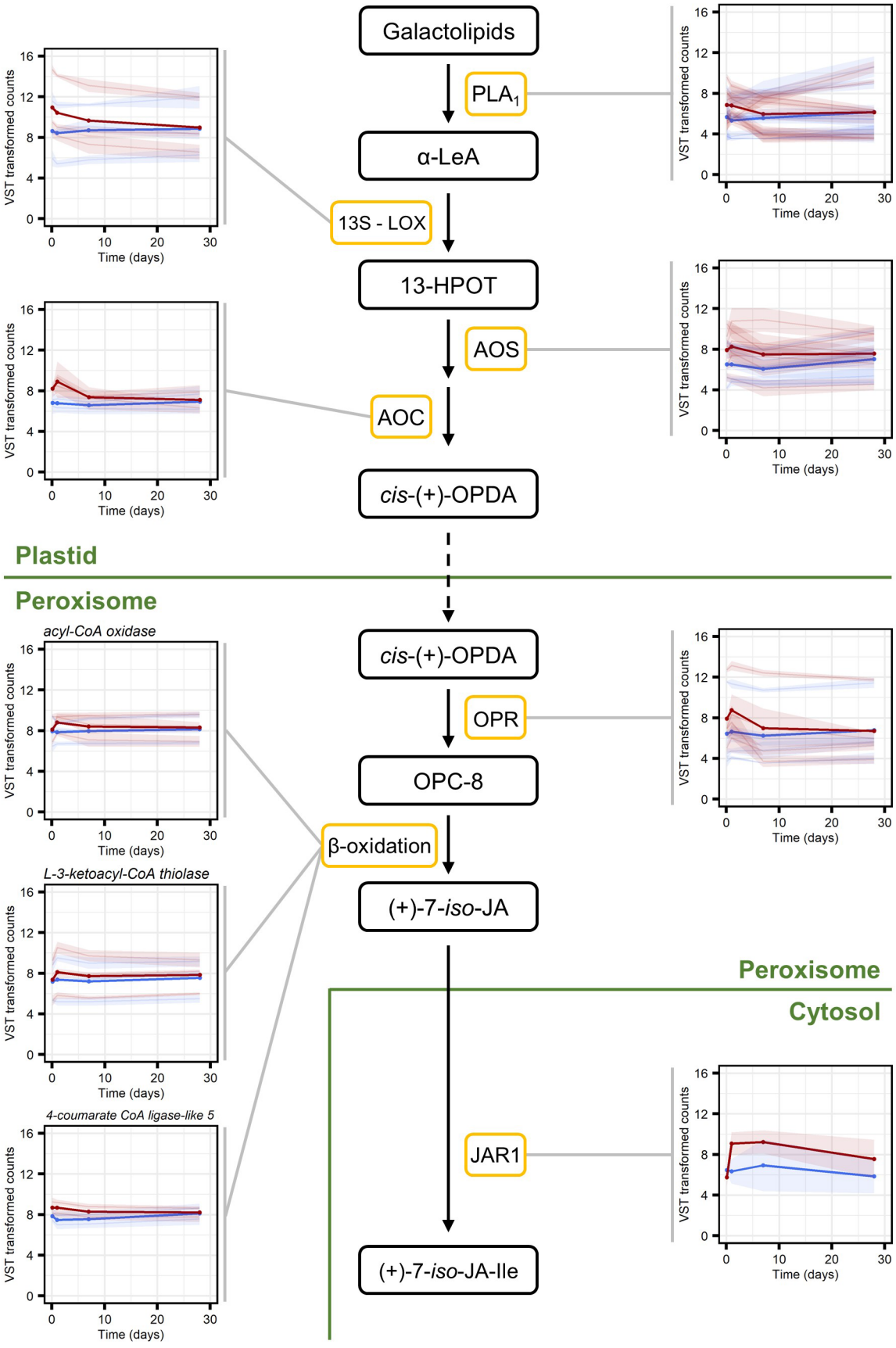
Galactolipids
PLA1
α-LeA
13S - LOX
13-HPOT
AOS
AOC
cis-(+)-OPDA
Plastid
Peroxisome
acyl-CoA oxidase
L-3-ketoacyl-CoA thiolase
4-coumarate CoA ligase-like 5
cis-(+)-OPDA
OPR
OPC-8
β-oxidation
(+)-7-iso-JA
Peroxisome
Cytosol
JAR1
(+)-7-iso-JA-Ile
VST transformed counts
Time (days)

3.3.6. Spruce Defence Genes are Differentially Expressed in Response to MeJA Pre-treatment

The upregulation of defence hormone biosynthesis genes along with downstream signalling genes, suggested that MeJA pre-treatment likely directly induced spruce defences. The functional analysis of the genes in the Figure 3.5A clusters provided evidence in support of this conclusion as it suggested that genes involved in the biosynthesis of terpenes, the major component of oleoresin, were differentially expressed in response to MeJA pre-treatment (Figure 3.5 and Supplemental Data Sets 3.2 and 3.3). This correlates with the previously reported MeJA-induced modulation of terpene levels (Martin et al., 2002; Zulak et al., 2009; Schiebe et al., 2012). It has also previously been shown that MeJA can induce an accumulation of phenolic defence related compounds derived from the phenylpropanoid pathway (Schiebe et al., 2012).

PAL enzymes catalyse what is generally considered the first step of the general phenylpropanoid pathway, conversion of phenylalanine to *trans*-cinnamic acid (*t*-CA) (Deng and Lu, 2017). Interestingly SA is also derived from *t*-CA and as mentioned above, genes annotated to encode for PAL were transiently upregulated in response to MeJA (Figure 3.7 and Supplemental Data Set 3.4). Furthermore, genes predicted to encode for the enzymes cinnamic acid 4-hydroxylase and 4-coumaroyl CoA ligase, which are involved in the next and final two steps of the general phenylpropanoid pathway (Deng and Lu, 2017), were also transiently upregulated and thus in group 1 clusters (Figure 3.5 and Supplemental Data Set 3.1). From the general

---

Figure 3.6. JA Biosynthesis Genes are Upregulated, Either Transiently or for at Least Four Weeks, in Response to MeJA Treatment (*Figure appears on previous page*).

Expression profiles of genes displaying a significantly (adjusted *p*-value < 0.001) altered expression pattern across time as a result of MeJA pre-treatment and which were annotated as encoding for enzymes involved in the (+)-7-iso-JA-Ile biosynthesis pathway. In each of the plots, the faint lines indicate the mean expression profiles, with 95% confidence intervals, of individual genes and the thicker lines depict the mean per enzyme category profile, for each of the two pre-treatments water (blue) and MeJA (red). Read counts were normalised for sequencing depth and transformed to approximately the $\log_2$ scale using the DESeq2 function vst (Love et al., 2014). The JA biosynthesis pathway is based on knowledge from angiosperms such as *Arabidopsis thaliana* and *Solanum lycopersicum* and was adapted from Wasternack and Hause (2013) and Wasternack and Song (2017). Compound abbreviations: α-LeA, α-linolenic acid; 13-HPOT, (13S)-hydroperoxyoctadecatrienoic acid; cis-(+)-OPDA, cis-(+)-12-oxophytodienoic acid; OPC-8, 3-oxo-2-(2-pentenyl)-cyclopentane-1-octanoic acid; (+)-7-iso-JA, (+)-7-iso-jasmonic acid; (+)-7-iso-JA-Ile, (+)-7-iso-jasmonoyl-L-isoleucine. Enzyme abbreviations: PLA1, phospholipase A1; 13S-LOX, 13S-lipoxygenase; AOS, allene oxide synthase; AOC, allene oxide cyclase; OPR, OPDA reductase; JAR1, JA-amino acid synthetase.

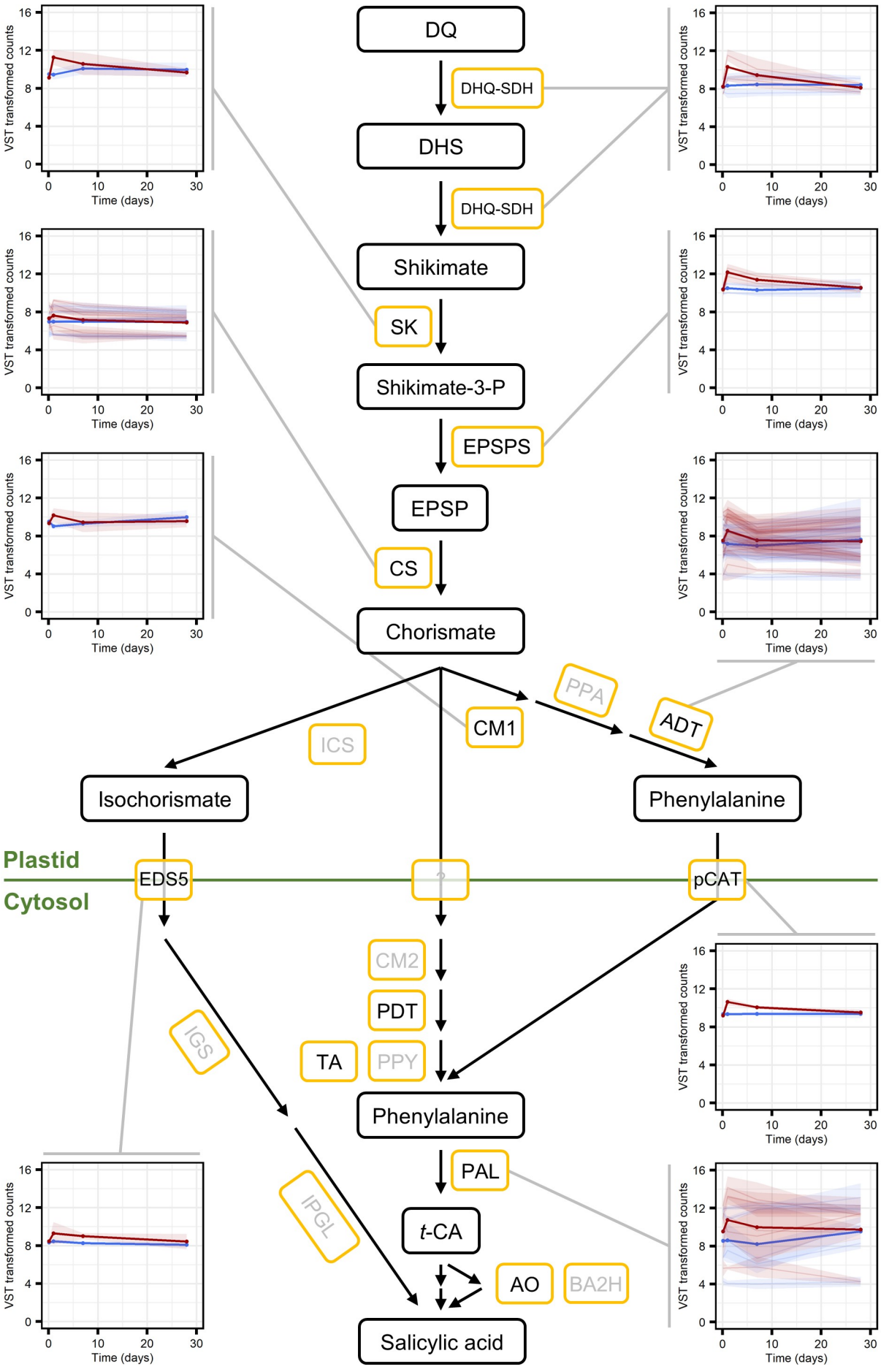
DQ
DHQ-SDH
DHS
DHQ-SDH
Shikimate
SK
Shikimate-3-P
EPSPS
EPSP
CS
Chorismate
ICS
CM1
PPA
ADT
Isochorismate
Phenylalanine
Plastid
Cytosol
EDS5
?
pCAT
CM2
PDT
TA
PPY
IGS
Phenylalanine
PAL
IPGL
t-CA
AO
BA2H
Salicylic acid
VST transformed counts
Time (days)

phenylpropanoid pathway a huge range of metabolites can be formed with a diversity of functions (Deng and Lu, 2017). To focus on the formation of metabolites most likely to be linked to MeJA-IR, we searched the list of 6330 genes showing an altered expression profile across time as a result of MeJA pre-treatment (Figure 3.5 and Supplemental Data Set 3.1) for those genes predicted to encode enzymes involved in the biosynthesis of phenylpropanoids that have been reported to be associated with defence of spruce against Ophiostomatoid fungal pathogens (Hammerbacher et al., 2011; Hammerbacher et al., 2014; Hammerbacher et al., 2018; Hammerbacher et al., 2019). Genes predicted to encode: chalcone synthase, chalcone isomerase, flavanone-3-hydroxylase, flavonol-3′-hydroxylase, flavonol-3′5′-hydroxylase, dihydroflavonol 4-reductase, anthocyanidin synthase, anthocyanidin reductase and leucoanthocyanidin reductase, were identified among the list of genes differentially expressed by MeJA pre-treatment (Supplemental Data Set 3.1). Generally, these biosynthesis genes were in group 1 clusters and were therefore upregulated in response to MeJA pre-treatment (Figure 3.5 and Supplemental Data Set 3.1). Notably, these genes are all involved in the production of phenylpropanoids of the flavonoid

---

Figure 3.7. Genes Involved in the Biosynthesis of the Precursors of Salicylic Acid (SA) and Phenolic Defence Compounds Including Flavonoids and Stilbenes, are Transiently Upregulated in Response to MeJA Treatment.

Expression profiles of genes displaying a significantly (adjusted *p*-value < 0.001) altered expression pattern across time as a result of MeJA pre-treatment and which were annotated as encoding for enzymes and transporters involved in the biosynthesis of the precursors of SA and other phenolic secondary metabolites such as flavonoids. In each of the plots, the faint lines indicate the mean expression profiles, with 95% confidence intervals, of individual genes and the thicker lines depict the mean per protein category profile, for each of the two pre-treatments water (blue) and MeJA (red). Read counts were normalised for sequencing depth and transformed to approximately the $\log_2$ scale using the DESeq2 function vst (Love et al., 2014). The pathway is based on what is known about the biosynthesis of SA in angiosperms and was adapted from Dempsey et al (2011), Ding and Ding (2020) and MetaCyc (Caspi et al., 2020). Enzymes in grey are involved in the biosynthesis pathway but no differentially expressed genes were annotated to encode for them. Due to space limitations not all enzymes have associated expression profiles, see Supplementary Data Set 3.4 for the full list of differentially expressed biosynthesis genes. Compound abbreviations: DQ, 3-dehydroquinate; DHS, 3-dehydroshikimate; Shikimate-3-P, shikimate 3-phosphate; EPSP; 5-enolpyruvoyl-shikimate 3-phosphate; t-CA, trans-cinnamic acid. Enzyme/transporter abbreviations: DHQ-SDH, dehydroquinate-shikimate dehydrogenase; SK, shikimate kinase; EPSPS, 5-enolpyruvylshikimate-3-phosphate synthase; CS, chorismate synthase; CM1, chorismate mutase 1; PPA, prephenate aminotransferase; ADT/PDT, arogenate dehydratase/prephenate dehydratase (annotated as being encoded for by the same genes); CM2, chorismate mutase 2; PPY, phenylpyruvate aminotransferase; TAT, tyrosine aminotransferase; pCAT, plastidial cationic amino-acid transporter; PAL, phenylalanine ammonia-lyase; AO, aldehyde oxidase; BA2H, benzoic acid 2-hydroxylase; ICS, isochorismate synthase; IGS, isochorismoyl-glutamate synthase; IPGL, IC-9-Glu pyruvoyl-glutamate lyase; EDS5, ENHANCED DISEASE SUSCEPTIBILITY 5.

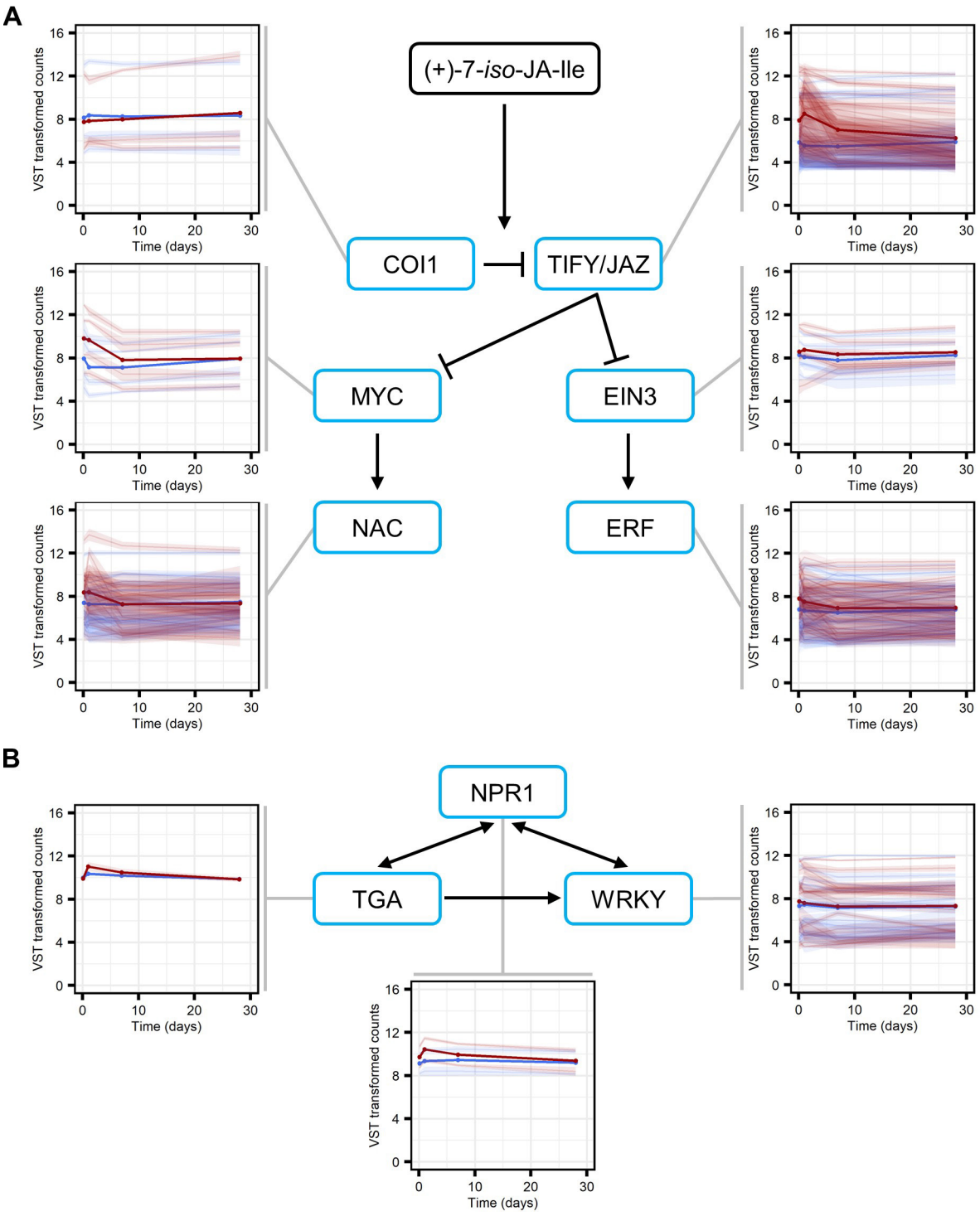

Figure 3.8. MeJA Treatment Induces a Rapid and Transient Upregulation of Regulators of JA and SA Dependent Defences.

Expression profiles of genes displaying a significantly (adjusted *p*-value < 0.001) altered expression pattern across time as a result of MeJA pre-treatment and which were annotated as encoding for proteins involved in regulation of JA (A) and SA (B) dependent defences. In each of the plots, the faint lines indicate the mean expression profiles, with 95% confidence intervals, of individual genes and the thicker lines depict the mean per protein category profile, for each of the two pre-treatments water (blue) and MeJA (red). Read counts were normalised for sequencing depth and transformed to approximately the $\log_2$ scale using the DESeq2 function vst (Love et al, 2014). The pathways are based on what is known in *Arabidopsis thaliana*. Compound abbreviations: (+)-7-iso-JA-Ile, (+)-7-iso-jasmonoyl-L-

group and none of the 6330 differentially expressed genes were annotated as encoding for stilbene synthases. Nevertheless, overall, the post pre-treatment transcriptome analysis suggests that the biosynthesis of defence related phenylpropanoids was upregulated by MeJA.

In addition to terpene and phenolic based defences, PR proteins are also thought to be an important component of spruce defence to biotic stress (Franceschi et al., 2005). Potentially MeJA treatment could trigger an upregulation of *PR* genes which in turn could result in a long-term accumulation of PR proteins, which would provide enhanced resistance to subsequent attack. To assess this, the list of 6330 differentially expressed genes (Supplemental Data Set 3.1) was searched for ones which were predicted to encode for PR proteins. Interestingly there was not a consensus pattern (Figure 3.9) and genes predicted to encode for PR proteins were found in clusters from all four groups (Figure 3.5 and Supplemental Data Set 3.4). Thus, while some PR proteins may accumulate in response to MeJA treatment, based on gene expression data alone, it is not the consensus pattern.

3.3.7. MeJA Pre-treatment Induces Differential Expression of Epigenetic Regulators

There is increasing evidence for an involvement of epigenetic mechanisms in immunological memory and maintenance of IR (Wilkinson et al., 2019). Interestingly, the GO term enrichment analysis suggested that genes encoding for epigenetic regulators were differentially expressed following MeJA pre-treatment. This pattern was exemplified by Figure 3.5 cluster 7 (MeJA-repressed) as overrepresented GO terms among its genes included “DNA methylation or demethylation” (GO:0044728), “chromatin silencing” (GO:0006342) and “histone modification” (GO:0016570; Supplemental Data Set 3.3). Thus, together with the evidence from the RT-qPCR analysis (Figure 3.3), it seems that MeJA pre-treatment alters the expression of epigenetic regulators which may in turn lead to an altered epigenetic landscape and be linked to the maintenance of MeJA-IR between pre-treatment and challenge.

Figure 3.8. (continued)

isoleucine. Protein abbreviations: COI1, CORONATINE INSENSITIVE1; JAZ, JASMONATE-ZIM-DOMAIN PROTEIN; NAC, Petunia NAM and Arabidopsis ATAF1, ATAF2, and CUC2; EIN3, ETHYLENE INSENSITIVE 3; ERF, ETHYLENE RESPONSIVE FACTOR; NPR1, NONEXPRESSER OF PR GENES 1; TGA, TGACG motif-binding.

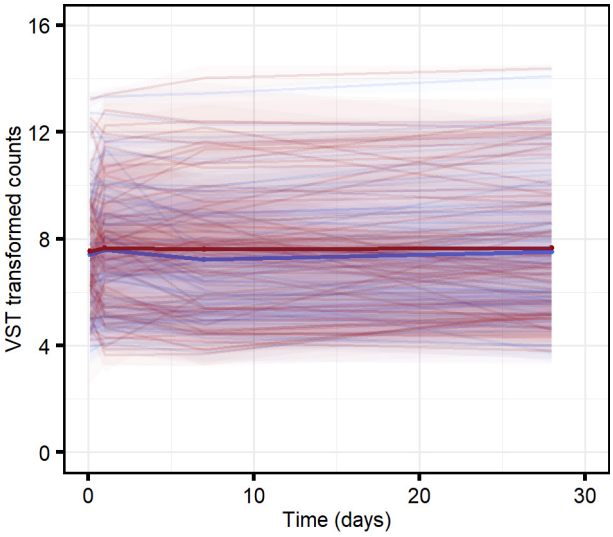

Figure 3.9. *Pathogenesis-related* (*PR*) Genes Response to MeJA Pre-treatment.

Expression profiles of genes displaying a significantly (adjusted *p*-value < 0.001) altered expression pattern across time as a result of MeJA pre-treatment and annotated as encoding for a PR protein. The faint lines depict the mean expression profiles, with 95% confidence intervals, of individual genes and the thicker lines depict the overall mean profile, for each of the two pre-treatments water (blue) and MeJA (red). Read counts were normalised for library size and transformed to approximately the $\log_2$ scale using the DESeq2 function vst (Love et al., 2014).

To further investigate the specific categories of epigenetic regulators which were differentially expressed in response to MeJA pre-treatment, we screened the 6330 genes in Figure 3.5A for those which featured in the list of Norway spruce epigenetic regulators compiled by (Mageroy et al., 2020b). Multiple epigenetic regulators, from a variety of categories, were differentially expressed in response to MeJA pre-treatment (Figure 3.10A). Furthermore, epigenetic regulator genes fell into all the thirteen Figure 3.5 clusters (Supplemental Data Set 3.5) and thus displayed was a variety of expression patterns (Figure 3.10B and Supplemental Figure 3.3). Nevertheless, some categories did exhibit an overall pattern, for instance on average MeJA induced a transient upregulation of histone acetyltransferase genes (Supplemental Figure 3.3).

In Chapter 2 of this thesis evidence was provided for a role of DNA methylation in within generation jasmonate-IR in Arabidopsis. Therefore, we focused on the expression profiles of the DNA methylation regulator categories. As can be seen in Figure 3.10B, the results of the targeted transcriptome analysis (Figure 3.3) match with the more general pattern, regulators of DNA methylation are repressed in response to MeJA pre-treatment. Interestingly, relevant to DNA methylation establishment and maintenance, it is particularly RdDM-related genes which are targeted for repression (Figure 3.10B and Supplemental Data Set 3.5). In addition to *NRPE1*, genes predicted to encode proteins involved in many different aspects of RdDM were repressed including NUCLEAR RNA POLYMERASE D 1 (NRPD1), the largest subunit of Pol IV, and RNA-DEPENDENT RNA POLYMERASE 2 (RDR2; see

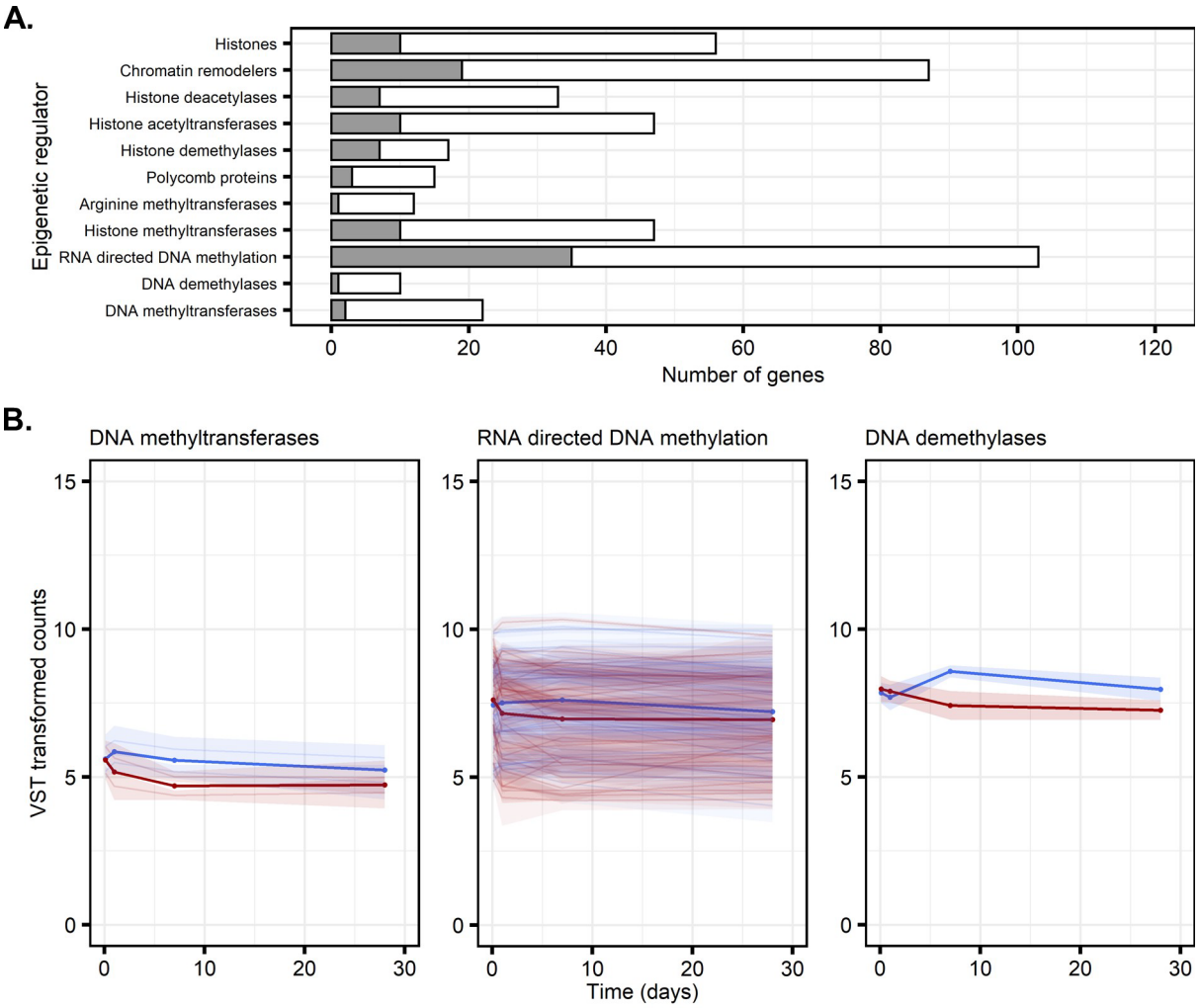

Figure 3.10. MeJA Pre-treatment Alters the Expression of Regulators of Multiple Epigenetic Modifications Including DNA Methylation.

(A) The total numbers of different classes of epigenetic regulator annotated in the spruce genome by Mageroy et al (2020b), are indicated by the white bars. The number of annotated genes which in this study exhibited a significantly (adjusted *p*-value < 0.001) altered expression pattern across time as a result of MeJA pre-treatment are indicated by the grey fill.
(B) The individual gene (faint lines) and category mean (solid lines) post water (blue) and MeJA (red) pre-treatment expression profiles for differentially expressed DNA methylation homeostasis regulators. The shading indicates the 95% confidence intervals for individual genes. Read counts were normalised for sequencing depth and transformed to approximately the $\log_2$ scale using the DESeq2 function vst (Love et al., 2014).

the sidebar titled RNA-directed DNA methylation in Chapter 1). Furthermore, both differentially expressed DNA methyltransferases were predicted to encode for DNA (cytosine-5)-methyltransferase (DRMs; Figure 3.10B and Supplemental Data Set 3.5). In Arabidopsis, DRMs are guided by Pol IV (or Pol II) derived small RNAs (sRNAs) to specific genome locations where they establish DNA methylation (Zhang et al., 2018b). Over 60% of the differentially expressed RdDM-related genes were in the group 3 clusters, with the mean pattern suggesting that RdDM began to be repressed

between 3 and 24 hrs post MeJA pre-treatment (Figure 3.10B and Supplemental Data Set 3.5).

The DNA glycosylase gene studied by RT-qPCR (Figure 3.3; *MA_68384g0010*) was not identified as differentially expressed in the post pre-treatment RNA-seq transcriptome analysis. Nevertheless, there was one DNA demethylase (*MA_111413g0010*) identified and it exhibited an analogous gene expression pattern. *MA_111413g0010* was in Figure 3.5 cluster 9 and thus was initially marginally upregulated before being downregulated to below basal expression levels (Figure 3.10B). It was not downregulated until at least 24 hrs post pre-treatment. Thus, there seems to be some delay between the downregulation of RdDM and the downregulation of DNA glycosylases, following MeJA pre-treatment. This suggests MeJA pre-treatment may induce genome-wide hypomethylation.

3.3.8. Characterisation of the Transcriptional Response to Challenge

The RT-qPCR analysis revealed that *PR* genes showing a primed response to challenge in mature trees, did not exhibit the same response in seedlings (Figure 3.3). While we did use a different challenge to our previous study, MeJA rather than wounding, this targeted analysis suggests that different mechanisms may underpin the MeJA-IR in seedlings. For instance, as suggested by the post pre-treatment transcriptome analysis, maybe there is more reliance on long-term altered expression of defence machinery (e.g. terpenoid and phenylpropanoid biosynthesis). However, in order to truly understand how the MeJA pre-treatment results in enhanced resistance to jasmonate-resisted attackers, we needed to study the response to subsequent challenge by MeJA in more detail. Thus, we performed a second untargeted transcriptomics analysis using only the post challenge RNA-seq samples. These were generated from plants pre-treated with water (W) or 10 mM MeJA, challenged 4 wks later with water (W_W or MeJA_W) or 5 mM MeJA (W_MeJA or MeJA_MeJA) and then harvested at 6 hrs post challenge (Figure 3.1). In our previous study (Mageroy et al., 2020b) the 24 hrs post challenge timepoint we used. This timepoint was not used in the present study as we wanted to try and investigate not only the defences underpinning MeJA-IR but also what regulates this response. In our RT-qPCR analysis the *MYC* TF gene reached peak upregulation by 3-6 hrs post MeJA treatment (Figure 3.3). Furthermore, our global transcriptome analysis demonstrated that in naïve plants,

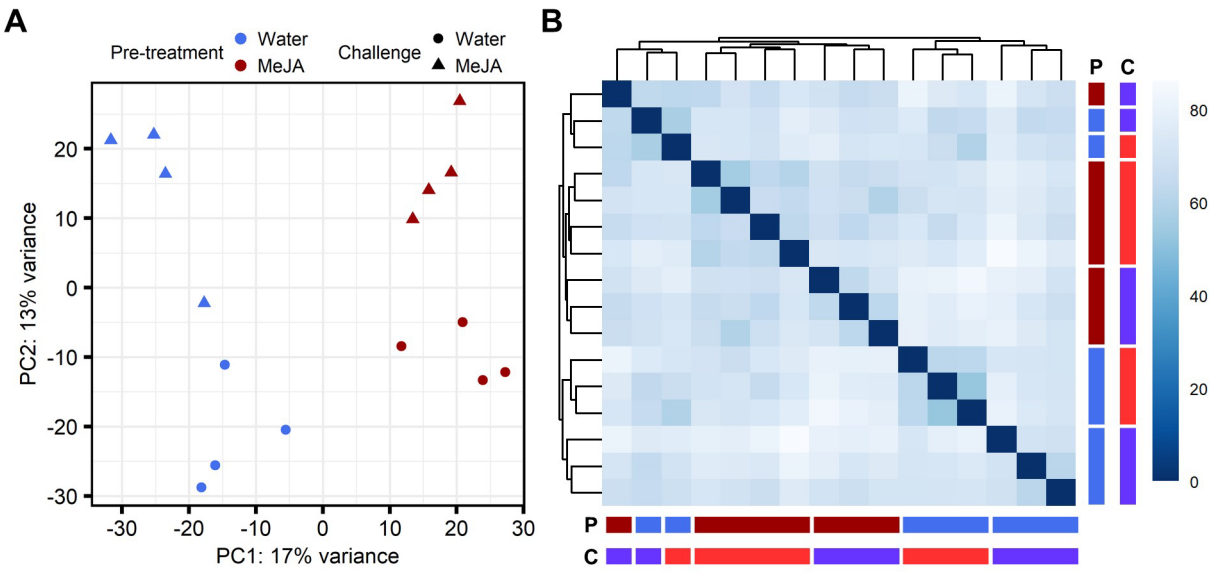

Figure 3.11. Impact of MeJA Pre-treatment and Challenge on the Bark Transcriptome.

A principle component analysis (PCA) **(A)** and hierarchical clustering analysis (HCA) **(B)** of bark tissue transcriptomes of 2-year-old seedlings pre-treatment (P) with water (blue) or 10 mM MeJA (red) and then challenged (C) with water (circle or dark blue) or 5 mM MeJA (triangle or light red) 4 weeks later. All genes with a total read count of ≥ 100 across the 16 samples (four replicates per pre-treatment and challenge combination) were included in the analyses. Both the PCA and HCA utilised read counts normalised for library size and transformed, to homogenise variances of genes from different expression levels, using the DESeq2 function vst (Love et al., 2014). The dendrogram and heatmap display the outcome of clustering samples using Euclidean distances (darker colours equate to a higher similarity) and the complete-linkage method.

numerous genes involved in defence regulation were already up regulated by 3 hrs post MeJA treatment and by 24 hrs could well have past peak differential expression (Figure 3.5). Thus, if we used the 24 hrs post challenge timepoint, we could miss the primed induction of many regulatory genes which respond rapidly to MeJA challenge in naïve plants. These regulatory genes are likely very important for the upregulation of defences which underpin MeJA-IR. Thus, out of the three timepoints available to us, 6 hrs post challenge was the most appropriate if we were going to identify key regulators and downstream defences involved in MeJA-IR.

To explore the global patterns in the post-challenge transcriptome data a PCA and HCA were performed. Although the replicates of the four post challenge treatment groups were not grouped perfectly by the HCA, they were separated by the PCA (Figure 3.11). Thus, together the analyses suggested that there were no mislabelled or outlier samples. PC1 of the PCA correlated with pre-treatment and in the HCA samples generally grouped by pre-treatment rather than challenge. Taken together the findings of these global analysis methods suggest that at the timepoint chosen (6

hrs post challenge), the effect of MeJA pre-treatment was stronger than the effect of MeJA challenge on the bark transcriptome.

To further explore the post challenge transcriptomes, all six possible pairwise comparisons between the four post challenge treatment groups were performed with DESeq2 (Figures 3.1 and 3.12 and Supplemental Data Set 3.6). In support of the PCA and HCA, there were a greater number of differentially expressed genes in the across pre-treatment comparisons (i.e. MeJA_ vs W_) than the within pre-treatment comparisons (i.e. W_ vs. W_ or MeJA_ vs. MeJA_; Figure 3.12 and Supplemental Data Set 3.6). The comparison between MeJA_MeJA and MeJA_W had the lowest number of differentially expressed genes and the W_MeJA and W_W comparison had the second lowest (Figure 3.12). Furthermore, the within pre-treatment comparisons had at least double the number of upregulated genes to downregulated genes, whereas the between pre-treatment comparisons generally had a similar number of up and down regulated genes (Figure 3.12B). A slight exception was the MeJA_W Vs W_MeJA comparison, which had more genes that were downregulated than upregulated. Furthermore, this comparison also had the highest total number of differentially expressed genes (Figure 3.12 and Supplemental Data Set 3.6), suggesting that there is a substantial difference between the short and long-term impacts of MeJA treatment on the transcriptomes of Norway spruce seedlings.

The DESeq2 pairwise comparisons identified a pool of genes which differed significantly ($p.adj < 0.05$) between at least two of the post challenge treatment groups (Supplemental Data Set 3.6). We explored these genes response to challenge in more detail by grouping them into 25 clusters based on expression pattern (Figure 3.13A). Next for each cluster, mean profiles were created for both the genes response to challenge and the initial pre-treatment (Figure 3.13B and Supplemental Figure 3.4). Finally, to gain some functional understanding, protein signature and GO term enrichment analysis was performed on a per cluster basis (Figure 3.13C and Supplemental Data Set 3.7 and 3.8).

Theoretically IR can be underpinned by two intertwined mechanisms, prolonged upregulation of inducible defences and priming of inducible defences (Wilkinson et al., 2019). Thus, we first looked for clusters displaying these patterns. There were no clusters displaying a classical primed pattern of no basal difference in

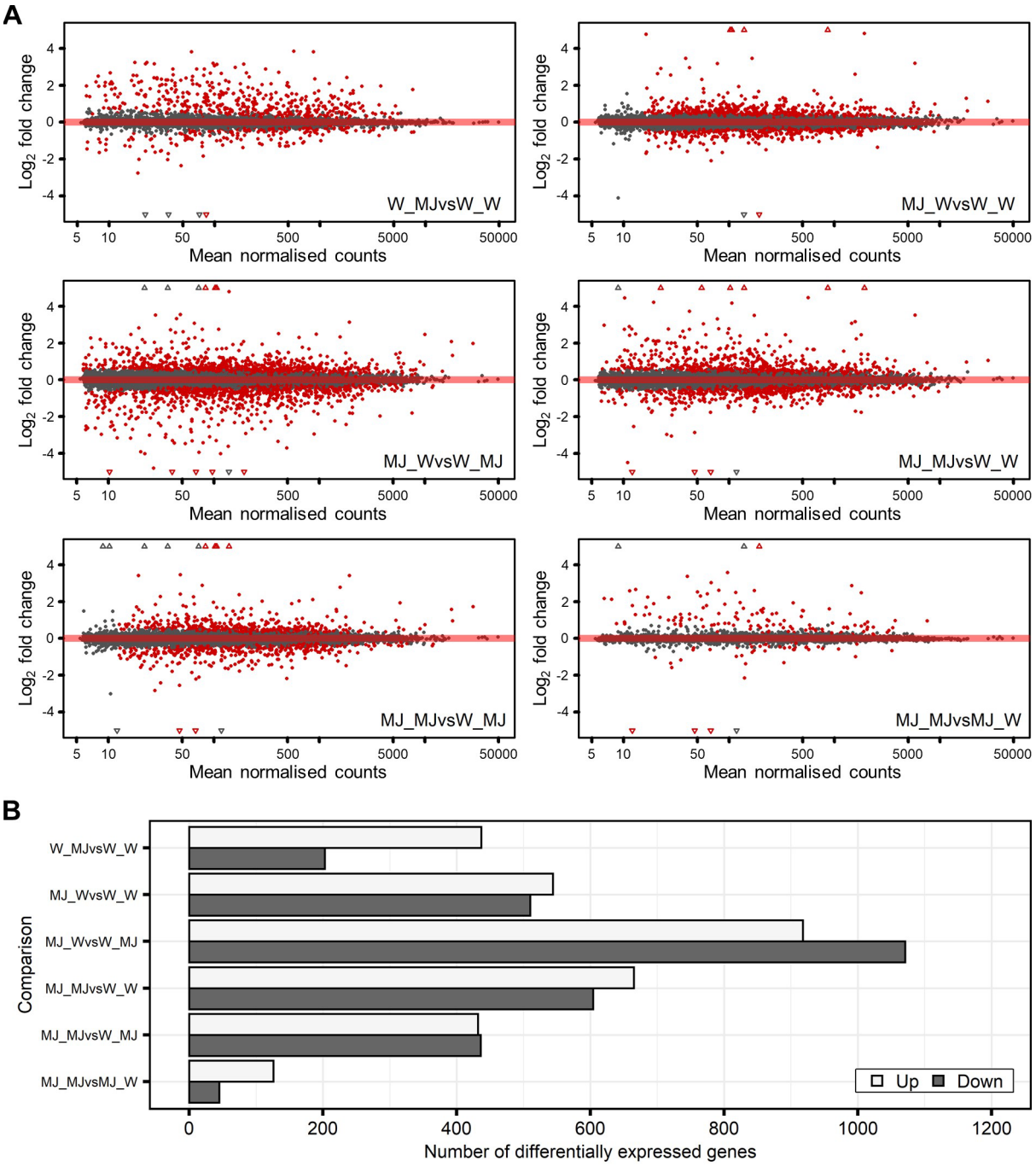

Figure 3.12. Hundreds of Genes are Differentially Expressed as a Consequence of MeJA Pre-treatment and Challenge Four Weeks and Six Hours Earlier, Respectively.

Numbers of differentially expressed genes in pairwise comparisons between samples from seedlings pre-treated with water (W) or 10 mM MeJA (MJ) and then challenged 4 weeks later with W (W_W and MJ_W) or 5 mM MJ (W_MJ and MJ_MJ). Bark material was harvested for RNA-seq at 6 hrs post challenge. For each comparison the second treatment group is the reference level. **(A)** MA-plots were created for each of the six possible pairwise comparison. Log_2 fold changes were shrunk using the DESeq2 function lfcShrink(type = "ashr") (Love et al, 2014; Stephens, 2016) and plotted against genes mean expression normalised for sequencing depth. Dots and triangles indicate individual genes in and out of the plotting area, respectively. Red coloured shapes indicate genes which have an adjusted *p*-value (*p.adj*) < 0.05. **(B)** The number of genes significantly (*p.adj*) up- and down-regulated in each of the pairwise comparisons.

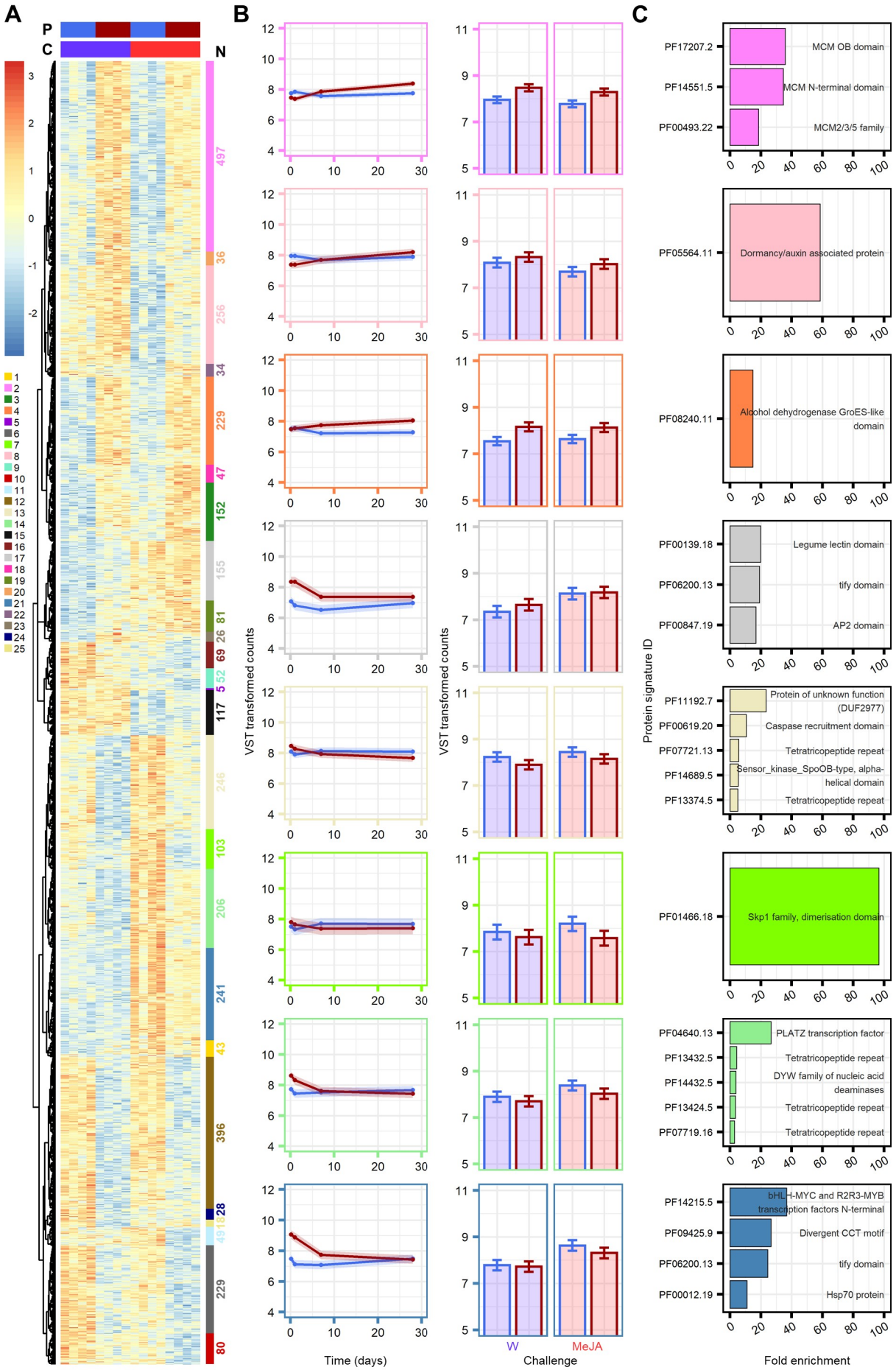
A
P
C
N
3
2
1
0
-1
-2
1 2 3 4 5 6 7 8 9 10 11 12 13 14 15 16 17 18 19 20 21 22 23 24 25
497 36 256 34 229 47 152 155 81 26 69 52 5 117 246 103 206 241 43 396 28 491 229 80
B
VST transformed counts
Time (days)
W
MeJA
Challenge
C
Protein signature ID
PF17207.2 MCM OB domain
PF14551.5 MCM N-terminal domain
PF00493.22 MCM2/3/5 family
PF05564.11 Dormancy/auxin associated protein
PF08240.11 Alcohol dehydrogenase GroES-like domain
PF00139.18 Legume lectin domain
PF06200.13 tify domain
PF00847.19 AP2 domain
PF11192.7 Protein of unknown function (DUF2977)
PF00619.20 Caspase recruitment domain
PF07721.13 Tetratricopeptide repeat
PF14689.5 Sensor_kinase_SpoOB-type, alpha-helical domain
PF13374.5 Tetratricopeptide repeat
PF01466.18 Skp1 family, dimerisation domain
PF04640.13 PLATZ transcription factor
PF13432.5 Tetratricopeptide repeat
PF14432.5 DYW family of nucleic acid deaminases
PF13424.5 Tetratricopeptide repeat
PF07719.16 Tetratricopeptide repeat
PF14215.5 bHLH-MYC and R2R3-MYB transcription factors N-terminal
PF09425.9 Divergent CCT motif
PF06200.13 tify domain
PF00012.19 Hsp70 protein
Fold enrichment

expression and post challenge a faster and/or stronger induction in MeJA pre-treated plants. However, clusters 3 (dark green), 18 (fluorescent pink) and 19 (olive green) displayed a mixture between prolonged upregulated and primed (Figures 3.13A and 3.13B and Supplemental Figure 3.4). Furthermore, cluster 17 (light grey) may also have displayed a mixed expression pattern as while at 6 hrs post challenge the W_MeJA and MeJA_MeJA groups had analogous levels of expression, the mean expression level of MeJA_W was slightly higher than that of W_W (Figure 3.13). Thus, the genes of this cluster may have initially been upregulated more quickly in the MeJA pre-treated group yet by 6 hrs post MeJA challenge their expression in the water pre-treated plants had caught up. Cluster 4 (orange) was prolonged upregulated and so were clusters 2 (pink) and 8 (pale pink), although the latter 2 clusters were repressed by MeJA challenge in both pre-treatment groups (Figures 3.13A and 3.13B).

The functional analysis suggested that several of the primed and/or prolonged upregulated clusters contained genes which were involved in defence against biotic stress. For instance, clusters 2 and 4 had the enriched GO terms “isoprenoid biosynthetic process” (GO:0008299) and “terpenoid biosynthetic process” (GO:0016114; Supplemental Data Set 3.8). Furthermore, enriched GO terms for clusters 8 and 18 included “response to ethylene stimulus” (GO:0009723) and “regulation of response to biotic stimulus” (GO:0002831), respectively (Supplemental Data Set 3.8). Finally, cluster 17 was enriched for multiple terms associated with the

---

Figure 3.13. Post Challenge Transcriptional Patterns (*Figure appears on previous page*).

(A) Post challenge expression profiles for all genes which were significantly (adjusted *p* value < 0.05) differentially expressed in at least one of the six possible pairwise comparisons between the four post challenge treatment groups: water (blue) pre-treatment (P) and water challenge (C), MeJA (red) pre-treatment and water challenge, water pre-treatment and MeJA challenge and MeJA pre-treatment and MeJA challenge. Genes were grouped by expression pattern using pearson sample to sample distances, complete-linkage clustering and read counts normalised for library size and transformed to approximately the $\log_2$ scale using the DESeq2 function vst (Love et al., 2014). The heatmap displays the outcome of the clustering with each row being a different gene and the expression values being represented by z-scores. The dendrogram was divided up into 25 clusters which are indicated by the coloured boxes and gene numbers (N) to the right of the heatmap.
(B) The mean expression profiles post pre-treatment (left) and post challenge (middle) for each of the eight clusters (from top: 2, 8, 4, 17, 13, 7, 14 and 21) with at least one significantly (adjusted *p*-value ≤ 0.05) enriched protein signature **(C)**. See Supplemental Figure 3.4 for the plots of all other clusters. Water and MeJA pre-treatments are indicated by the blue and red lines (left hand side plots) and bar outlines (middle plots). Water and MeJA challenges are indicated by the blue and red bar fill (middle plots). The shading and error bars depict 95% confidence intervals.
(C) If a cluster had more than five significantly enriched protein signatures, only the five with the highest fold enrichment are displayed. See Supplemental Data Set 3.7 for all significantly overrepresented protein signatures.

regulation of defence to biotic stress. For example, overrepresented GO terms and protein signatures among the genes of cluster 17 included “immune system process” (GO:0002376), “defense response” (GO:0006952) and “AP2 domain” (PF00847.19; Figures 3.13C and Supplemental Data Set 3.7 and 3.8). Furthermore, blastp annotations suggested that cluster 17 genes encoded for defence regulatory transcription (co-)factors (e.g. NONEXPRESSOR OF PATHOGENESIS-RELATED GENES 1 (NPR1), ETHYLENE INSENSITIVE 3-LIKE 1 and ETHYLENE-RESPONSIVE TRANSCRIPTION FACTOR 1 homologs), disease resistance proteins (e.g. TIR-NBS-LRR class disease resistance protein), pattern recognition receptors (receptor-like kinases) and signalling cascade components (e.g. Mitogen-activated protein kinases (MAPKs); Supplemental Data Set 3.6).

Cluster 21, which exhibited an unchanged basal expression but a lower post MeJA challenge expression in MeJA pre-treated plants, was also overrepresented with functional annotations which linked it to defence (Figure 3.13 and Supplemental Data Sets 3.6, 3.7 and 3.8). For example, overrepresented protein signatures and GO terms for the cluster included: “bHLH-MYC and R2R3-MYB TFs N-terminal” (PF14215.5), “response to chitin” (GO:0010200), “response to jasmonic acid stimulus” (GO:0009753), “response to ethylene stimulus” (GO:0009723) and “response to salicylic acid stimulus” (GO:0009751; Figure 3.13 and Supplemental Data Sets 3.7 and 3.8). Unsurprisingly considering the enriched functional annotation terms, *MYC2*, *EIN3* and *WRKY* homologs were among the cluster 21 genes (Supplemental Data Set 3.6). In fact, cluster 21 contained numerous genes encoding for TFs (e.g. MYCs, NACs, MYBs, ERFs) and master regulators (e.g. JAZ repressors). Furthermore, as with cluster 17, numerous genes in cluster 21 were annotated as encoding for disease resistance proteins and pattern recognition receptors (Supplemental Data Set 3.6). Finally, there were genes in cluster 21 annotated as being involved in the regulation of flavonoid biosynthesis and encoding for PR proteins (Supplemental Data Sets 3.6 and 3.8). Considering this strong association of cluster 21 with defence, it is very plausible that the cluster 21 genes were primed yet 6 hrs post challenge was too late to observe this, with the genes having reached peak upregulation and were returning to basal levels in MeJA pre-treated plants.

3.4. Discussion

The plant hormone MeJA has previously been demonstrated to elicit IR against pests and pathogens in Norway spruce trees of a variety of ages (Kozlowski et al., 1999; Erbilgin et al., 2006; Zeneli et al., 2006; Krokene et al., 2008; Zhao et al., 2011; Mageroy et al., 2020a). In this study we confirmed this phenomenon showing that MeJA treatment of 2-year-old seedlings induced enhanced resistance to infection over a month later by the Ophiostomatoid fungal pathogen, *G. penicillata* (Figure 3.2). Subsequently, we explored the molecular mechanisms behind MeJA-IR. A transcriptome analysis of a time-course post MeJA pre-treatment allowed for the mechanisms underpinning both the establishment and maintenance of MeJA-IR in Norway spruce to be explored. Furthermore, this analysis also provided an understanding of the general transcriptional response to MeJA in the bark tissue of spruce seedlings. In a previous study, we wounded mature trees pre-treated 4 wks earlier with MeJA and then profiled their transcriptional response 24 hrs later (Mageroy et al., 2020b). In the present study, a transcriptome analysis of an earlier timepoint (6 hrs) was used to further our understanding of the response to challenge by MeJA-IR expressing trees.

3.4.1. Transcriptional Response of Seedling Bark to MeJA

The transcriptional response to jasmonate treatment has been explored by multiple previous studies working with numerous different species (e.g. Men et al., 2013; Shi et al., 2015; Hickman et al., 2017; Liu et al., 2017; Benevenuto et al., 2019). Although these previous analyses were generally conducted over much shorter timeframes (hours and days rather than hours, days and weeks) and were conducted using leaf rather than woody stem tissue, their findings had many similarities to those of this study. For instance, Liu et al (2017) demonstrated that in the needle tissue of whitebark pine (*Pinus albicaulis*) seedlings, MeJA treatment resulted in a transient upregulation of numerous defence related genes including hormone related transcriptional regulators (e.g. homologs of *MYC2* and ethylene responsive TFs) and phenylpropanoid and terpenoid biosynthesis genes. We found similar genes upregulated in this study. Furthermore, genes predicted to encode for the ethylene biosynthesis enzymes SAM synthetase and ACC oxidase were also upregulated in whitebark pine needles in response to MeJA. This is analogous to the pattern we

observed, with SAM synthetase and ACC oxidase but not ACC synthase genes being upregulated (Supplemental Data Set 3.4). Among the genes downregulated in whitebark pine needles in response to MeJA were multiple that were involved in photosynthesis (Liu et al., 2017). We also found genes involved in photosynthesis to be repressed, at least in the first 24 hrs post MeJA pre-treatment (Figure 3.5 and Supplemental Data Sets 3.1, 3.2 and 3.3). Although bark tissue, particularly of mature trees, appears brown and lacking in chlorophyll, it is known that stem photosynthesis occurs in conifers including Norway spruce (Berveiller et al., 2007; Pfanz, 2008; Vandegehuchte et al., 2015; Tarvainen et al., 2018).

In Arabidopsis, the transcriptional response to MeJA has been explored in great detail. For instance, Hickman et al (2017) performed RNA-seq on samples harvested at 14 timepoints over a 16 hour period post MeJA treatment. This high-resolution time course analysis suggested that in Arabidopsis there is a pulse of differential expression, with many genes showing peak change before 3 hrs post treatment. While we similarly observed a pulse of change, the peak up or downregulation of majority of genes appeared to occur many hours later (Figure 3.5). One possible explanation is that maybe it takes longer for MeJA to enter and move through the thick bark tissue of the large tree species Norway spruce than the thin leaf tissue of the small stature herbaceous annual Arabidopsis. If so, there would be a longer delay between treatment and MeJA entering cells, being converted to the bioactive form of JA, JA-isoleucine, and thus stimulating changes in transcription. A cell-type specific metabolomics and transcriptomics approach, the latter as demonstrated by Celedon et al (2017), could be used to test this hypothesis.

3.4.2. Direct Induction of Spruce Defences May be Key to MeJA-IR

IR can be underpinned by a prolonged upregulation of defences directly induced by the IR eliciting stimuli (Wilkinson et al., 2019). In spruce, MeJA treatment has previously been shown to directly induce a range of defences. For example, Zulak et al (2009) demonstrated that in 2-year-old seedlings terpene biosynthesis and the subsequent accumulation of terpenes was induced in bark tissue in response to MeJA treatment. Similarly, in this study we also found an upregulation of certain terpene biosynthesis genes. For example, genes predicted to encode for terpene (e.g. Pinene and Carene) synthases were found in the group 1 clusters (Figure 3.5 and

Supplemental Data Set 3.1). However, we did not find that all terpene biosynthesis genes were upregulated.

The precursors of monoterpenes, sesquiterpenes and diterpenes are geranyl diphosphate (GPP), farnesyl diphosphate (FPP) and geranylgeranyl diphosphate (GGPP), respectively (Celedon and Bohlmann, 2019). These metabolites, which are the substrates for terpene synthases, are produced in reactions catalysed by isoprenyl diphosphate synthases (IDS). In this study, we found that four *IDS* genes were differentially expressed in response to MeJA treatment (Supplemental Data Set 3.1). Interestingly, three of these genes were found among repressed clusters. This finding appears somewhat at odds to the expected accumulation of terpenes in the bark in response to MJ treatment (Zulak et al., 2009). However, it has been shown in Norway spruce that there are some *IDS* genes which are not induced by MeJA and instead can be mildly repressed (Schmidt and Gershenzon, 2007; Schmidt and Gershenzon, 2008; Schmidt et al., 2011). The MeJA unresponsive or repressed *IDS* genes could be involved in basal terpene production or the production of other metabolites derived from GPP, FPP and GGPP. Thus, despite the repression of some predicted IDS encoding genes in response to MeJA, it is very plausible that as in previous studies terpenes would have accumulated in the bark tissue of the MeJA treated trees used in this study. However, it is unclear whether such a bark specific terpene level increase contributes substantially to IR lasting longer than a few weeks. Previous studies have shown that often the increase of terpene levels in the bark of spruce seedlings is transient and by 1 or 2 months post MeJA treatment the levels of only specific terpenes remain enhanced (Martin et al., 2002; Zulak et al., 2009). This is in line with our findings that by 4 weeks post MeJA pre-treatment the group 1 clusters associated with terpene biosynthesis were nearly back to basal levels of expression (Figure 3.5). Spruce is a long-lived tree species and 4 weeks will generally represent a short portion of a spruce tree's life. Thus, the MeJA induced accumulation of terpenes in bark tissue and the IR we have studied here should perhaps be referred to as short- or medium-term responses. Nevertheless, MeJA treatment also induces a substantial increase of terpenes in wood tissue which is associated with the formation of traumatic resin ducts (TRDs) (Martin et al., 2002). It takes a couple of weeks for TRDs to form and start filling with resin however they remain active for many years and are thought to play an important role in long-term MeJA-IR against herbivores by providing an large reservoir

of defence-related and terpene-rich oleoresin (Krokene, 2015). Presumably such TRDs could also have played a role in the MeJA-IR against *G. penicillata* observed here (Figure 3.2). In our inoculation method (chapter section 3.5.6) bark was wounded prior to deposition of the fungal inoculum. This wounding may have released resin from TRDs. As resin can inhibit the growth of Ophiostomatoid fungi (Solheim, 1991), such a resin release could partially explain the resistance exhibited by MeJA pre-treated trees.

An accumulation of terpenes in bark and wood tissue in response to MeJA treatment, is likely one key mechanism behind MeJA-IR. Another is likely the accumulation of phenolics. Multiple studies have provided evidence that MeJA treatment induces the enlargement of PP cells and that this is linked to an accumulation of phenolic compounds (Franceschi et al., 2002; Krokene et al., 2008; Li et al., 2012b). Furthermore, over the past decade, multiple studies by Hammerbacher, Gershenzon and colleagues have provided an increased understanding of the biosynthesis of specific polyphenolic compounds (e.g. stilbenes and flavonoids) which provide resistance to Ophiostomatoid fungi in spruce bark (e.g. Hammerbacher et al., 2011; Hammerbacher et al., 2014; Hammerbacher et al., 2019). In this study, we found that genes predicted to encode for enzymes involved in the biosynthesis of anti-Ophiostomatoid fungi flavonoid metabolites were upregulated following MeJA pre-treatment (Supplemental Data Set 3.1). Furthermore, the upstream general phenylpropanoid pathway which provides the precursor metabolites was also transiently upregulated. Thus, although most studies have worked with the model Ophiostomatoid fungal species *E. polonica*, it is likely that an accumulation of phenylpropanoid pathway derived phenolic compounds in the bark would have been key to the resistance against *G. penicillata* exhibited by the MeJA pre-treated trees in this study. To begin to investigate this hypothesis, future studies should aim to profile protein levels and activity of phenolic biosynthesis enzymes in addition to phenolic metabolite levels in response to MeJA treatment. Such a holistic study was performed by Zulak et al (2009) for terpenes. Accumulated phenolic metabolites should then be tested for the ability to inhibit *G. penicillata* growth.

PR proteins are another important anti-fungal pathogen defence. Numerous genes predicted to encode for PR proteins were differentially expressed in response to MeJA pre-treatment. While there was not a consensus expression pattern exhibited

by *PR* genes, there were some interesting results. For instance, some were transiently induced (upregulated < 4 wks) while others were mildly prolonged upregulated (upregulated > 4 wks) in response to MeJA pre-treatment (Figure 3.9 and Supplemental Data Set 3.4). This jasmonate inducibility of *PR* genes is consistent with previous work in conifers (Davis et al., 2002; Pervieux et al., 2004). It also suggests that much like the accumulation of terpenes and polyphenolic compounds, a prolonged accumulation of PR proteins could underpin MeJA-IR. Additionally, MeJA likely primes some *PR* genes for a faster and stronger induction upon subsequent challenge. In a previous study, we demonstrated that following wounding there was a stronger upregulation of numerous *PR* genes in the bark of mature trees pre-treated with MeJA compared to the bark of those which were pre-treated with water (Mageroy et al., 2020b). Notably, we did not find any of the previously highlighted *PR* genes as primed in this study (Figure 3.3 and Supplemental Data Set 3.6). Furthermore, more generally we found little evidence of a widespread primed response of *PR* genes post challenge. This could be because the 6 hrs post challenge timepoint was too early to observe an induction of *PR* genes. Alternatively, it could be because the challenge we used, MeJA painted onto the stem, elicits a weaker and/or substantially different response compared to wounding. The seedlings were grown outside and not in a controlled environment chamber. Thus, another explanation for the lack of a primed response among *PR* genes may be that because of exposure to various uncontrolled environmental stimuli, the basal expression of often very responsive *PR* genes was already very high and therefore the MeJA pre-treatment and/or challenge had no or an inconsistent impact on expression. Finally, the lack of a primed response could represent a developmental or genetic difference between the seedlings used in this study and the mature trees used in our previous work. To determine whether *PR* genes are good markers of MeJA-IR in seedlings as well as mature trees and in turn whether the PR proteins they encode are a key defence mechanism underpinning the MeJA-IR phenomena, additional experiments are required. For instance, RNA-seq experiments in seedlings using alternative challenge treatments (e.g. wounding and pathogen inoculation) and post challenge harvest timepoints, should be conducted. Furthermore, if consistently primed and/or prolonged upregulated *PR* genes are identified, these genes should be transiently expressed in tobacco to determine if their products can provide resistance against necrotrophic pathogens.

PR genes were not unique as generally we did not find much evidence of genes exhibiting solely primed responses to MeJA challenge. However, there was some evidence of defence related genes exhibiting a mixture between a prolonged upregulated and primed expression pattern. For instance, a gene (*MA_70145g0010*) annotated as encoding for a carene synthase was still slightly upregulated 4 wks post MeJA pre-treatment and also exhibited an augmented response to MeJA challenge in MeJA pre-treated plants (Supplemental Data Set 3.6). Interestingly, this gene was identified as showing a primed response to challenge in our previous study in mature trees (Mageroy et al., 2020b), suggesting that it is a good candidate for being a marker of MeJA-IR in spruce. Nevertheless, as in our previous study, the expression pattern of the carene synthase was not the consensus of terpene biosynthesis genes. In our post challenge analysis, enriched terpenoid biosynthesis GO terms were associated with the prolonged upregulated clusters. Few terpene biosynthesis genes exhibited a primed response in addition to a prolonged upregulation. Thus, a faster and stronger *de novo* biosynthesis of terpenes is unlikely to majorly contribute to MeJA-IR. Instead, as discussed above, the accumulation of terpenes in the bark and/or wood in response to the initial MeJA pre-treatment is likely to be more important.

3.4.3. Hormonal Regulation of MeJA Induced Defences

Many of the genes in the clusters upregulated post MeJA pre-treatment were associated with defence regulation (Figure 3.5 and Supplemental Data Sets 3.1-3.3). Furthermore, many of the same clusters were also associated with hormone biosynthesis and signalling (Figures 3.5, 3.6, 3.7 and 3.8 and Supplemental Data Sets 3.1, 3.2, 3.3. and 3.4). More specifically, there was a strong association with the known major defence regulatory hormones JA and SA along with the supporting hormone ET. Genes encoding many of the enzymes required to produce these hormones were upregulated, generally transiently, following MeJA pre-treatment. However, a notable absence was genes encoding for ACS. Ralph et al (2006a) reported that mechanical wounding and herbivory induced multiple *ACS* genes in 2-year-old Sitka spruce (*Picea sitchensis*). In line with many studies in angiosperms including Arabidopsis, these authors concluded that the ACS enzyme was the rate limiting step in ethylene biosynthesis. Nevertheless, as it is thought that under some conditions ACC oxidase can be the rate limiting enzyme (Houben and Van de Poel, 2019), it is still plausible that ET levels increase in Norway spruce bark in response to MeJA treatment.

Additional support for this comes from a previous study which demonstrated that MeJA induced ET accumulation in in saplings (4 years old) of another *Pinaceae* species, *P. menziesii* (Hudgins and Franceschi, 2004). MeJA treatment has also previously been demonstrated to induce an accumulation of JA and SA in the bark of Norway spruce saplings (6-7 years old) (Schmidt et al., 2011). Thus, the upregulated JA and SA biosynthesis pathways likely lead to an accumulation of these hormones in our system. This is despite the fact that as no *ISOCHORISMATE SYNTHASE* (*ICS*) genes have been reported in spruce (Schmidt et al., 2011) the closest enzymes to SA in our pathway which had differentially expressed genes were PAL and aldehyde oxidase. PAL is the first member of the general phenylpropanoid pathway (Deng and Lu, 2017) and therefore many other metabolites aside from SA could have been produced from the PAL product *t*-CA. Furthermore, while an aldehyde oxidase has been shown to be involved in benzoic acid (BA) production in Arabidopsis (Ibdah et al., 2009) and BA is thought to be converted to SA by benzoic acid 2-hydroxylase (León et al., 1995), aldehyde oxidases are also involved in many other processes in plants including ABA biosynthesis (Seo et al., 2000).

An accumulation of JA, SA and ET in response to MeJA treatment would explain the upregulation of many homologs of angiosperm genes which encode for components of downstream hormone signalling. For instance, *MYC*, *EIN3/EIL1* and *NPR1* homologs were all upregulated and are known to be major regulators of JA, JA/ET and SA dependent signalling pathways and defence responses, respectively (Lorenzo et al., 2004; Fernández-Calvo et al., 2011; Chang et al., 2013; Du et al., 2017; Ding et al., 2018). Studies mainly in Arabidopsis and tomato have demonstrated that JA activates MYC and EIN3/EIL1 by targeting JAZ repressors for degradation. When concentrations of the bioactive JA-Ile are low, JAZ repressors inhibit the activity of the master regulatory TFs. However, when JA-Ile accumulates, the coreceptor complex of JA-Ile, JAZ and the F-box protein CORONATINE INSENSITIVE1 (COI1) is formed resulting in JAZ proteins being ubiquinated and thus targeted for degradation (Howe et al., 2018). As reported in other species (e.g. Hoo et al., 2008; Hickman et al., 2017; Sun et al., 2017; Wang et al., 2020), we found that numerous genes encoding for JAZ proteins were upregulated by MeJA treatment. It is likely that this upregulation acts to prevent over activation of the JA dependent responses.

Several Petunia NAM and Arabidopsis ATAF1, ATAF2, and CUC2 (NAC), myb domain protein (MYB), ethylene response factor (ERF) and WRKY family TFs were also upregulated in response to MeJA treatment. In Arabidopsis and other well studied angiosperm species, members of these TF families can play an intermediate role in JA, JA/ET and SA signalling pathways and are important for the regulation of defence responses (Huang et al., 2016; Chen et al., 2017; Erb and Reymond, 2019; Yuan et al., 2019). For instance, MYB TFs are known to be key regulators of phenylpropanoid biosynthesis in many species (Liu et al., 2015). Thus, the defence responses upregulated by MeJA treatment may well depend on the accumulation of JA, ET and SA and in turn upregulation of signalling pathways involving similar components to that in Arabidopsis and other angiosperms. However, there are a number of caveats and clarifications which must be mentioned. Firstly, there were differentially expressed ERFs, MYBs, NACs and WRKYs which were downregulated by MeJA treatment. This could be because they are negative regulators of defences or alternatively, they regulate other pathways and processes which are repressed by MeJA treatment (e.g. growth and development). Secondly, while we assigned TF families to specific signalling pathways, members of these families may well function in the other hormones signalling pathway. Thirdly, while NAC, ERF, MYB and WRKY TFs can act below the master regulators in hormone signalling pathways (e.g. MYC2) (Zander et al., 2020), this is not always the case. For example, there is evidence that specific MYBs can interact directly with JAZ repressors (Qi et al., 2011; Zhou et al., 2017). Finally, we are basing our conclusions entirely off gene expression data. Future studies should aim to perform RNA interference (RNAi) in Norway spruce, as demonstrated by (Hammerbacher et al., 2019), to repress MeJA inducible TFs and thus assess their importance in the regulation of key MeJA inducible defence response in spruce (e.g. *PR* gene expression, and terpene and phenolic accumulation).

3.4.4. Defence Regulators: are they Primed by MeJA Pre-treatment?

Genes predicted to encode for components of hormone signalling pathways were also a key feature of particularly two the post challenge transcriptomics analysis clusters, cluster 17 and cluster 21 (Figure 3.13). The genes within these clusters included ones which were predicted to encode for master regulators (e.g. MYC, EIL1) and downstream TFs (e.g. ERF1) in addition to JAZ repressors (Supplemental Data Set 3.6). Furthermore, these clusters also contained genes predicted to encode for

proteins involved in biotic stress perception (e.g. PRRs, R genes) and downstream signalling (e.g. MAPKs). Interestingly, both clusters displayed a mean expression pattern which suggested genes were upregulated to a similar extent in both pre-treatment groups or even slightly more weakly in the plants pre-treated with MeJA (Figure 3.13). This matched the targeted transcriptome analysis of both a MYC and EIN3/EIL1 homolog (Figure 3.3B). These results could suggest that the MeJA pre-treatment may induce a long-lasting reduced sensitivity to challenge of defence regulator genes. Alternatively, the upregulation of these genes may have occurred very rapidly, with peak expression being reached before 6 hrs post challenge. Future studies should conduct an intense time course experiment over the first 24 hrs post challenge, including multiple timepoints before 6 hrs, to understand how the cluster 17 and 21 type genes truly respond to challenge. Furthermore, maybe the challenge used should either be a high concentration of MeJA or a combination of wounding and MeJA treatment. In the present study, the challenge did not induce a very strong response which made it harder to pick out patterns and explore how MeJA pre-treatment influenced the subsequent response to a JA eliciting stress.

3.4.5. Role of Epigenetics Mechanisms in Maintenance of MeJA-IR

We demonstrated here that MeJA pre-treatment induced an upregulation of defence regulators (e.g. MYC) and downstream defence genes (e.g. defence metabolite biosynthesis genes, *PR* genes) which lasted for many weeks and longer than 4 weeks in some cases. Alongside this prolonged upregulation, we also found some evidence of defence priming (e.g. carene synthase). Moreover, our previous work provided strong evidence of *PR* genes showing an augmented induction in response to wounding in MeJA pre-treated trees (Mageroy et al., 2020b). Together this evidence suggests that both a prolonged upregulation and priming of genes underpin MeJA-IR in spruce. It is very plausible that long-term changes in basal gene expression and/or gene responsiveness could be underpinned by epigenetic mechanisms (Wilkinson et al., 2019). For instance, histone tail modifications leading to chromatin decompaction and enhanced TF binding to promoter regions has been linked with defence gene priming in Arabidopsis (Jaskiewicz et al., 2011; Schillheim et al., 2018; Baum et al., 2019). Furthermore, changes in DNA methylation both in gene promoters and elsewhere in the genome has been linked to both a prolonged upregulation and priming of genes (Yu et al., 2013; López Sánchez et al., 2016;

Cambiagno et al., 2018; Furci et al., 2019). In order to implement histone tail modifications, changes in DNA methylation and chromatin remodelling, a suite of different proteins are required (Van Oosten et al., 2014; Pikaard and Mittelsten Scheid, 2014). Interestingly, we found that in response to the resistance inducing MeJA pre-treatment, many genes predicted to encode for these epigenetic regulators were differentially expressed. This suggests MeJA induce changes to the epigenetic landscape in spruce bark which in turn could explain the changes in gene expression associated with MeJA-IR. To confirm this hypothesis techniques such as whole genome bisulfite sequencing (WGBS), Chromatin Immunoprecipitation Sequencing (ChIP-seq) and Formaldehyde-Assisted Isolation of Regulatory Elements sequencing (FAIRE-seq) are needed to explore the methylomes and histone and chromatin landscape of MeJA pre-treated trees. Analysis of data generated by these next generation sequencing approaches will be complex due to the size and repetitive nature of the Norway spruce genome (Nystedt et al., 2013). Nevertheless, WGBS has already been successfully conducted in *P. abies* (Ausin et al., 2016). Thus, we decided to perform WGBS on DNA extracted from seedlings treated with MeJA or water 4 wks previously. However, due to a COVID-19 pandemic induced delay in the sequencing and data acquisition, downstream analysis will have to be performed in future research projects.

Based on our gene expression data, one outcome we could expect to find from WGBS would be widespread hypomethylation in MeJA pre-treated trees. In Arabidopsis, DNA methylation is established, and CHH context methylation is maintained, by RdDM (Zhang et al., 2018b). The canonical RdDM pathway involves 24 nucleotide (nt) small RNAs (sRNAs) and long noncoding scaffold RNAs produced in a Pol IV and V dependent manner, respectively (see sidebar titled RNA-directed DNA methylation in Chapter 1) (Matzke and Mosher, 2014; Matzke et al., 2015). These noncoding RNAs, along with numerous proteins (e.g. ARGONAUTE 4), recruit de novo methyltransferase DRM enzymes to specific loci where they catalyse the methylation of cytosines. Interestingly, aside from in reproductive tissue, the expression of 24 nt sRNAs is very low in Norway spruce (Nystedt et al., 2013; Chávez Montes et al., 2014; Nakamura et al., 2019). However, it is has been reported in Arabidopsis that 21/22 nt sRNAs generated from Pol II, or Pol IV, transcripts in an RDR6 (RDR2 for Pol IV) and DICER-LIKE 2/4 (DCL2/4) dependent manner, are involved in a non-canonical RdDM

pathway (Nuthikattu et al., 2013; McCue et al., 2015; Cuerda-Gil and Slotkin, 2016; Panda et al., 2020). Taken together with the existence of many predicted DNA methylation pathway genes in Norway spruce, it is likely that RdDM and also other DNA methylation pathways described in angiosperms function in this tree species and also conifers more generally (Huang et al., 2015; Ausin et al., 2016; Bewick et al., 2017; Nakamura et al., 2019). Thus, we explored the expression patterns of DNA methylation genes. We found that many of the Norway spruce RdDM genes were repressed by MeJA pre-treatment (e.g. *DRM2*, *NRPE1, RDR6*). Arabidopsis and rice (*Oryza sativa*) RdDM mutants are hypomethylated at many, particularly CHH context, loci (Stroud et al., 2013; Tan et al., 2016; Tang et al., 2016). This suggests that MeJA treatment may induce DNA hypomethylation. It would be interesting to explore the dynamics of this predicted hypomethylation by performing WGBS not only at the challenge timepoint but also at various timepoints post MeJA pre-treatment.

In addition to RdDM genes, we also found that MeJA pre-treatment repressed genes encoding for DNA glycosylases, enzymes which catalyse the first step in active DNA methylation removal (Zhang et al., 2018b). However, this repression occurred later than the RdDM pathway further supporting the idea that MeJA triggers a loss of DNA methylation. The later repression of the DNA glycosylases also provides evidence for an RdDM DNA glycosylase feedback phenomenon previously observed in Arabidopsis. Two studies in 2015 provided evidence that the expression of *ROS1*, the major vegetative DNA glycosylase in Arabidopsis, is regulated by the RdDM pathway (Lei et al., 2015; Williams et al., 2015). Decreased or increased methylation in a specific region of *ROS1's* promoter leads to reduced or enhanced gene expression, respectively. Future studies should aim to explore the methylation in the DNA glycosylase promoters in response to changes in RdDM expression triggered by MeJA treatment.

3.5. Methods

3.5.1. Plant Materials and Growth Conditions

In May 2018, 2-year-old M95 Norway spruce seedlings were purchased from the nursery Norgesplanter AS. The seedlings, which had overwintered at 7 ºC with the root plugs wrapped in Clingfilm, were transferred to 0.8 L pots (7.5 cm x 7.5 cm x 12 cm; Nelson Garden, Product No. 5726) containing mineral fertiliser supplemented compost (Plantasjen, EAN:7058782362802). Seedlings were subsequently grown outside with an irrigation system providing additional water when required.

It has previously been demonstrated that susceptibility of spruce seedlings to necrotrophic pathogens increases during yearly bud development and shoot elongation, before returning to basal levels once new buds have formed (Krokene et al., 2012). To prevent this impact of phenology on resistance complicating our analyses, we performed all manipulations and experimentation from the end of July 2018 onwards, following the cessation of yearly growth (Supplemental Figure 3.1) and development.

3.5.2. Methyl Jasmonate (MeJA) Treatments

On the 31st July 2018, half of the spruce seedlings were sprayed with a 10 mM MeJA solution while the remaining half received a control solution. The MeJA solution consisted of MeJA (Sigma-Aldrich, 392707) dissolved in tap water and supplemented with 0.1% Tween 20 (Sigma-Aldrich, P9416) to ensure even coating across all sprayed tissues. The control solution was identical apart from it did not contain any MeJA. Each plant was sprayed, using a 1.5 L pressurised spray bottle (Bürkle GmbH, 0309-0100), with a similar volume of solution, which was enough to saturate the entire stem surface. Following spraying, plants of the two pre-treatments were kept separate for > 4 hrs to allow excess solution to evaporate prior to being put back into close proximity to one another.

On the 28th August 2018, 4 weeks post pre-treatment, seedlings from both of the pre-treatment groups (control and 10 mM MeJA) were challenged with either a 5 mM MeJA solution or a water control solution (Figure 3.1). Both challenge solutions were supplemented with 0.1 % TWEEN 20 and were applied by painting them across the entirety of the first internode bark surface.

3.5.3. Growth Measurements

Both tree and apical leader height were recorded prior to pre-treatment and then again 4 weeks later prior to challenge. The distance between the base of the stem and the tip of the new buds on top of the apical leader equated to the plant height. Whereas the apical leader height was recorded as the distance from the top whorl of branches to the tip of the present year's buds. For the confirmation of growth cessation and assessment of the impact of MeJA pre-treatment (Supplementary Figure 3.1), only plants which were still present at the time of challenge, and hence measured twice, were used.

3.5.4. Growth Measurement Statistical Analysis

Due to the repeated measurement of the same trees, a two-way mixed design ANOVA was used to analyse the effect of pre-treatment, measurement timepoint and the interaction on plant height. Whereas, due to a lack of normality and variance homogeneity, the effect of pre-treatment, measurement timepoint and the interaction on apical leader height was analysed using a robust two-way mixed design ANOVA. All statistical analysis and plotting was performed in R version 3.6.1 (R Core Team, 2019) with the assistance of the packages WRS2 version 1.0-0 (Mair and Wilcox, 2020) and ggplot2 version 3.2.1 (Wickham, 2016).

3.5.5. Pathogen Material

Grosmannia penicillata isolate 1980-91/54 (Collected: 1980, Akershus (Ås), Norway) from the Norwegian Institute of Bioeconomy Research (NIBIO) fungal culture collection, was revived from a -150 ºC culture stock and propagated on malt agar (2% Malt Extract and 1% Agar).

3.5.6. Necrotrophic Pathogen (*Grosmannia penicillata*) Bioassay

Seedlings were inoculated approximately 4 weeks (29th August 2018) after pre-treatment with water or 10 mM MeJA (Figure 3.1). From each pre-treatment group, 15 plants were inoculated with *G. penicillata* and 15 plants were mock inoculated with sterile malt agar. The inoculation procedure was identical for all plants regardless of whether they were inoculated with a fungal or sterile agar inoculum. First a wound, approximately 1 cm in length and half the circumference of the stem, was created in the middle of the first internode by slicing off outer layers of phloem with a scalpel. The

phloem tissue was not completely detached from the stem and instead a bark flap was created. A 5 mm^3 droplet of inoculum was placed behind the bark flap with a 5 ml needless syringe. In order to seal the inoculum droplet in place behind the bark flap and to prevent contamination and/or drying out of the wounds, parafilm was wrapped around the stem at the location of the wound site. The inoculums were created by homogenising 56 cm^2 worth of malt agar, with or without fungal tissue, using two 60 ml syringes. Inoculated plants were arranged into eight blocks. Seven blocks had two plants of each pre-treatment and inoculation type combination, while one block only had one plant of each combination. Plants were randomised in each block.

Approximately 8 weeks (wks) after inoculation (25th October 2018), resistance was assessed by measuring the inner phloem lesion length around the wounding site of each plant. Parafilm and bark flaps were removed, and the inner phloem was revealed by slicing off the outer layers of phloem tissue above and below the wound site using a scalpel. In both mock and fungal inoculated plants there was a clear area of darkened tissue (See Figure 3.2) around the wound site. The length, in the direction parallel to the stem, of each lesion was measured using callipers (Digital Vernier Caliper, Cocraft).

3.5.7. Pathogen Bioassay Statistical Analysis

R version 3.6.1 (R Core Team, 2019) was used to perform a three-factor ANOVA, which assessed the effect of pre-treatment and challenge on lesion length. To ensure fulfilment of ANOVA's normality assumption, lesion lengths were log-transformed. Pre-treatment, challenge and block were included as fixed effects however only the interaction between the first two factors was studied. Due to an imbalance in the number of replicates in each block and a significant effect of the interaction, type III sum of squares were used. A tukey post-hoc test, with a statistical significance threshold of $P < 0.05$, was used to evaluate whether the mean lesion lengths per pre-treatment and challenge combinations were significantly different.

3.5.8. Bark Harvesting and RNA Extractions

At 3 hours (hrs), 6 hrs, 24 hrs, 72 hrs, 1 wk and 4 wks post pre-treatment on the 31st July 2018, the bark was harvested from the first internode of four seedlings from each of the two pre-treatment groups (Water and 10 mM MeJA). Bark was also harvested from the first internode of four seedlings, from each of the four pre-treatment

(Water or 10 mM MeJA) and chemical challenge (Water or 5 mM MeJA) combinations, at 6, 24 and 48 hrs post chemical challenge on the 28th August 2018. Each seedling represented a separate sample therefore each treatment group (e.g. MeJA pre-treated and 3 hrs harvest timepoint) had four replicates. Immediately following harvesting the bark of all samples was flash frozen in liquid nitrogen before being stored at -80 ºC.

Using a pestle and mortar, all harvested bark was ground to powder independently for each sample. The one exception was the 4 wks post pre-treatment samples which only had half of the harvested bark ground to a powder. Total RNA was extracted from 30-50 mg of bark tissue powder of each sample using the MasterPure Complete DNA and RNA Purification Kit (Lucigen, MC85200). In order to denature ribonucleases and reduce polyphenolic contamination of extracted nucleic acids, 0.5 % β-mercaptoethanol (Sigma-Aldrich, M3148) and 1 % Polyvinylpyrrolidone (PVP; Sigma-Aldrich, P-5288) were added to the extraction buffer. To reduce carbohydrate contamination, nucleic acids were precipitated via the use of 0.5 volumes of 7.5 M lithium chloride precipitation solution (ThermoFisher Scientific, AM9480), an incubation at -20 ºC for 2 hours and centrifugation for 30 minutes at 16500 x *g* and 4 ºC. Nucleic acids were resuspended in 60 µl of nuclease free water.

3.5.9. Reverse Transcriptase-Quantitative Polymerase Chain Reactions (RT-qPCRs)

The Maxima First Strand cDNA Synthesis Kit for RT-qPCR with dsDNase (ThermoFisher Scientific, K1671) was used, according to manufacturer's instructions, to remove contaminant genomic DNA and reverse transcribe extracted mRNA to cDNA. For each sample, 200 ng of total RNA was used for cDNA synthesis. qPCR assessment of gene expression was performed with 2-fold diluted cDNA, SYBR™ Select Master Mix (ThermoFisher Scientific, 4472919) and the Applied Biosystems® ViiA™ 7 Real-Time PCR System. qPCRs were set up according to manufacturer's recommendations. Primer sequences are shown in Table 3.1. Post pre-treatment and post challenge samples were analysed separately, with four blocks of qPCRs for each. Within every block there was one biological replicate of each treatment group and primer sets for all genes studied in the experiment. Relative gene expression values were calculated using the following pipeline: (i) C_t values, outputted by the ViiA™ 7 system, adjusted for amplification efficiency calculated using the program LinRegPCR

(Ruijter et al., 2009) (ii) adjusted values put relative to a calibrator sample (a water control) (ii) relative values normalised using the mean relative expression of two endogenous reference genes, *actin* and *alpha-tubulin* (iii) normalised values put relative to the mean normalised expression of the water pre-treated, or water pre-treated and water challenged, replicates from the earliest timepoint (3 hrs post pre-treatment or 6 hrs post challenge). Plots displaying relative expression values were created using the R package ggplot2.

Table 3.1. – RT-qPCR Primers

Target Gene	Forward primer (5'-3')	Reverse primer (5'-3')	Reference
Actin	TGAGCTCCCTGATGGGCAGGTGA	TGGATACCAGCAGCTTCCATCCCAAT	(Yakovlev et al., 2006)
Alpha-Tubulin	GGCATACCGGCAGCTCTTC	AAGTTGTTGGCGGCGTCTT	(Hietala et al., 2004)
MA_10432716g0010 – PR2	TCCCAACATCCCACTCATCGT	GCTCCTTCCCGGCCTCTT	This Study
MA_394599g0010 – PR4	AGTCTGCTTGTGGCTGTATTTC	CGGACGGGTTGTAGTCATTGT	This Study
MA_83505g0010 – PR3.1	GCAGGACACCGCCGATTG	TGATGAACAGACAGCCGATAGAGA	This Study
MA_9682123g0010 – PR3.2	TGTCGGATATTGCTACCCAAGA	CCTGTTGTGCCAAAGCTAGAA	This Study
MA_19953g0020 – PR5	TGCCACTGACTACTCGAAGGT	GCCTGGGTGCAGGTGAAAG	This Study
MA_68384g0010 – DML	AGGCACACTGCTGATACCTT	TTGTTTCATGGTCTGCAAATACCT	This Study
MA_8720349g0010 – NRPE1	GGTCTGGCAAAGCTAAATTCATGT	CAGGTATCTTTCTCCCAGCCCTTA	This Study
MA_52817g0010 – EIN3/EIL1	AGTTGGTGACTTCTCGTTTAGG	TGCTCAAATGCTGTGTTTCTCT	This Study
MA_10425932g0020 - WRKY	ACGATGGCGGAAATGTTAAGGA	ACCTGGCTTCTGGTCTGAAATG	This Study
MA_10435905g0020 - MYC	AGGCATCTGTGTTCGCTGAA	GGCTTCGGTCTGCTGAGTTA	This Study

3.5.10. RT-qPCR statistical analysis

Analysis of the relative expression data was conducted separately for each gene and for the post pre-treatment and post challenge experiments. If the data was normally distributed and the treatment groups had homogeneous variances, an ANOVA followed by a Tukey post-hoc test was performed. Whereas if the variances were not homogeneous but the data was normal, a welch ANOVA followed by pairwise t-tests was used. A Kruskal Wallis test followed by pairwise Wilcox tests was used if a log transformation could not rectify non-normal data. The *p*-value's of the pairwise t-tests and Wilcox tests were adjusted using the Benjamini and Hochberg correction (Benjamini and Hochberg, 1995). Pairwise comparisons were only conducted if a significant effect of treatment group was identified with the ANOVA or Kruskal Wallis test. All statistical analyses were performed using R version 3.6.1.

3.5.11. mRNA-Sequencing (RNA-Seq)

3.5.11.1. Library Preparation and Sequencing

The RNA samples from each of the 3 hrs, 24 hrs and 1 wk post pre-treatment timepoints and from each of the four pre-treatment and challenge combinations, at 6 hrs post challenge, were selected for transcriptome analysis. Prior to sequencing, quantity and quality of RNA was assessed using a Nanodrop and Agilent 2100 Bioanalyzer. All samples had an RNA integrity number (RIN) value ≥ 8.5.

Library preparation and sequencing of all RNA samples was performed by BGI Tech Solutions (Hongkong) Company Limited (16 Dai Fu Street, Tai Po Industrial Estate, Tai Po, Hong Kong). As the BGI-seq (quantification) service was used, a standard protocol was followed for library preparation and sequencing. Briefly, total RNA was treated with DNase I to remove any contaminating genomic DNA. mRNAs were isolated via the selection for poly(A) tails using oligo dT sequences attached to magnetic beads. Following fragmentation of the purified mRNAs, first strand cDNA was synthesised with the help of random hexamer primers. Subsequent second strand cDNA synthesis was followed by end-repair and adenylation of the 3' end. Adaptors were ligated at the 3' adenylated ends before the cDNA was amplified by PCR. Purification of the amplified cDNA was performed using SPRI beads. Via denaturation and circularization with the help of a DNA splint, double stranded PCR products were converted to single strand circle DNA (ssCir DNA). The phi29 DNA polymerase

created DNA nanoballs by amplifying the ssCir DNA. The DNA nanoballs were loaded onto a sequencing chip and then sequenced using the BGISEQ-500 functioning in its paired end mode. More information on the technical details of BGI's in house sequencing platform, and evidence that its output is comparable to that of Illumina's HiSeq4000 platform when it comes to sequencing plant transcriptomes, can be found in the following references: Huang et al (2017) and Zhu et al (2018).

Across the 40 samples, 1.4 billion 150 bp paired-end (PE) clean reads were generated in total, with the minimum, maximum and mean number of read pairs per sample of 14, 38.1 and 35.2 million, respectively (Supplemental Data Set 3.9). The reads delivered by BGI were defined as clean because adapter sequences, contamination and low-quality reads had been removed. BGI reported that for all samples, ≥ 96% of nucleotides had a Phred quality score of > 20. To confirm BGI's read filtering had been comprehensive and the sequencing quality was sufficient, FastQC version 0.11.8 (Andrews, 2010) was used to analyse the FASTQ files containing BGI cleaned reads. Per sample FastQC reports were grouped into a single report using MultiQC version 1.7 (Ewels et al., 2016). The only issues flagged by FASTQC were higher than expected levels of read duplication and the first 10-15 positions having an uneven proportion of the four bases and showing a K-mer bias. Both issues are common for RNA-seq datasets and are simply an artefact of highly expressed transcripts and the use of random hexamer primers for cDNA synthesis, respectively.

3.5.11.2. Read Alignment and Counting

The Bowtie 2 package version 2.3.1 (Langmead and Salzberg, 2012) was used to align reads to the curated Norway spruce reference transcriptome described in (Mageroy et al., 2020b). First the transcriptome was indexed using the bowtie2-build function, and then reads were aligned using bowtie2 function run with the parameter settings: '--very-sensitive' '-q' '-k 10'. With option k being set to 10, up to 10 valid alignments were reported per read pair rather than the single best alignment being reported as would happen by default. This reporting method allowed multi-mapping reads to be recognised and removed. On average, 22.5% (7.9 million) of each samples raw read pairs remained following alignment and subsequent multi-mapper removal (Supplemental Data Set 3.9). The number of uniquely aligned fragments mapping to

each gene were counted with the featureCounts function from the Rsubread R package version 2.0.1 (Liao et al., 2014; Liao et al., 2019). The following options were specified in the featureCounts function: ‘isGTFAnnotationFile = TRUE’, ‘isPairedEnd = TRUE’. The GTF reference transcriptome annotation file was created using AUGUSTUS run with the parameter settings: ‘--strand=both’, ‘--genemodel=partial’, ‘--species=arabidopsis’ (Stanke et al., 2004).

3.5.11.3. Differential Expression Analysis

Two separate transcriptome analyses were conducted. The first aimed to understand how over time the transcriptome responded to MeJA pre-treatment and the second aimed to investigate how that pre-treatment influenced the subsequent response to challenge. The first analysis utilised the 3 hrs, 24 hrs and 1 wk post pre-treatment samples along with the water challenged samples (i.e. water or MeJA pre-treated and water challenged) which acted as the 4 wk timepoint. The second analysis used only the post challenge samples. The transcriptome analyses were conducted in R, primarily using the package DEseq2 version 1.24.0 (Love et al., 2014).

Prior to differential expression analysis, an assessment of global patterns was performed separately for the samples of the two transcriptome analyses. Count tables created by featureCounts were loaded into R and all genes with total read counts across all samples < 100 were removed. To account for between sample differences in sequencing depth and reduce the level of heteroskedasticity (i.e. flatten the mean normalized gene expression vs dispersion trend), read counts were both normalized for library size and transformed with a variance stabilising transformation (vst) (Anders and Huber, 2010) using the DESeq2 vst function run with the following option settings: ‘blind=TRUE’, ‘nsub=1000’, ‘fitType = "parametric"’. Transformed count data was used for principle component analysis (PCA), hierarchical clustering analysis (HCA) and heatmaps of sample to sample distances. The PCAs were performed using the DEseq2 plotPCA function run with the following options: ‘intgroup=c(“Pre.Treatment","Challenge")’, ‘ntop = all genes ≥ 100 read counts’, ‘returnData = TRUE’. The outcome of the PCAs were displayed using the R package ggplot2. Another R package, pheatmap version 1.0.12 (Kolde, 2019), was used to cluster samples and create heatmaps displaying sample to sample distances.

Samples were clustered using the complete-linkage method and the euclidean distances between samples.

Genes which showed a significantly altered expression profile across time as a result of MeJA pre-treatment were identified using the DESeq2 DEseq function run with the following parameter settings: ‘test="LRT"’, ‘full = ~ time + pre.treatment:time’, ‘reduced = ~ time’. Genes with an adjusted *p*-value (Benjamini and Hochberg correction) (Benjamini & Hochberg, 1995) < 0.001 were selected from the results table created by the DESeq2 results function which was run with the parameter settings: ‘alpha = 0.001’, ‘cooksCutoff = T’, ‘lfcThreshold = 0’.

For the second transcriptome analysis, all six possible pairwise comparisons between the four post challenge treatment groups (e.g. “water pre-treatment and MeJA challenge”) were conducted using the DESeq2 functions, DESeqDataSetFromMatrix run with the option setting: “design ~ treatment_group”, DEseq run with default settings and results run six times with the following argument values: ‘contrast = c("treatment_group",x,y)’(x and y being the different treatment groups), ‘alpha = 0.05’, ‘cooksCutoff = T’, ‘lfcThreshold = 0’. Genes were regarded as differentially expressed between two treatment groups if they had an adjusted *p*-value (Benjamini and Hochberg correction) < 0.05.

3.5.11.4. Hierarchical Clustering and Expression Pattern Visualisation

Genes were grouped by expression pattern using agglomerative hierarchical clustering. Correlation-based distance measures were used to calculate between gene dissimilarity based on counts transformed with the DESeq2 vst function run with the argument values: ‘blind=FALSE’, ‘nsub=1000’, ‘fitType = "parametric"’. Dendrograms were created from the dissimilarity data using the complete linkage or Ward's minimum variance clustering methods. For visualisation, the dendrograms were displayed together with heatmaps, each row of which was a separate gene with transformed counts displayed as Z-scores. All aforementioned steps were conducted using the aheatmap function from the NMF R package version 0.21.0 (Gaujoux and Seoighe, 2010).

MA-plots, which displayed the relationship between log fold change and gene expression level, were created using DESeq2’s plotMA function. To reduce the emphasis on highly variable non-significant lowly expressed genes and thus aid

visualisation, log fold changes were shrunk using the DESeq2 function lfcShrink(type = "ashr“) (Love et al., 2014; Stephens, 2017). All bar charts and line plots showing numbers of differentially expressed genes and gene expression profiles, respectively, were created using the R package ggplot2. Expression profile plots used the same transformed counts as used for the hierarchical clustering.

3.5.11.5. Protein Signature Enrichment Analysis

Predicted protein sequences for all genes with total read counts ≥ 100 across all samples of a particular transcriptome analysis, were annotated with protein signatures (e.g. protein domain) using the Pfam database version 32.0 (El-Gebali et al., 2019) and hmmscan from the HMMER package version 3.2.1 (Eddy and Wheeler, 2015). These genes provided the background distribution of Pfam protein signatures for enrichment analysis which was conducted using the enrichment function from the bc3net R package version 1.0.4 (de Matos Simoes and Emmert-Streib, 2016). For a Pfam protein signature to be found as enriched in a candidate protein list, it had to have an adjusted *p*-value (Benjamini and Hochberg correction) ≤ 0.05. Fold enrichment plots displaying significantly enriched protein signatures were created using ggplot2.

3.5.11.6. Gene Ontology (GO) Enrichment Analysis

Per gene cluster over-enrichment analysis of biological function GO terms was conducted using the enrichment tool of ConGenIE (http://congenie.org/), the online host of information and data relating to the Norway spruce genome project (Nystedt et al., 2013; Sundell et al., 2015). The background for the analysis consisted of all genes in the spruce genome assigned at least one biological function GO term. For a GO term to be reported it had to be assigned to 1 or more genes in a cluster and it had to have a false discovery rate (FDR) adjusted *p*-value < 0.05.

3.5.11.7. Identification of Differentially Expressed Genes Related to Defence or Epigenetics

Differentially expressed genes were annotated using predicted amino acid sequences, blastp version 2.8.1, (Altschul et al., 1990; Altschul et al., 1997; Camacho et al., 2009) and the Swiss-Prot database (The UniProt Consortium, 2019). Those genes predicted to encode for hormone biosynthesis enzymes, defence regulators,

defence metabolite biosynthesis enzymes or pathogenesis-related (PR) proteins, were identified by searching the blastp outputs for key terms (e.g. "WRKY", " Pathogenesis-related" and “anthocyanidin reductase”). Differentially expressed genes predicted to encode for epigenetic regulators were identified using the lists of epigenetic regulator genes provided in Mageroy et al (2020b).

3.6. Supplemental Figures

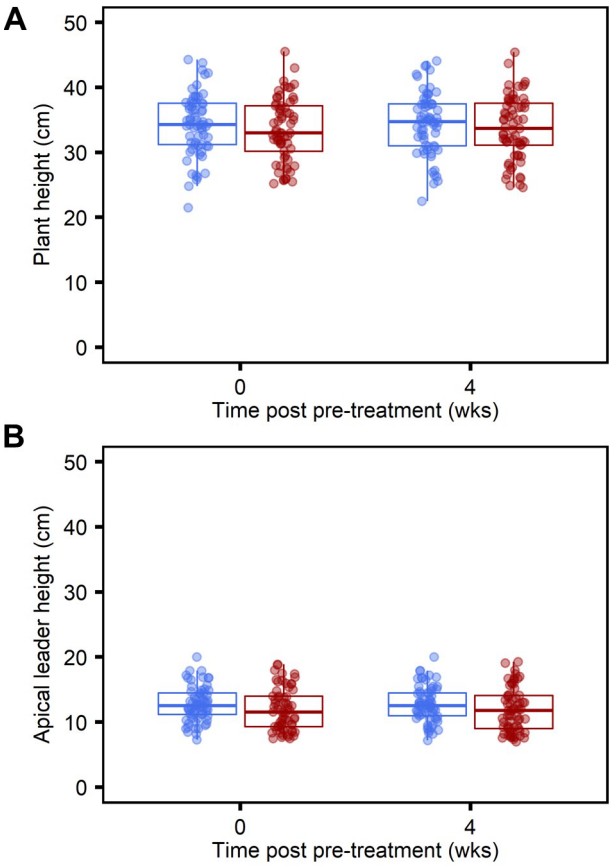

Supplemental Figure 3.1. Impact of MeJA Pre-treatment on Plant and Apical Leader Height.

Plant **(A)** and apical leader height **(B)** for seedlings pre-treated with water (blue) or 10 mM MeJA (red). Trees were measured prior to pre-treatment (0 weeks) and then again 4 weeks (wks) later prior to challenge. Points represent individual replicates (n = 64-65). The lower, middle and upper horizontal lines in the boxplots equate to the first, second and third quartiles. Whiskers extend to the lowest and highest data points within 1.5*interquartile range below and above the first and third quartiles. Apart from the effect of measurement timepoint on plant height (two-factor mixed ANOVA; F = 19.93, df = 1, 64, $p < 0.001$) and pre-treatment on apical leader height (robust two-factor mixed ANOVA; F = 6.36, df = 1,76, $p < 0.05$), there were no other significant effects.

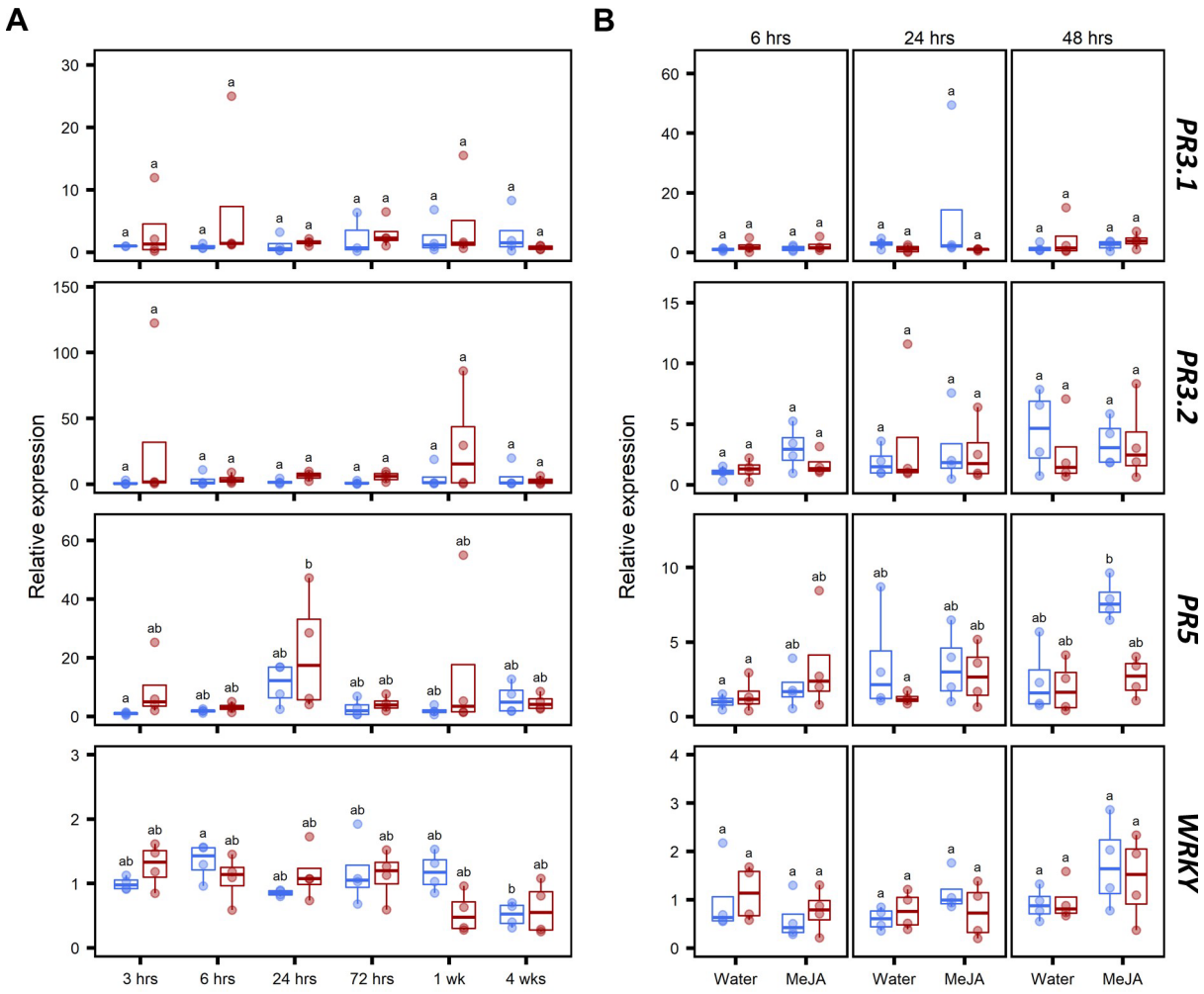

Supplemental Figure 3.2. Expression Profiles of Pathogenesis-related (PR) and WRKY Transcription Factor Genes in Response to MeJA Pre-treatment and Challenge.

The expression pattern of three *PR* genes (*PR3.1 - MA_83505g0010, PR3.2 - MA_9682123g0010* and *PR5 - MA_19953g0020*) and one WRKY transcription factor (*MA_10425932g0020*), in response to water (blue) or 10 mM MeJA (red) pre-treatment and subsequent challenge four-weeks-later with water or 5 mM MeJA. Expression of the four genes was assessed at six timepoints post pre-treatment **(A)** and three timepoints post challenge **(B)**. Points represent individual replicates (n = 4) with expression relative to the mean, which equals 1, of the 3 hrs water pre-treated samples **(A)** or the 6 hrs water pre-treated and water challenged replicates **(B)**. Those treatment groups which do not share the same letter are significantly different (ANOVA followed by Tukey post hoc, $p < 0.05$ (**(A)** *PR5* and *WRKY* **(B)** *PR5*); No pairwise comparison as no significant effect of treatment group (**(A)** *PR3.1* and *PR3.2* **(B)** *WRKY*, *PR3.1* and *PR3.2*).

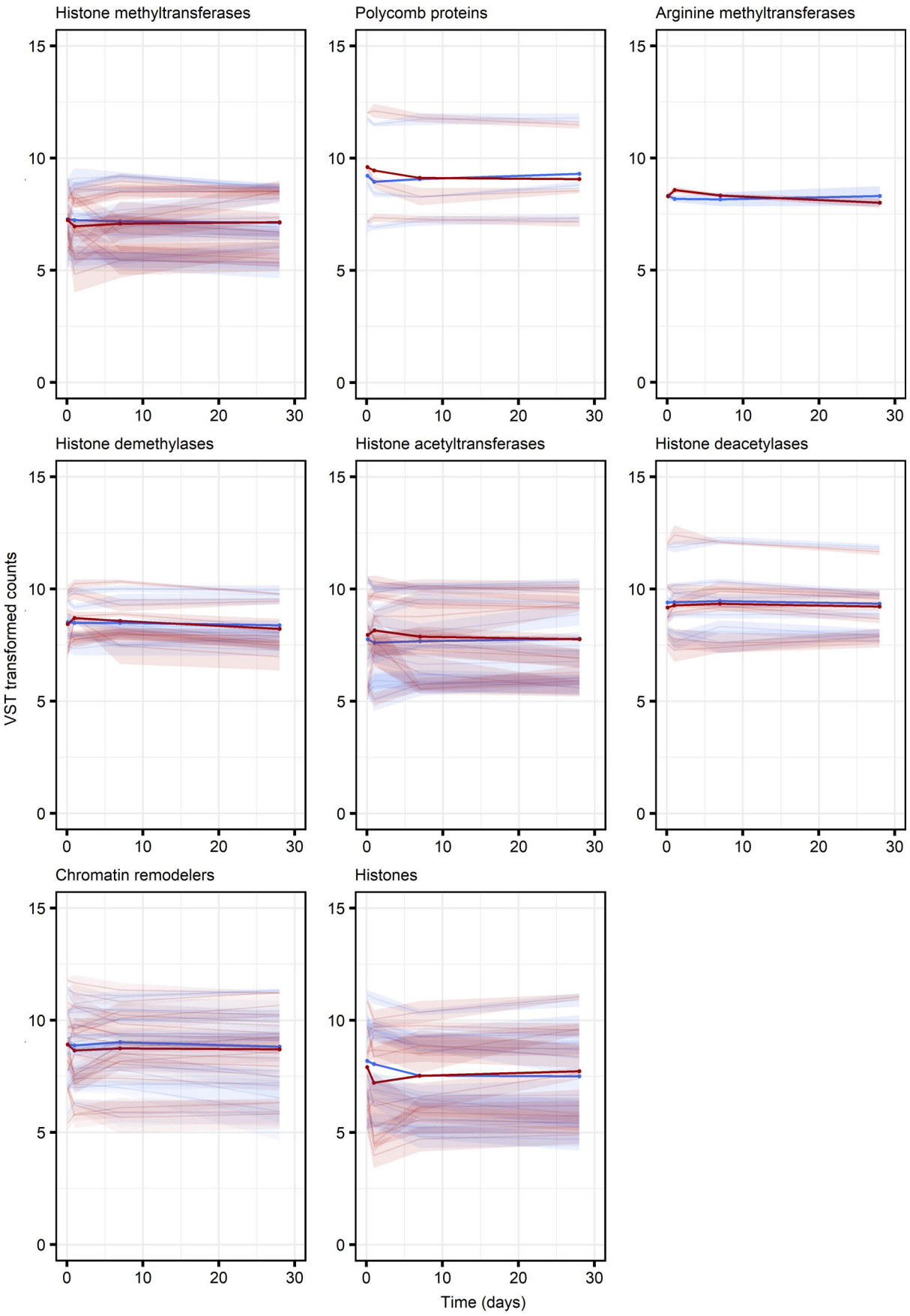
Histone methyltransferases
Polycomb proteins
Arginine methyltransferases
Histone demethylases
Histone acetyltransferases
Histone deacetylases
Chromatin remodelers
Histones
VST transformed counts
Time (days)
0
5
10
15
0
10
20
30

Supplemental Figure 3.3. Epigenetic Regulators Transcriptional Response to MeJA Pre-treatment (*Figure appears on previous page*).

Expression profiles of epigenetic regulator genes that were annotated in the spruce genome by Mageroy et al (2020b) and which showed a significantly (adjusted *p*-value < 0.001) altered expression pattern across time as a result of MeJA pre-treatment (Figure 3.5). Each of the expression plots represents a specific category of epigenetic regulators. The faint lines with shading indicate individual genes with 95% confidence intervals and the thicker lines depict the category means, for each of the two pre-treatments, water (blue) and MeJA (red). Read counts were normalised for sequencing depth and transformed to approximately the log2 scale using the DESeq2 function vst (Love et al., 2014).

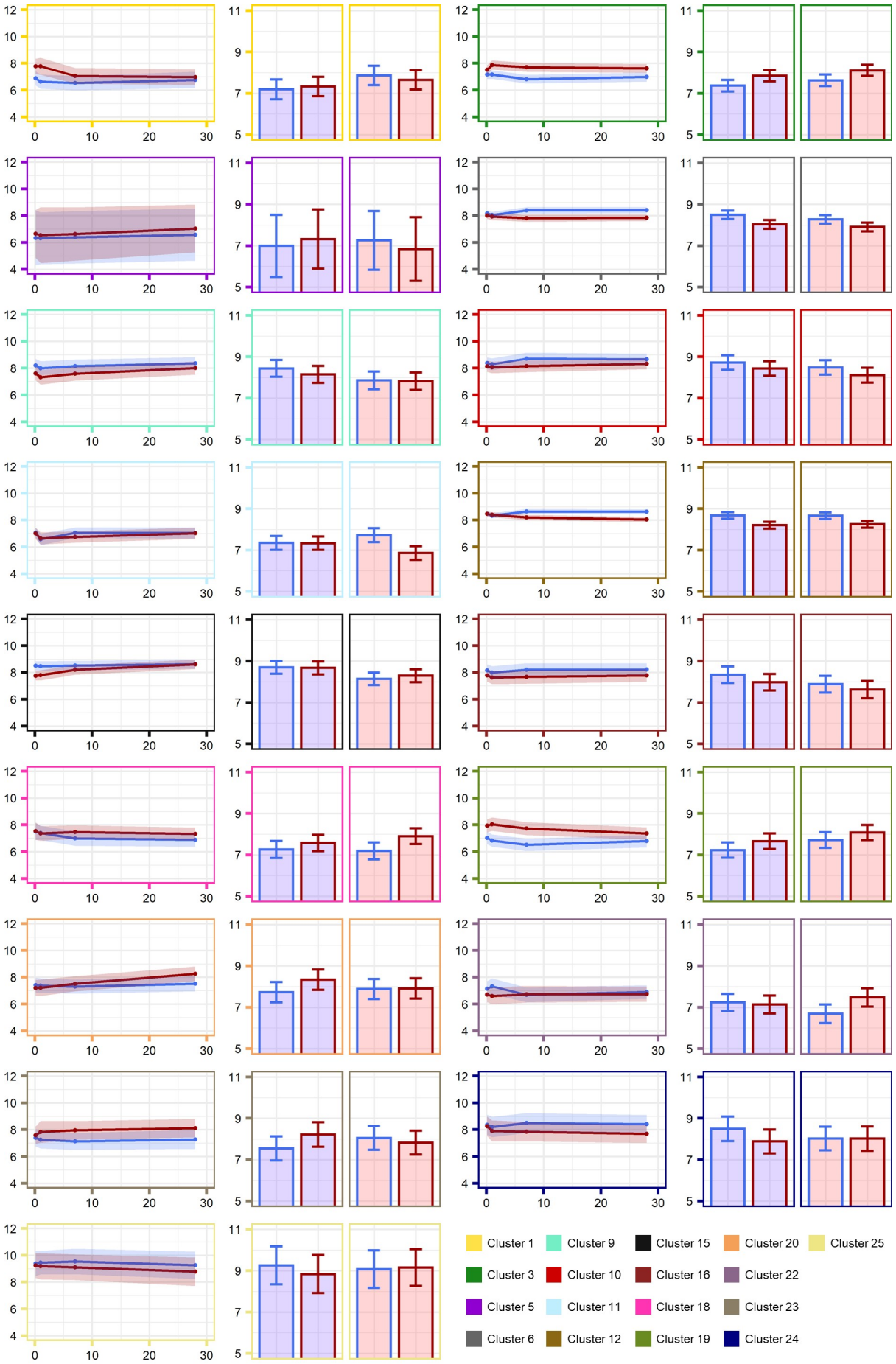
Cluster 1
Cluster 9
Cluster 15
Cluster 20
Cluster 25
Cluster 3
Cluster 10
Cluster 16
Cluster 22
Cluster 5
Cluster 11
Cluster 18
Cluster 23
Cluster 6
Cluster 12
Cluster 19
Cluster 24

Supplemental Figure 3.4. Post Challenge Transcriptional Patterns – Extension of Figure 3.13 (*Figure appears on previous page*).

The mean expression profiles post pre-treatment (line plots) and post challenge (bar plots) for gene clusters from the dendrogram displayed in Figure 3.13A, which did not have at least one significantly (adjusted *p*-value ≤ 0.05) enriched protein signature. Water and MeJA pre-treatments are indicated by the blue and red lines or bar outlines. Water and MeJA challenges are indicated by the blue and red bar fill. The y axis on all plots displays counts normalised for sequencing depth and transformed to approximately the log2 scale by the DESeq2 function vst (Love et al., 2014). The x axis of the post pre-treatment line plots is time in days. 95% confidence intervals are displayed as shading and error bars.

Chapter 4

General Discussion

Text and figures in this chapter were adapted from:

Wilkinson SW[1,2], Magerøy MH[2], López Sánchez A[1,3], Smith LM[1], Furci L[1], Cotton TEA[1], Krokene P[2], Ton J[1] (2019) Surviving in a Hostile World: Plant Strategies to Resist Pests and Diseases. *Annual Review of Phytopathology* 57: 505–529

Affiliations:

[1] Department of Animal and Plant Sciences, The University of Sheffield, Sheffield S10 2TN, United Kingdom

[2] Department of Molecular Plant Biology, Division for Biotechnology and Plant Health, Norwegian Institute for Bioeconomy Research (NIBIO), 1431 Ås, Norway

[3] Department of Plant Molecular Genetics, Centro Nacional de Biotecnología, Consejo Superior de Investigaciones Científicas (CNB-CSIC), 28049 Madrid, Spain

Author contributions:

SWW (the candidate) and JT conceived the original idea and structure of the review. All authors contributed to the writing of the article and/or production of the figures. SWW, MHM, PK and JT reviewed and finalised the manuscript for submission.

All material in this chapter, which is not in the publication, was created by SWW.

Chapter 4. General Discussion

4.1. Summary and Highlights from Experimental Chapters

The primary aim of this PhD was to better understand the (epi)genetic mechanisms behind long-lasting within generation jasmonate-induced resistance (IR). This was achieved by conducting experiments in two species, Arabidopsis (Chapter 2) and Norway spruce (Chapter 3). It is well described that defences effective against chewing herbivores and necrotrophic pathogens are positively regulated by jasmonate signalling (Wasternack and Hause, 2013; Erb and Reymond, 2019). In agreement, this PhD study found that Arabidopsis exhibits short-term IR following challenge by a chewing herbivore or a necrotrophic pathogen at 1 day after treatment with jasmonic acid (JA). However, strikingly, while the JA-IR against the herbivore was maintained over a time span of 3 weeks, the short-term JA-IR against the necrotrophic pathogen was reverted to long-term JA-induced susceptibility (IS) over the same time period. Chapter 2 explores the mechanism behind these opposing long-term phenotypes, using a combination of mutant lines, mRNA sequencing (RNA-seq) and whole genome bisulfite sequencing (WGBS). Highlights from this work include clear transcriptomic evidence for MYC-dependent augmentation of anti-herbivore defences coupled with suppression of anti-pathogen defences. Furthermore, it was shown that long-term JA-IR requires active regulation of DNA methylation at transposable elements (TEs), which was associated with random hypomethylation that appeared to be targeted to TEs of the *ATREP2* family.

Multiple studies have demonstrated that treatment of Norway spruce with methyl jasmonate (MeJA) elicits IR against necrotrophic pathogens and chewing herbivores, which can last for at least several weeks (Erbilgin et al., 2006; Zeneli et al., 2006; Krokene et al., 2008; Mageroy et al., 2020a). Nevertheless, the (epi)genetic mechanisms behind this response have only just begun to be explored in detail. Mageroy et al (2020b) demonstrated that MeJA pre-treatment primed mature spruce tree bark for an augmented induction of *PR* genes in response to wounding challenge 4 weeks later. Furthermore, it was also shown that wounding stress induced differential expression of epigenetic regulators. As wounding can elicit IR in other species (Chassot et al., 2008), these findings suggest that IR in spruce could be associated with epigenetic changes. Chapter 3 carried on from this recent study, using

an experiment that was conducted in 2-year-old Norway spruce seedlings. This study firstly demonstrates long-term MeJA-IR against a necrotrophic pathogen. Secondly, by using RNA-seq analysis, Chapter 3 provides global transcriptomic patterns that potentially mark the underlying mechanisms of the MeJA-IR response. While this analysis revealed similarities with the response of Arabidopsis to jasmonates, there were also noticeable differences. Considering the evolutionary distance between these plant species, these differences are perhaps unsurprising. The next section will discuss the similarities and differences in long-term jasmonate-IR between Arabidopsis and Norway spruce. Subsequently, this Chapter will go into further detail about the possible impacts of long-term jasmonate-IR on interactions with other organisms, including defence strategies that rely on tri-trophic interactions (see Figure 1.1). Finally, this Chapter will discuss possible implications of my PhD research for agriculture and forestry.

4.2. Jasmonate Induced Resistance: Similarities and Differences Between Arabidopsis and Norway spruce

The most obvious difference between the results presented in Chapter 2 (Arabidopsis) and Chapter 3 (Norway spruce) relates to the long-term impact of jasmonates on resistance against necrotrophic pathogens. In Arabidopsis, treatment of seedlings with JA resulted in long-term IS against the necrotrophic fungus *Plectosphaerella cucumerina* (Figure 2.1C). By contrast, treatment of Norway spruce with MeJA resulted in long-term IR against the necrotrophic fungus *Grosmannia penicillata* (Figure 3.2). There are several possible explanations for this difference. For instance, the concentration of JA-Ile reaching the COI1-JAZ co-receptor may have been different between the two species. For the Arabidopsis and spruce experiments, 1 mM JA and 10 mM MeJA pre-treatments were used respectively. In both cases, the entire plants were sprayed with jasmonate solutions. MeJA is more volatile than JA and therefore more MeJA may have evaporated during the application procedure resulting in a difference between the Arabidopsis and spruce in the active concentrations inside tissues (leaves or stem). Furthermore, dissimilarities in active concentrations in tissues may also have been driven by differences between the two species in plant form and the properties of the outer surfaces of leaves and stems. Arabidopsis is an herbaceous plant with ovate-shaped leaves, whereas Norway spruce is a woody tree species with a thick stem cortex and needle-shaped leaves

that have thick waxy cuticles. Once inside cells, JA and MeJA had to be converted into the bioactive jasmonate, JA-isoleucine (JA-Ile) in order to be effective. It should be mentioned, however, that while it is likely that JA-Ile is the bioactive form of jasmonate in Norway spruce, there is no direct evidence to support this. Nevertheless, assuming that JA-Ile is the active jasmonate in spruce, MeJA would have gone through a two-step conversion to form JA-Ile. Firstly, MeJA specific esterase's would have converted MeJA into JA, before secondly, the JA could then have been conjugated into active JA-Ile by jasmonoyl isoleucine conjugate synthase enzymes, such as JAR1 (Staswick and Tiryaki, 2004; Jong et al., 2013). All these factors listed could have led to a lower activation of JA signalling in spruce compared to Arabidopsis. Accordingly, it is possible that only relatively high internal JA-Ile concentrations trigger long-term IS against necrotrophic pathogens, and therefore lower initial concentrations of JA-Ile may lead to long-lasting JA-IR in Arabidopsis. However, this hypothesis was not supported by a preliminary Arabidopsis experiment, which revealed that lower concentrations of JA failed to trigger both JA-IR and JA-IS to *P. cucumerina*, while higher JA concentrations resulted in a dose-dependent increase in JA-IS (Supplemental Figure 2.1). In order to fully exclude the hypothesis, more experiments are needed that compare internal JA-Ile concentrations and long-term resistance to necrotrophic pathogens after treatment of both Arabidopsis and Norway spruce with jasmonate solutions of a range of concentrations.

An alternative explanation for the absence of jasmonate-IS in spruce is a lack of antagonistic crosstalk within the JA response. It has been hypothesised that antagonistic crosstalk between hormonal signalling pathways exists in Arabidopsis as a means to optimise available resources and thus ensure that the plant both survives and has a good reproductive output (Koornneef and Pieterse, 2008; Pieterse et al., 2012). *Arabidopsis thaliana* is a short-lived annual plant species that can complete its lifecycle in as little as 6 weeks. Thus, in order to both survive and reproduce, it must prioritise the biotic threats that are the most imminent. In contrast, Norway spruce generally lives for 100s of years (Caudullo et al., 2016). Accordingly, an investment for multiple hours, days and weeks in defence against multiple biotic threats, potentially controlled by multiple separate signalling pathways, is likely to be less of an issue. Indeed, evidence suggesting a lack of antagonistic crosstalk in spruce comes from the previous reports that defences which are thought to be effective against both

necrotrophic pathogens and herbivores appear to be regulated by JA and ET (Hudgins and Franceschi, 2004). By contrast, while ET signalling in Arabidopsis positively regulates resistance against necrotrophic pathogens, it negatively regulates resistance against generalist chewing herbivores through negative signalling-cross talk between the EIN3/EIL1-dependent JA response and the MYC-dependent JA response (Bodenhausen and Reymond, 2007; Song et al., 2014). Furthermore, from previous studies, it is unclear whether the classical SA-JA crosstalk exists in spruce (Germain et al., 2012; Arnerup et al., 2013; Mageroy et al., 2020b). In Chapter 2, it was demonstrated that in addition to many genes involved in synthesising upstream precursors of SA, genes predicted to encode for the master regulator of SA-dependent defences, NPR1, were transiently upregulated in response to MeJA treatment. This contrasts Arabidopsis, where MeJA treatment of seedlings slightly represses *NPR1* (Arabidopsis eFP Browser, http://bar.utoronto.ca/efp/cgi-bin/efpWeb.cgi, (Winter et al., 2007)). It is plausible that the *NPR1* homologues in spruce do not regulate SA dependent defences. However, against this conclusion is the fact that the non-vascular moss species *Physcomitrella patens*, has a functional NPR1-like protein, which at least partially complements the Arabidopsis *npr1-1* mutant with regards to SA-dependent defence against biotrophic pathogens (Peng et al., 2017). This suggests conservation of functional NPR1-dependent SA signalling across land plants and that by activating NPR1 MeJA was activating SA-dependent defences in spruce bark tissue. Thus, it seems plausible that JA and SA may not be antagonistic in spruce and that in general antagonistic crosstalk within and between hormonal signalling pathways does not exist in this tree species. This provides a possible explanation for why over longer timeframes following jasmonate pre-treatment, spruce can prioritise both branches of JA pathway, but Arabidopsis can only prioritise one branch.

The lack of jasmonate-IS in Norway spruce could also be because 4 weeks is not that long-term when you consider that the species has a lifespan of multiple centuries. It would be interesting to assess resistance to necrotrophic pathogens multiple years after a strong jasmonate treatment as potentially the jasmonate-IR would switch to jasmonate-IS after such a time period in spruce. In addition to lifespan, the reproductive strategy of Norway spruce also differs from that of *Arabidopsis thaliana*, as Norway spruce is an obligate outcrosser rather than being a predominant self-fertiliser. It has been reported that mating system variation can influence defence

traits and resistance to biotic stress (Campbell, 2015). Thus, differences in mating system could also explain the dissimilarities between Arabidopsis and spruce in the response to jasmonate treatment at the seedling stage.

While Chapter 3 demonstrated long-term MeJA-IR against a necrotrophic pathogen, the impacts of MeJA treatment on resistance of Norway spruce against chewing herbivores was not tested. Nevertheless, based on previous studies in spruce, it is likely that the MeJA elicits IR against herbivores in this tree species (Erbilgin et al., 2006; Berglund et al., 2016; Fedderwitz et al., 2016; Mageroy et al., 2020a). In Arabidopsis, MYC TFs are essential for long-term jasmonate-IR against herbivores (Figure 2.7). Multiple lines of evidence suggest that MYC TFs also orchestrate this long-lasting response in spruce. Firstly, in Chapter 3 it was shown that genes predicted to encode for MYC TFs are upregulated in response to MeJA treatment (Figures 3.3 and 3.8 and Supplemental Data Set 3.4). Secondly, in spruce, production of defence-related terpene-rich oleoresin plays a role in resistance against herbivores and is thought to contribute to MeJA-IR (Zhao et al., 2011; Schiebe et al., 2012; Krokene, 2015; Celedon and Bohlmann, 2019). Thirdly, production of terpenes in spruce is known to be induced in response to MeJA treatment (Martin et al., 2002; Martin et al., 2003; Zulak et al., 2009). Fourthly, in species across the plant kingdom, including the liverwort *Marchantia polymorpha* and the conifer Chinese Yew (*Taxus chinensis*), MYC TFs positively regulate terpene biosynthesis genes and/or terpene production (Hong et al., 2012; Spyropoulou et al., 2014; Roos et al., 2015; Shen et al., 2016; Zhang et al., 2018c; Peñuelas et al., 2019; Aslam et al., 2020). Finally, many of these studies in diverse plant species demonstrated that MYCs are required for jasmonate induced terpene production. In summary, together these lines of evidence strongly suggest that MYCs are important, if not essential, for jasmonate-IR against chewing herbivores in spruce.

The lack of causal evidence about the function of MYC TFs in Norway spruce epitomises the limited knowledge about jasmonate signalling in this plant species. For instance, in addition to the lack of direct evidence that JA-Ile is the bioactive jasmonate, it is also unknown whether COI1 and JAZ act as the jasmonate co-receptors in spruce. It is, nevertheless, likely that these jasmonate pathway components are conserved between Arabidopsis and spruce. Firstly, JA-Ile accumulates in spruce tissue in response to MeJA treatment or necrotrophic pathogen

infection (Schmidt et al., 2011; Zhao et al., 2019). Secondly, evidence suggests that COI1 and JAZ are the co-receptors of the bioactive jasmonate in the liverwort *M. polymorpha* (Monte et al., 2018). Thus, as liverworts diverged very early following the colonisation of land (Bowman et al., 2017), it is likely that the common ancestor of all land plants had functional jasmonate signalling which required COI1 and JAZ. Downstream of the bioactive jasmonate receptors, it is also likely that spruce and Arabidopsis have conserved transcriptional regulators of JA dependent defences. In addition to the discussion about MYCs in the previous paragraph, evidence in support of this conclusion was provided by Germain et al (2012) who demonstrated that a GUS reporter gene fused to the promoter sequence of a jasmonate-inducible *PR* gene from white spruce was induced by JA when expressed in Arabidopsis. Nevertheless, more research into the evolutionary conservation of the JA signalling pathway and its regulation of defences would be desirable. This could be achieved by using RNA interference (RNAi) to silence homologs of COI1, MYC or other JA signalling components. (Hammerbacher et al., 2019) successfully employed RNAi in Norway spruce to reduce the expression of a flavonoid biosynthesis gene. Additional insight could also be gained by using jasmonate pathway inhibitors (Meesters et al., 2014; Monte et al., 2014; Vadassery et al., 2019). For instance, to determine the importance of JA-Ile in jasmonate signalling and the induction of defences in spruce, the JA-Ile synthetase inhibitor jasmonate response inhibitor-1 (jarin-1) could be utilised (Meesters et al., 2014). Alternatively coronatine-O-methyloxime (COR-MO) could be used to assess the requirement of the COI1-JAZ co-receptor complex, since COR-MO is a JA-Ile antagonist which prevents the interaction between COI1 and JAZ and thus in turn the targeting of JAZ repressors for degradation (Monte et al., 2014). In addition to understanding the role of the JA signalling pathway in basal resistance, future studies using RNAi and the jasmonate pathway inhibitors could also confirm the involvement of individual signalling components, or the JA signalling pathway as a whole, in long-term MeJA-IR in spruce.

Another potential similarity between the two plant species featured in this thesis, is a role for DNA methylation in regulating long-term resistance responses to jasmonates. There is increasing evidence that epigenetic mechanisms play a role in IR responses of plants (Jaskiewicz et al., 2011; Luna et al., 2012; López Sánchez et al., 2016; Schillheim et al., 2018; Baum et al., 2019; Furci et al., 2019; Wilkinson et al.,

2019). Indeed, Chapter 2 established causal evidence for the importance of DNA methylation homeostasis in long-term JA-IR against herbivory. Bioassays with mutants in RNA-directed DNA methylation (RdDM; See the sidebar titled RNA-directed DNA methylation in Chapter 1) or the DNA demethylase ROS1, which predominantly target TEs (Tang et al., 2016; Zhang et al., 2018b), provided causal evidence that active homeostasis of TE methylation is critical (Figure 2.11). Furthermore, WGBS confirmed these results by demonstrating that JA induces genome-wide hypomethylation at TEs at 3 weeks after seedling treatment (Figure 2.13). Interestingly, Chapter 3 showed that spruce genes predicted to encode for regulatory components in RdDM were long-term repressed following MeJA treatment, which could result in long-term hypomethylation of TEs (Figure 3.10). The spruce genome is inundated with TEs (Nystedt et al., 2013) and therefore there is plenty of scope for regulation of defence gene expression by changes in DNA methylation at these mobile elements. However, the way in which the TE silencing RdDM pathway functions in spruce bark tissue remains somewhat unclear as there is a paucity of 24 nucleotide (nt) small RNAs (sRNAs; M. Magerøy, personal communication), which are known to be required for canonical RdDM in Arabidopsis (Zhang et al., 2018b). Nevertheless, there is a greatly expanded miRNA and phased secondary small interfering RNAs (phasiRNAs) network in Norway spruce (Xia et al., 2015) and recent evidence for non-canonical RdDM pathways that rely on such 21/22 nt sRNAs (Cuerda-Gil and Slotkin, 2016). Furthermore, genes predicted to encode the majority of the components of the RdDM pathway and also other DNA methylation pathways, have been identified in the Norway spruce genome (Huang et al., 2015; Ausin et al., 2016). Thus, based on the results presented in Chapter 3 (Figure 3.10), it is plausible that MeJA induces DNA hypomethylation in Norway spruce.

DNA has been extracted from 2-year-old spruce seedlings treated with either water or MeJA 4 weeks previously and is awaiting analysis by WGBS to confirm that MeJA indeed induces long-term hypomethylation in spruce. Unfortunately, due to the COVID-19 pandemic, the sequencing data was received too late for any preliminary results to be included in this thesis and will therefore have to be explored as part of future research projects. Nevertheless, as Norway spruce methylomes have only so far been generated for naïve needle and somatic embryonic tissues (Ausin et al., 2016), this dataset will provide an excellent opportunity to expand our knowledge and

explore how the Norway spruce methylome is changed in response to stress. Furthermore, if the WGBS confirms that MeJA treatment induces long-lasting hypomethylation, it will pave the way for numerous follow-up experiments. For instance, to attempt to confirm that the hypomethylation is important for long-term IR, trees could be treated with 5-azacytidine prior to challenge with a necrotrophic pathogen or chewing herbivore. This chemical inhibits the activity of DNA methyltransferases resulting in a rapid DNA hypomethylation (Christman, 2002). Furthermore, the chemical has been used successfully to induce resistance in plants. For example, a recent study treated rice (*Oryza sativa*) with 5-azacytidine and demonstrated that this caused a global DNA hypomethylation and enhanced resistance to the root-knot nematode *Meloidogyne graminicola* (Atighi et al., 2020). This study also used RdDM mutants to establish causal evidence for the role of RdDM in rice resistance against nematodes. Unfortunately, mutants are not readily available in Norway spruce. However, RNAi, and perhaps even CRISPR/Cas9 gene editing technology, could be used to impair RdDM.

Finally, another possible similarity between Arabidopsis and spruce relates to the mode of action underpinning long-term jasmonate-IR. As hypothesised in Chapter 1, IR can be based on a prolonged upregulation of defences, and/or a prolonged priming of inducible defences, mediating a faster and/or stronger induction of these defences after subsequent pathogen/herbivore attack (Figure 1.3). Chapter 2 suggests involvement of both mechanisms in long-term JA-IR of Arabidopsis. For example, genes encoding anti-herbivore proteins, such as *VSP2*, showed a stronger induction upon challenge (Figure 2.3 and Figure 2.7), whereas numerous gene transcripts encoding for enzymes in secondary defence metabolism (e.g. glucosinolates) showed prolonged up-regulation (Figure 2.7 and Supplemental Figure 2.2). Results from Chapter 3 and preceding studies, including (Martin et al., 2002; Zulak et al., 2009; Zhao et al., 2011; Schiebe et al., 2012; Mageroy et al., 2020b), have suggested that MeJA-IR in spruce involves a combination of a prolonged upregulation of metabolic defences (e.g. oleoresin and polyphenolic accumulation) and priming of inducible defence proteins. Nevertheless, more research is needed to identify the key defences and potential trade-offs associated with long-term IR in spruce.

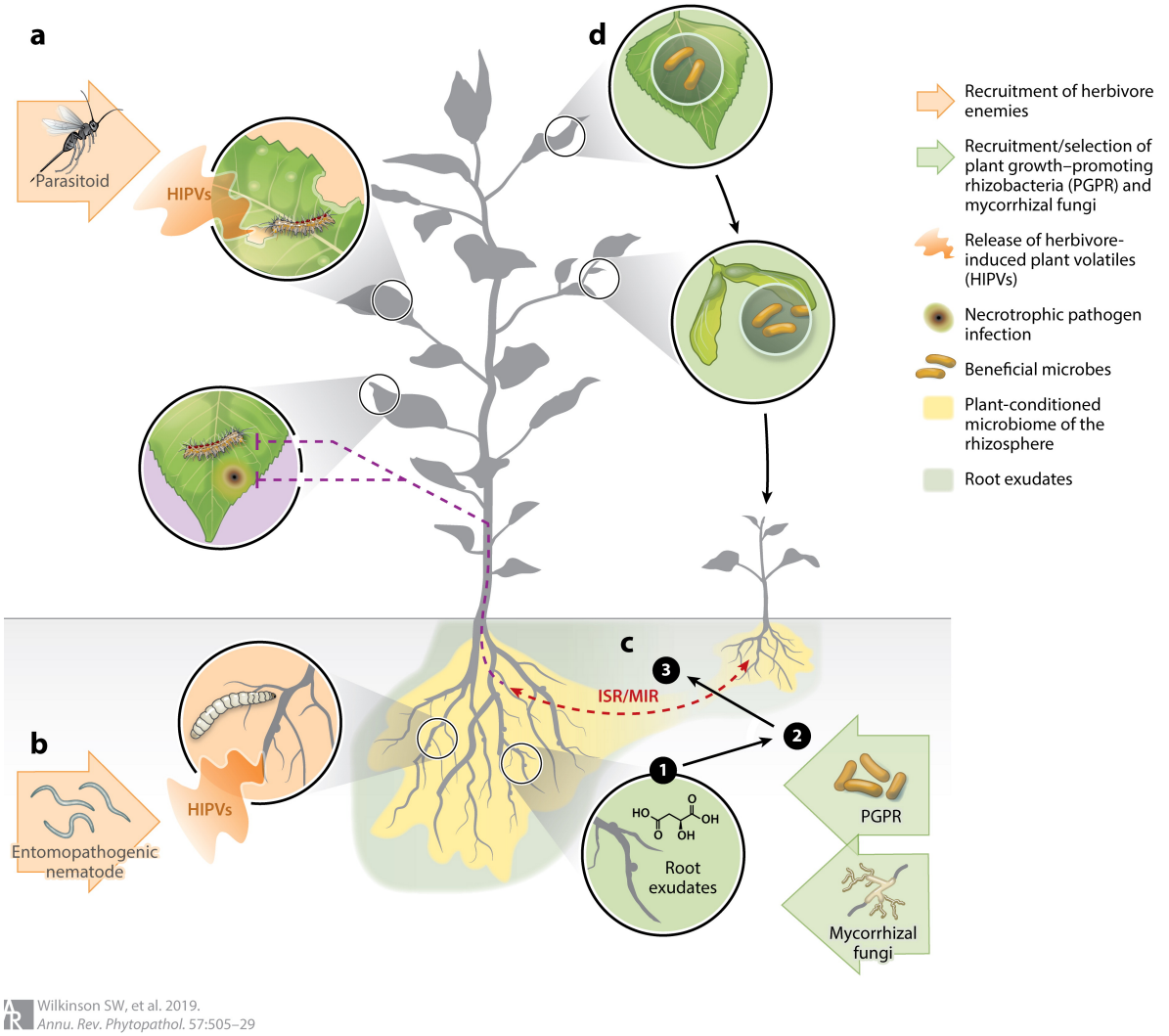

Figure 4.1. External Strategies by Which Plants Resist Pests and Diseases.

Volatile-based strategies that involve tritrophic interactions are shown on the left in orange shading. In response to egg deposition and/or feeding by herbivores, plants release herbivore-induced plant volatiles (HIPVs) that can recruit herbivore enemies, such as **(A)** parasitoid wasps and **(B)** entomopathogenic nematodes. These beneficial organisms kill the herbivore and so reduce damage to the host plant. Strategies involving recruitment of disease-suppressing microbial communities are shown to the right in green shading. **(C)** Plants can change their rhizosphere microbiome upon exposure to disease or herbivory. (1) Biotic stress changes the quantity and composition of root exudates, resulting in (2) increased recruitment of beneficial microbes. (3) The recruited microbes can antagonize soilborne pathogens and/or trigger an induced resistance (IR; ISR/MIR) response in the host plant (red dashed line), leading to augmented defence expression upon pathogen/herbivore attack (purple dashed line and purple shading). The conditioned microbiome (yellow shading) can spread to and protect neighbouring plants including nearby progeny (as indicated by the small plant). **(D)** Plants may also shape their phyllosphere microbiome and transfer the associated microbes to their progeny via seeds. Abbreviations: ISR, induced systemic resistance; MIR, mycorrhiza-induced resistance. Reproduced with permission from the Annual Review of Phytopathology, Volume 57 © 2019 by Annual Reviews, http://www.annualreviews.org

4.3. Impact of Jasmonate Pre-treatment on External Defences

Strategies utilised by plants to resist pests and diseases can broadly be split into internal and external (Figure 1.1). In Chapter's 2 and 3 it was demonstrated that jasmonate treatment can mimic an attacker and trigger the innate immune system. Furthermore, it was also shown that jasmonates can elicit IR which is associated with an augmentation of basal defences that directly antagonise attackers (e.g. anti-insect and -microbial proteins). These are both examples of internal strategies. Whereas, the influence of jasmonate treatment on external strategies was not explored. Plants constantly interact with beneficial organisms, such as insect pollinators, animal seed dispersers, nitrogen-fixing bacteria, and nutrient-providing fungi (Bronstein et al., 2006; Martin et al., 2017). These organisms can protect plants from pests and pathogens and thus plants have evolved to recruit them for their defence. For instance, plants can recruit parasitoid wasps which kill attacking herbivores or bacteria which can antagonise soil borne pathogens (Turlings and Erb, 2018; Rolfe et al., 2019). Defence strategies involving the recruitment of beneficial organisms can be described as external strategies and they are summarised in Figure 4.1.

In response to feeding or egg deposition by herbivores, plants often emit herbivore-induced plant volatiles (HIPVs) (Turlings et al., 1990; Rasmann et al., 2005; Baldwin, 2010; Mumm and Dicke, 2010; Clavijo McCormick et al., 2014; Turlings and Erb, 2018). HIPVs can mediate tritrophic interactions by attracting predators and/or parasitoids of the attacking herbivore (Figure 4.1) (Dicke and Sabelis, 1988; Turlings et al., 1990; Rasmann et al., 2005; Clavijo McCormick et al., 2014; Turlings and Erb, 2018). The recruitment of natural enemies of plant attackers by HIPVs is commonly referred to as indirect induced defence because plants are not directly antagonizing their attackers (Mumm and Dicke, 2010). In numerous plant species, exogeneous treatment with jasmonates has been reported to induce the emission of volatiles that can recruit natural enemies of herbivores, thereby protecting the plants indirectly against damage (Dicke et al., 1999; Thaler, 1999; Lou et al., 2005; Rodriguez-Saona et al., 2013; Li et al., 2015a; Mrazova and Sam, 2018). Thus, if used in a natural setting, the jasmonate pre-treatments applied in Chapter's 2 and 3 may not only provide long-lasting protection through defences which directly antagonise the attacker (e.g. PR proteins, glucosinolates), but also via the enhanced release of volatiles that recruit natural enemies. In support of this, a previous study, using an

analogous setup to the one used in Chapter 3, demonstrated that MeJA treatment enhances the release of terpene volatiles, including oxygenated monoterpenes, from above ground Norway spruce seedling tissue for at least 7 days (Martin et al., 2003). Numerous previous studies have provided evidence that natural enemies of the bark beetle *Ips typographus*, a devasting pest of Norway spruce, are attracted by a blend of beetle pheromones and/or host tree monoterpenes (Hansen, 1983; Pettersson, 2001; Pettersson and Boland, 2003; Hulcr et al., 2005; Hulcr et al., 2006). Thus, while *I. typographus* may not attack spruce seedlings, this suggests indirect defences could indeed play a role in the protection of spruce by MeJA treatment. However, constitutive emission of airborne signals recruiting natural enemies may not be a sustainable strategy and result in a "crying wolf" scenario, where the parasitoids and predatory insects learn to ignore the cue, which would alleviate the effectiveness of the tritrophic interaction. Thus, it would be interesting to explore whether treatment with jasmonates induces constitutive emission of volatiles over several weeks, or whether it primes the plants for augmented volatile emissions after subsequent herbivore challenge.

In Chapter 2, we provided evidence from dual-choice assays that JA pre-treatment reduced plants attractiveness to *Spodoptera littoralis* larvae (Figure 2.11B). This could result from altered volatile emissions by JA pre-treated plants, as *S. littoralis* larvae are attracted and repelled by specific plant volatile organic compounds (Rharrabe et al., 2014). However, to assess this, volatile organic compounds which differ substantially in their emission between 5-week-old plants from water and JA treated seedlings, need to be identified. Mutant plants deficient in the release of these volatiles can be tested for expression of long-term JA-IR associated reduced attractiveness to larvae (Figure 2.11B). Furthermore, the ability of the identified volatiles to repel *S. littoralis* larvae can also be evaluated. Nevertheless, it is plausible that the JA pre-treated plants may release increased amounts of volatiles which recruit the herbivore and it is following subsequent feeding that *S. littoralis* larvae are repelled. Notably, this attract then repel strategy was observed in a recent study which used mature Norway spruce trees (Mageroy et al., 2020a). Trees pre-treated with MeJA attracted higher numbers of *I. typographus* bark beetles yet received far less herbivory damage than the water controls. Work is ongoing to understand the exact mechanisms behind this phenomenon.

There is mounting evidence that treatment of above ground tissues with jasmonate can also influence the recruitment of beneficial organisms in the soil. For example, foliar treatment of maize (*Zea mays*) plants with MeJA makes them more attractive to the entomopathogenic nematode *Heterorhabditis amazonensis*, a natural enemy of the root damaging cucurbit beetle (*Diabrotica speciosa*) larvae (Filgueiras et al., 2016). Furthermore, jasmonate can also influence a plants rhizosphere microbiome (Carvalhais et al., 2017). The rhizosphere is defined as the narrow region of root-surrounding soil, which is influenced by root exudation chemicals and associated microorganisms. There is mounting evidence for the so-called belowground 'cry-for-help' hypothesis, where plants under attack by pests and diseases change the composition of their rhizosphere microbiome, resulting in the presence, or enhanced presence, of microbes that are capable of protecting their hosts against pests and diseases (Figure 4.1) (Rolfe et al., 2019). Foliar treatment of Arabidopsis with MeJA results in a shift in the rhizosphere microbiome composition (Carvalhais et al., 2013). Furthermore, the jasmonate signalling mutant *myc2* has an altered root exudation profile and rhizosphere microbiome (Carvalhais et al., 2015). However, as yet, there are no clear examples pulling everything together and demonstrating that jasmonate treatment enhances the release of specific exudates that recruit specific microbial species which can promote resistance to future attacks by pests and/or pathogens. Nevertheless, particularly when grown in natural soils, it is plausible that the belowground microbiome could also contribute to the jasmonate-IR phenotype. Additional support for this conclusion comes from a recent study which demonstrated that in Arabidopsis and tomato (*Solanum lycopersicum*), DNA methylation regulates the production of a root exudate which recruits a plant growth promoting rhizobacterium (Vílchez et al., 2020; Wilkinson and Ton, 2020). It is well known that plant growth–promoting rhizobacteria can elicit induced systemic resistance (ISR) in plants (Pieterse et al., 2014). Furthermore, Chapter 2 demonstrated that JA treatment causes long-lasting changes in DNA methylation and that DNA methylation machinery is required for long-lasting JA-IR. Future studies should explore whether jasmonates induce long-term changes in root exudation, which can then be linked to changes in DNA methylation. In turn, it should be assessed whether the observed change in root exudation chemistry actually recruits and/or selects for a rhizosphere microbiome that provides long-lasting protection against pests and pathogens.

4.4. Implications for Agriculture and Forestry

The rapidly changing climate coupled with a growing and increasingly interconnected global population, will inevitably force us to change the way we use and manage our land and the crops that grow upon it. For instance, a diversification of species used to provide food and timber is a necessity. A warming climate coupled with inter country movement of goods and people will likely result in shifts in the distribution of pests and pathogens. A reliance on a minimal number of species for food and timber makes our food and forestry systems very vulnerable to collapse following an outbreak of a novel pest or disease. A diversification of tree species being used in commercial forestry is also important to ensure the success of large areas of new productive forest which are to be created across the globe. Following the increased public interest in the “climate crisis”, governments are now keen to plant millions of trees and create numerous new forests to mitigate the impacts of, and counteract, climate change.

When selecting new crop species, it is vital that the management tools of the future are also considered. Agriculture and commercial forestry are reliant on chemical pesticides for management of pests and diseases. However, as a result of the regulation of pesticide use becoming more stringent, the evolution of pesticide resistance and changes in public opinion, this reliance on a single strategy is going to have to change. It is widely believed that an integrated pest management approach will be required to ensure that there are resilient agricultural and forestry systems moving forward. This approach will require a multitude of different pest and disease management strategies, many of which may build on the plants innate ability to fend off pests and pathogens. In order for this to be a success, it is essential that appropriate varieties and species of plant are selected for the diversification of agriculture and forestry. For instance, if we are to maximise the use of resistance-inducing chemicals, we should select varieties and species of plant which are genetically predisposed to be able to maintain their defences as primed over timeframes which are useful for agriculture or forestry. Enhancing our understanding of the (epi)genetic mechanisms behind long-term IR, as done in this thesis, is therefore of great importance and can even lead to new innovative breeding opportunities that target the epigenome, rather than the genome, which would allow crop breeders to tap into heritable diversity that is not limited by species boundaries. Indeed, it is known

that hypomethylation of selected pericentromeric regions in the model plant Arabidopsis can yield a substantial increase in SA-dependent quantitative disease resistance, which mimics the effects of priming agents for this type of defence (Furci et al., 2019). It is also paramount that the costs and benefits of IR associated with a species over a range of timescales are considered. Chapter 2 provided clear support for this conclusion. In Arabidopsis, JA induced short-term enhanced resistance to both the chewing herbivore *S. littoralis* and the necrotrophic pathogen *P. cucumerina*. Whereas, in the long-term it induced enhanced resistance to the herbivore but enhanced susceptibility to the pathogen. Notably, as discussed above, this long-term resistance trade-off may not exist in spruce. Thus, jasmonate treatment could be utilised by nurseries and forest managers to protect spruce seedlings that will go onto establish the new woodlands which are being demanded. Field trials using MeJA to protect conifer seedlings against the large pine weevil (*Hylobius abietis*), a chewing herbivore, have already had some success (Zas et al., 2014).

While BREXIT has many downsides and is not very popular among the scientific community, it does provide the UK with an excellent opportunity to revolutionise its farming and forestry systems. This revolution should involve the implementation of the ideas discussed in the previous paragraphs, including the wider use of alternative pest and disease management strategies. Induced resistance is one such strategy and therefore the future success of human society is heavily dependent upon acquired immunity.

References

Abbott E, Hall D, Hamberger B, Bohlmann J (2010) Laser microdissection of conifer stem tissues: isolation and analysis of high quality RNA, terpene synthase enzyme activity and terpenoid metabolites from resin ducts and cambial zone tissue of white spruce (*Picea glauca*). BMC Plant Biol **10**: 106

Abe H, Urao T, Ito T, Seki M, Shinozaki K (2003) Arabidopsis AtMYC2 (bHLH) and AtMYB2 (MYB) function as transcriptional activators in abscisic acid signaling. Plant Cell **15**: 63–78

Abe H, Yamaguchi-Shinozaki K, Urao T, Iwasaki T, Hosokawa D, Shinozaki K (1997) Role of Arabidopsis MYC and MYB homologs in drought- and abscisic acid-regulated gene expression. Plant Cell **9**: 1859–1868

Ade J, DeYoung BJ, Golstein C, Innes RW (2007) Indirect activation of a plant nucleotide binding site-leucine-rich repeat protein by a bacterial protease. Proc Natl Acad Sci U S A **104**: 2531–2536

Agrawal AA, Laforsch C, Tollrian R (1999) Transgenerational induction of defences in animals and plants. Nature **401**: 60–63

Ahmad S, Gordon-Weeks R, Pickett J, Ton J (2010) Natural variation in priming of basal resistance: from evolutionary origin to agricultural exploitation. Mol Plant Pathol **11**: 817–827

Ahmad S, Van Hulten M, Martin J, Pieterse CMJ, Van Wees SCM, Ton J (2011) Genetic dissection of basal defence responsiveness in accessions of *Arabidopsis thaliana*. Plant Cell Environ **34**: 1191–1206

Akalin A, Franke V, Vlahoviček K, Mason CE, Schübeler D (2015) genomation: a toolkit to summarize, annotate and visualize genomic intervals. Bioinformatics **31**: 1127–1129

Aleman F, Yaza J, Lee M, Takahashi Y, Kim AY, Li Z, Kinoshita T, Ecker JR, Schroeder JI (2016) An ABA-increased interaction of the PYL6 ABA receptor with MYC2 transcription factor: a putative link of ABA and JA signaling. Sci Rep **6**: 28941

Ali S, Ganai BA, Kamili AN, Bhat AA, Mir ZA, Bhat JA, Tyagi A, Islam ST,

Mushtaq M, Yadav P, et al (2018) Pathogenesis-related proteins and peptides as promising tools for engineering plants with multiple stress tolerance. Microbiol Res **212**–**213**: 29–37

Alonso JM, Hirayama T, Roman G, Nourizadeh S, Ecker JR (1999) EIN2, a bifunctional transducer of ethylene and stress responses in *Arabidopsis.* Science 284:

Alonso JM, Stepanova AN, Solano R, Wisman E, Ferrari S, Ausubel FM, Ecker JR (2003) Five components of the ethylene-response pathway identified in a screen for weak *ethylene-insensitive* mutants in *Arabidopsis*. Proc Natl Acad Sci U S A **100**: 2992–2997

Altschul SF, Gish W, Miller W, Myers EW, Lipman DJ (1990) Basic local alignment search tool. J Mol Biol **215**: 403–410

Altschul SF, Madden TL, Schäffer AA, Zhang J, Zhang Z, Miller W, Lipman DJ (1997) Gapped BLAST and PSI-BLAST: a new generation of protein database search programs. Nucleic Acids Res **25**: 3389–3402

An F, Zhao Q, Ji Y, Li W, Jiang Z, Yu X, Zhang C, Han Y, He W, Liu Y, et al (2010) Ethylene-induced stabilization of ETHYLENE INSENSITIVE3 and EIN3-LIKE1 is mediated by proteasomal degradation of EIN3 binding F-box 1 and 2 that requires EIN2 in *Arabidopsis*. Plant Cell **22**: 2384–23401

Anders S, Huber W (2010) Differential expression analysis for sequence count data. Genome Biol **11**: R106

Anders S, Pyl PT, Huber W (2015) HTSeq-a Python framework to work with high-throughput sequencing data. Bioinformatics **31**: 166–169

Anderson JP, Badruzsaufari E, Schenk PM, Manners JM, Desmond OJ, Ehlert C, Maclean DJ, Ebert PR, Kazan K (2004) Antagonistic interaction between abscisic acid and jasmonate-ethylene signaling pathways modulates defense gene expression and disease resistance in Arabidopsis. Plant Cell **16**: 3460–3479

Anderson JP, Gleason CA, Foley RC, Thrall PH, Burdon JB, Singh KB (2010) Plants versus pathogens: an evolutionary arms race. Funct Plant Biol **37**: 499–

512

Andrews SR (2010) FastQC: a quality control tool for high throughput sequence data. Available online: http://www.bioinformatics.babraham.ac.uk/projects/fastqc/

Arnerup J, Nemesio-Gorriz M, Lundén K, Asiegbu FO, Stenlid J, Elfstrand M (2013) The primary module in Norway spruce defence signalling against *H. annosum* s.l. seems to be jasmonate-mediated signalling without antagonism of salicylate-mediated signalling. Planta **237**: 1037–1045

Aslam MZ, Lin X, Li X, Yang N, Chen L (2020) Molecular cloning and functional characterization of *CpMYC2* and *CpBHLH13* transcription factors from Wintersweet (*Chimonanthus praecox* L.). Plants **9**: 785

Atighi MR, Verstraeten B, De Meyer T, Kyndt T (2020) Genome-wide DNA hypomethylation shapes nematode pattern-triggered immunity in plants. New Phytol **227**: 545–558

Audenaert K, De Meyer GB, Höfte MM (2002) Abscisic acid determines basal susceptibility of tomato to *Botrytis cinerea* and suppresses salicylic acid-dependent signaling mechanisms. Plant Physiol **128**: 491–501

Ausin I, Feng S, Yu C, Liu W, Kuo HY, Jacobsen EL, Zhai J, Gallego-Bartolome J, Wang L, Egertsdotter U, et al (2016) DNA methylome of the 20-gigabase Norway spruce genome. Proc Natl Acad Sci **113**: E8106–E8113

Axtell MJ, Staskawicz BJ (2003) Initiation of *RPS2*-specified disease resistance in *Arabidopsis* is coupled to the AvrRpt2-directed elimination of RIN4. Cell **112**: 369–377

Baldwin IT (2010) Plant volatiles. Curr Biol **20**: R392–R397

Bari R, Jones JDG (2009) Role of plant hormones in plant defence responses. Plant Mol Biol **69**: 473–488

Bartee L, Malagnac F, Bender J (2001) *Arabidopsis cmt3* chromomethylase mutations block non-CG methylation and silencing of an endogenous gene. Genes Dev **15**: 1753–1758

Barth C, Jander G (2006) Arabidopsis myrosinases TGG1 and TGG2 have redundant function in glucosinolate breakdown and insect defense. Plant J **46**: 549–562

Baum S, Reimer-Michalski EM, Bolger A, Mantai AJ, Benes V, Usadel B, Conrath U (2019) Isolation of open chromatin identifies regulators of systemic acquired resistance. Plant Physiol **181**: 817–833

Baum S, Reimer-Michalski EM, Jaskiewicz MR, Conrath U (2020) Formaldehyde-assisted isolation of regulatory DNA elements from *Arabidopsis* leaves. Nat Protoc **15**: 713–733

Beckers GJM, Jaskiewicz M, Liu Y, Underwood WR, He SY, Zhang S, Conrath U (2009) Mitogen-activated protein kinases 3 and 6 are required for full priming of stress responses in *Arabidopsis thaliana*. Plant Cell **21**: 944–953

Bednarek P, Piślewska-Bednarek M, Svatoš A, Schneider B, Doubský J, Mansurova M, Humphry M, Consonni C, Panstruga R, Sanchez-Vallet A, et al (2009) A glucosinolate metabolism pathway in living plant cells mediates broad-spectrum antifungal defense. Science **323**: 101–106

Beekweelder J, van Leeuwen W, van Dam NM, Bertossi M, Grandi V, Mizzi L, Soloviev M, Szabados L, Molthoff JW, Schipper B, et al (2008) The impact of the absence of aliphatic glucosinolates on insect herbivory in Arabidopsis. PLoS One **3**: e2068

Bekaert M, Edger PP, Hudson CM, Pires JC, Conant GC (2012) Metabolic and evolutionary costs of herbivory defense: systems biology of glucosinolate synthesis. New Phytol **196**: 596–605

Bender J (2004) DNA methylation and epigenetics. Annu Rev Plant Biol **55**: 41–68

Benevenuto RF, Seldal T, Hegland SJ, Rodriguez-Saona C, Kawash J, Polashock J (2019) Transcriptional profiling of methyl jasmonate-induced defense responses in bilberry (*Vaccinium myrtillus* L.). BMC Plant Biol **19**: 70

Benjamini Y, Hochberg Y (1995) Controlling the false discovery rate: a practical and powerful approach to multiple testing. J R Stat Soc Ser B **57**: 289–300

Berendsen RL, Vismans G, Yu K, Song Y, De Jonge R, Burgman WP, Burmølle

M, Herschend J, Bakker PAHM, Pieterse CMJ (2018) Disease-induced assemblage of a plant-beneficial bacterial consortium. ISME J **12**: 1496–1507

Berglund T, Lindström A, Aghelpasand H, Stattin E, Ohlsson AB (2016) Protection of spruce seedlings against pine weevil attacks by treatment of seeds or seedlings with nicotinamide, nicotinic acid and jasmonic acid. Forestry **89**: 127–135

Berrocal-Lobo M, Molina A, Solano R (2002) Constitutive expression of *ETHYLENE-RESPONSE-FACTOR1* in *Arabidopsis* confers resistance to several necrotrophic fungi. Plant J **29**: 23–32

Berveiller D, Kierzkowski D, Damesin C (2007) Interspecific variability of stem photosynthesis among tree species. Tree Physiol **27**: 53–61

Bewick AJ, Ji L, Niederhuth CE, Willing E-M, Hofmeister BT, Shi X, Wang L, Lu Z, Rohr NA, Hartwig B, et al (2016) On the origin and evolutionary consequences of gene body DNA methylation. Proc Natl Acad Sci U S A **113**: 9111–6

Bewick AJ, Niederhuth CE, Ji L, Rohr NA, Griffin PT, Leebens-Mack J, Schmitz RJ (2017) The evolution of CHROMOMETHYLASES and gene body DNA methylation in plants. Genome Biol **18**: 65

Biedermann PHW, Müller J, Grégoire JC, Gruppe A, Hagge J, Hammerbacher A, Hofstetter RW, Kandasamy D, Kolarik M, Kostovcik M, et al (2019) Bark beetle population dynamics in the anthropocene: challenges and solutions. Trends Ecol Evol **34**: 914–924

Van Der Biezen EA, Jones JDG (1998) Plant disease-resistance proteins and the gene-for-gene concept. Trends Biochem Sci **23**: 454–456

Bigeard J, Colcombet J, Hirt H (2015) Signaling mechanisms in pattern-triggered immunity (PTI). Mol Plant **8**: 521–539

Birch ANE, Wynne Griffiths D, Hopkins RJ, Macfarlane Smith WH, McKinlay RG (1992) Glucosinolate responses of swede, kale, forage and oilseed rape to root damage by turnip root fly (*Delia floralis*) larvae. J Sci Food Agric **60**: 1–9

Birkenbihl RP, Kracher B, Somssich IE (2017) Induced genome-wide binding of

three Arabidopsis WRKY transcription factors during early MAMP-triggered immunity. Plant Cell **29**: 20–38

Boatwright JL, Pajerowska-Mukhtar K (2013) Salicylic acid: an old hormone up to new tricks. Mol Plant Pathol **14**: 623–634

Bodenhausen N, Reymond P (2007) Signaling pathways controlling induced resistance to insect herbivores in *Arabidopsis*. Mol Plant-Microbe Interact MPMI **20**: 1406–1420

Bodnaryk RP (1994) Potent effect of jasmonates on indole glucosinolates in oilseed rape and mustard. Phytochemistry **35**: 301–305

Bolger AM, Lohse M, Usadel B (2014) Trimmomatic: a flexible trimmer for Illumina sequence data. Bioinformatics **30**: 2114–2120

Boter M, Ruíz-Rivero O, Abdeen A, Prat S (2004) Conserved MYC transcription factors play a key role in jasmonate signaling in both in tomato and *Arabidopsis*. Genes Dev **18**: 1577–1591

Boughton AJ, Hoover K, Felton GW (2005) Methyl jasmonate application induces increased densities of glandular trichomes on tomato, *Lycopersicon esculentum*. J Chem Ecol **31**: 2211–2216

Boutrot F, Zipfel C (2017) Function, discovery, and exploitation of plant pattern recognition receptors for broad-spectrum disease resistance. Annu Rev Phytopathol **55**: 257–286

Bowman JL, Kohchi T, Yamato KT, Jenkins J, Shu S, Ishizaki K, Yamaoka S, Nishihama R, Nakamura Y, Berger F, et al (2017) Insights into land plant evolution garnered from the *Marchantia polymorpha* genome. Cell **171**: 287–304

Bozarth RF, Ross AF (1964) Systemic resistance induced by localized virus infections: extent of changes in uninfected plant parts. Virology **24**: 446–455

Bricchi I, Occhipinti A, Bertea CM, Zebelo SA, Brillada C, Verrillo F, De Castro C, Molinaro A, Faulkner C, Maule AJ, et al (2013) Separation of early and late responses to herbivory in Arabidopsis by changing plasmodesmal function. Plant J **73**: 14–25

Broekgaarden C, Caarls L, Vos IA, Pieterse CMJ, Van Wees SCM (2015) Ethylene: traffic controller on hormonal crossroads to defense. Plant Physiol **169**: 2371–2379

Bronstein JL, Alarcón R, Geber M (2006) The evolution of plant-insect mutualisms. New Phytol **172**: 412–428

Brooks DM, Bender CL, Kunkel BN (2005) The *Pseudomonas syringae* phytotoxin coronatine promotes virulence by overcoming salicylic acid-dependent defences in *Arabidopsis thaliana*. Mol Plant Pathol **6**: 629–639

Bruce TJA, Matthes MC, Napier JA, Pickett JA (2007) Stressful “memories” of plants: evidence and possible mechanisms. Plant Sci **173**: 603–608

Bruce TJA, Smart LE, Birch ANE, Blok VC, MacKenzie K, Guerrieri E, Cascone P, Luna E, Ton J (2017) Prospects for plant defence activators and biocontrol in IPM – concepts and lessons learnt so far. Crop Prot **97**: 128–134

Bu Q, Jiang H, Li C-B, Zhai Q, Zhang J, Wu X, Sun J, Xie Q, Li C (2008) Role of the *Arabidopsis thaliana* NAC transcription factors ANAC019 and ANAC055 in regulating jasmonic acid-signaled defense responses. Cell Res **18**: 756–767

Burow M, Halkier BA (2017) How does a plant orchestrate defense in time and space? Using glucosinolates in Arabidopsis as case study. Curr Opin Plant Biol **38**: 142–147

Buswell W, Schwarzenbacher RE, Luna E, Sellwood M, Chen B, Flors V, Pétriacq P, Ton J (2018) Chemical priming of immunity without costs to plant growth. New Phytol **218**: 1205–1216

Caarls L, Pieterse CMJ, Van Wees SCM (2015) How salicylic acid takes transcriptional control over jasmonic acid signaling. Front Plant Sci **6**: 170

Camacho C, Coulouris G, Avagyan V, Ma N, Papadopoulos J, Bealer K, Madden TL (2009) BLAST+: architecture and applications. BMC Bioinformatics **10**: 421

Cambiagno DA, Nota F, Zavallo D, Rius S, Casati P, Asurmendi S, Alvarez ME (2018) Immune receptor genes and pericentromeric transposons as targets of common epigenetic regulatory elements. Plant J **96**: 1178–1190

La Camera S, L'Haridon F, Astier J, Zander M, Abou-Mansour E, Page G, Thurow C, Wendehenne D, Gatz C, Métraux JP, et al (2011) The glutaredoxin ATGRXS13 is required to facilitate *Botrytis cinerea* infection of *Arabidopsis thaliana* plants. Plant J **68**: 507–519

Cameron DD, Neal AL, Van Wees SCM, Ton J (2013) Mycorrhiza-induced resistance: more than the sum of its parts? Trends Plant Sci **18**: 539–545

Campbell SA (2015) Ecological mechanisms for the coevolution of mating systems and defence. New Phytol **205**: 1047–1053

Campos ML, Yoshida Y, Major IT, De Oliveira Ferreira D, Weraduwage SM, Froehlich JE, Johnson BF, Kramer DM, Jander G, Sharkey TD, et al (2016) Rewiring of jasmonate and phytochrome B signalling uncouples plant growth-defense tradeoffs. Nat Commun **7**: 12570

Cao H, Bowling SA, Gordon AS, Xinnian D (1994) Characterization of an *Arabidopsis* mutant that is nonresponsive to inducers of systemic acquired resistance. Plant Cell **6**: 1583–1592

Carlson M (2019) org.At.tair.db: genome wide annotation for Arabidopsis. R package

Carretero-Paulet L, Galstyan A, Roig-Villanova I, Martínez-García JF, Bilbao-Castro JR, Robertson DL (2010) Genome-wide classification and evolutionary analysis of the bHLH family of transcription factors in Arabidopsis, poplar, rice, moss, and algae. Plant Physiol **153**: 1398–1412

Carvalhais LC, Dennis PG, Badri D V., Kidd BN, Vivanco JM, Schenk PM (2015) Linking jasmonic acid signaling, root exudates, and rhizosphere microbiomes. Mol plant-microbe Interact **28**: 1049–1058

Carvalhais LC, Dennis PG, Badri D V., Tyson GW, Vivanco JM, Schenk PM (2013) Activation of the jasmonic acid plant defence pathway alters the composition of rhizosphere bacterial communities. PLoS One **8**: e56457

Carvalhais LC, Schenk PM, Dennis PG (2017) Jasmonic acid signalling and the plant holobiont. Curr Opin Microbiol **37**: 42–47

Caspi R, Billington R, Keseler IM, Kothari A, Krummenacker M, Midford PE,

Ong WK, Paley S, Subhraveti P, Karp PD (2020) The MetaCyc database of metabolic pathways and enzymes - a 2019 update. Nucleic Acids Res **48**: D455–D453

Caudullo G, Tinner W, Rigo D De (2016) *Picea abies* in Europe: distribution, habitat, usage and threats. *In* J San-Miguel-Ayanz, D de Rigo, G Caudullo, T Houston Durrant, A Mauri, eds, Eur. Atlas For. Tree Species. Publication Office of the European Union, Luxembourg, pp 114–116

Celedon JM, Bohlmann J (2019) Oleoresin defenses in conifers: chemical diversity, terpene synthases and limitations of oleoresin defense under climate change. New Phytol **224**: 1444–1463

Celedon JM, Yuen MMS, Chiang A, Henderson H, Reid KE, Bohlmann J (2017) Cell-type- and tissue-specific transcriptomes of the white spruce (*Picea glauca*) bark unmask fine-scale spatial patterns of constitutive and induced conifer defense. Plant J **92**: 710–726

Chang KN, Zhong S, Weirauch MT, Hon G, Pelizzola M, Li H, Carol Huang SS, Schmitz RJ, Urich MA, Kuo D, et al (2013) Temporal transcriptional response to ethylene gas drives growth hormone cross-regulation in *Arabidopsis*. Elife **2**: e00675

Chassot C, Buchala A, Schoonbeek HJ, Métraux JP, Lamotte O (2008) Wounding of Arabidopsis leaves causes a powerful but transient protection against *Botrytis* infection. Plant J **55**: 555–567

Chávez Montes RA, De Fátima Rosas-Cárdenas F, De Paoli E, Accerbi M, Rymarquis LA, Mahalingam G, Marsch-Martínez N, Meyers BC, Green PJ, De Folter S (2014) Sample sequencing of vascular plants demonstrates widespread conservation and divergence of microRNAs. Nat Commun **5**: 3722

Chen F, Hu Y, Vannozzi A, Wu K, Cai H, Qin Y, Mullis A, Lin Z, Zhang L (2017) The WRKY transcription factor family in model plants and crops. CRC Crit Rev Plant Sci **36**: 311–335

Chen H, Xue L, Chintamanani S, Germain H, Lin H, Cui H, Cai R, Zuo J, Tang X, Li X, et al (2009) ETHYLENE INSENSITIVE3 and ETHYLENE INSENSITIVE3-

LIKE1 repress *SALICYLIC ACID INDUCTION DEFICIENT2* expression to negatively regulate plant innate immunity in *Arabidopsis*. Plant Cell **21**: 2527–2540

Cheng YT, Germain H, Wiermer M, Bi D, Xu F, Garcia A V., Wirthmueller L, Després C, Parker JE, Zhang Y, et al (2009) Nuclear pore complex component MOS7/Nup88 is required for innate immunity and nuclear accumulation of defense regulators in *Arabidopsis*. Plant Cell **21**: 2503–2516

Cheng Z, Sun L, Qi T, Zhang B, Peng W, Liu Y, Xie D (2011) The bHLH transcription factor MYC3 interacts with the jasmonate ZIM-domain proteins to mediate jasmonate response in *Arabidopsis*. Mol Plant **4**: 279–288

Chini A, Fonseca S, Fernández G, Adie B, Chico JM, Lorenzo O, García-Casado G, López-Vidriero I, Lozano FM, Ponce MR, et al (2007) The JAZ family of repressors is the missing link in jasmonate signalling. Nature **448**: 666–671

Chini A, Gimenez-Ibanez S, Goossens A, Solano R (2016) Redundancy and specificity in jasmonate signalling. Curr Opin Plant Biol **33**: 147–156

Chini A, Monte I, Zamarreño AM, Hamberg M, Lassueur S, Reymond P, Weiss S, Stintzi A, Schaller A, Porzel A, et al (2018) An OPR3-independent pathway uses 4,5-didehydrojasmonate for jasmonate synthesis. Nat Chem Biol **14**: 171–178

Chodavarapu RK, Feng S, Bernatavichute Y V., Chen PY, Stroud H, Yu Y, Hetzel JA, Kuo F, Kim J, Cokus SJ, et al (2010) Relationship between nucleosome positioning and DNA methylation. Nature **466**: 388–392

Christman JK (2002) 5-Azacytidine and 5-aza-2′-deoxycytidine as inhibitors of DNA methylation: mechanistic studies and their implications for cancer therapy. Oncogene **21**: 5483–5495

Cipollini D, Enright S, Traw MB, Bergelson J (2004) Salicylic acid inhibits jasmonic acid-induced resistance of *Arabidopsis thaliana* to *Spodoptera exigua*. Mol Ecol **13**: 1643–1653

Clavijo McCormick A, Irmisch S, Reinecke A, Boeckler GA, Veit D, Reichelt M, Hansson BS, Gershenzon J, Köllner TG, Unsicker SB (2014) Herbivore-

induced volatile emission in black poplar: regulation and role in attracting herbivore enemies. Plant Cell Environ **37**: 1909–1923

Cohen Y, Vaknin M, Mauch-Mani B (2016) BABA-induced resistance: milestones along a 55-year journey. Phytoparasitica **44**: 513–538

Cokus SJ, Feng S, Zhang X, Chen Z, Merriman B, Haudenschild CD, Pradhan S, Nelson SF, Pellegrini M, Jacobsen SE (2008) Shotgun bisulphite sequencing of the *Arabidopsis* genome reveals DNA methylation patterning. Nature **452**: 215–219

Conrath U (2011) Molecular aspects of defence priming. Trends Plant Sci **16**: 524–531

Conrath U, Beckers GJM, Flors V, Garcia-Agustin P, Jakab G, Mauch F, Newman M-A, Pieterse CMJ, Poinssot B, Pozo MJ, et al (2006) Priming: getting ready for battle. Mol Pant-Microbe Interact **19**: 1062–1071

Conrath U, Beckers GJM, Langenbach CJG, Jaskiewicz MR (2015) Priming for enhanced defense. Annu Rev Phytopathol **53**: 97–119

Cook DE, Mesarich CH, Thomma BPHJ (2015) Understanding plant immunity as a surveillance system to detect invasion. Annu Rev Phytopathol **53**: 541–563

Couto D, Zipfel C (2016) Regulation of pattern recognition receptor signalling in plants. Nat Rev Immunol **16**: 537–552

Cuerda-Gil D, Slotkin RK (2016) Non-canonical RNA-directed DNA methylation. Nat Plants **2**: 16163

Cui H, Tsuda K, Parker JE (2015) Effector-triggered tmmunity: from pathogen perception to robust defense. Annu Rev Plant Biol **66**: 487–511

Cui J, Bahrami AK, Pringle EG, Hernandez-Guzman G, Bender CL, Pierce NE, Ausubel FM (2005) *Pseudomonas syringae* manipulates systemic plant defenses against pathogens and herbivores. Proc Natl Acad Sci U S A **102**: 1791–1796

Czechowski T, Stitt M, Altmann T, Udvardi MK, Scheible W-R (2005) Genome-wide identification and testing of superior reference genes for transcript

normalization in Arabidopsis. Plant Physiol **139**: 5–17

Van Dam NM, Witjes L, Svatoš A (2004) Interactions between aboveground and belowground induction of glucosinolates in two wild *Brassica* species. New Phytol **161**: 801–810

Davis JM, Wu H, Cooke JEK, Reed JM, Luce KS, Michler CH (2002) Pathogen challenge, salicylic acid, and jasmonic acid regulate expression of chitinase gene homologs in pine. Mol Plant-Microbe Interact **15**: 380–387

Deal RB, Henikoff S (2011) Histone variants and modifications in plant gene regulation. Curr Opin Plant Biol **14**: 116–122

Delaney TP, Friedrich L, Ryals JA (1995) *Arabidopsis* signal transduction mutant defective in chemically and biologically induced disease resistance. Proc Natl Acad Sci U S A **92**: 6602–6606

Dempsey DA, Vlot AC, Wildermuth MC, Klessig DF (2011) Salicylic acid biosynthesis and metabolism. Arab B **9**: e0156

Deng Y, Lu S (2017) Biosynthesis and regulation of phenylpropanoids in plants. CRC Crit Rev Plant Sci **36**: 257–290

DeRose RJ, Bekker MF, Long JN (2017) Traumatic resin ducts as indicators of bark beetle outbreaks. Can J For Res **47**: 1168–1174

Després C, Delong C, Glaze S, Liu E, Fobert PR (2000) The Arabidopsis NPR1/NIM1 protein enhances the DNA binding activity of a subgroup of the TGA family of bZIP transcription factors. Plant Cell **12**: 279–290

Devoto A, Nieto-Rostro M, Xie D, Ellis C, Harmston R, Patrick E, Davis J, Sherratt L, Coleman M, Turner JG (2002) COI1 links jasmonate signalling and fertility to the SCF ubiquitin-ligase complex in *Arabidopsis*. Plant J **32**: 457–466

Dicke M, Gols R, Ludeking D, Posthumus MA (1999) Jasmonic acid and herbivory differentially induce carnivore-attracting plant volatiles in lima bean plants. J Chem Ecol **25**: 1907–1922

Dicke M, Sabelis MW (1988) How plants obtain predatory mites as bodyguards. Netherlands J Zool **38**: 148–165

Ding P, Ding Y (2020) Stories of salicylic acid: a plant defense hormone. Trends Plant Sci **25**: 549–565

Ding Y, Sun T, Ao K, Peng Y, Zhang Y, Li X, Zhang Y (2018) Opposite roles of salicylic acid receptors NPR1 and NPR3/NPR4 in transcriptional regulation of plant immunity. Cell **173**: 1454–1467

Dobin A, Davis CA, Schlesinger F, Drenkow J, Zaleski C, Jha S, Batut P, Chaisson M, Gingeras TR (2013) STAR: ultrafast universal RNA-seq aligner. Bioinformatics **29**: 15–21

Van der Does D, Leon-Reyes A, Koornneef A, Van Verk MC, Rodenburg N, Pauwels L, Goossens A, Körbes AP, Memelink J, Ritsema T, et al (2013) Salicylic acid suppresses jasmonic acid signaling downstream of SCF^{COI1}-JAZ by targeting GCC promoter motifs via transcription factor ORA59. Plant Cell **25**: 744–761

Dombrecht B, Ping Xue G, Sprague SJ, Kirkegaard JA, Ross JJ, Reid JB, Fitt GP, Sewelam N, Schenk PM, Manners JM, et al (2007) MYC2 differentially modulates diverse jasmonate-dependent functions in *Arabidopsis*. Plant Cell **19**: 2225–2245

Douma JC, Vermeulen PJ, Poelman EH, Dicke M, Anten NPR (2017) When does it pay off to prime for defense? A modeling analysis. New Phytol **216**: 782–797

Dowen RH, Pelizzola M, Schmitz RJ, Lister R, Dowen JM, Nery JR, Dixon JE, Ecker JR (2012) Widespread dynamic DNA methylation in response to biotic stress. Proc Natl Acad Sci U S A **109**: E2183–E2191

Du J, Johnson LM, Groth M, Feng S, Hale CJ, Li S, Vashisht AA, Gallego-Bartolome J, Wohlschlegel JA, Patel DJ, et al (2014a) Mechanism of DNA methylation-directed histone methylation by KRYPTONITE. Mol Cell **55**: 495–504

Du J, Zhong X, Bernatavichute Y V, Stroud H, Feng S, Caro E, Vashisht AA, Terragni J, Chin HG, Tu A, et al (2012) Dual binding of chromomethylase domains to H3K9me2-containing nucleosomes directs DNA methylation in plants. Cell **151**: 167–180

Du M, Zhai Q, Deng L, Li S, Li H, Yan L, Huang Z, Wang B, Jiang H, Huang T, et al (2014b) Closely related NAC transcription factors of tomato differentially regulate stomatal closure and reopening during pathogen attack. Plant Cell **26**: 3167–3184

Du M, Zhao J, Tzeng DTW, Liu Y, Deng L, Yang T, Zhai Q, Wu F, Huang Z, Zhou M, et al (2017) MYC2 orchestrates a hierarchical transcriptional cascade that regulates jasmonate-mediated plant immunity in tomato. Plant Cell **29**: 1883–1906

Dubois M, Van den Broeck L, Inzé D (2018) The pivotal role of ethylene in plant growth. Trends Plant Sci **23**: 311–323

Eddy SR, Wheeler TJ (2015) HMMER: biosequence analysis using profile hidden Markov models. http://hmmer.org/

El-Gebali S, Mistry J, Bateman A, Eddy SR, Luciani A, Potter SC, Qureshi M, Richardson LJ, Salazar GA, Smart A, et al (2019) The Pfam protein families database in 2019. Nucleic Acids Res **47**: D427–D432

Van Der Ent S, Van Hulten M, Pozo MJ, Czechowski T, Udvardi MK, Pieterse CMJ, Ton J (2009) Priming of plant innate immunity by rhizobacteria and β-aminobutyric acid: differences and similarities in regulation. New Phytol **183**: 419–431

Erb M, Reymond P (2019) Molecular interactions between plants and insect herbivores. Annu Rev Plant Biol **70**: 527–557

Erbilgin N, Krokene P, Christiansen E, Zeneli G, Gershenzon J (2006) Exogenous application of methyl jasmonate elicits defenses in Norway spruce (*Picea abies*) and reduces host colonization by the bark beetle *Ips typographus*. Oecologia **148**: 426–436

Ewels P, Magnusson M, Lundin S, Käller M (2016) MultiQC: summarize analysis results for multiple tools and samples in a single report. Bioinformatics **32**: 3047–3048

Eyles A, Bonello P, Ganley R, Mohammed C (2010) Induced resistance to pests and pathogens in trees. New Phytol **185**: 893–908

Faccoli M, Schlyter F (2007) Conifer phenolic resistance markers are bark beetle antifeedant semiochemicals. Agric For Entomol **9**: 237–245

Fan J, Crooks C, Lamb C (2008) High-throughput quantitative luminescence assay of the growth in planta of *Pseudomonas syringae* chromosomally tagged with *Photorhabdus luminescens luxCDABE*. Plant J **53**: 393–399

Fan W, Dong X (2002) In vivo interaction between NPR1 and transcription factor TGA2 leads to salicylic acid–mediated gene activation in Arabidopsis. Plant Cell **14**: 1377–1389

Farmer EE (2007) Plant biology: jasmonate perception machines. Nature **448**: 659–660

Fedderwitz F, Nordlander G, Ninkovic V, Björklund N (2016) Effects of jasmonate-induced resistance in conifer plants on the feeding behaviour of a bark-chewing insect, *Hylobius abietis*. J Pest Sci (2004) **89**: 97–105

Feng H, Conneely KN, Wu H (2014a) A Bayesian hierarchical model to detect differentially methylated loci from single nucleotide resolution sequencing data. Nucleic Acids Res **42**: e69–e69

Feng S, Cokus SJ, Schubert V, Zhai J, Pellegrini M, Jacobsen SE (2014b) Genome-wide Hi-C analyses in wild-type and mutants reveal high-resolution chromatin interactions in *Arabidopsis*. Mol Cell **55**: 694–707

Fernández-Calvo P, Chini A, Fernández-Barbero G, Chico J-M, Gimenez-Ibanez S, Geerinck J, Eeckhout D, Schweizer F, Godoy M, Franco-Zorrilla JM, et al (2011) The *Arabidopsis* bHLH transcription factors MYC3 and MYC4 are targets of JAZ repressors and act additively with MYC2 in the activation of jasmonate responses. Plant Cell **23**: 701–715

Feys BJF, Benedetti CE, Penfold CN, Turner JG (1994) *Arabidopsis* mutants selected for resistance to the phytotoxin coronatine are male sterile, insensitive to methyl jasmonate, and resistant to a bacterial pathogen. Plant Cell **6**: 751–759

Filgueiras CC, Willett DS, Pereira RV, Moino Junior A, Pareja M, Duncan LW (2016) Eliciting maize defense pathways aboveground attracts belowground

biocontrol agents. Sci Rep **6**: 36484

Foissner I, Wendehenne D, Langebartels C, Durner J (2000) In vivo imaging of elicitor-induced nitric oxide burst in tobacco. Plant J **23**: 817–824

Fonseca S, Chini A, Hamberg M, Adie B, Porzel A, Kramell R, Miersch O, Wasternack C, Solano R (2009) (+)-7-*iso*-Jasmonoyl-L-isoleucine is the endogenous bioactive jasmonate. Nat Chem Biol **5**: 344–350

Franceschi VR, Krekling T, Berryman AA, Christiansen E (1998) Specialized phloem parenchyma cells in Norway spruce (Pinaceae) bark are an important site of defense reactions. Am J Bot **85**: 601–615

Franceschi VR, Krekling T, Christiansen E (2002) Application of methyl jasmonate on *Picea abies* (Pinaceae) stems induces defense-related responses in phloem and xylem. Am J Bot **89**: 578–586

Franceschi VR, Krokene P, Christiansen E, Krekling T (2005) Anatomical and chemical defenses of conifer bark against bark beetles and other pests. New Phytol **167**: 353–376

Franceschi VR, Krokene P, Krekling T, Christiansen E (2000) Phloem parenchyma cells are involved in local and distant defense responses to fungal inoculation or bark-beetle attack in Norway spruce (Pinaceae). Am J Bot **87**: 314–326

Frerigmann H (2016) Glucosinolate regulation in a complex relationship – MYC and MYB – no one can act without each other. Adv Bot Res **80**: 57–97

Frerigmann H, Berger B, Gigolashvili T (2014) bHLH05 is an interaction partner of MYB51 and a novel regulator of glucosinolate biosynthesis in Arabidopsis. Plant Physiol **166**: 349–369

Frerigmann H, Gigolashvili T (2014) MYB34, MYB51, and MYB122 distinctly regulate indolic glucosinolate biosynthesis in *Arabidopsis thaliana*. Mol Plant **7**: 814–828

Frerigmann H, Piślewska-Bednarek M, Sánchez-Vallet A, Molina A, Glawischnig E, Gigolashvili T, Bednarek P (2016) Regulation of pathogen-triggered tryptophan metabolism in *Arabidopsis thaliana* by MYB transcription

factors and indole glucosinolate conversion products. Mol Plant **9**: 682–695

Fritz VA, Justen VL, Bode AM, Schuster T, Wang M (2010) Glucosinolate enhancement in cabbage induced by jasmonic acid application. HortScience **45**: 1188–1191

Fu ZQ, Dong X (2013) Systemic acquired resistance: turning local infection into global defense. Annu Rev Plant Biol **64**: 839–863

Fu ZQ, Yan S, Saleh A, Wang W, Ruble J, Oka N, Mohan R, Spoel SH, Tada Y, Zheng N, et al (2012) NPR3 and NPR4 are receptors for the immune signal salicylic acid in plants. Nature **486**: 228–232

Furci L, Jain R, Stassen J, Berkowitz O, Whelan J, Roquis D, Baillet V, Colot V, Johannes F, Ton J (2019) Identification and characterisation of hypomethylated DNA loci controlling quantitative resistance in *Arabidopsis*. Elife **8**: e40655

Furniss MM, Solheim H, Christiansen E (1990) Transmission of blue-stain fungi by *Ips typographus* (Coleoptera: Scolytidae) in Norway spruce. Ann Entomol Soc Am **83**: 712–716

Gagne JM, Smalle J, Gingerich DJ, Walker JM, Yoo SD, Yanagisawa S, Vierstra RD (2004) *Arabidopsis* EIN3-binding F-box 1 and 2 form ubiquitin-protein ligases that repress ethylene action and promote growth by directing EIN3 degradation. Proc Natl Acad Sci U S A **101**: 6803–6808

Galili T (2015) dendextend: An R package for visualizing, adjusting and comparing trees of hierarchical clustering. Bioinformatics **31**: 3718–3720

Gallego-Bartolomé J, Gardiner J, Liu W, Papikian A, Ghoshal B, Kuo HY, Zhao JMC, Segal DJ, Jacobsen SE (2018) Targeted DNA demethylation of the *Arabidopsis* genome using the human TET1 catalytic domain. Proc Natl Acad Sci U S A **115**: E2125–E2134

Gamir J, Darwiche R, van't Hof P, Choudhary V, Stumpe M, Schneiter R, Mauch F (2017) The sterol-binding activity of PATHOGENESIS-RELATED PROTEIN 1 reveals the mode of action of an antimicrobial protein. Plant J **89**: 502–509

Gao QM, Venugopal S, Navarre D, Kachroo A (2011) Low oleic acid-derived repression of jasmonic acid-inducible defense responses requires the WRKY50

and WRKY51 proteins. Plant Physiol **155**: 464–476

Gaujoux R, Seoighe C (2010) A flexible R package for nonnegative matrix factorization. BMC Bioinformatics **11**: 367

Germain H, Lachance D, Pelletier G, Fossdal CG, Solheim H, Séguin A (2012) The expression pattern of the *Picea glauca Defensin 1* promoter is maintained in *Arabidopsis thaliana*, indicating the conservation of signalling pathways between angiosperms and gymnosperms. J Exp Bot **63**: 785–795

Gershenzon J (1994) Metabolic costs of terpenoid accumulation in higher plants. J Chem Ecol **20**: 1281–1328

Gfeller A, Dubugnon L, Liechti R, Farmer EE (2010) Jasmonate biochemical pathway. Sci Signal **3**: cm3

Gigolashvili T, Berger B, Mock HP, Müller C, Weisshaar B, Flügge UI (2007) The transcription factor HIG1/MYB51 regulates indolic glucosinolate biosynthesis in *Arabidopsis thaliana*. Plant J **50**: 886–901

Gimenez-Ibanez S, Boter M, Ortigosa A, García-Casado G, Chini A, Lewsey MG, Ecker JR, Ntoukakis V, Solano R (2017) JAZ2 controls stomata dynamics during bacterial invasion. New Phytol **213**: 1378–1392

Glauser G, Dubugnon L, Mousavi SAR, Rudaz S, Wolfender J-L, Farmer EE (2009) Velocity estimates for signal propagation leading to systemic jasmonic acid accumulation in wounded *Arabidopsis*. J Biol Chem **284**: 34506–34513

Glazebrook J (2005) Contrasting mechanisms of defense against biotrophic and necrotrophic pathogens. Annu Rev Phytopathol **43**: 205–227

Gleason C, Leelarasamee N, Meldau D, Feussner I (2016) OPDA has key role in regulating plant susceptibility to the root-knot nematode *Meloidogyne hapla* in *Arabidopsis*. Front Plant Sci **7**: 1565

Gong Z, Morales-Ruiz T, Ariza R, Roldan-Arjona T, David L, Zhu J-K (2002) *ROS1*, a repressor of transcriptional gene silencing in *Arabidopsis*, encodes a DNA glycosylase/lyase. Cell **111**: 803–814

Goossens J, Fernández-Calvo P, Schweizer F, Goossens A (2016) Jasmonates:

signal transduction components and their roles in environmental stress responses. Plant Mol Biol **91**: 673–689

Gravino M, Savatin DV, MacOne A, De Lorenzo G (2015) Ethylene production in *Botrytis cinerea*- and oligogalacturonide-induced immunity requires calcium-dependent protein kinases. Plant J **84**: 1073–1086

Guan L, Denkert N, Eisa A, Lehmann M, Sjuts I, Weiberg A, Soll J, Meinecke M, Schwenkert S (2019) JASSY, a chloroplast outer membrane protein required for jasmonate biosynthesis. Proc Natl Acad Sci U S A **116**: 10568–10575

Guan R, Su J, Meng X, Li S, Liu Y, Xu J, Zhang S (2015) Multilayered regulation of ethylene induction plays a positive role in Arabidopsis resistance against *Pseudomonas syringae*. Plant Physiol **169**: 299–312

Guo H, Ecker JR (2003) Plant responses to ethylene gas are mediated by $SCF^{EBF1/EBF2}$-dependent proteolysis of EIN3 transcription factor. Cell **115**: 667–677

Guo Q, Yoshida Y, Major IT, Wang K, Sugimoto K, Kapali G, Havko NE, Benning C, Howe GA (2018) JAZ repressors of metabolic defense promote growth and reproductive fitness in *Arabidopsis*. Proc Natl Acad Sci **115**: E10768–E10777

Gupta GP, Rani S, Birah A, Raghuraman M (2005) Improved artificial diet for mass rearing of the tobacco caterpillar, *Spodoptera litura* (Lepidoptera: Noctuidae). Int J Trop Insect Sci **25**: 55–58

Halkier BA (2016) General introduction to glucosinolates. *In* S Kopriva, ed, Adv. Bot. Res. Elsevier, Amsterdam, pp 1–14

Hammerbacher A, Kandasamy D, Ullah C, Schmidt A, Wright LP, Gershenzon J (2019) Flavanone-3-hydroxylase plays an important role in the biosynthesis of spruce phenolic defenses against bark beetles and their fungal associates. Front Plant Sci **10**: 208

Hammerbacher A, Paetz C, Wright LP, Fischer TC, Bohlmann J, Davis AJ, Fenning TM, Gershenzon J, Schmidt A (2014) Flavan-3-ols in Norway spruce: biosynthesis, accumulation, and function in response to attack by the bark

beetle-associated fungus *Ceratocystis polonica*. Plant Physiol **164**: 2107–2122

Hammerbacher A, Raguschke B, Wright LP, Gershenzon J (2018) Gallocatechin biosynthesis via a flavonoid 3′,5′-hydroxylase is a defense response in Norway spruce against infection by the bark beetle-associated sap-staining fungus *Endoconidiophora polonica*. Phytochemistry **148**: 78–86

Hammerbacher A, Ralph SG, Bohlmann J, Fenning TM, Gershenzon J, Schmidt A (2011) Biosynthesis of the major tetrahydroxystilbenes in spruce, astringin and isorhapontin, proceeds via resveratrol and is enhanced by fungal infection. Plant Physiol **157**: 876–890

Han L, Li GJ, Yang KY, Mao G, Wang R, Liu Y, Zhang S (2010) Mitogen-activated protein kinase 3 and 6 regulate *Botrytis cinerea*-induced ethylene production in Arabidopsis. Plant J **64**: 114–127

Hansen K (1983) Reception of bark beetle pheromone in the predaceous clerid beetle, *Thanasimus formicarius* (Coleoptera: Cleridae). J Comp Physiol A **150**: 371–378

Heil M (2001) Induced systemic resistance (ISR) against pathogens – a promising field for ecological research. Perspect Plant Ecol Evol Syst **4**: 65–79

Heil M, Land WG (2014) Danger signals - damaged-self recognition across the tree of life. Front Plant Sci **5**: 578

Hewezi T, Lane T, Piya S, Rambani A, Rice JH, Staton M (2017) Cyst nematode parasitism induces dynamic changes in the root epigenome. Plant Physiol **174**: 405–420

Hickman R, Van Verk MC, Van Dijken AJH, Mendes MP, Vroegop-Vos IA, Caarls L, Steenbergen M, Van der Nagel I, Wesselink GJ, Jironkin A, et al (2017) Architecture and dynamics of the jasmonic acid gene regulatory network. Plant Cell **29**: 2086–2105

Hietala AM, Kvaalen H, Schmidt A, Johnk N, Solheim H, Fossdal CG (2004) Temporal and spatial profiles of chitinase expression by Norway spruce in response to bark colonization by *Heterobasidion annosum*. Appl Environ Microbiol **70**: 3948–3953

Hlásny T, Krokene P, Liebhold A, Montagné-Huck C, Müller J, Qin H, Raffa K, Schelhaas M-J, Seidl R, Svoboda M, et al (2019) Living with bark beetles : impacts, outlook and management options. From Sci. to Policy 8. European Forest Institute.

Holeski LM (2007) Within and between generation phenotypic plasticity in trichome density of *Mimulus guttatus*. J Evol Biol **20**: 2092–2100

Hong GJ, Xue XY, Mao YB, Wang LJ, Chen XY (2012) *Arabidopsis* MYC2 interacts with DELLA proteins in regulating sesquiterpene synthase gene expression. Plant Cell **24**: 2635–2648

Hoo SC, Koo AJK, Gao X, Jayanty S, Thines B, Jones AD, Howe GA (2008) Regulation and function of Arabidopsis *JASMONATE ZIM*-domain genes in response to wounding and herbivory. Plant Physiol **146**: 952–964

Hopkins RJ, van Dam NM, van Loon JJ a (2009) Role of glucosinolates in insect-plant relationships and multitrophic interactions. Annu Rev Entomol **54**: 57–83

Houben M, Van de Poel B (2019) 1-aminocyclopropane-1-carboxylic acid oxidase (ACO): The enzyme that makes the plant hormone ethylene. Front Plant Sci **10**: 695

Howe GA, Major IT, Koo AJ (2018) Modularity in jasmonate signaling for multistress resilience. Annu Rev Plant Biol **69**: 387–415

Hu L, Robert CAM, Cadot S, Zhang X, Ye M, Li B, Manzo D, Chervet N, Steinger T, van Der Heijden MGA, et al (2018) Root exudate metabolites drive plant-soil feedbacks on growth and defense by shaping the rhizosphere microbiota. Nat Commun **9**: 2738

Huang J, Liang X, Xuan Y, Geng C, Li Y, Lu H, Qu S, Mei X, Chen H, Yu T, et al (2017) A reference human genome dataset of the BGISEQ-500 sequencer. Gigascience **6**: 1–9

Huang P, Dong Z, Guo P, Zhang X, Qiu Y, Li B, Wang Y, Guo H (2020a) Salicylic acid suppresses apical hook formation via NPR1-mediated repression of EIN3 and EIL1 in Arabidopsis. Plant Cell **32**: 612–629

Huang PY, Catinot J, Zimmerli L (2016) Ethylene response factors in Arabidopsis

immunity. J Exp Bot **67**: 1231–1241

Huang W, Wang Y, Li X, Zhang Y (2020b) Biosynthesis and regulation of salicylic acid and n-hydroxypipecolic acid in plant immunity. Mol Plant **13**: 31–41

Huang Y, Kendall T, Forsythe ES, Dorantes-Acosta A, Li S, Caballero-Pérez J, Chen X, Arteaga-Vázquez M, Beilstein MA, Mosher RA (2015) Ancient origin and recent innovations of RNA polymerase IV and V. Mol Biol Evol **32**: 1788–1799

Hudgins JW, Franceschi VR (2004) Methyl jasmonate-induced ethylene production is responsible for conifer phloem defense responses and reprogramming of stem cambial zone for traumatic resin duct formation. Plant Physiol **135**: 2134–2149

Hulcr J, Pollet M, Ubik K, Vrkoč J (2005) Exploitation of kairomones and synomones by *Medetera* spp. (Diptera: Dolichopodidae), predators of spruce bark beetles. Eur J Entomol **102**: 655–662

Hulcr J, Ubik K, Vrkoc J (2006) The role of semiochemicals in tritrophic interactions between the spruce bark beetle *Ips typographus*, its predators and infested spruce. J Appl Entomol **130**: 275–283

Van Hulten M, Pelser M, Van Loon LC, Pieterse CMJ, Ton J (2006) Costs and benefits of priming for defense in *Arabidopsis*. Proc Natl Acad Sci U S A **103**: 5602–5607

Ibdah M, Chen YT, Wilkerson CG, Pichersky E (2009) An aldehyde oxidase in developing seeds of arabidopsis converts benzaldehyde to benzoic acid. Plant Physiol **150**: 416–423

Innes R (2018) The positives and negatives of NPR: a unifying model for salicylic acid signaling in plants. Cell **173**: 1314–1315

Irieda H, Inoue Y, Mori M, Yamada K, Oshikawa Y, Saitoh H, Uemura A, Terauchi R, Kitakura S, Kosaka A, et al (2019) Conserved fungal effector suppresses PAMP-triggered immunity by targeting plant immune kinases. Proc Natl Acad Sci U S A **116**: 496–505

Ito H, Gaubert H, Bucher E, Mirouze M, Vaillant I, Paszkowski J (2011) An siRNA

pathway prevents transgenerational retrotransposition in plants subjected to stress. Nature **472**: 115–119

Jackson JP, Lindroth AM, Cao X, Jacobsen SE (2002) Control of CpNpG DNA methylation by the KRYPTONITE histone H3 methyltransferase. Nature **416**: 556–560

Jaskiewicz M, Conrath U, Peterhänsel C (2011) Chromatin modification acts as a memory for systemic acquired resistance in the plant stress response. EMBO Rep **12**: 50–55

Jeger M, Bragard C, Caffier D, Candresse T, Chatzivassiliou E, Dehnen-Schmutz K, Gilioli G, Jaques Miret JA, MacLeod A, Navajas Navarro M, et al (2017) Pest categorisation of *Ips typographus*. EFSA J **15**: 4881

Jeschke V, Gershenzon J, Vassão DG (2016) A mode of action of glucosinolate-derived isothiocyanates: detoxification depletes glutathione and cysteine levels with ramifications on protein metabolism in *Spodoptera littoralis*. Insect Biochem Mol Biol **71**: 37–48

Jeworutzki E, Roelfsema MRG, Anschütz U, Krol E, Elzenga JTM, Felix G, Boller T, Hedrich R, Becker D (2010) Early signaling through the Arabidopsis pattern recognition receptors FLS2 and EFR involves Ca^{2+}-associated opening of plasma membrane anion channels. Plant J **62**: 367–378

Johnson LM, Bostick M, Zhang X, Kraft E, Henderson I, Callis J, Jacobsen SE (2007) The SRA methyl-cytosine-binding domain links DNA and histone methylation. Curr Biol **17**: 379–384

Johnson ML, Schenk PM, Cribb BW, Moore C, Perkins LE, Zalucki MP (2011) Is the effect of priming plants, and a functional JAR1, negligible on the foraging behaviour and development of a generalist lepidopteran, *Helicoverpa armigera*? Entomol Exp Appl **141**: 78–87

Jones JDG, Dangl JL (2006) The plant immune system. Nature **444**: 323–329

Jong Y, Eun K, Yoon S, Sung J, Kim SJ, Do Y (2013) Characterization of a methyl jasmonate specific esterase in Arabidopsis. J Korean Soc Appl Biol Chem **56**: 27–33

Joo S, Liu Y, Lueth A, Zhang S (2008) MAPK phosphorylation-induced stabilization of ACS6 protein is mediated by the non-catalytic C-terminal domain, which also contains the *cis*-determinant for rapid degradation by the 26S proteasome pathway. Plant J **54**: 129–140

Ju C, Yoon GM, Shemansky JM, Lin DY, Ying ZI, Chang J, Garrett WM, Kessenbrock M, Groth G, Tucker ML, et al (2012) CTR1 phosphorylates the central regulator EIN2 to control ethylene hormone signaling from the ER membrane to the nucleus in *Arabidopsis*. Proc Natl Acad Sci U S A **109**: 19486–19491

Jung HW, Tschaplinski TJ, Wang L, Glazebrook J, Greenberg JT (2009) Priming in systemic plant immunity. Science **324**: 89–91

Kandasamy D, Gershenzon J, Andersson MN, Hammerbacher A (2019) Volatile organic compounds influence the interaction of the Eurasian spruce bark beetle (*Ips typographus*) with its fungal symbionts. ISME J **13**: 1788–1800

Kankel MW, Ramsey DE, Stokes TL, Flowers SK, Haag JR, Jeddeloh JA, Riddle NC, Verbsky ML, Richards EJ (2003) Arabidopsis *MET1* cytosine methyltransferase mutants. Genetics **163**: 1109–1122

Kathiria P, Sidler C, Golubov A, Kalischuk M, Kawchuk LM, Kovalchuk I (2010) Tobacco mosaic virus infection results in an increase in recombination frequency and resistance to viral, bacterial, and fungal pathogens in the progeny of infected tobacco plants. Plant Physiol **153**: 1859–1870

Katsir L, Schilmiller AL, Staswick PE, Sheng YH, Howe GA (2008) COI1 is a critical component of a receptor for jasmonate and the bacterial virulence factor coronatine. Proc Natl Acad Sci U S A **105**: 7100–7105

Kellenberger RT, Desurmont GA, Schlüter PM, Schiestl FP (2018) Trans-generational inheritance of herbivory-induced phenotypic changes in *Brassica rapa*. Sci Rep **8**: 3536

Kellenberger RT, Schlüter PM, Schiestl FP (2016) Herbivore-induced DNA demethylation changes floral signalling and attractiveness to pollinators in *Brassica rapa*. PLoS One **11**: e0166646

Khan M, Subramaniam R, Desveaux D (2016) Of guards, decoys, baits and traps: Pathogen perception in plants by type III effector sensors. Curr Opin Microbiol **29**: 49–55

Kim J, Kim JH, Richards EJ, Chung KM, Woo HR (2014) *Arabidopsis* VIM proteins regulate epigenetic silencing by modulating DNA methylation and histone modification in cooperation with MET1. Mol Plant **7**: 1470–1485

Kim KC, Lai Z, Fan B, Chen Z (2008) *Arabidopsis* WRKY38 and WRKY62 transcription factors interact with histone deacetylase 19 in basal defense. Plant Cell **20**: 2357–2371

Klessig DF, Choi HW, Dempsey DA (2018) Systemic acquired resistance and salicylic acid: past, present, and future. Mol Plant-Microbe Interact **31**: 871–888

Kliebenstein DJ, Rowe HC (2008) Ecological costs of biotrophic versus necrotrophic pathogen resistance, the hypersensitive response and signal transduction. Plant Sci **174**: 551–556

Kloek AP, Verbsky ML, Sharma SB, Schoelz JE, Vogel J, Klessig DF, Kunkel BN (2001) Resistance to *Pseudomonas syringae* conferred by an *Arabidopsis thaliana* coronatine-insensitive (*coi1*) mutation occurs through two distinct mechanisms. Plant J **26**: 509–522

Kolde R (2019) pheatmap: Pretty Heatmaps. R package

Kong W, Li J, Yu Q, Cang W, Xu R, Wang Y, Ji W (2016) Two novel flavin-containing monooxygenases involved in biosynthesis of aliphatic glucosinolates. Front Plant Sci **7**: 1292

Koo AJK, Gao X, Daniel Jones A, Howe GA (2009) A rapid wound signal activates the systemic synthesis of bioactive jasmonates in Arabidopsis. Plant J **59**: 974–986

Koornneef A, Leon-reyes A, Ritsema T, Verhage A, Otter FC Den, Pieterse MJ (2008) Kinetics of salicylate-mediated suppression of jasmonate signaling reveal a role for redox modulation. Plant Physiol **147**: 1358–1368

Koornneef A, Pieterse CMJ (2008) Cross talk in defense signaling. Plant Physiol **146**: 839–844

Kozlowski G, Buchala A, Metraux J-P (1999) Methyl jasmonate protects Norway spruce [*Picea abies* (L.) Karst.] seedlings against *Pythium ultimum* Trow. Physiol Mol Plant Pathol **55**: 53–58

Krasileva K V., Dahlbeck D, Staskawicz BJ (2010) Activation of an *Arabidopsis* resistance protein is specified by the in planta association of its leucine-rich repeat domain with the cognate oomycete effector. Plant Cell **22**: 2444–2458

Krekling T, Franceschi VR, Krokene P, Solheim H (2004) Differential anatomical response of Norway spruce stem tissues to sterile and fungus infected inoculations. Trees - Struct Funct **18**: 1–9

Krokene P (2015) Conifer defense and resistance to bark beetles. *In* RW Vega. Fernando E.; Hofstetter, ed, Bark Beetles Biol. Ecol. Nativ. invasive Species. Academic Press, United States, pp 177–206

Krokene P, Christiansen E, Solheim H, Franceschi V, Berryman A (1999) Induced resistance to pathogenic fungi in Norway spruce. Plant Physiol **121**: 565–570

Krokene P, Lahr E, Dalen LS, Skrøppa T, Solheim H (2012) Effect of phenology on susceptibility of Norway spruce (*Picea abies*) to fungal pathogens. Plant Pathol **61**: 57–62

Krokene P, Nagy NE, Solheim H (2008) Methyl jasmonate and oxalic acid treatment of Norway spruce: anatomically based defense responses and increased resistance against fungal infection. Tree Physiol **28**: 29–35

Krokene P, Solheim H (1996) Fungal associates of five bark beetle species colonizing Norway spruce. Can J For Res **26**: 2115–2122

Krokene P, Solheim H, Krekling T, Christiansen E (2003) Inducible anatomical defense responses in Norway spruce stems and their possible role in induced resistance. Tree Physiol **23**: 191–197

Krol E, Mentzel T, Chinchilla D, Boller T, Felix G, Kemmerling B, Postel S, Arents M, Jeworutzki E, Al-Rasheid KAS, et al (2010) Perception of the *Arabidopsis* danger signal peptide 1 involves the pattern recognition receptor *At*PEPR1 and its close homologue *At*PEPR2. J Biol Chem **285**: 13471–13479

Krueger F, Andrews SR (2011) Bismark: a flexible aligner and methylation caller for bisulfite-seq applications. Bioinformatics **27**: 1571–1572

Kuc J (1982) Induced immunity to plant disease. Bioscience **32**: 854–860

Kunz BA, Dando PK, Grice DM, Mohr PG, Schenk PM, Cahill DM (2008) UV-induced DNA damage promotes resistance to the biotrophic pathogen *Hyaloperonospora parasitica* in Arabidopsis. Plant Physiol **148**: 1021–1031

Laha D, Johnen P, Azevedo C, Dynowski M, Weiß M, Capolicchio S, Mao H, Iven T, Steenbergen M, Freyer M, et al (2015) VIH2 regulates the synthesis of inositol pyrophosphate $InsP_8$ and jasmonate-dependent defenses in Arabidopsis. Plant Cell **27**: 1082–1097

Lai Z, Vinod K, Zheng Z, Fan B, Chen Z (2008) Roles of *Arabidopsis* WRKY3 and WRKY4 transcription factors in plant responses to pathogens. BMC Plant Biol **8**: 68

Langmead B, Salzberg SL (2012) Fast gapped-read alignment with Bowtie 2. Nat Methods **9**: 357–359

Laurie-berry N, Joardar V, Street IH, Kunkel BN (2006) The *Arabidopsis thaliana JASMONATE INSENSITIVE 1* gene is required for suppression of salicylic acid-dependent defenses during infection by *Pseudomonas syringae*. Mol Plant-Microbe Interact **19**: 789–800

Law JA, Du J, Hale CJ, Feng S, Krajewski K, Palanca AMS, Strahl BD, Patel DJ, Jacobsen SE (2013) Polymerase IV occupancy at RNA-directed DNA methylation sites requires SHH1. Nature **498**: 385–389

Law JA, Jacobsen SE (2010) Establishing, maintaining and modifying DNA methylation patterns in plants and animals. Nat Rev Genet **11**: 204–220

Lawrence M, Huber W, Pagès H, Aboyoun P, Carlson M, Gentleman R, Morgan MT, Carey VJ (2013) Software for computing and annotating genomic ranges. PLoS Comput Biol **9**: e1003118

Le T-N, Schumann U, Smith NA, Tiwari S, Au P, Zhu Q-H, Taylor JM, Kazan K, Llewellyn DJ, Zhang R, et al (2014) DNA demethylases target promoter transposable elements to positively regulate stress responsive genes in

Arabidopsis. Genome Biol **15**: 458

Lee H, Raskin I (1998) Glucosylation of salicylic acid in *Nicotiana tabacum* cv. Xanthi-nc. Phytopathology **88**: 692–697

Lei M, Zhang H, Julian R, Tang K, Xie S, Zhu J (2015) Regulatory link between DNA methylation and active demethylation in *Arabidopsis*. Proc Natl Acad Sci **112**: 3553–3557

Leon-reyes A, Spoel SH, Lange ES De, Abe H, Kobayashi M, Tsuda S, Millenaar FF, Welschen RAM, Ritsema T, Pieterse CMJ (2009) Ethylene modulates the role of NONEXPRESSOR OF PATHOGENESIS-RELATED GENES1 in cross talk between salicylate and jasmonate signaling. Plant Physiol **149**: 1797–1809

León J, Shulaev V, Yalpani N, Lawton MA, Raskin I (1995) Benzoic acid 2-hydroxylase, a soluble oxygenase from tobacco, catalyzes salicylic acid biosynthesis. Proc Natl Acad Sci U S A **92**: 10413–10417

Li B, Meng X, Shan L, He P (2016) Transcriptional regulation of pattern-triggered immunity in plants. Cell Host Microbe **19**: 641–650

Li G, Meng X, Wang R, Mao G, Han L, Liu Y, Zhang S (2012a) Dual-level regulation of ACC synthase activity by MPK3/MPK6 cascade and its downstream WRKY transcription factor during ethylene induction in arabidopsis. PLoS Genet **8**: e1002767

Li H, Handsaker B, Wysoker A, Fennell T, Ruan J, Homer N, Marth G, Abecasis G, Durbin R (2009) The sequence alignment/map format and SAMtools. Bioinformatics **25**: 2078–2079

Li J, Brader G, Palva ET (2004) The WRKY70 transcription factor: a node of convergence for jasmonate-mediated and salicylate-mediated signals in plant defense. Plant Cell **16**: 319–331

Li J, Zhong R, Palva ET (2017a) WRKY70 and its homolog WRKY54 negatively modulate the cell wall-associated defenses to necrotrophic pathogens in Arabidopsis. PLoS One **12**: e0183731

Li M, Ma X, Chiang YH, Yadeta KA, Ding P, Dong L, Zhao Y, Li X, Yu Y, Zhang L, et al (2014a) Proline isomerization of the immune receptor-interacting protein

RIN4 by a cyclophilin inhibits effector-triggered immunity in *Arabidopsis*. Cell Host Microbe **16**: 473–483

Li Q, Eigenbrode SD, Stringam GR, Thiagarajah MR (2000) Feeding and growth of *Plutella xylostella* and *Spodoptera eridania* on *Brassica juncea* with varying glucosinolate concentrations and myrosinase activities. J Chem Ecol **26**: 2401–2419

Li Q, Zheng J, Li S, Huang G, Skilling SJ, Wang L, Li L, Li M, Yuan L, Liu P (2017b) Transporter-mediated nuclear entry of jasmonoyl-isoleucine is essential for jasmonate signaling. Mol Plant **10**: 695–708

Li R, Weldegergis BT, Li J, Jung C, Qu J, Sun Y, Qian H, Tee C, Van Loon JJA, Dicke M, et al (2014b) Virulence factors of geminivirus interact with MYC2 to subvert plant resistance and promote vector performance. Plant Cell **26**: 4991–5008

Li S, Han X, Yang L, Deng X, Wu H, Zhang M, Liu Y, Zhang S, Xu J (2018) Mitogen-activated protein kinases and calcium-dependent protein kinases are involved in wounding-induced ethylene biosynthesis in *Arabidopsis thaliana*. Plant Cell Environ **41**: 134–147

Li S, Wang H, Li F, Chen Z, Li X, Zhu L, Wang G, Yu J, Huang D, Lang Z (2015a) The maize transcription factor *EREB58* mediates the jasmonate-induced production of sesquiterpene volatiles. Plant J **84**: 296–308

Li S, Zhou X, Chen L, Huang W, Yu D (2010) Functional characterization of *Arabidopsis thaliana* WRKY39 in heat stress. Mol Cells **29**: 475–483

Li SH, Nagy NE, Hammerbacher A, Krokene P, Niu XM, Gershenzon J, Schneider B (2012b) Localization of phenolics in phloem parenchyma cells of Norway spruce (*Picea abies*). ChemBioChem **13**: 2707–2713

Li W, Ma M, Feng Y, Li H, Wang Y, Ma Y, Li M, An F, Guo H (2015b) EIN2-Directed translational regulation of ethylene signaling in *Arabidopsis*. Cell **163**: 670–683

Lian T fei, Xu Y ping, Li L fen, Su XD (2017) Crystal structure of tetrameric *Arabidopsis* MYC2 reveals the mechanism of enhanced interaction with DNA.

Cell Rep **19**: 1334–1342

Liao Y, Smyth GK, Shi W (2014) FeatureCounts: an efficient general purpose program for assigning sequence reads to genomic features. Bioinformatics **30**: 923–930

Liao Y, Smyth GK, Shi W (2019) The R package Rsubread is easier, faster, cheaper and better for alignment and quantification of RNA sequencing reads. Nucleic Acids Res **47**: e47–e47

Lieutier F, Yart A, Salle A (2009) Stimulation of tree defenses by Ophiostomatoid fungi can explain attack success of bark beetles on conifers. Ann For Sci **66**: 801–801

Lin Z, Zhong S, Grierson D (2009) Recent advances in ethylene research. J Exp Bot **60**: 3311–3336

Lindroth AM, Cao X, Jackson JP, Zilberman D, McCallum CM, Henikoff S, Jacobsen SE (2001) Requirement of *CHROMOMETHYLASE3* for maintenance of CpXpG methylation. Science **292**: 2077–2080

Linnakoski R, Mahilainen S, Harrington A, Vanhanen H, Eriksson M, Mehtatalo L, Pappinen A, Wingfield MJ (2016) Seasonal succession of fungi associated with *Ips typographus* beetles and their phoretic mites in an outbreak region of Finland. PLoS One **11**: e0155622

Lippert DN, Ralph SG, Phillips M, White R, Smith D, Hardie D, Gershenzon J, Ritland K, Borchers CH, Bohlmann J (2009) Quantitative iTRAQ proteome and comparative transcriptome analysis of elicitor-induced Norway spruce (*Picea abies*) cells reveals elements of calcium signaling in the early conifer defense response. Proteomics **9**: 350–367

Liu C, Xin Y, Xu L, Cai Z, Xue Y, Liu Y, Xie D, Liu Y, Qi Y (2018) *Arabidopsis* ARGONAUTE 1 binds chromatin to promote gene transcription in response to hormones and stresses. Dev Cell **44**: 348–361

Liu H, Stone SL (2010) Abscisic acid increases *Arabidopsis* ABI5 transcription factor levels by promoting KEG E3 ligase self-ubiquitination and proteasomal degradation. Plant Cell **22**: 2630–2641

Liu J, Osbourn A, Ma P (2015) MYB transcription factors as regulators of phenylpropanoid metabolism in plants. Mol Plant **8**: 689–708

Liu JJ, Williams H, Li XR, Schoettle AW, Sniezko RA, Murray M, Zamany A, Roke G, Chen H (2017) Profiling methyl jasmonate-responsive transcriptome for understanding induced systemic resistance in whitebark pine (*Pinus albicaulis*). Plant Mol Biol **95**: 359–374

Liu Y, Ahn JE, Datta S, Salzman RA, Moon J, Huyghues-Despointes B, Pittendrigh B, Murdock LL, Koiwa H, Zhu-Salzman K (2005) Arabidopsis vegetative storage protein is an anti-insect acid phosphatase. Plant Physiol **139**: 1545–1556

Liu Y, Zhang S (2004) Phosphorylation of 1-Aminocyclopropane-1-Carboxylic Acid Synthase by MPK6, a stress-responsive Mitogen-Activated Protein Kinase , induces ethylene biosynthesis in Arabidopsis. Plant Cell **16**: 3386–3399

Van Loon LC, Rep M, Pieterse CMJ (2006) Significance of inducible defense-related proteins in infected plants. Annu Rev Phytopathol **44**: 135–162

López A, Ramírez V, García-Andrade J, Flors V, Vera P (2011) The RNA silencing enzyme RNA polymerase V is required for plant immunity. PLoS Genet **7**: e1002434

López Sánchez A, Pardo DP, Furci L, Roberts M, Ton J (2021) Costs and benefits of transgenerational acquired resistance in Arabidopsis. Front Plant Sci **12**: 644999

López Sánchez A, Stassen JHM, Furci L, Smith LM, Ton J (2016) The role of DNA (de)methylation in immune responsiveness of Arabidopsis. Plant J **88**: 361–374

Lorang J, Kidarsa T, Bradford CS, Gilbert B, Curtis M, Tzeng S-C, Maier CS, Wolpert TJ (2012) Tricking the guard: exploiting plant defense for disease susceptibility. Science **338**: 659–662

Lorang JM, Sweat TA, Wolpert TJ (2007) Plant disease susceptibility conferred by a “resistance” gene. Proc Natl Acad Sci U S A **104**: 14861–14866

Lorenzo O, Chico JM, Sánchez-Serrano JJ, Solano R (2004) *JASMONATE-*

INSENSITIVE1 encodes a MYC transcription factor essential to discriminate between different jasmonate-regulated defense responses in Arabidopsis. Plant Cell **16**: 1938–1950

Lorenzo O, Piqueras R, Sánchez-Serrano JJ, Solano R (2003) ETHYLENE RESPONSE FACTOR1 integrates signals from ethylene and jasmonate pathways in plant defense. Plant Cell **15**: 165–178

Lou YG, Du MH, Turlings TCJ, Cheng JA, Shan WF (2005) Exogenous application of jasmonic acid induces volatile emissions in rice and enhances parasitism of *Nilaparvata lugens* eggs by the parasitoid *Anagrus nilaparvatae*. J Chem Ecol **31**: 1985–2002

Love MI, Huber W, Anders S (2014) Moderated estimation of fold change and dispersion for RNA-seq data with DESeq2. Genome Biol **15**: 550

van der Luit a H, Piatti T, van Doorn a, Musgrave a, Felix G, Boller T, Munnik T (2000) Elicitation of suspension-cultured tomato cells triggers the formation of phosphatidic acid and diacylglycerol pyrophosphate. Plant Physiol **123**: 1507–1516

Luna E, Beardon EG, Ravnskov S, Scholes JD, Ton J (2016) Optimizing chemically induced resistance in tomato against *Botrytis cinerea*. Plant Dis **100**: 704–710

Luna E, Bruce TJA, Roberts MR, Flors V, Ton J (2012) Next-generation systemic acquired resistance. Plant Physiol **158**: 844–853

Luna E, Hulten M Van, Zhang Y, Berkowitz O, López A, Pétriacq P, Sellwood MA, Chen B, Burrell M, Meene A Van De, et al (2014a) Plant perception of β-aminobutyric acid is mediated by an aspartyl-tRNA synthetase. Nat Chem Biol **10**: 450–456

Luna E, López A, Kooiman J, Ton J (2014b) Role of NPR1 and KYP in long-lasting induced resistance by β-aminobutyric acid. Front Plant Sci **5**: 184

Luna E, Ton J (2012) The epigenetic machinery controlling transgenerational systemic acquired resistance. Plant Signal Behav **7**: 615–618

Luo X, Chen Z, Gao J, Gong Z (2014) Abscisic acid inhibits root growth in

Arabidopsis through ethylene biosynthesis. Plant J **79**: 44–55

Maag D, Köhler A, Robert CAM, Frey M, Wolfender J-L, Turlings TCJ, Glauser G, Erb M (2016) Highly localized and persistent induction of *Bx1*-dependent herbivore resistance factors in maize. Plant J **88**: 976–991

Mageroy MH, Christiansen E, Långström B, Borg-Karlson AK, Solheim H, Björklund N, Zhao T, Schmidt A, Fossdal CG, Krokene P (2020a) Priming of inducible defenses protects Norway spruce against tree-killing bark beetles. Plant Cell Environ **43**: 420–430

Mageroy MH, Wilkinson SW, Tengs T, Cross H, Almvik M, Pétriacq P, Vivian-Smith A, Zhao T, Fossdal CG, Krokene P (2020b) Molecular underpinnings of methyl jasmonate-induced resistance in Norway spruce. Plant Cell Environ **43**: 1827–1843

Mair P, Wilcox R (2020) Robust statistical methods in R using the WRS2 package. Behav Res Methods **52**: 464–488

Major IT, Yoshida Y, Campos ML, Kapali G, Xin XF, Sugimoto K, de Oliveira Ferreira D, He SY, Howe GA (2017) Regulation of growth–defense balance by the JASMONATE ZIM-DOMAIN (JAZ)-MYC transcriptional module. New Phytol **215**: 1533–1547

Malinovsky FG, Fangel JU, Willats WGT (2014) The role of the cell wall in plant immunity. Front Plant Sci **5**: 178

Mao G, Meng X, Liu Y, Zheng Z, Chen Z, Zhang S (2011) Phosphorylation of a WRKY transcription factor by two pathogen-responsive MAPKs drives phytoalexin biosynthesis in *Arabidopsis*. Plant Cell **23**: 1639–1653

Martin D, Tholl D, Gershenzon J, Bohlmann J (2002) Methyl jasmonate induces traumatic resin ducts, terpenoid resin biosynthesis, and terpenoid accumulation in developing xylem of norway spruce stems. Plant Physiol **129**: 1003–1018

Martin DM, Gershenzon J, Bohlmann J (2003) Induction of volatile terpene biosynthesis and diurnal emission by methyl jasmonate in foliage of Norway spruce. Plant Physiol **132**: 1586–1599

Martin FM, Uroz S, Barker DG (2017) Ancestral alliances: plant mutualistic

symbioses with fungi and bacteria. Science **356**: eaad4501

Martinez-Medina A, Flors V, Heil M, Mauch-Mani B, Pieterse CMJ, Pozo MJ, Ton J, van Dam NM, Conrath U (2016) Recognizing plant defense priming. Trends Plant Sci **21**: 818–822

de Matos Simoes R, Emmert-Streib F (2016) bc3net: gene regulatory network inference with Bc3net. R package

Matzke M a, Kanno T, Matzke AJM (2015) RNA-directed DNA methylation: the evolution of a complex epigenetic pathway in flowering plants. Annu Rev Plant Biol **66**: 243–267

Matzke MA, Mosher RA (2014) RNA-directed DNA methylation: an epigenetic pathway of increasing complexity. Nat Rev Genet **15**: 394–408

Mauch-Mani B, Baccelli I, Luna E, Flors V (2017) Defense priming: an adaptive part of induced resistance. Annu Rev Plant Biol **68**: 485–512

McConn M, Creelman R a, Bell E, Mullet JE, Browse J (1997) Jasmonate is essential for insect defense in *Arabidopsis*. Proc Natl Acad Sci U S A **94**: 5473–5477

McCue AD, Nuthikattu S, Reeder SH, Slotkin RK (2012) Gene expression and stress response mediated by the epigenetic regulation of a transposable element small RNA. PLoS Genet **8**: e1002474

McCue AD, Panda K, Nuthikattu S, Choudury SG, Thomas EN, Slotkin RK (2015) ARGONAUTE 6 bridges transposable element mRNA-derived siRNAs to the establishment of DNA methylation. EMBO J **34**: 20–35

McGrath KC, Dombrecht B, Manners JM, Schenk PM, Edgar CI, Maclean DJ, Scheible WR, Udvardi MK, Kazan K (2005) Repressor- and activator-type ethylene response factors functioning in jasmonate signaling and disease resistance identified via a genome-wide screen of Arabidopsis transcription factor gene expression. Plant Physiol **139**: 949–959

Meesters C, Mönig T, Oeljeklaus J, Krahn D, Westfall CS, Hause B, Jez JM, Kaiser M, Kombrink E (2014) A chemical inhibitor of jasmonate signaling targets JAR1 in *Arabidopsis thaliana*. Nat Chem Biol **10**: 830–836

Melotto M, Mecey C, Niu Y, Chung HS, Katsir L, Yao J, Zeng W, Thines B, Staswick P, Browse J, et al (2008a) A critical role of two positively charged amino acids in the Jas motif of Arabidopsis JAZ proteins in mediating coronatine- and jasmonoyl isoleucine-dependent interactions with the COI1 F-box protein. Plant J **55**: 979–988

Melotto M, Underwood W, He SY (2008b) Role of stomata in plant innate immunity and foliar bacterial diseases. Annu Rev Phytopathol **46**: 101–122

Melotto M, Underwood W, Koczan J, Nomura K, He SY (2006) Plant stomata function in innate immunity against bacterial invasion. Cell **126**: 969–980

Melotto M, Zhang L, Oblessuc PR, He SY (2017) Stomatal defense a decade later. Plant Physiol **174**: 561–571

Men L, Yan S, Liu G (2013) De novo characterization of *Larix gmelinii* (Rupr.) Rupr. transcriptome and analysis of its gene expression induced by jasmonates. BMC Genomics **14**: 548

Merchante C, Brumos J, Yun J, Hu Q, Spencer KR, Enríquez P, Binder BM, Heber S, Stepanova AN, Alonso JM (2015) Gene-specific translation regulation mediated by the hormone-signaling molecule EIN2. Cell **163**: 684–697

Mewis I, Appel HM, Hom A, Raina R, Schultz JC (2005) Major signaling pathways modulate arabidopsis glucosinolate accumulation and response to both phloem-feeding and chewing insects. Plant Physiol **138**: 1149–1162

Mine A (2019) Multifaceted involvement of abscisic acid in plant interactions with pathogenic and mutualistic microbes. Adv Bot Res **92**: 219–253

Mine A, Berens ML, Nobori T, Anver S, Fukumoto K, Winkelmüller TM, Takeda A, Becker D, Tsuda K (2017) Pathogen exploitation of an abscisic acid- and jasmonate-inducible MAPK phosphatase and its interception by *Arabidopsis* immunity. Proc Natl Acad Sci **114**: 7456–7461

Mishra P, Asaari MSM, Herrero-Langreo A, Lohumi S, Diezma B, Scheunders P (2017) Close range hyperspectral imaging of plants: a review. Biosyst Eng **164**: 49–67

Mithöfer A, Boland W (2012) Plant defense against herbivores: chemical aspects. Annu Rev Plant Biol **63**: 431–450

Monte I, Franco-Zorrilla JM, García-Casado G, Zamarreño AM, García-Mina JM, Nishihama R, Kohchi T, Solano R (2019) A Single JAZ repressor controls the jasmonate pathway in *Marchantia polymorpha*. Mol Plant **12**: 185–198

Monte I, Hamberg M, Chini A, Gimenez-Ibanez S, García-Casado G, Porzel A, Pazos F, Boter M, Solano R (2014) Rational design of a ligand-based antagonist of jasmonate perception. Nat Chem Biol **10**: 671–676

Monte I, Ishida S, Zamarreño AM, Hamberg M, Franco-Zorrilla JM, García-Casado G, Gouhier-Darimont C, Reymond P, Takahashi K, García-Mina JM, et al (2018) Ligand-receptor co-evolution shaped the jasmonate pathway in land plants. Nat Chem Biol **14**: 480–488

Morel J, Dangl JL (1999) Suppressors of the Arabidopsis *lsd5* cell death mutation identify genes involved in regulating disease resistance responses. Genetics **151**: 305–319

Morris JL, Puttick MN, Clark JW, Edwards D, Kenrick P, Pressel S, Wellman CH, Yang Z, Schneider H, Donoghue PCJ (2018) The timescale of early land plant evolution. Proc Natl Acad Sci U S A **115**: E2274–E2283

Mosblech A, Thurow C, Gatz C, Feussner I, Heilmann I (2011) Jasmonic acid perception by COI1 involves inositol polyphosphates in *Arabidopsis thaliana*. Plant J **65**: 949–957

Mou Z, Fan W, Dong X (2003) Inducers of plant systemic acquired resistance regulate NPR1 function through redox changes. Cell **113**: 935–944

Mrazova A, Sam K (2018) Application of methyl jasmonate to grey willow (*Salix cinerea*) attracts insectivorous birds in nature. Arthropod Plant Interact **12**: 1–8

Müller R, de Vos M, Sun JY, Sønderby IE, Halkier BA, Wittstock U, Jander G (2010) Differential effects of indole and aliphatic glucosinolates on lepidopteran herbivores. J Chem Ecol **36**: 905–913

Mumm R, Dicke M (2010) Variation in natural plant products and the attraction of bodyguards involved in indirect plant defense. Can J Zool **88**: 628–667

Murmu J, Wilton M, Allard G, Pandeya R, Desveaux D, Singh J, Subramaniam R (2014) *Arabidopsis* GOLDEN2-LIKE (GLK) transcription factors activate jasmonic acid (JA)-dependent disease susceptibility to the biotrophic pathogen *Hyaloperonospora arabidopsidis*, as well as JA-independent plant immunity against the necrotrophic pathogen *Botrytis cinerea*. Mol Plant Pathol **15**: 174–184

Musser RO, Hum-Musser SM, Eichenseer H, Peiffer M, Ervin G, Murphy JB, Felton GW (2002) Caterpillar saliva beats plant defences. Nature **416**: 599–600

Nagy NE, Franceschi VR, Solheim H, Krekling T, Christiansen E (2000) Wound-induced traumatic resin duct development in stems of Norway spruce (Pinaceae): anatomy and cytochemical traits. Am J Bot **87**: 302–313

Nakamura M, Köhler C, Hennig L (2019) Tissue-specific transposon-associated small RNAs in the gymnosperm tree, Norway spruce. BMC Genomics **20**: 997

Nakano RT, Piślewska-Bednarek M, Yamada K, Edger PP, Miyahara M, Kondo M, Böttcher C, Mori M, Nishimura M, Schulze-Lefert P, et al (2017) PYK10 myrosinase reveals a functional coordination between endoplasmic reticulum bodies and glucosinolates in *Arabidopsis thaliana*. Plant J **89**: 204–220

Nawrath C, Métraux J (1999) Salicylic acid induction – deficient mutants of Arabidopsis express *PR-2* and *PR-5* and accumulate high levels of camalexin after pathogen inoculation. Plant Cell **11**: 1393–1404

Neilson EH, Goodger JQD, Woodrow IE, Møller BL (2013) Plant chemical defense: at what cost? Trends Plant Sci **18**: 250–258

Nguyen CT, Martinoia E, Farmer EE (2017) Emerging jasmonate transporters. Mol Plant **10**: 659–661

Niederhuth CE, Bewick AJ, Ji L, Alabady MS, Kim K Do, Li Q, Rohr NA, Rambani A, Burke JM, Udall JA, et al (2016) Widespread natural variation of DNA methylation within angiosperms. Genome Biol **17**: 194

Niederhuth CE, Schmitz RJ (2014) Covering your bases: inheritance of DNA methylation in plant genomes. Mol Plant **7**: 472–480

Niu Y, Figueroa P, Browse J (2011) Characterization of JAZ-interacting bHLH

transcription factors that regulate jasmonate responses in *Arabidopsis*. J Exp Bot **62**: 2143–2154

Nühse TS, Bottrill AR, Jones AME, Peck SC (2007) Quantitative phosphoproteomic analysis of plasma membrane proteins reveals regulatory mechanisms of plant innate immune responses. Plant J **51**: 931–940

Nuthikattu S, McCue AD, Panda K, Fultz D, DeFraia C, Thomas EN, Slotkin RK (2013) The initiation of epigenetic silencing of active transposable elements is triggered by RDR6 and 21-22 nucleotide small interfering RNAs. Plant Physiol **162**: 116–131

Nystedt B, Street NR, Wetterbom A, Zuccolo A, Lin Y-C, Scofield DG, Vezzi F, Delhomme N, Giacomello S, Alexeyenko A, et al (2013) The Norway spruce genome sequence and conifer genome evolution. Nature **497**: 579–584

O'Malley RC, Huang S shan C, Song L, Lewsey MG, Bartlett A, Nery JR, Galli M, Gallavotti A, Ecker JR (2016) Cistrome and epicistrome features shape the regulatory DNA landscape. Cell **165**: 1280–1292

El Oirdi M, El Rahman TA, Rigano L, El Hadrami A, Rodriguez MC, Daayf F, Vojnov A, Bouarab K (2011) *Botrytis cinerea* manipulates the antagonistic effects between immune pathways to promote disease development in tomato. Plant Cell **23**: 2405–2421

Van Oosten MJ, Bressan RA, Zhu J-K, Bohnert HJ, Chinnusamy V (2014) The role of the epigenome in gene expression control and the epimark changes in response to the environment. Crit Rev Plant Sci **33**: 64–87

Ossowski S, Schneeberger K, Lucas-Lledó JI, Warthmann N, Clark RM, Shaw RG, Weigel D, Lynch M (2010) The rate and molecular spectrum of spontaneous mutations in *Arabidopsis thaliana*. Science **327**: 92–94

Panda K, Ji L, Neumann DA, Daron J, Schmitz RJ, Slotkin RK (2016) Full-length autonomous transposable elements are preferentially targeted by expression-dependent forms of RNA-directed DNA methylation. Genome Biol **17**: 170

Panda K, McCue AD, Slotkin RK (2020) *Arabidopsis* RNA Polymerase IV generates 21–22 nucleotide small RNAs that can participate in RNA-directed

DNA methylation and may regulate genes. Philos Trans R Soc B Biol Sci **375**: 20190417

Panda K, Slotkin RK (2020) Long-read cDNA sequencing enables a “Gene-Like” transcript annotation of transposable elements. Plant Cell **32**: 2687–2698

Pandey SP, Roccaro M, Schön M, Logemann E, Somssich IE (2010) Transcriptional reprogramming regulated by WRKY18 and WRKY40 facilitates powdery mildew infection of Arabidopsis. Plant J **64**: 912–923

Pastor V, Balmer A, Gamir J, Flors V, Mauch-Mani B (2014) Preparing to fight back: generation and storage of priming compounds. Front Plant Sci **5**: 295

Pastor V, Luna E, Mauch-mani B, Ton J, Flors V (2013) Primed plants do not forget. Environ Exp Bot **94**: 46–56

Patkar RN, Benke PI, Qu Z, Chen YYC, Yang F, Swarup S, Naqvi NI (2015) A fungal monooxygenase-derived jasmonate attenuates host innate immunity. Nat Chem Biol **11**: 733–740

Pauwels L, Barbero GF, Geerinck J, Tilleman S, Grunewald W, Pérez AC, Chico JM, Bossche R Vanden, Sewell J, Gil E, et al (2010) NINJA connects the co-repressor TOPLESS to jasmonate signalling. Nature **464**: 788–791

Pauwels L, Goossens A (2011) The JAZ proteins: a crucial interface in the jasmonate signaling cascade. Plant Cell **23**: 3089–3100

Pauwels L, Ritter A, Goossens J, Durand AN, Liu H, Gu Y, Geerinck J, Boter M, Vanden Bossche R, De Clercq R, et al (2015) The RING E3 ligase KEEP ON GOING modulates JASMONATE ZIM-DOMAIN12 stability. Plant Physiol **169**: 1405–1417

Pavet V, Quintero C, Cecchini NM, Rosa AL, Alvarez ME (2006) *Arabidopsis* displays centromeric DNA hypomethylation and cytological alterations of heterochromatin upon attack by *Pseudomonas syringae*. Mol Plant-Microbe Interact **19**: 577–587

Pel MJC, Pieterse CMJ (2013) Microbial recognition and evasion of host immunity. J Exp Bot **64**: 1237–1248

Peng Y, Sun T, Zhang Y (2017) Perception of salicylic acid in *Physcomitrella patens*. Front Plant Sci **8**: 2145

Penninckx I a, Eggermont K, Terras FR, Thomma BP, De Samblanx GW, Buchala A, Métraux JP, Manners JM, Broekaert WF (1996) Pathogen-induced systemic activation of a plant defensin gene in Arabidopsis follows a salicylic acid-independent pathway. Plant Cell **8**: 2309–2323

Penninckx IAMA, Thomma BPHJ, Buchala A, Métraux J-P, Broekaert WF (1998) Concomitant activation of jasmonate and ethylene response pathways is required for induction of a plant defensin gene in Arabidopsis. Plant Cell **10**: 2103–2113

Penterman J, Zilberman D, Huh JH, Ballinger T, Henikoff S, Fischer RL (2007) DNA demethylation in the *Arabidopsis* genome. Proc Natl Acad Sci U S A **104**: 6752–6757

Peñuelas M, Monte I, Schweizer F, Vallat A, Reymond P, García-Casado G, Franco-Zorrilla JM, Solano R (2019) Jasmonate-related MYC transcription factors are functionally conserved in *Marchantia polymorpha*. Plant Cell **31**: 2491–2509

Pervieux I, Bourassa M, Laurans F, Hamelin R, Séguin A (2004) A spruce defensin showing strong antifungal activity and increased transcript accumulation after wounding and jasmonate treatments. Physiol Mol Plant Pathol **64**: 331–341

Pétriacq P, Stassen J, Ton J (2016) Spore density determines infection strategy by the plant-pathogenic fungus *Plectosphaerella cucumerina*. Plant Physiol **170**: 2325–2339

Pettersson EM (2001) Volatile attractants for three Pteromalid parasitoids attacking concealed spruce bark beetles. Chemoecology **11**: 89–95

Pettersson EM, Boland W (2003) Potential parasitoid attractants, volatile composition throughout a bark beetle attack. Chemoecology **13**: 27–37

Pfalz M, Mukhaimar M, Perreau F, Kirk J, Hansen CIC, Olsen CE, Agerbirk N, Kroymann J (2016) Methyl transfer in glucosinolate biosynthesis mediated by

indole glucosinolate O-methyltransferase 5. Plant Physiol **172**: 2190–2203

Pfalz M, Vogel H, Kroymann J (2009) The gene controlling the *Indole Glucosinolate Modifier1* quantitative trait locus alters indole glucosinolate structures and aphid resistance in *Arabidopsis*. Plant Cell **21**: 985–999

Pfanz H (2008) Bark photosynthesis. Trees - Struct Funct **22**: 137–138

Piasecka A, Jedrzejczak-Rey N, Bednarek P (2015) Secondary metabolites in plant innate immunity: conserved function of divergent chemicals. New Phytol **206**: 948–964

Pieterse CMJ, Van der Does D, Zamioudis C, Leon-Reyes A, Van Wees SCM (2012) Hormonal modulation of plant immunity. Annu Rev Cell Dev Biol **28**: 489–521

Pieterse CMJ, Leon-Reyes A, Van der Ent S, Van Wees SCM (2009) Networking by small-molecule hormones in plant immunity. Nat Chem Biol **5**: 308–316

Pieterse CMJ, Van Pelt JA, Ton J, Parchmann S, Mueller MJ, Buchala AJ, Métraux JP, Van Loon LC (2000) Rhizobacteria-mediated induced systemic resistance (ISR) in *Arabidopsis* requires sensitivity to jasmonate and ethylene but is not accompanied by an increase in their production. Physiol Mol Plant Pathol **57**: 123–134

Pieterse CMJ, Zamioudis C, Berendsen RL, Weller DM, Van Wees SCM, Bakker PAHM (2014) Induced systemic resistance by beneficial microbes. Annu Rev Phytopathol **52**: 347–375

Pikaard CS, Mittelsten Scheid O (2014) Epigenetic regulation in plants. Cold Spring Harb Perspect Biol **6**: a019315

Pontier D, Yahubyan G, Vega D, Bulski A, Saez-Vasquez J, Hakimi MA, Lerbs-Mache S, Colot V, Lagrange T (2005) Reinforcement of silencing at transposons and highly repeated sequences requires the concerted action of two distinct RNA polymerases IV in *Arabidopsis*. Genes Dev **19**: 2030–2040

Potuschak T, Lechner E, Parmentier Y, Yanagisawa S, Grava S, Koncz C, Genschik P (2003) EIN3-dependent regulation of plant ethylene hormone signaling by two *Arabidopsis* F box proteins: EBF1 and EBF2. Cell **115**: 679–

689

Pré M, Atallah M, Champion A, De Vos M, Pieterse CMJ, Memelink J (2008) The AP2/ERF domain transcription factor ORA59 integrates jasmonic acid and ethylene signals in plant defense. Plant Physiol **147**: 1347–1357

Proietti S, Caarls L, Coolen S, Van Pelt JA, Van Wees SCM, Pieterse CMJ (2018) Genome-wide association study reveals novel players in defense hormone crosstalk in *Arabidopsis*. Plant Cell Environ **41**: 2342–2356

Qi G, Chen J, Chang M, Chen H, Hall K, Korin J, Liu F, Wang D, Fu ZQ (2018) Pandemonium breaks out: disruption of salicylic acid-mediated defense by plant pathogens. Mol Plant **11**: 1427–1439

Qi T, Song S, Ren Q, Wu D, Huang H, Chen Y, Fan M, Peng W, Ren C, Xiea D (2011) The jasmonate-ZIM-domain proteins interact with the WD-repeat/bHLH/MYB complexes to regulate jasmonate-mediated anthocyanin accumulation and trichome initiation in *Arabidopsis thaliana*. Plant Cell **23**: 1795–1814

Qiao H, Shen Z, Huang SSC, Schmitz RJ, Urich MA, Briggs SP, Ecker JR (2012) Processing and subcellular trafficking of ER-tethered EIN2 control response to ethylene gas. Science **338**: 390–393

Quesneville H (2020) Twenty years of transposable element analysis in the *Arabidopsis thaliana* genome. Mob DNA **11**: 28

R Core Team (2019) R: A language and environment for statistical computing. R Foundation for Statistical Computing, Vienna

Ralph SG, Hudgins JW, Jancsik S, Franceschi VR, Bohlmann J (2006a) Aminocyclopropane carboxylic acid synthase is a regulated step in ethylene-dependent induced conifer defense. Full-length cDNA cloning of a multigene family, differential constitutive, and wound- and insect-induced expression, and cellular and subcellular localization in spruce and Douglas fir. Plant Physiol **143**: 410–424

Ralph SG, Yueh H, Friedmann M, Aeschliman D, Zeznik JA, Nelson CC, Butterfield YSN, Kirkpatrick R, Liu J, Jones SJM, et al (2006b) Conifer

defence against insects: microarray gene expression profiling of Sitka spruce (*Picea sitchensis*) induced by mechanical wounding or feeding by spruce budworms (*Choristoneura occidentalis*) or white pine weevils (*Pissodes strobi*) reveals large-scale changes of the host transcriptome. Plant, Cell Environ **29**: 1545–1570

Rasmann S, Kollner TG, Degenhardt J, Hiltpold I, Toepfer S, Kuhlmann U, Gershenzon J, Turlings TC (2005) Recruitment of entomopathogenic nematodes by insect-damaged maize roots. Nature **434**: 732–737

Rasmann S, De Vos M, Casteel CL, Tian D, Halitschke R, Sun JY, Agrawal AA, Felton GW, Jander G (2012) Herbivory in the previous generation primes plants for enhanced insect resistance. Plant Physiol **158**: 854–863

Rekhter D, Lüdke D, Ding Y, Feussner K, Zienkiewicz K, Lipka V, Wiermer M, Zhang Y, Feussner I (2019) Isochorismate-derived biosynthesis of the plant stress hormone salicylic acid. Science **365**: 498–502

Ren D, Liu Y, Yang KY, Han L, Mao G, Glazebrook J, Zhang S (2008) A fungal-responsive MAPK cascade regulates phytoalexin biosynthesis in *Arabidopsis*. Proc Natl Acad Sci U S A **105**: 5638–5643

Rharrabe K, Jacquin-Joly E, Marion-Poll F (2014) Electrophysiological and behavioral responses of *Spodoptera littoralis* caterpillars to attractive and repellent plant volatiles. Front Ecol Evol **2**: 5

Robinson JT, Thorvaldsdóttir H, Winckler W, Guttman M, Lander ES, Getz G, Mesirov JP (2011) Integrative genomics viewer. Nat Biotechnol **29**: 24–26

Rochon A, Boyle P, Wignes T, Fobert PR, Després C (2006) The coactivator function of *Arabidopsis* NPR1 requires the core of its BTB/POZ domain and the oxidation of C-terminal cysteines. Plant Cell **18**: 3670–3685

Rodriguez-Saona CR, Polashock J, Malo EA (2013) Jasmonate-mediated induced volatiles in the American cranberry, *Vaccinium macrocarpon*: from gene expression to organismal interactions. Front Plant Sci **4**: 115

Roeder KA, Kuriachan I, Vinson SB, Behmer ST (2010) Evaluation of a microbial inhibitor in artificial diets of a generalist caterpillar, *Heliothis virescens*. J Insect

Sci **10**: 197

Rojo E, León J, Sánchez-Serrano JJ (1999) Cross-talk between wound signalling pathways determines local versus systemic gene expression in *Arabidopsis thaliana*. Plant J **20**: 135–142

Rolfe SA, Griffiths J, Ton J (2019) Crying out for help with root exudates: adaptive mechanisms by which stressed plants assemble health-promoting soil microbiomes. Curr Opin Microbiol **49**: 73–82

De Román M, Fernández I, Wyatt T, Sahrawy M, Heil M, Pozo MJ (2011) Elicitation of foliar resistance mechanisms transiently impairs root association with arbuscular mycorrhizal fungi. J Ecol **99**: 36–45

Roos J, Bejai S, Mozuraitis R, Dixelius C (2015) Susceptibility to *Verticillium longisporum* is linked to monoterpene production by TPS23/27 in Arabidopsis. Plant J **81**: 572–585

Ross AF (1961) Systemic acquired resistance induced by localized virus infections in plants. Virology **14**: 340–358

Ruijter JM, Ramakers C, Hoogaars WMH, Karlen Y, Bakker O, van den hoff MJB, Moorman AFM (2009) Amplification efficiency: linking baseline and bias in the analysis of quantitative PCR data. Nucleic Acids Res **37**: e45

Ryals JA, Uknes SJ, Ward ER (1994) Systemic acquired resistance. Plant Physiol **104**: 1109–1112

Sánchez-vallet A, López G, Ramos B, Delgado-cerezo M, Riviere M, Llorente F, Fernández PV, Miedes E, Estevez JM, Grant M, et al (2012) Disruption of abscisic acid signaling constitutively activates Arabidopsis resistance to the necrotrophic fungus *Plectosphaerella cucumerina*. Plant Physiol **160**: 2109–2124

Sanchez-Vallet A, Ramos B, Bednarek P, López G, Piślewska-Bednarek M, Schulze-Lefert P, Molina A (2010) Tryptophan-derived secondary metabolites in *Arabidopsis thaliana* confer non-host resistance to necrotrophic *Plectosphaerella cucumerina* fungi. Plant J **63**: 115–127

Saze H, Mittelsten Scheid O, Paszkowski J (2003) Maintenance of CpG

methylation is essential for epigenetic inheritance during plant gametogenesis. Nat Genet **34**: 65–69

Schiebe C, Hammerbacher A, Birgersson G, Witzell J, Brodelius PE, Gershenzon J, Hansson BS, Krokene P, Schlyter F (2012) Inducibility of chemical defenses in Norway spruce bark is correlated with unsuccessful mass attacks by the spruce bark beetle. Oecologia **170**: 183–198

Schillheim B, Jansen I, Baum S, Beesley A, Bolm C, Conrath U (2018) Sulforaphane modifies histone H3, unpacks chromatin, and primes defense. Plant Physiol **176**: 2395–2405

Schmelz EA, Carroll MJ, LeClere S, Phipps SM, Meredith J, Chourey PS, Alborn HT, Teal PEA (2006) Fragments of ATP synthase mediate plant perception of insect attack. Proc Natl Acad Sci U S A **103**: 8894–8899

Schmidt A, Gershenzon J (2007) Cloning and characterization of isoprenyl diphosphate synthases with farnesyl diphosphate and geranylgeranyl diphosphate synthase activity from Norway spruce (*Picea abies*) and their relation to induced oleoresin formation. Phytochemistry **68**: 2649–2659

Schmidt A, Gershenzon J (2008) Cloning and characterization of two different types of geranyl diphosphate synthases from Norway spruce (*Picea abies*). Phytochemistry **69**: 49–57

Schmidt A, Nagel R, Krekling T, Christiansen E, Gershenzon J, Krokene P (2011) Induction of isoprenyl diphosphate synthases, plant hormones and defense signalling genes correlates with traumatic resin duct formation in Norway spruce (*Picea abies*). Plant Mol Biol **77**: 577–590

Scholz SS, Vadassery J, Heyer M, Reichelt M, Bender KW, Snedden WA, Boland W, Mithöfer A (2014) Mutation of the *Arabidopsis* calmodulin-like protein CML37 deregulates the jasmonate pathway and enhances susceptibility to herbivory. Mol Plant **7**: 1712–1726

Schultz MD, Schmitz RJ, Ecker JR (2012) “Leveling” the playing field for analyses of single-base resolution DNA methylomes. Trends Genet **28**: 583–585

Schweizer F, Bodenhausen N, Lassueur S, Masclaux FG, Reymond P (2013a)

Differential contribution of transcription factors to *Arabidopsis thaliana* defense against *Spodoptera littoralis*. Front Plant Sci **4**: 13

Schweizer F, Fernández-Calvo P, Zander M, Diez-Diaz M, Fonseca S, Glauser G, Lewsey MG, Ecker JR, Solano R, Reymond P (2013b) *Arabidopsis* basic helix-loop-helix transcription factors MYC2, MYC3, and MYC4 regulate glucosinolate biosynthesis, insect performance, and feeding behavior. Plant Cell **25**: 3117–3132

Seo M, Peeters AJM, Koiwai H, Oritani T, Marion-Poll A, Zeevaart JAD, Koornneef M, Kamiya Y, Koshiba T (2000) The *Arabidopsis* aldehyde oxidase 3 (AAO3) gene product catalyzes the final step in abscisic acid biosynthesis in leaves. Proc Natl Acad Sci U S A **97**: 12908–12913

Shah J, Tsui F, Klessig DF (1997) Characterization of a salicylic acid-insensitive mutant (*sai1*) of *Arabidopsis thaliana*, identified in a selective screen utilizing the SA- inducible expression of the *tms2* gene. Mol Plant-Microbe Interact **10**: 69–78

Shakeel SN, Gao Z, Amir M, Chen YF, Rai MI, Haq NU, Schaller GE (2015) Ethylene regulates levels of ethylene receptor/CTR1 signaling complexes in *Arabidopsis thaliana*. J Biol Chem **290**: 12415–12424

Shannon P, Richards M (2019) MotifDb: an annotated collection of protein-DNA binding sequence motifs. R package

Sheard LB, Tan X, Mao H, Withers J, Ben-Nissan G, Hinds TR, Kobayashi Y, Hsu FF, Sharon M, Browse J, et al (2010) Jasmonate perception by inositol-phosphate-potentiated COI1-JAZ co-receptor. Nature **468**: 400–407

Shen Q, Lu X, Yan T, Fu X, Lv Z, Zhang F, Pan Q, Wang G, Sun X, Tang K (2016) The jasmonate-responsive AaMYC2 transcription factor positively regulates artemisinin biosynthesis in *Artemisia annua*. New Phytol **210**: 1269–1281

Shi J, Ma CY, Qi DD, Lv HP, Yang T, Peng QH, Chen ZM, Lin Z (2015) Transcriptional responses and flavor volatiles biosynthesis in methyl jasmonate-treated tea leaves. BMC Plant Biol **15**: 233

Shyu C, Figueroa P, de Pew CL, Cooke TF, Sheard LB, Moreno JE, Katsir L,

Zheng N, Browse J, Howea GA (2012) JAZ8 lacks a canonical degron and has an EAR motif that mediates transcriptional repression of jasmonate responses in *Arabidopsis*. Plant Cell **24**: 536–550

Simon JM, Giresi PG, Davis IJ, Lieb JD (2012) Using formaldehyde-assisted isolation of regulatory elements (FAIRE) to isolate active regulatory DNA. Nat Protoc **7**: 256–267

Singh M, Bag SK, Bhardwaj A, Ranjan A, Mantri S, Nigam D, Sharma YK, Sawant SV (2015) Global nucleosome positioning regulates salicylic acid mediated transcription in *Arabidopsis thaliana*. BMC Plant Biol **15**: 13

Skelly MJ, Furniss JJ, Grey HL, Wong KW, Spoel SH (2019) Dynamic ubiquitination determines transcriptional activity of the plant immune coactivator NPR1. Elife **8**: e47005

Skrautvol TO (2018) Vaccinating Norway spruce – physiological and morphological effects of methyl jasmonate (master's thesis). Norwegian University of Life Sciences, Ås, Norway.

Slaughter A, Daniel X, Flors V, Luna E, Hohn B, Mauch-Mani B (2012) Descendants of primed Arabidopsis plants exhibit resistance to biotic stress. Plant Physiol **158**: 835–843

Slowikowski K (2019) ggrepel: automatically position non-overlapping text labels with “ggplot2.” R package

Solano R, Stepanova A, Chao Q, Ecker JR (1998) Nuclear events in ethylene signaling: a transcriptional cascade mediated by ETHYLENE-INSENSITIVE3 and ETHYLENE-RESPONSE-FACTOR1. Genes Dev **12**: 3703–3714

Solheim H (1991) Oxygen deficiency and spruce resin inhibition of growth of blue stain fungi associated with *Ips typographus*. Mycol Res **95**: 1387–1392

Sønderby IE, Burow M, Rowe HC, Kliebenstein DJ, Halkier BA (2010a) A complex interplay of three R2R3 MYB transcription factors determines the profile of aliphatic glucosinolates in Arabidopsis. Plant Physiol **153**: 348–363

Sønderby IE, Geu-Flores F, Halkier BA (2010b) Biosynthesis of glucosinolates - gene discovery and beyond. Trends Plant Sci **15**: 283–290

Song JT (2006) Induction of a salicylic acid glucosyltransferase, AtSGT1, is an early disease response in *Arabidopsis thaliana*. Mol Cells **22**: 233–238

Song S, Huang H, Gao H, Wang J, Wu D, Liu X, Yang S, Zhai Q, Li C, Qi T, et al (2014) Interaction between MYC2 and ETHYLENE INSENSITIVE3 modulates antagonism between jasmonate and ethylene signaling in *Arabidopsis*. Plant Cell **26**: 263–279

Song S, Huang H, Wang J, Liu B, Qi T, Xie D (2017) *MYC5* is involved in jasmonate-regulated plant growth, leaf senescence and defense responses. Plant Cell Physiol **58**: 1752–1763

Spoel SH, Dong X (2012) How do plants achieve immunity? Defence without specialized immune cells. Nat Rev Immunol **12**: 89–100

Spoel SH, Johnson JS, Dong X (2007) Regulation of tradeoffs between plant defenses against pathogens with different lifestyles. Proc Natl Acad Sci U S A **104**: 18842–18847

Spoel SH, Koornneef A, Claessens SMC, Korzelius JP, Van Pelt JA, Mueller MJ, Buchala AJ, Métraux JP, Brown R, Kazan K, et al (2003) NPR1 modulates cross-talk between salicylate- and jasmonate-dependent defense pathways through a novel function in the cytosol. Plant Cell **15**: 760–770

Spoel SH, Mou Z, Tada Y, Spivey NW, Genschik P, Dong X (2009) Proteasome-mediated turnover of the transcription coactivator NPR1 plays dual roles in regulating plant immunity. Cell **137**: 860–872

Spyropoulou EA, Haring MA, Schuurink RC (2014) RNA sequencing on *Solanum lycopersicum* trichomes identifies transcription factors that activate terpene synthase promoters. BMC Genomics **15**: 402

Stanke M, Steinkamp R, Waack S, Morgenstern B (2004) AUGUSTUS: a web server for gene finding in eukaryotes. Nucleic Acids Res **32**: W309–W312

Stassen JHM, López A, Jain R, Pascual-Pardo D, Luna E, Smith LM, Ton J (2018) The relationship between transgenerational acquired resistance and global DNA methylation in Arabidopsis. Sci Rep **8**: 14761

Staswick PE, Tiryaki I (2004) The oxylipin signal jasmonic acid is activated by an

enzyme that conjugate it to isoleucine in Arabidopsis W inside box sign. Plant Cell **16**: 2117–2127

Stephens M (2017) False discovery rates: A new deal. Biostatistics **18**: 275–294

Stojnic R, Diez D (2019) PWMEnrich: PWM enrichment analysis. R package

Stokes TL, Kunkel BN, Richards EJ (2002) Epigenetic variation in *Arabidopsis* disease resistance. Genes Dev **16**: 171–182

Stotz HU, Biedermann A, Weniger K, Mitchell-olds T (2002) Evidence for regulation of resistance in *Arabidopsis* to Egyptian cotton worm by salicylic and jasmonic acid signaling pathways. Planta **214**: 648–652

Stotz HU, Pittendrigh BR, Kroymann J, Weniger K, Fritsche J, Bauke A, Mitchell-Olds T (2000) Induced plant defense responses against chewing insects. Ethylene signaling reduces resistance of Arabidopsis against Egyptian cotton worm but not diamondback moth. Plant Physiol **124**: 1007–1017

Stroud H, Greenberg MVC, Feng S, Bernatavichute Y V., Jacobsen SE (2013) Comprehensive analysis of silencing mutants reveals complex regulation of the *Arabidopsis* methylome. Cell **152**: 352–364

Stuart T, Buckberry S, Lister R (2018) Approaches for the analysis and interpretation of whole genome bisulfite sequencing data. *In* A Jeltsch, MG Rots, eds, Epigenome Ed. Methods Protoc. Methods Mol. Biol. Humana Press, pp 299–310

Sun H, Chen L, Li J, Hu M, Ullah A, He X, Yang X, Zhang X (2017) The JASMONATE ZIM-domain gene family mediates JA signaling and stress response in cotton. Plant Cell Physiol **58**: 2139–2154

Sun T, Li Y, Zhang Q, Ding Y, Zhang Y, Zhang Y (2015) ChIP-seq reveals broad roles of SARD1 and CBP60g in regulating plant immunity. Nat Commun **6**: 10159

Sundell D, Mannapperuma C, Netotea S, Delhomme N, Lin Y-C, Sjödin A, Van de Peer Y, Jansson S, Hvidsten TR, Street NR (2015) The Plant Genome Integrative Explorer Resource: PlantGenIE.org. New Phytol **208**: 1149–1156

Suzuki M, Liao W, Wos F, Johnston AD, DeGrazia J, Ishii J, Bloom T, Zody MC, Germer S, Greally JM (2018) Whole-genome bisulfite sequencing with improved accuracy and cost. Genome Res **28**: 1364–1371

Tada Y, Spoel SH, Pajerowska-Mukhtar K, Mou Z, Song J, Wang C, Zuo J, Dong X (2008) Plant immunity requires conformational charges of NPR1 via S-nitrosylation and thioredoxins. Science **321**: 952–956

Taki N, Sasaki-Sekimoto Y, Obayashi T, Kikuta A, Kobayashi K, Ainai T, Yagi K, Sakurai N, Suzuki H, Masuda T, et al (2005) 12-Oxo-phytodienoic acid triggers expression of a distinct set of genes and plays a role in wound-induced gene expression in Arabidopsis. Plant Physiol **139**: 1268–1283

Takuno S, Ran J-H, Gaut BS (2016) Evolutionary patterns of genic DNA methylation vary across land plants. Nat Plants **2**: 15222

Tan F, Zhou C, Zhou Q, Zhou S, Yang W, Zhao Y, Li G, Zhou DX (2016) Analysis of chromatin regulators reveals specific features of rice DNA methylation pathways. Plant Physiol **171**: 2041–2054

Tang K, Lang Z, Zhang H, Zhu J (2016) The DNA demethylase ROS1 targets genomic regions with distinct chromatin modification. Nat Plants **2**: 16169

Tarvainen L, Wallin G, Lim H, Linder S, Oren R, Löfvenius MO, Räntfors M, Tor-Ngern P, Marshall J (2018) Photosynthetic refixation varies along the stem and reduces CO_2 efflux in mature boreal *Pinus sylvestris* trees. Tree Physiol **38**: 558–569

Tateda C, Zhang Z, Shrestha J, Jelenska J, Chinchilla D, Greenberg JT (2014) Salicylic acid regulates *Arabidopsis* microbial pattern receptor kinase levels and signaling. Plant Cell **26**: 4171–4187

Thaler JS (1999) Jasmonate-inducible plant defences cause increased parasitism of herbivores. Nature **399**: 686–688

The UniProt Consortium (2019) UniProt: a worldwide hub of protein knowledge. Nucleic Acids Res **47**: D506–D515

Thines B, Katsir L, Melotto M, Niu Y, Mandaokar A, Liu G, Nomura K, He SY, Howe GA, Browse J (2007) JAZ repressor proteins are targets of the SCF^{COI1}

complex during jasmonate signalling. Nature **448**: 661–665

Thomma BPHJ, Eggermont K, Broekaert WF, Cammue BPA (2000) Disease development of several fungi on Arabidopsis can be reduced by treatment with methyl jasmonate. Plant Physiol Biochem **38**: 421–427

Thomma BPHJ, Eggermont K, Penninckx IAMA, Mauch-Mani B, Vogelsang R, Cammue BPA, Broekaert WF (1998) Separate jasmonate-dependent and salicylate-dependent defense-response pathways in *Arabidopsis* are essential for resistance to distinct microbial pathogens. Proc Natl Acad Sci U S A **95**: 15107–15111

Thomma BPHJ, Eggermont K, Tierens KFMJ, Broekaert WF (1999) Requirement of functional *ethylene-insensitive 2* gene for efficient resistance of Arabidopsis to infection by *Botrytis cinerea*. Plant Physiol **121**: 1093–1101

Thorvaldsdottir H, Robinson JT, Mesirov JP (2013) Integrative Genomics Viewer (IGV): high-performance genomics data visualization and exploration. Brief Bioinform **14**: 178–192

Thulke O, Conrath U (1998) Salicylic acid has a dual role in the activation of defence-related genes in parsley. Plant J **14**: 35–42

Ton J, D'Alessandro M, Jourdie V, Jakab G, Karlen D, Held M, Mauch-Mani B, Turlings TCJ (2007) Priming by airborne signals boosts direct and indirect resistance in maize. Plant J **49**: 16–26

Ton J, Jakab G, Toquin V, Flors V, Iavicoli A, Maeder MN, Métraux J-P, Mauch-Mani B (2005) Dissecting the β-aminobutyric acid–induced priming phenomenon in Arabidopsis. Plant Cell **17**: 987–999

Ton J, Mauch-Mani B (2004) *β*-amino-butyric acid-induced resistance against necrotrophic pathogens is based on ABA-dependent priming for callose. Plant J **38**: 119–130

Torrens-Spence MP, Bobokalonova A, Carballo V, Glinkerman CM, Pluskal T, Shen A, Weng JK (2019) PBS3 and EPS1 complete salicylic acid biosynthesis from isochorismate in *Arabidopsis*. Mol Plant **12**: 1577–1586

Toruño TY, Stergiopoulos I, Coaker G (2016) Plant-pathogen effectors: cellular

probes interfering with plant defenses in spatial and temporal manners. Annu Rev Phytopathol **54**: 419–441

Tsuchisaka A, Yu G, Jin H, Alonso JM, Ecker JR, Zhang X, Gao S, Theologis A (2009) A combinatorial interplay among the 1-aminocyclopropane-1-carboxylate isoforms regulates ethylene biosynthesis in *Arabidopsis thaliana*. Genetics **183**: 979–1003

Tsuchiya T, Eulgem T (2013) An alternative polyadenylation mechanism coopted to the *Arabidopsis RPP7* gene through intronic retrotransposon domestication. Proc Natl Acad Sci U S A **110**: E3535–E3543

Turlings TCJ, Erb M (2018) Tritrophic interactions mediated by herbivore-induced plant volatiles: mechanisms, ecological relevance, and application potential. Annu Rev Entomol **63**: 433–452

Turlings TCJ, Tumlinson JH, Lewis WJ (1990) Exploitation of herbivore-induced plant odors by host-seeking parasitic wasps. Science **250**: 1251–1253

Vadassery J, Ballhorn DJ, Fleming SR, Mazars C, Pandey SP, Schmidt A, Schuman MC, Yeh KW, Yilamujiang A, Mithöfer A (2019) Neomycin: an effective inhibitor of jasmonate-induced reactions in plants. J Plant Growth Regul **38**: 713–722

Vandegehuchte MW, Bloemen J, Vergeynst LL, Steppe K (2015) Woody tissue photosynthesis in trees: salve on the wounds of drought? New Phytol **208**: 998–1002

VanEtten HD, Mansfield JW, Baily JA, Farmer EE (1994) Two classes of plant antibiotics : phytoalexins versus “ phytoanticipins .” Plant Cell **6**: 1191–1192

Verdugo RA, Orostica KY (2019) chromPlot: global visualization tool of genomic data. R package

Verhage A, Vlaardingerbroek I, Raaymakers C, Van Dam NM, Dicke M, Van Wees SCM, Pieterse CMJ (2011) Rewiring of the Jasmonate signaling pathway in Arabidopsis during insect herbivory. Front Plant Sci **2**: 47

Verhoeven KJF, Van Gurp TP (2012) Transgenerational effects of stress exposure on offspring phenotypes in apomictic dandelion. PLoS One **7**: e38605

Vijayan P, Shockey J, Lévesque C a, Cook RJ, Browse J (1998) A role for jasmonate in pathogen defense of *Arabidopsis*. Proc Natl Acad Sci U S A **95**: 7209–7214

Vílchez JI, Yang Y, He D, Zi H, Peng L, Lv S, Kaushal R, Wang W, Huang W, Liu R, et al (2020) DNA demethylases are required for *myo*-inositol-mediated mutualism between plants and beneficial rhizobacteria. Nat Plants **6**: 983–995

Vlot AC, Dempsey DA, Klessig DF (2009) Salicylic acid, a multifaceted hormone to combat disease. Annu Rev Phytopathol **47**: 177–206

Vos I, Verhage A, Watt L, Vlaardingerbroek I, Schuurink R, Pieterse CM, Van Wees SC (2019) Abscisic acid is essential for rewiring of jasmonic acid-dependent defenses during herbivory. bioRxiv doi: 10.1101/747345

Vos IA, Moritz L, Pieterse CMJ, Van Wees SCM (2015) Impact of hormonal crosstalk on plant resistance and fitness under multi-attacker conditions. Front Plant Sci **6**: 639

Vos IA, Verhage A, Schuurink RC, Watt LG, Pieterse CMJ, Van Wees SCM (2013) Onset of herbivore-induced resistance in systemic tissue primed for jasmonate-dependent defenses is activated by abscisic acid. Front Plant Sci **4**: 539

Vos M De, Oosten VR Van, Poecke RMP Van, Pelt JA Van, Pozo MJ, Mueller MJ, Buchala AJ, Métraux J-P, Loon LC Van, Dicke M, et al (2005) Signal signature and transcriptome changes of *Arabidopsis* during pathogen and insect attack. Mol Plant-Microbe Interact **18**: 923–937

De Vries J, Poelman EH, Anten N, Evers JB (2018) Elucidating the interaction between light competition and herbivore feeding patterns using functional–structural plant modelling. Ann Bot **121**: 1019–1031

Waddington C (1942) The epigenotype. Endeavor **1**: 18–20

Walters DR, Paterson L, Walsh DJ, Havis ND (2009) Priming for plant defense in barley provides benefits only under high disease pressure. Physiol Mol Plant Pathol **73**: 95–100

Walters DR, Ratsep J, Havis ND (2013) Controlling crop diseases using induced

resistance: challenges for the future. J Exp Bot **64**: 1263–1280

Wambui Mbichi R, Wang QF, Wan T (2020) RNA directed DNA methylation and seed plant genome evolution. Plant Cell Rep **39**: 983–996

Wang KLC, Li H, Ecker JR (2002) Ethylene biosynthesis and signaling networks. Plant Cell **14**: S131–S151

Wang L, Qiao H (2019) New insights in transcriptional regulation of the ethylene response in *Arabidopsis*. Front Plant Sci **10**: 790

Wang L, Tsuda K, Truman W, Sato M, Nguyen L V., Katagiri F, Glazebrook J (2011) CBP60g and SARD1 play partially redundant critical roles in salicylic acid signaling. Plant J **67**: 1029–1041

Wang P, Yu S, Han X, Xu J, He Q, Xu S, Wang R (2020) Identification, molecular characterization and expression of *JAZ* genes in *Lycoris aurea*. PLoS One **15**: e0230177

Wasternack C (2007) Jasmonates: an update on biosynthesis, signal transduction and action in plant stress response, growth and development. Ann Bot **100**: 681–697

Wasternack C (2015) How jasmonates earned their laurels: past and present. J Plant Growth Regul **34**: 761–794

Wasternack C, Feussner I (2018) The oxylipin pathways: biochemistry and function. Annu Rev Plant Biol **69**: 363–386

Wasternack C, Hause B (2013) Jasmonates: biosynthesis, perception, signal transduction and action in plant stress response, growth and development. An update to the 2007 review in *Annals of Botany*. Ann Bot **111**: 1021–1058

Wasternack C, Hause B (2019) The missing link in jasmonic acid biosynthesis. Nat Plants **5**: 776–777

Wasternack C, Song S (2017) Jasmonates: biosynthesis, metabolism, and signaling by proteins activating and repressing transcription. J Exp Bot **68**: 1303–1321

Weiberg A, Wang M, Lin F, Zhao H, Zhang Z, Kaloshian I, Huang H-D, Jin H

(2013) Fungal small RNAs suppress plant immunity by hijacking host RNA interference pathways. Science **342**: 118–123

Wen X, Zhang C, Ji Y, Zhao Q, He W, An F, Jiang L, Guo H (2012) Activation of ethylene signaling is mediated by nuclear translocation of the cleaved EIN2 carboxyl terminus. Cell Res **22**: 1613–1616

Wermelinger B (2004) Ecology and management of the spruce bark beetle *Ips typographus* - A review of recent research. For Ecol Manage **202**: 67–82

Wicker T, Sabot F, Hua-Van A, Bennetzen JL, Capy P, Chalhoub B, Flavell A, Leroy P, Morgante M, Panaud O, et al (2007) A unified classification system for eukaryotic transposable elements. Nat Rev Genet **8**: 973–982

Wickham H (2016) ggplot2: elegant graphics for data analysis. doi: 10.1007/978-0-387-98141-3

Widhalm JR, Dudareva N (2015) A familiar ring to it: biosynthesis of plant benzoic acids. Mol Plant **8**: 83–97

Wildermuth MC, Dewdney J, Wu G, Ausubel FM (2001) Isochorismate synthase is required to synthesize salicylic acid for plant defence. Nature **414**: 562–565

Wilkinson SW, Magerøy MH, López Sánchez A, Smith LM, Furci L, Cotton TEA, Krokene P, Ton J (2019) Surviving in a hostile world: plant strategies to resist pests and diseases. Annu Rev Phytopathol **57**: 505–529

Wilkinson SW, Pastor V, Paplauskas S, Pétriacq P, Luna E (2018) Long-lasting β-aminobutyric acid-induced resistance protects tomato fruit against *Botrytis cinerea*. Plant Pathol **67**: 30–41

Wilkinson SW, Ton J (2020) Methylation moulds microbiomes. Nat Plants **6**: 910–911

Williams BP, Pignatta D, Henikoff S, Gehring M (2015) Methylation-sensitive expression of a DNA demethylase gene serves as an epigenetic rheostat. PLoS Genet **11**: e1005142

Winter D, Vinegar B, Nahal H, Ammar R, Wilson G V., Provart NJ (2007) An "electronic fluorescent pictograph" browser for exploring and analyzing large-

scale biological data sets. PLoS One **2**: e718

Wittstock U, Burow M (2010) Glucosinolate breakdown in Arabidopsis: mechanism, regulation and biological significance. Arab B **8**: e0134

Wittstock U, Kurzbach E, Herfurth AM, Stauber EJ (2016) Glucosinolate breakdown. Adv Bot Res **80**: 125–169

Worrall D, Holroyd GH, Moore JP, Glowacz M, Croft P, Taylor JE, Paul ND, Roberts MR (2012) Treating seeds with activators of plant defence generates long-lasting priming of resistance to pests and pathogens. New Phytol **193**: 770–778

Wu H, Hu ZH (1997) Comparative anatomy of resin ducts of the Pinaceae. Trees - Struct Funct **11**: 135–143

Wu H, Xu T, Feng H, Chen L, Li B, Yao B, Qin Z, Jin P, Conneely KN (2015) Detection of differentially methylated regions from whole-genome bisulfite sequencing data without replicates. Nucleic Acids Res **43**: e141

Wu Y, Zhang D, Chu JY, Boyle P, Wang Y, Brindle ID, De Luca V, Després C (2012) The *Arabidopsis* NPR1 protein is a receptor for the plant defense hormone salicylic acid. Cell Rep **1**: 639–647

Xia R, Xu J, Arikit S, Meyers BC (2015) Extensive families of miRNAs and *PHAS* loci in Norway spruce demonstrate the origins of complex phasiRNA networks in seed plants. Mol Biol Evol **32**: 2905–2918

Xie DX, Feys BF, James S, Nieto-Rostro M, Turner JG (1998) *COI1*: An *Arabidopsis* gene required for jasmonate-regulated defense and fertility. Science **280**: 1091–1094

Xin X-F, He SY (2013) *Pseudomonas syringae* pv. *tomato* DC3000: a model pathogen for probing disease susceptibility and hormone signaling in plants. Annu Rev Phytopathol **51**: 473–498

Xu J, Xie J, Yan C, Zou X, Ren D, Zhang S (2014) A chemical genetic approach demonstrates that MPK3/MPK6 activation and NADPH oxidase-mediated oxidative burst are two independent signaling events in plant immunity. Plant J **77**: 222–234

Xu J, Zhang S (2014) Regulation of ethylene biosynthesis and signaling by protein kinases and phosphatases. Mol Plant **7**: 939–942

Xu L, Liu F, Lechner E, Genschik P, Crosby WL, Ma H, Peng W, Huang D, Xie D (2002) The SCF^{COI1} ubiquitin-ligase complexes are required for jasmonate response in Arabidopsis. Plant Cell **14**: 1919–1935

Xu X, Chen C, Fan B, Chen Z (2006) Physical and functional interactions between pathogen-induced *Arabidopsis* WRKY18, WRKY40 and WRKY60 transcription factors. Plant Cell **18**: 1310–1326

Yakovlev IA, Fossdal CG, Johnsen Ø, Junttila O, Skrøppa T (2006) Analysis of gene expression during bud burst initiation in Norway spruce via ESTs from subtracted cDNA libraries. Tree Genet Genomes **2**: 39–52

Yan C, Fan M, Yang M, Zhao J, Zhang W, Su Y, Xiao L, Deng H, Xie D (2018) Injury activates Ca^{2+}/calmodulin-dependent phosphorylation of JAV1-JAZ8-WRKY51 complex for jasmonate biosynthesis. Mol Cell **70**: 136–149

Yan J, Li S, Gu M, Yao R, Li Y, Chen J, Yang M, Tong J, Xiao L, Nan F, et al (2016) Endogenous bioactive jasmonate is composed of a set of (+)-7-iso-JA-amino acid conjugates. Plant Physiol **172**: 2154–2164

Yan J, Zhang C, Gu M, Bai Z, Zhang W, Qi T, Cheng Z, Peng W, Luo H, Nan F, et al (2009) The *Arabidopsis* CORONATINE INSENSITIVE1 protein is a jasmonate receptor. Plant Cell **21**: 2220–2236

Yan Y, Stolz S, Chételat A, Reymond P, Pagni M, Dubugnon L, Farmer EE (2007) A downstream mediator in the growth repression limb of the jasmonate pathway. Plant Cell **19**: 2470–2483

Yang L, Li B, Zheng XY, Li J, Yang M, Dong X, He G, An C, Deng XW (2015) Salicylic acid biosynthesis is enhanced and contributes to increased biotrophic pathogen resistance in *Arabidopsis* hybrids. Nat Commun **6**: 7309

Yatusevich R, Mugford SG, Matthewman C, Gigolashvili T, Frerigmann H, Delaney S, Koprivova A, Flügge UI, Kopriva S (2010) Genes of primary sulfate assimilation are part of the glucosinolate biosynthetic network in *Arabidopsis thaliana*. Plant J **62**: 1–11

Yi H, Richards EJ (2009) Gene duplication and hypermutation of the pathogen resistance gene *SNC1* in the Arabidopsis *bal* variant. Genetics **183**: 1227–1234

Yu A, Lepère G, Jay F, Wang J, Bapaume L, Wang Y, Abraham A-L, Penterman J, Fischer RL, Voinnet O, et al (2013) Dynamics and biological relevance of DNA demethylation in *Arabidopsis* antibacterial defense. Proc Natl Acad Sci U S A **110**: 2389–2394

Yu G, Li F, Qin Y, Bo X, Wu Y, Wang S (2010) GOSemSim: An R package for measuring semantic similarity among GO terms and gene products. Bioinformatics **26**: 976–978

Yu G, Wang LG, Han Y, He QY (2012) ClusterProfiler: An R package for comparing biological themes among gene clusters. Omi A J Integr Biol **16**: 284–287

Yuan X, Wang H, Cai J, Li D, Song F (2019) NAC transcription factors in plant immunity. Phytopathol Res **1**: 3

Zander M, Chen S, Imkampe J, Thurow C, Gatz C (2012) Repression of the *Arabidopsis thaliana* jasmonic acid/ethylene-induced defense pathway by tga-interacting glutaredoxins depends on their c-terminal alwl motif. Mol Plant **5**: 831–840

Zander M, Lewsey MG, Clark NM, Yin L, Bartlett A, Saldierna Guzmán JP, Hann E, Langford AE, Jow B, Wise A, et al (2020) Integrated multi-omics framework of the plant response to jasmonic acid. Nat Plants **6**: 290–302

Zander M, Thurow C, Gatz C (2014) TGA transcription factors activate the salicylic acid-suppressible branch of the ethylene-induced defense program by regulating *ORA59* expression. Plant Physiol **165**: 1671–1683

Zas R, Bjorklund N, Nordlander G, Cendan C, Hellqvist C, Sampedro L (2014) Exploiting jasmonate-induced responses for field protection of conifer seedlings against a major forest pest, *Hylobius abietis*. For Ecol Manage **313**: 212–223

Zemach A, Kim MY, Hsieh P-H, Coleman-Derr D, Eshed-Williams L, Thao K, Harmer SL, Zilberman D (2013) The Arabidopsis nucleosome remodeler DDM1 allows DNA methyltransferases to access H1-containing heterochromatin. Cell **153**: 193–205

Zeneli G, Krokene P, Christiansen E, Krekling T, Gershenzon J (2006) Methyl jasmonate treatment of mature Norway spruce (*Picea abies*) trees increases the accumulation of terpenoid resin components and protects against infection by *Ceratocystis polonica*, a bark beetle-associated fungus. Tree Physiol **26**: 977–988

Zhai Q, Yan L, Tan D, Chen R, Sun J, Gao L, Dong MQ, Wang Y, Li C (2013) Phosphorylation-coupled proteolysis of the transcription factor MYC2 is important for jasmonate-signaled plant immunity. PLoS Genet **9**: e1003422

Zhang F, Ke J, Zhang L, Chen R, Sugimoto K, Howe GA, Xu HE, Zhou M, He SY, Melcher K (2017a) Structural insights into alternative splicing-mediated desensitization of jasmonate signaling. Proc Natl Acad Sci U S A **114**: 1720–1725

Zhang F, Qi B, Wang L, Zhao B, Rode S, Riggan ND, Ecker JR, Qiao H (2016) EIN2-dependent regulation of acetylation of histone H3K14 and non-canonical histone H3K23 in ethylene signalling. Nat Commun **7**: 13018

Zhang F, Wang L, Ko EE, Shao K, Qiao H (2018a) Histone deacetylases SRT1 and SRT2 interact with ENAP1 to mediate ethylene-induced transcriptional repression. Plant Cell **30**: 153–166

Zhang F, Wang L, Qi B, Zhao B, Ko EE, Riggan ND, Chin K, Qiao H (2017b) EIN2 mediates direct regulation of histone acetylation in the ethylene response. Proc Natl Acad Sci U S A **114**: 10274–10279

Zhang F, Yao J, Ke J, Zhang L, Lam VQ, Xin XF, Zhou XE, Chen J, Brunzelle J, Griffin PR, et al (2015) Structural basis of JAZ repression of MYC transcription factors in jasmonate signalling. Nature **525**: 269–273

Zhang H, Lang Z, Zhu JK (2018b) Dynamics and function of DNA methylation in plants. Nat Rev Mol Cell Biol **19**: 489–506

Zhang H, Ma ZY, Zeng L, Tanaka K, Zhang CJ, Ma J, Bai G, Wang P, Zhang SW, Liu ZW, et al (2013) DTF1 is a core component of RNA-directed DNA methylation and may assist in the recruitment of Pol IV. Proc Natl Acad Sci U S A **110**: 8290–8295

Zhang M, Jin X, Chen Y, Wei M, Liao W, Zhao S, Fu C, Yu L (2018c) TcMYC2a, a basic helix–loop–helix transcription factor, transduces JA-signals and regulates taxol biosynthesis in *Taxus chinensis*. Front Plant Sci **9**: 863

Zhang PJ, Zheng SJ, Van Loon JJA, Boland W, David A, Mumm R, Dicke M (2009) Whiteflies interfere with indirect plant defense against spider mites in Lima bean. Proc Natl Acad Sci U S A **106**: 21202–21207

Zhang X, Zhu Z, An F, Hao D, Li P, Song J, Yi C, Guo H (2014) Jasmonate-activated MYC2 represses ETHYLENE INSENSITIVE3 activity to antagonize ethylene-promoted apical hook formation in *Arabidopsis*. Plant Cell **26**: 1105–1117

Zhang Y, Cheng YT, Qu N, Zhao Q, Bi D, Li X (2006) Negative regulation of defense responses in Arabidopsis by two *NPR1* paralogs. Plant J **48**: 647–656

Zhang Y, Fan W, Kinkema M, Li X, Dong X (1999) Interaction of NPR1 with basic leucine zipper protein transcription factors that bind sequences required for salicylic acid induction of the *PR-1* gene. Proc Natl Acad Sci U S A **96**: 6523–6528

Zhang Y, Li X (2019) Salicylic acid: biosynthesis, perception, and contributions to plant immunity. Curr Opin Plant Biol **50**: 29–36

Zhang Y, Xu S, Ding P, Wang D, Cheng YT, He J, Gao M, Xu F, Li Y, Zhu Z, et al (2010) Control of salicylic acid synthesis and systemic acquired resistance by two members of a plant-specific family of transcription factors. Proc Natl Acad Sci U S A **107**: 18220–18225

Zhang Y, Zhang Y, Tessaro MJ, Tessaro MJ, Lassner M, Lassner M, Li X, Li X (2003) Knockout analysis of Arabidopsis transcription factors *TGA2*, *TGA5*, and *TGA6* reveals their redundant and essential roles in systemic acquired resistance. Plant Cell **15**: 2647–2653

Zhao D, Ferguson AA, Jiang N (2016) What makes up plant genomes: the vanishing line between transposable elements and genes. Biochim Biophys Acta **1859**: 366–380

Zhao T, Borg-Karlson A-K, Erbilgin N, Krokene P (2011) Host resistance elicited

by methyl jasmonate reduces emission of aggregation pheromones by the spruce bark beetle, *Ips typographus*. Oecologia **167**: 691–699

Zhao T, Kandasamy D, Krokene P, Chen J, Gershenzon J, Hammerbacher A (2019) Fungal associates of the tree-killing bark beetle, *Ips typographus*, vary in virulence, ability to degrade conifer phenolics and influence bark beetle tunneling behavior. Fungal Ecol **38**: 71–79

Zheng X, Spivey NW, Zeng W, Liu P-P, Fu ZQ, Klessig DF, He SY, Dong X (2012) Coronatine promotes *Pseudomonas syringae* virulence in plants by activating a signaling cascade that inhibits salicylic acid accumulation. Cell Host Microbe **11**: 587–596

Zheng Z, Qamar SA, Chen Z, Mengiste T (2006) Arabidopsis WRKY33 transcription factor is required for resistance to necrotrophic fungal pathogens. Plant J **48**: 592–605

Zhou JM, Trifa Y, Silva H, Pontier D, Lam E, Shah J, Klessig DF (2000) NPR1 differentially interacts with members of the TGA/OBF family of transcription factors that bind an element of the *PR-1* gene required for induction by salicylic acid. Mol Plant-Microbe Interact **13**: 191–202

Zhou M, Sun Z, Ding M, Logacheva MD, Kreft I, Wang D, Yan M, Shao J, Tang Y, Wu Y, et al (2017) FtSAD2 and FtJAZ1 regulate activity of the FtMYB11 transcription repressor of the phenylpropanoid pathway in *Fagopyrum tataricum*. New Phytol **216**: 814–828

Zhu FY, Chen MX, Ye NH, Qiao WM, Gao B, Law WK, Tian Y, Zhang D, Zhang D, Liu TY, et al (2018) Comparative performance of the BGISEQ-500 and Illumina HiSeq4000 sequencing platforms for transcriptome analysis in plants. Plant Methods **14**: 69

Zhu J-K (2009) Active DNA demethylation mediated by DNA glycosylases. Annu Rev Genet **43**: 143–66

Zhu Z, An F, Feng Y, Li P, Xue L, A M, Jiang Z, Kim JM, To TK, Li W, et al (2011) Derepression of ethylene-stabilized transcription factors (EIN3/EIL1) mediates jasmonate and ethylene signaling synergy in *Arabidopsis*. Proc Natl Acad Sci U

S A **108**: 12539–12544

Zimmerli L, Jakab G, Metraux JP, Mauch-Mani B (2000) Potentiation of pathogen-specific defense mechanisms in *Arabidopsis* by *β*-aminobutyric acid. Proc Natl Acad Sci U S A **97**: 12920–12925

Zipfel C (2014) Plant pattern-recognition receptors. Trends Immunol **35**: 345–351

Zipfel C, Robatzek S, Navarro L, Oakeley EJ, Jones JDG, Felix G, Boller T (2004) Bacterial disease resistance in *Arabidopsis* through flagellin perception. Nature **428**: 764–767

Zulak KG, Dullat HK, Keeling CI, Lippert D, Bohlmann J (2010) Immunofluorescence localization of levopimaradiene/abietadiene synthase in methyl jasmonate treated stems of Sitka spruce (*Picea sitchensis*) shows activation of diterpenoid biosynthesis in cortical and developing traumatic resin ducts. Phytochemistry **71**: 1695–1699

Zulak KG, Lippert DN, Kuzyk MA, Domanski D, Chou T, Borchers CH, Bohlmann J (2009) Targeted proteomics using selected reaction monitoring reveals the induction of specific terpene synthases in a multi-level study of methyl jasmonate-treated Norway spruce (*Picea abies*). Plant J **60**: 1015–1030